

# **Role of inflammatory cytokine signaling in the regulation of detoxifying functions in human hepatocytes and liver**

Von der Fakultät Energie-, Verfahrens- und Biotechnik der Universität Stuttgart  
zur Erlangung der Würde eines Doktors der  
Naturwissenschaften (Dr. rer. nat.) genehmigte Abhandlung

Vorgelegt von

**Marcus Klein**

aus Dresden

Hauptberichter: Prof. Dr. Ulrich M. Zanger

Mitberichterin: Prof. Dr. Monilola Olayioye

Tag der mündlichen Prüfung: 27.08.2014

Dr. Margarete Fischer-Bosch-Institut für Klinische Pharmakologie  
und

Institut für Zellbiologie und Immunologie der Universität Stuttgart

2014

For Pilar Hazel

**TABLE OF CONTENTS**

**ABBREVIATIONS ..... VI**

**ZUSAMMENFASSUNG .....VIII**

**SUMMARY..... XII**

**1 INTRODUCTION..... 1**

**1.1 Drug metabolism and its variability ..... 1**

    1.1.1 Introduction to drug metabolism ..... 1

    1.1.2 Factors affecting drug metabolism activity ..... 5

**1.2 Inflammation and the acute phase response ..... 8**

    1.2.1 The role of cytokines ..... 9

    1.2.2 C-reactive protein: an exquisitely sensitive systemic marker of inflammation ..... 10

**1.3 Impact of inflammation and infection on drug metabolism ..... 11**

    1.3.1 Clinical relevance ..... 12

    1.3.2 Molecular mechanisms ..... 14

**1.4 *In vitro* test systems ..... 19**

    1.4.1 Primary human hepatocytes ..... 19

    1.4.2 HepaRG cells ..... 20

**1.5 Objectives ..... 21**

**2 MATERIALS..... 22**

**2.1 Chemical reagents ..... 22**

**2.2 Buffers and solutions ..... 24**

**2.3 Kits ..... 25**

**2.4 Equipment ..... 25**

**2.5 Consumables ..... 26**

**2.6 TaqMan® assays ..... 27**

**2.7 Antibodies ..... 28**

## TABLE OF CONTENTS

---

<b>2.8</b>	<b>Primary cells and cell lines</b> .....	<b>28</b>
2.8.1	Primary human hepatocytes .....	28
2.8.2	HepaRG cells .....	28
2.8.3	Cell culture media .....	29
<b>2.9</b>	<b>Liver samples</b> .....	<b>29</b>
<b>2.10</b>	<b>Software and online tools</b> .....	<b>30</b>
<b>3</b>	<b>METHODS</b> .....	<b>31</b>
<b>3.1</b>	<b>Cell culture</b> .....	<b>31</b>
3.1.1	Cultivation of cells .....	31
3.1.1.1	Primary human hepatocytes.....	31
3.1.1.2	HepaRG cells.....	31
3.1.2	Cytokine stimulation .....	32
3.1.3	Chemical activation of signaling pathways.....	32
3.1.4	Chemical inhibition of signaling pathways.....	33
3.1.5	siRNA-mediated knock-down.....	33
<b>3.2</b>	<b>Quantitative methods</b> .....	<b>34</b>
3.2.1	RNA isolation and quantification.....	34
3.2.2	cDNA synthesis by reverse transcription .....	34
3.2.3	Real-time PCR with the BioMark HD System.....	35
3.2.3.1	Specific target amplification.....	35
3.2.3.2	qPCR using the BioMark HD System .....	35
3.2.3.3	$\Delta\Delta$ CT method for analysis of qPCR data .....	36
3.2.3.4	Statistical analysis .....	37
3.2.4	Quantification of total protein content .....	37
3.2.5	Quantification of proteins by SDS-PAGE and immunoblotting .....	37
3.2.6	Quantification of phosphoproteins by reverse phase protein array .....	38
3.2.7	Quantification of P450 activities.....	39
3.2.7.1	Internal standards and calibration.....	39
3.2.7.2	Statistical analysis .....	40
<b>3.3</b>	<b>Transcriptome analyses</b> .....	<b>41</b>
3.3.1	Affymetrix <i>ex vivo</i> transcriptome study.....	41
3.3.1.1	Affymetrix Human Gene ST 2.0 array processing .....	41
3.3.1.2	Data processing and statistical analysis.....	41
3.3.2	Retrospective <i>in vivo</i> transcriptome study .....	42
3.3.3	Annotation enrichment analyses .....	42
3.3.3.1	Gene Ontology .....	42

## TABLE OF CONTENTS

---

3.3.3.2	Kyoto Encyclopedia of Genes and Genomes .....	43
<b>4</b>	<b>RESULTS.....</b>	<b>44</b>
<b>4.1</b>	<b>Impact of the inflammatory mediator interleukin-6 on the drug detoxification system in primary human hepatocytes.....</b>	<b>44</b>
4.1.1	Stimulation with interleukin-6 .....	46
4.1.1.1	Identification of differentially expressed genes.....	46
4.1.1.2	Cytochrome P450 protein expression.....	51
4.1.1.3	Cytochrome P450 activities.....	51
4.1.2	Interleukin-6 response pathways.....	53
4.1.2.1	Major signaling pathways activated by interleukin-6.....	53
4.1.2.2	Chemical inhibition of major signaling pathways.....	55
4.1.2.3	Chemical activation of the PI3K/AKT pathway.....	62
4.1.2.4	Knock-down of the central nuclear receptor RXR- $\alpha$ .....	64
<b>4.2</b>	<b>Impact of inflammatory mediators on the drug detoxification system in HepaRG cells .....</b>	<b>67</b>
4.2.1	HepaRG cells as a model for interleukin-6-induced effects.....	67
4.2.1.1	Identification of differentially expressed genes.....	68
4.2.1.2	Cytochrome P450 protein expression.....	72
4.2.1.3	Cytochrome P450 activities.....	73
4.2.2	Stimulation with interleukin-1 $\beta$ and tumor necrosis factor- $\alpha$ .....	74
4.2.2.1	Identification of differentially expressed genes.....	75
4.2.2.2	Cytochrome P450 activities.....	78
<b>4.3</b>	<b>Transcriptome-wide impact of inflammatory mediators.....</b>	<b>79</b>
4.3.1	Affymetrix microarray study in primary human hepatocytes treated with interleukin-6 .....	80
4.3.1.1	Identification of differentially expressed genes.....	80
4.3.1.2	Validation of microarray data by qPCR .....	82
4.3.1.3	Identification of over-represented annotation terms .....	84
4.3.1.4	Identification of over-represented regulatory pathways .....	86
4.3.2	Retrospective transcriptome study in patients with elevated CRP .....	87
4.3.2.1	Identification of differentially expressed genes.....	87
4.3.2.2	Identification of over-represented annotation terms and regulatory pathways.....	90
4.3.3	Combined and comparative analyses .....	92
<b>5</b>	<b>DISCUSSION .....</b>	<b>94</b>
<b>5.1</b>	<b>Influence of the inflammatory mediator interleukin-6 on drug metabolizing enzymes and transporters .....</b>	<b>95</b>

## TABLE OF CONTENTS

---

<b>5.2</b>	<b>Inflammatory signaling pathways involved in the regulation of drug metabolizing enzymes and transporters .....</b>	<b>99</b>
<b>5.3</b>	<b>HepaRG cells as a model for studying the influence of inflammatory mediators on human drug metabolism.....</b>	<b>103</b>
<b>5.4</b>	<b>The hepatic transcriptome during inflammation.....</b>	<b>106</b>
<b>5.5</b>	<b>Conclusions .....</b>	<b>111</b>
<b>5.6</b>	<b>Future directions .....</b>	<b>112</b>
<b>6</b>	<b>REFERENCES .....</b>	<b>114</b>
<b>7</b>	<b>PUBLICATIONS .....</b>	<b>130</b>
<b>7.1</b>	<b>Publications in peer reviewed journals.....</b>	<b>130</b>
<b>7.2</b>	<b>Posters presented at national and international meetings .....</b>	<b>130</b>
<b>7.3</b>	<b>Other publications .....</b>	<b>130</b>
<b>8</b>	<b>ACKNOWLEDGEMENTS.....</b>	<b>131</b>
<b>9</b>	<b>DECLARATION/ERKLÄRUNG.....</b>	<b>133</b>
<b>10</b>	<b>SUPPLEMENTS .....</b>	<b>134</b>

**ABBREVIATIONS**

ABC	ATP binding cassette
ADH	alcohol dehydrogenase
ADME	absorption, distribution, metabolism, and excretion
AhR	aryl hydrocarbon receptor
AKT	proteine kinase B/PKB
ALDH	aldehyde dehydrogenase
AMET	arzneimittelmetabolisierende Enzyme und Transporter
AP	acute phase
APP	acute phase protein
APR	acute phase response
ATP	adenosine triphosphate
bp	base pairs
BSA	bovine serum albumin
C/EBP	CCAAT-enhancer binding protein
CAR	constitutive androstane receptor
cDNA	complementary DNA
cRNA	complementary RNA
CRP	C-reactive protein
CYP	cytochrome P450 (usually used to describe the gene)
Da	Dalton
DDI	drug-drug interaction
DMET	drug metabolizing enzymes and transporters
DNA	deoxyribonucleic acid
EDTA	ethylendiamintetraacetic acid
ER	estrogen receptor
ERK	extracellular-signal regulated kinase
ERMBT	erythromycin breath test
FC	fold change
FXR	farnesoid X-activated receptor
g	gravitational
Gab1	Grb2-associated binding protein 1
GDP	guanosine diphosphate
GO	gene ontology
gp	glycoprotein
GR	glucocorticoid receptor
Grb2	growth factor receptor-bound protein 2
GST	glutathione S-transferase
GTP	guanosine triphosphate
h	hour(s)
IFN	interferon
IKK	I $\kappa$ B kinase
IL	interleukin
ISTD	internal standard
JAK	janus kinase
KD	knock-down
KEGG	Kyoto Encyclopedia of Genes and Genomes
LAP	liver activating protein
LC-MS/MS	Liquid Chromatography-Tandem Mass Spectrometry

## ABBREVIATIONS

---

LIP	liver inhibiting protein
LPS	lipopolysaccharide
LXR	liver X-receptor
MAPK	mitogen-activated protein kinase
MEK	mitogen-activated protein kinase kinase
min	minute(s)
NAT	N-acetyltransferase
NF-kB	nuclear factor kappa B
NR	nuclear receptor
P450	cytochrome P450 (usually used to describe the enzyme)
PAPS	3'-phosphoadenosine 5'-phosphosulphate
PCR	polymerase chain reaction
PHH	primary human hepatocytes
PI3K	phosphoinositide 3-kinase
PKC	protein kinase C
PP	phosphoprotein
PPAR	peroxisome proliferator-activated receptor
PXR	pregnane X receptor
qPCR	real-time PCR
Raf	rapidly accelerated fibrosarcoma protein kinase
RAR	retinoid acid receptor
Ras	from: Rat sarcoma, small GTPase
RFI	relative fluorescence intensity
RNA	ribonucleic acid
ROS	reactive oxygen species
RXR	retinoid X receptor
S	serine
SAA	serum amyloid A
sec	second(s)
SHP2	SH2-containing protein tyrosine phosphatase 2
siRNA	small interfering RNA
SLC	solute carrier
SNP	single-nucleotide polymorphism
SOCS	suppressor of cytokine signaling
SOS	son of sevenless
STAT	signal transducer and activator of transcription
SULT	sulfotransferase
T	threonine
TAE	tris-acetate-EDTA
TBS	tris buffered saline
TNF	tumor necrosis factor
TPMT	thiopurine S-methyltransferase
TR	thyroid hormone receptor
UDP	uridine 5'-diphosphate
UGT	UDP-glucuronosyltransferase
VDR	vitamin-D receptor
WB	Western blot
Y	tyrosine

## ZUSAMMENFASSUNG

Die Entzündungsreaktion ist vor allem von pro-entzündlichen Zytokinen, wie z.B. TNF- $\alpha$ , IL-1 $\beta$  und IL-6, geprägt. Diese werden u.a. von Kupffer-Zellen, Makrophagen und Tumorzellen produziert und spielen eine wichtige Rolle in hepatozellulären Signalwegen sowie in der Regulation der zellulären Homöostase. Hauptsächlich aktivieren diese Zytokine die Akut-Phase-Reaktion (APR), beeinflussen jedoch gleichzeitig die Genexpression von vielen arzneimittelmetabolisierenden Enzymen und Transportern (AMET), was zu einer dramatischen Verminderung der Kapazität des Arzneimittelstoffwechsels (Fremdstoffmetabolismus) führen kann. IL-6 aktiviert verschiedene Signalkaskaden, wie z.B. JAK/STAT, MAPK/ERK und PI3K/AKT. Frühere Arbeiten zeigten eine JAK/STAT- und MAPK/ERK-unabhängige Herunterregulation des bedeutenden Cytochroms P450 (CYP)3A4. Es gibt jedoch Hinweise, dass MAP-Kinasen Kernrezeptoren (nukleäre Rezeptoren, NRs), wie z.B. RXR- $\alpha$ , phosphorylieren und somit deren Funktion verändern. Möglicherweise kann die AKT-Kinase, welche der PI3-Kinase nachgeschaltet ist, die nukleäre Translokation von NF- $\kappa$ B induzieren, was zu einer Antagonisierung von RXR- $\alpha$  und anderer NRs führen kann. RXR- $\alpha$ , welches mit anderen NRs der Unterfamilie 1 (z.B. CAR und PXR) dimerisiert, ist ein wichtiger Regulator der Entgiftungsfunktion der Leber. Eine Inhibition dieses oder anderer NRs könnte daher eine koordinierte Herunterregulation von ganzen Gengruppen inklusive vieler AMET-Gene erklären. Die beteiligten Signaltransduktionswege und Mechanismen sind jedoch noch größtenteils ungeklärt.

Ziel dieser Arbeit war es, den Einfluss des wichtigen pro-entzündlichen Mediators IL-6 auf die Entgiftungskapazität der Leber sowie dessen Regulation zu untersuchen. Dafür wurde mittels Hochdurchsatz-qPCR auf mikrofluidischen Chips (Fluidigm) eine umfangreiche Analyse von AMET-Genexpressionsänderungen in IL-6-behandelten primären humanen Hepatozyten (PHH) durchgeführt. Viele wichtige AMET-Gene waren herunterreguliert. Am stärksten supprimiert waren Gene, welche für CYPs (z.B. *CYP1A2*, *2C9*, *2D6* und *3A4*) und Transportproteine der ABC- (z.B. *ABCB1* und *ABCC2*) sowie SLC-Familie (z.B. *SLC10A1* und *SLCO1B1*) kodieren. Die Expression von Genen des Phase II-Metabolismus waren nur moderat betroffen und zeigten eine sehr viel stärkere Variabilität, mit teilweise erhöhter Expression (*SULTs*). Vor allem für die *CYP*-Gene war eine sehr koordinierte Reaktion auf die IL-6-Stimulation in PHH auffallend. Übereinstimmend dazu konnten anhand von spezifischen Marker-Reaktionen eine Beeinträchtigung der Aktivität der wichtigen Isoenzyme CYP1A2,

2B6, 2C8, 2C9, 2C19 und 3A4 bestimmt werden. Es wurde somit gezeigt, dass die IL-6-Signalwirkung störend in den Fremdstoffmetabolismus in humanen Hepatozyten eingreift.

Mittels Phosphoprotein-Mikroarray-Analysen konnten eine IL-6-abhängige Aktivierung der JAK/STAT-, MAPK- und PI3K-Signalkaskaden gezeigt werden. Während eine individuelle chemische Hemmung der MAPK- oder PI3K-Kaskade viele Effekte abschwächte, führte deren gleichzeitige Hemmung fast vollständig zur Aufhebung der IL-6-vermittelten Effekte auf die AMET-Genexpression. Eine Hemmung des JAK/STAT-Signalwegs hatte nur einen geringen Einfluss auf die IL-6-vermittelten Effekte. Interessanterweise führten die Aktivierung von PI3K sowie der Knockdown (KD) von RXR- $\alpha$  im Vergleich zur IL-6-Stimulation zu bemerkenswert ähnlichen AMET-Genexpressionsmustern. Demzufolge deuten diese Ergebnisse auf eine MAPK/ERK- und PI3K/AKT-abhängige, jedoch aber JAK/STAT-unabhängige, IL-6-vermittelte Herunterregulation von AMET-Genen hin. Möglicherweise geschieht dies durch Interaktion mit RXR- $\alpha$ . Zusammenfassend geben diese Daten zu erkennen, dass sowohl MAP-Kinasen als auch durch AKT aktiviertes NF- $\kappa$ B NR-Signalwege antagonisieren und somit zu einer koordinierten Repression von AMET-Genen führen können.

Die interindividuelle Variabilität von primären Hepatozyten erschwert die Untersuchung von sensitiven regulatorischen Mechanismen. In der hepatozellulären Karzinomzelllinie HepaRG sind viele Eigenschaften von PHH erhalten inklusive der funktionellen Expression von AMET. Der Einfluss der Entzündungsreaktion auf den Arzneimittelmetabolismus wurde in dieser Zelllinie jedoch noch nicht untersucht. Folglich wurden HepaRG Zellen für ihre Eignung sowie Robustheit in der Erforschung der entzündungsvermittelten Wirkung auf den Medikamentenstoffwechsel in der humanen Leber untersucht. Tatsächlich führte eine IL-6-Stimulation in HepaRG zu einer stark erhöhten Expression von Akut-Phase (AP) Genen (z.B. *CRP*) sowie zu einer koordinierten Herunterregulation der AMET-Genexpression. Selektivität und Ausmaß der Effekte waren denen in IL-6-behandelten humanen Hepatozyten sehr ähnlich, mit nur wenigen Ausnahmen (z.B. *CYP2E1* und *SULTs*). Dies wurde bestätigt durch eine stark positive Korrelation von IL-6-vermittelten Expressionsänderungen von AMET-Genen sowie wichtigen Modulatoren in beiden Zellmodellen, PHH und HepaRG. Des Weiteren konnten in HepaRG Zellen, ähnlich wie in PHH, eine verminderte Proteinexpression sowie Aktivität von wichtigen Cytochromen P450 bestimmt werden. Die Behandlung von HepaRG Zellen mit verschiedenen Zytokinen resultierte in differenziellen Genexpressionsmustern, was auf eine spezifische Empfindlichkeit gegenüber bestimmten pro-entzündlichen

Zytokinen hinweist. Insgesamt zeigen diese Daten, dass HepaRG Zellen die regulatorischen Mechanismen der Herunterregulation des Fremdstoffmetabolismus während einer Entzündung bewahren. Diese Zelllinie könnte somit ein gutes alternatives Modellsystem für mechanistische Analysen während pathophysiologischer Bedingungen, wie Entzündungen, darstellen.

Die durch Entzündung verursachten Genexpressionsänderungen, welche schwerwiegende Auswirkungen auf den Arzneimittelmetabolismus in der Leber haben, wurden bisher noch nicht auf transkriptomweiter Ebene untersucht. Somit wurden im letzten Teil dieser Arbeit mittels Mikroarray-Analysen die genomweiten Transkriptveränderungen in Folge einer Entzündungsreaktion in der humanen Leber gemessen. Es wurden Transkriptomdaten von IL-6-behandelten PHH mit bereits verfügbaren Daten aus einer Leberkohorte, welche Patienten mit einer APR einschloss (erhöhtes CRP), verglichen. Bemerkenswerterweise zählten die wichtigen *CYPs 2C8, 3A4* und *2A6* zu den am stärksten herunterregulierten Genen in IL-6-behandelten PHH. Deren Transkription war mindestens vierfach reprimiert. Insgesamt wurden 40 signifikant veränderte AMET-Gene identifiziert, von denen 30 herunterreguliert waren, inklusive vieler Transkripte von wichtigen *CYPs* (z.B. *1A2, 2A6, 2B6, 2C8, 2C9, 2C19, 3A4* und *3A5*), Phase II-metabolisierenden Enzymen (z.B. *GSTAs, SULTs* und *UGTs*) sowie Medikamententransportern (*ABCS* und *SLCs*). In Leberproben von Patienten mit einem erhöhten CRP-Serumlevel waren 29 AMET-Gene herunterreguliert. Diese umfassten wichtige Gene, welche für Phase I/II-metabolisierende Enzyme (z.B., *ADHs, ALDHs, CYPs, GSTs* und *UGTs*) sowie Medikamententransporter (z.B. *ABCG2* und *SLCs*) kodieren. Genannotationsanalysen in beiden Studien deuteten auf einen sehr starken Einfluss auf Prozesse des Fremdstoffmetabolismus hin, welche hauptsächlich herunterregulierte AMET-Gene enthalten. Des Weiteren zeigte eine Signalweg-Analyse (KEGG), dass die am stärksten beeinflussten Netzwerke dem Medikamenten- sowie dem Fremdstoffmetabolismus angehörten. Dadurch konnte gezeigt werden, dass das Entgiftungssystem der Leber während einer Entzündung stark beeinträchtigt wird. Weitere Genannotationsanalysen zeigten außerdem eine Anreicherung von diversen Fettstoffwechselprozessen, wie z.B. des Fettsäure- und Steroidstoffwechsels. In den Leberproben von Patienten mit erhöhtem CRP-Serumlevel waren ferner vermehrt biologische Prozesse und Signalwege betroffen, welche dem Aminosäurestoffwechsel angehören. Die Daten deuteten auf eine Konservierung sowie eine gerichtete Verteilung von spezifischen Aminosäuren, zugunsten der Akut-Phase-Protein (APP)-Synthese, hin. Zusammenfassend zeigen diese Daten das Ausmaß, in welchem das

Transkriptom der humanen Leber während einer Entzündung beeinflusst wird. Eine umfangreiche Reorganisation des Fremdstoff-, Fett- und Aminosäurestoffwechsel findet statt. Es scheint, als ob die Leber ihre transkriptionelle Maschinerie der Immunantwort widmet während andere wichtige Leberfunktionen eingestellt werden. Diese Beobachtungen könnten den Weg in Richtung eines besseren Verständnisses der Leber, ihrer Funktionen und wie diese ihre diversen Aufgaben unter verschiedenen Bedingungen organisiert und anpasst, ebnet.

**SUMMARY**

During inflammation, circulating pro-inflammatory cytokines such as TNF $\alpha$ , IL-1 $\beta$ , and IL-6, which are produced by, e.g., Kupffer cells, macrophages, or tumor cells, play important roles in hepatocellular signalling pathways and in the regulation of cellular homeostasis. In particular, these cytokines are responsible for the acute phase response (APR) but also for a dramatic reduction of drug detoxification capacity due to impaired expression of numerous genes coding for drug metabolic enzymes and transporters (DMETs). Several pathways are known to be activated by IL-6 such as the JAK/STAT, MAPK/ERK, and PI3K/AKT pathways. Earlier work by others has shown that downregulation of CYP3A4 is independent of the JAK/STAT and MAPK/ERK pathways. However, there is evidence that MAPKs are able to phosphorylate nuclear receptors (NRs) such as RXR- $\alpha$ , which alters their function. Moreover, AKT, downstream of PI3K, may induce nuclear translocation of NF- $\kappa$ B which antagonizes RXR- $\alpha$  and other NRs. RXR- $\alpha$ , which heterodimerizes with subfamily 1 NRs (e.g., CAR and PXR), is an important regulator of detoxifying functions in liver. Inhibition of RXR- $\alpha$  or other NRs could therefore explain the simultaneous downregulation of large gene batteries including many DMET genes. The contributing signaling events and mechanisms remained, however, largely unexplained.

Therefore, the major focus of this thesis was the investigation of the impact of the major inflammatory mediator IL-6 on the regulation of detoxifying functions in human liver. For this purpose, a large-scale investigation of DMET gene expression changes in IL-6-stimulated primary human hepatocytes (PHH) was carried out. Many important DMET genes were found to be downregulated in response to IL-6 stimulation of PHH. Most significantly suppressed were genes coding for cytochrome P450s (e.g., *CYP1A2*, *2C9*, *2D6*, and *3A4*) and ATP-binding cassette (e.g., *ABCB1* and *ABCC2*) and solute carrier (e.g., *SLC10A1* and *SLCO1B1*) drug transporters. The average phase II metabolism gene expression appeared to be only moderately affected by IL-6, showing much stronger variability in gene expression, including genes with a trend towards upregulation (*SULTs*). Most notably, CYPs appeared to be highly downregulated in a coordinated fashion, demonstrating the broad suppressive potency of IL-6 towards this particular family of drug metabolizing enzymes (DMEs). Moreover, determination of metabolite formation rates in IL-6-treated PHH revealed impaired metabolic functionality of the major CYP isoenzymes CYP1A2, 2B6, 2C8, 2C9, 2C19, and 3A4. Therefore, it was shown that IL-6 signaling extensively interferes with drug detoxification capacity in human hepatocytes.

Phosphoprotein analyses revealed activation of the JAK/STAT, MAPK, and PI3K cascades by IL-6. Whereas individual chemical inhibition of the two latter pathways attenuated many IL-6-mediated effects on DMET gene expression, co-inhibition almost completely abolished these effects. Inhibition of JAK/STAT signaling barely affected IL-6-mediated effects. Notably, activation of PI3K and knock-down (KD) of RXR- $\alpha$  demonstrated strikingly similar DMET gene expression patterns compared to IL-6 stimulation. Therefore, these data indicated a MAPK/ERK- and PI3K/AKT-dependent but JAK/STAT-independent downregulation of DMET genes in response to IL-6, possibly via interference with RXR- $\alpha$ . In conclusion, these data suggest that MAPKs and AKT-activated NF- $\kappa$ B antagonize NR signaling, causing a coordinated downregulation of DMET genes.

The investigation of sensitive regulatory mechanisms is complicated by the interindividual variability of PHH. The human hepatocellular carcinoma derived HepaRG cell line has been shown to retain many functional characteristics of PHH, including the expression of functional DMETs, but the influence of inflammation has not been investigated so far. Thus, HepaRG cells were tested for their robustness and suitability in studying the inflammation-mediated impact on the drug detoxification capacity in human liver. Indeed, IL-6 stimulation of HepaRG cells led to highly induced expression of acute phase (AP) genes (e.g., *CRP*) and significantly repressed DMET gene expression in a coordinated fashion. The selectivity and magnitude of these effects were strikingly similar to those observed in IL-6-exposed PHH, with only few exceptions (e.g., *CYP2E1* and *SULTs*). This was further supported by a strong positive correlation of IL-6-mediated expression changes of DMET and critical modifier genes in both cell models. Moreover, decreased protein expression and activity of major P450s could be determined in HepaRG cells, comparable to PHH. Exposure of HepaRG cells to different cytokines resulted in moderately different gene expression patterns, indicating specific responsiveness to particular pro-inflammatory cytokines. These data indicate that HepaRG cells retain the regulatory mechanisms that are responsible for the downregulation of the liver's drug detoxification capacity during inflammation. This cell line may therefore provide a good alternative model for detailed mechanistic analyses during such conditions.

The inflammation-mediated transcriptional changes that have major effects on drug detoxification in the liver have not been analyzed on a transcriptome-wide scale so far. Therefore, the last part of this work focused on the unbiased assessment of genome-wide transcriptional changes in response to inflammatory signaling in the human liver. For this purpose, microarray analysis was carried out in IL-6-stimulated PHH and compared to

transcriptome data, previously acquired in samples from a liver cohort, including patients having undergone an APR (elevated CRP). Remarkably, major human-relevant *CYPs*, *2C8*, *3A4*, and *2A6* were the most strongly downregulated genes in IL-6-challenged PHH. Their transcription was at least 4-fold repressed. A total of 40 DMET genes were identified as significantly altered, of which 30 were downregulated, including almost all transcripts of major *CYPs* of importance in humans (e.g., *1A2*, *2A6*, *2B6*, *2C8*, *2C9*, *2C19*, *3A4* and *3A5*), phase II drug metabolizing enzymes (e.g., *GSTAs*, *SULTs* and *UGTs*), and drug transporters (*ABCs* and *SLCs*). In liver samples from patients with elevated CRP, 29 DMET genes were downregulated including important genes coding for phase I/II drug metabolizing enzymes (e.g., *ADHs*, *ALDHs*, *CYPs*, *GSTs* and *UGTs*) and drug transporters (e.g., *ABCG2* and *SLCs*). In both studies, gene term enrichment analyses indicated a very strong influence on xenobiotic metabolic and related processes, containing mostly downregulated DMET genes. Moreover, pathway enrichment (KEGG) analyses revealed that drug and xenobiotic metabolic signaling pathways were the most strongly impacted reaction networks, clearly demonstrating that the drug detoxification system in the liver is largely affected during inflammation. Gene annotation analysis also identified enriched processes related to diverse lipid metabolic processes such as fatty-acid and steroid metabolism. Moreover, enriched biological processes and regulatory pathways related to amino acid metabolism were found, particularly in the retrospective study. The data indicated a conservation and allocation of specific amino acids, possibly in favor of acute phase protein (APP) synthesis. Taken together, these findings highlight the scale on which the human liver transcriptome is affected during inflammation. Extensive reorganization related to xenobiotic, lipid, and amino acid metabolism takes place. It appears that the liver devotes its transcriptional machinery to the immune response while other major liver functions are shut down. This may help to pave the way towards a better understanding of how the liver organizes its many responsibilities in different conditions.

# 1 INTRODUCTION

## 1.1 Drug metabolism and its variability

### 1.1.1 Introduction to drug metabolism

In order to be sufficiently absorbed by the body, most clinically used drugs have lipophilic properties. Such substances are difficult to eliminate by the kidneys and therefore are prone to accumulate in fat deposits or cell membranes. Thus, the major function of drug metabolism is the biotransformation of lipophilic foreign substances (xenobiotic biotransformation) to more hydrophilic products in order to enable their efficient elimination through the kidneys or the intestine (**Figure 1**). This function is also referred to as detoxification due to frequent loss of pharmacological activity. However, formation of toxic metabolites is also possible. Hence, it is important to reach an optimal balance between positive and negative effects in drug therapy. A steady-state plasma concentration within a “therapeutic window” is desirable, where the drug shows a pharmacological effect with the least side effects (Zanger, 2012).

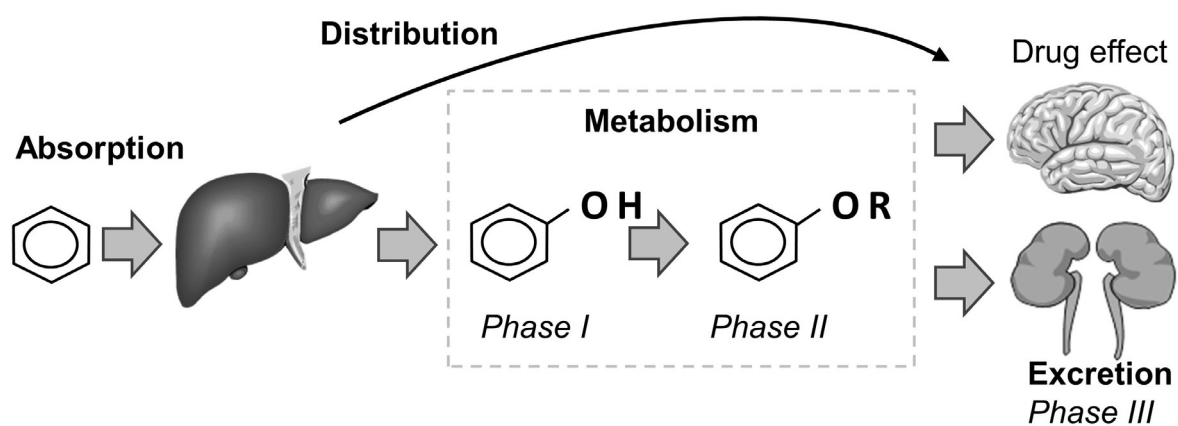


**Figure 1** Schematic of absorption, distribution, metabolism, and excretion (ADME) processes that determine the fate of a foreign lipophilic compound in the human body. This figure was adapted and modified from Zanger, 2012.

The major organ for biotransformation of drugs is the liver, in which hepatocytes constitute up to 80% of the tissue volume in adults (Kmiec, 2001). These express diverse and various drug metabolizing enzymes and transporters (DMETs). Traditionally, they were grouped into phase I and II drug metabolizing enzymes and phase III transporters (Anzenbacher and Anzenbacherová, 2012; Xu et al., 2005). This classification reflects the fact that drugs are often primarily transformed into polar metabolites (phase I) and subsequently conjugated (phase II) with polar groups to facilitate their excretion (phase III). It needs to be considered, however, that there are exceptions to this general rule. Although other classifications based on the chemical nature of processes have been proposed (David Josephy et al., 2005), the traditional classification is still extensively used.

The cytochromes P450 (CYPs) are the most important phase I drug metabolizing enzymes that catalyze the oxidative biotransformation of more than three-quarters of today's clinically used drugs (Zanger and Schwab, 2013). With heme in their active site, they mostly catalyze oxidation reactions, activating and splitting molecular oxygen, yielding a water molecule and a monooxygenated (mostly hydroxylated) product (Anzenbacher and Anzenbacherová, 2012). The P450s are well known to metabolize a large number of structurally diverse xenobiotics (Pelkonen et al., 2008). The human genome comprises 57 presumably functional CYP genes and a similar number of non-functional pseudogenes. Only about a dozen of isoenzymes of the families CYP1, CYP2, and CYP3 are responsible for most biotransformations of drugs (**Figure 2, A**), with the CYPs 3A4, 2C9, 1A2, and 2E1 being the most abundant forms in the liver (Zanger et al., 2014).

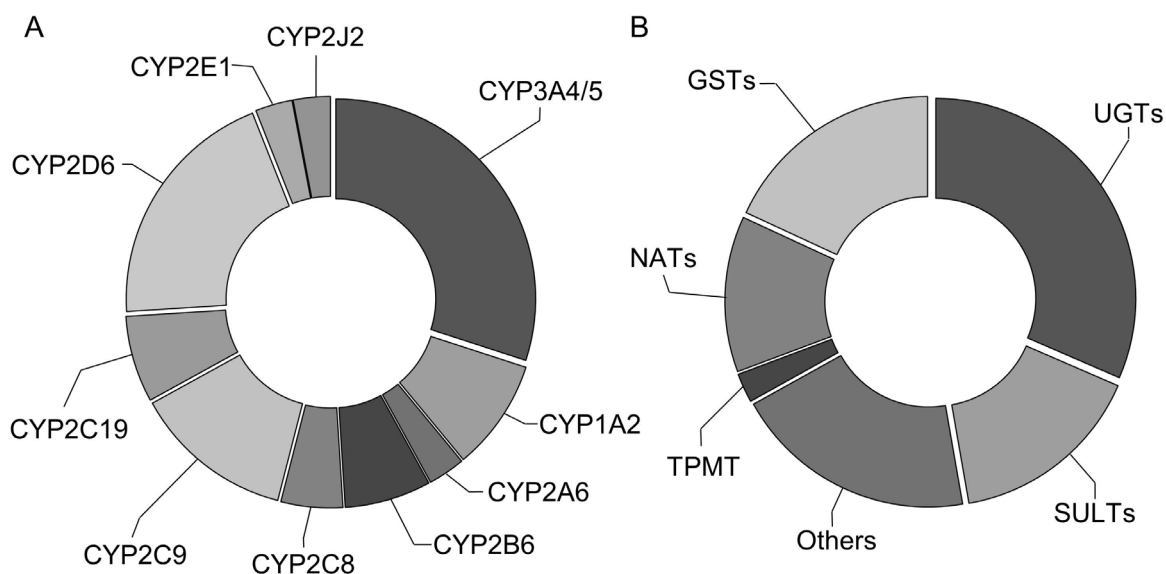


**Figure 2** Contribution of major phase I and II enzymes to metabolism of clinically used drugs. The relative size of each section represents an estimated percentaged fraction of drugs metabolized by the major (A) phase I and (B) phase II drug metabolizing enzymes (sometimes, several enzymes are responsible for the metabolism of a single drug). This figure was adapted and modified from Gonzalez and Tukey, 2005; Jancova et al., 2010; Zanger et al., 2014.

The phase II drug metabolizing enzymes play an important role in the biotransformation of endogenous compounds and xenobiotics to more water soluble products that can be easily excreted (Anzenbacher and Anzenbacherová, 2012). They perform conjugating reactions, including acetylation, glucuronidation, methylation, sulfation, and glutathione and amino acid conjugation. These reactions are mostly carried out by transferases, including glutathione S-transferases (GSTs), N-acetyltransferases (NATs), sulfotransferases (SULTs), various methyltransferases (e.g., thiopurine S-methyltransferase TPMT), and UDP-glucuronosyltransferases (UGTs) (Jancova et al., 2010). The participation of these enzymes in metabolism of clinically used drugs is shown in **Figure 2, B**. The membrane-bound UGTs form glycosidic bonds by transferring the sugar moiety from sugar nucleotide donors to another compound (Mackenzie et al., 2005). The most common type of drug conjugation is the glucuronidation, performed by enzymes of the UGT1A and UGT2B subfamily, utilizing UDP-glucuronic acid as a donor. Other enzymes in the UGT superfamily (117 members) are of minor importance in drug metabolism (Jancova et al., 2010). The SULTs are members of an enzyme superfamily that catalyzes the conjugation of a sulfonyl moiety from the universal donor molecule PAPS (3'-phosphoadenosine 5'-phosphosulphate) to an acceptor group with an O-, N-, or S-

nucleophilic atom. Hence, they facilitate sulfonation reactions of endogenous and exogenous compounds (Anzenbacher and Anzenbacherová, 2012; Jancova et al., 2010). The majority of SULTs in human liver are represented by SULT1A1 (Riches et al., 2009), which primarily catalyzes sulfate conjugation of phenolic xenobiotics such as acetaminophen (Anzenbacher and Anzenbacherová, 2012). The cytosolic NATs, typically found in human liver, catalyze (in two steps) the transfer of an acetyl group from acetyl-CoA to the amino group of a substrate (aromatic amines and hydrazines). Only two NATs are known in humans, NAT1 and NAT2, and they are able to catalyze various reactions that may lead to activation or inactivation (detoxification) of compounds. Their role in endogenous metabolism is rather unknown (Anzenbacher and Anzenbacherová, 2012; Jancova et al., 2010). The GSTs constitute another major group of phase II drug metabolizing enzymes (DMEs) which are involved in the metabolism of xenobiotics as well as endogenous compounds such as prostaglandins and steroids (van Bladeren, 2000). They catalyze the formation of thioether conjugates between glutathione and xenobiotic compounds (Jancova et al., 2010). The three main classes of GSTs (cytosolic, mitochondrial and microsomal) are widely associated with detoxification reactions, however, they may also facilitate activation of xenobiotics (Anzenbacher and Anzenbacherová, 2012; Wheeler et al., 2001). Another major biological function of GSTs appears to be defense against reactive oxygen species (ROS) that are mainly formed by cellular oxidative reactions which are catalyzed by, e.g., P450s (Jancova et al., 2010). The cytosolic enzyme TPMT is one of the few important methyltransferases, catalyzing the S-methylation of aromatic heterocyclic sulfhydryl compounds such as thiopurines (e.g., anticancer and immunosuppressive drugs). The TPMT enzyme is highly expressed in liver. Its role in endogenous metabolism remains unknown (Anzenbacher and Anzenbacherová, 2012).

Numerous drugs, metabolites, and xenobiotics are actively transported across membranes during processes of absorption, distribution, and excretion. Drug transporters play a major role in defining pharmacokinetics of many drugs because they are expressed in epithelia of the blood-brain barrier, intestine, kidney, and liver (Petrovic et al., 2007). Only a limited number of transport proteins influence drug disposition, as shown by clinical evidence (International Transporter Consortium et al., 2010). These include several uptake solute carriers (SLCs) and some ATP-binding-cassette (ABC) efflux transporters. The latter constitute the largest family of transmembrane proteins identified to date. They are involved in the transport of various substrates including drugs, hormones, lipids, and other xenobiotics (Scotto, 2003). However, for the disposition of many clinically used drugs, only a few ABCs

are of particular importance, namely, P-glycoprotein (P-gp)/MDR1 (ABCB1), multidrug resistance protein 1 & 2 (MRP1 & 2/ABCC1 & 2), and breast cancer resistance protein (BCRP/ABCG2) (Schinkel and Jonker, 2003). They are mostly known to confer multidrug resistance in tumor cells and are capable of transporting a variety of substrates including lipophilic anionic, cationic, and neutrally charged drugs and toxins as well as conjugated organic anions. These ABC transporters are expressed in tissues of absorption (e.g., lung and gut) and metabolism and elimination (liver and kidney), thus are able to modulate the pharmacokinetics of xenobiotics (Leslie et al., 2005). Another important determinant of drug absorption and availability is the cellular uptake which is mediated by the Solute Carrier (SLC) superfamily of transporters. The SLC22As form a distinct family of proteins within the SLC superfamily, and include the organic anion transporters (OATs). They are responsible for the translocation of organic anions and drugs as well as endogenous substances and toxins (Nigam et al., 2007). The OATPs (SLCs) represent a family of important sodium-independent transporters of various endogenous compounds and xenobiotics (International Transporter Consortium et al., 2010). The latter includes anti-cancer drugs, antibiotics, non-steroidal anti-inflammatory drugs, and peptides, whereas their endogenous substrates comprise bile acids, thyroid hormones, and conjugated steroids (Mikkaichi et al., 2004). The sodium/taurocholate cotransporting polypeptide (NTCP/SLC10A1) is an example of a sodium-dependent transporter. It belongs to the SLC10 family of transport proteins that mediate the uptake of bile acids, steroidal hormones, and various drugs (Claro da Silva et al., 2013).

### **1.1.2 Factors affecting drug metabolism activity**

A variety of factors affect the metabolism of drugs and xenobiotics, including intrinsic factors such as genetics, sex, age, race, or disease and extrinsic factors such as drug-drug interactions (DDIs), smoking, diet, and environmental factors (Thummel and Lin, 2014). Some of these factors are rather constant (genetics and sex), whereas others are dynamic (age, DDIs, and disease). Interindividual variability of drug metabolism can in part be explained by genetic polymorphisms which virtually exist in all genes coding for DMEs. Clinically relevant genetic polymorphisms, affecting the baseline drug metabolism capacity, occur in CYPs of the CYP2 family (2D6, 2C19, 2C9, and 2B6), CYP3A5, and phase II enzymes such as UGT1A1, NAT2, TPMT, GSTM1, and SULT1A1 (Jancova et al., 2010; Zanger, 2012). Variations of more than 100-fold are possible and can be even higher in the case of complete enzyme deficiency caused by null alleles in, e.g., CYP2C19 and CYP2D6 (Zanger et al., 2008). Less pronounced

variations caused by polymorphisms may lead to relative gain or loss of expression and/or activity of DMEs.

In some cases, sex may contribute to interindividual variability of drug metabolism by influencing factors such as body weight, plasma volume, fat distribution, liver blood flow, DME activity, drug transporter function, and excretion activity (Beierle et al., 1999; Gandhi et al., 2004; Scandlyn et al., 2008). Whereas in humans the sex differences are rather subtle, differences in expression of hepatic drug metabolizing enzymes in rodents can be very pronounced, due to different growth hormone profiles between male and female animals (Waxman and Holloway, 2009). In humans to date, not many differences in drug metabolism between men and women have been reported. It was shown that women exhibit greater CYP3A4 activity, influencing the metabolism of drugs such as antipyrine, midazolam, or verapamil (Wolbold et al., 2003). In men, activities of CYP2E1 and CYP1A2 appeared to be higher, leading to a more rapid metabolism of, e.g., caffeine or acetaminophen (Scandlyn et al., 2008; Zanger, 2012). Very recently it was shown that different methylation patterns partially explain such sex-biased differences in expression of P450 family members (Penalzo et al., 2014).

Another established factor, influencing several aspects of drug metabolism capacity is age. Age-associated alterations in functions of mostly P450s, but also other DMEs, have been reported. In neonates, some clinically important CYPs (e.g., CYP2C9 and 2C19) as well as several SULTs demonstrated immaturity, fully developing only during the first months of life (Duanmu et al., 2006; Koukouritaki et al., 2004). In the elderly, previous studies associated age with reduced inducibility of DMEs which, however, could not be reproduced and therefore remain controversial (George et al., 1990). More likely to play a role in reduced drug clearance with advancing age are decrease of liver volume and blood flow (Kinirons and O'Mahony, 2004), as well as impaired renal function (Cotreau et al., 2005).

Among many others, the most influential environmental sources of drug metabolism variability are DDIs, diet, alcohol consumption, and smoking. Many DDIs involve inhibition of DMETs, resulting in increased systemic exposure and subsequent adverse drug reactions (ADRs) (Zhang et al., 2009). P450s, in particular, are commonly affected by reversible (competitive or non-competitive) or irreversible inhibition (mechanism-based inactivation). The latter usually involves bioactivation of the xenobiotic to a reactive intermediate, covalently binding to the P450 enzyme and thereby inactivating it (Kalgutkar et al., 2007).

Some clinically relevant irreversible inhibitors of, e.g., the important CYP3A4 are antimicrobials (e.g., erythromycin and ritonavir), antihypertensives (e.g., verapamil), anti-cancer drugs (tamoxifen), and some herbal compounds (e.g., bergamottin) as well as grapefruit juice (Pelkonen et al., 2008).

In other cases, induction of drug metabolizing enzymes and transporters can result in reduced systemic exposure, accompanied by the risk of loss of efficacy of co-administered drugs (Zhang et al., 2009). This is, to a major extent, mediated by the three ligand-activated xenosensors or nuclear receptors (NRs) aryl hydrocarbon receptor (AhR), pregnane X receptor (PXR/NR1I2), and constitutive androstane receptor (CAR/NR1I3) (Pascussi et al., 2008). These NRs exert their regulatory effects by functioning as pleiotropic receptors of a large diversity of endogenous and xenobiotic compounds in order to adjust the organism to the chemical environment (Pelkonen et al., 2008; Sonoda et al., 2003). The formation and degradation of these compounds is often catalyzed by P450s whose expression in turn is regulated by NRs via tightly controlled feedback networks (Honkakoski and Negishi, 2000). Apart from regulating many different CYPs, NRs are also involved in the regulation of phase II DMEs and drug transporters (Xu et al., 2005). Particularly, the retinoid X receptor (RXR) plays an important role due to its ability to form heterodimers with all subfamily 1 nuclear receptors: CAR, FXR, LXR, PPAR, PXR, RAR, TR and VDR (Germain et al., 2006; Mangelsdorf and Evans, 1995; Wang and LeCluyse, 2003).

Moreover, AhR, CAR, and PXR can establish crosstalks with many other steroid and nuclear receptors such as estrogen receptor (ER)  $\alpha$  (NR3A1), glucocorticoid receptor (GR/NR3C1), liver X receptor (LXR/NR1H3), farnesoyl X receptor (FXR/NR1H4), peroxisome proliferator-activated receptor (PPAR- $\alpha$ /NR1C1), and retinoic acid receptor (RAR- $\alpha$ /NR1B1) (Pascussi et al., 2008; Zanger, 2012). Coordinated expression of gene batteries therefore is not only dependent on one particular stimulus but also on the function of other signaling pathways. This tangle of regulatory networks is even further complicated by the increasing importance of corepressors and coactivators, of which more than 200 are known to date (Lonard and O'Malley, 2006; Pascussi et al., 2008).

Disease states are generally associated with negative effects on drug metabolism capacity. For instance, liver cirrhosis leads to reduced blood flow and loss of functional hepatocytes which results in reduced drug clearance and loss of drug metabolic capacity, respectively (Zanger, 2012). In numerous examples, compromised metabolism, distribution, and elimination of

drugs was also reported to occur during infections and disease states that involve an inflammatory component (Renton, 2005). These effects result from mostly transcriptional suppression of major P450s and drug transporters during the generation of host defense mechanisms (Jover et al., 2002; Morgan et al., 2008; Petrovic et al., 2007). The common pathophysiological factors during such conditions are pro-inflammatory cytokines such as interleukin-1 $\beta$  (IL-1 $\beta$ ), interleukin-6 (IL-6), and tumor necrosis factor- $\alpha$  (TNF- $\alpha$ ) that ultimately modify the expression and function of specific transcription factors (Aitken et al., 2006). The components of the inflammatory response and its clinical relevance in drug therapy, including regulatory aspects, are discussed in the following chapters.

### **1.2 Inflammation and the acute phase response**

Inflammation is a complex response of vascular tissue to injury, infection, trauma, immunological disorder, or neoplastic growth (cancer), accompanied by increased blood flow and vascular permeability as well as accumulation of fluid, leukocytes, and various soluble factors (Feghali and Wright, 1997; Gruys et al., 2005). The latter are responsible for activation of resident cells (e.g., endothelial cells, fibroblasts, macrophages, and mast cells) and the recruitment of leukocytes (e.g., eosinophils, lymphocytes, monocytes, and neutrophils) by increased expression of cellular adhesion molecules and chemoattraction, thereby initiating the innate immunity (Beutler, 2004; Feghali and Wright, 1997). These soluble factors include lipid metabolites such as prostaglandins (causing pain and inducing fever), soluble proteases and substrates involved in coagulation, the complement system and the kinin system, nitric oxide (causing vasodilation of vessels), and various cell-derived polypeptides known as cytokines (Feghali and Wright, 1997; Slaviero et al., 2003). Cytokines trigger and modulate the hepatic acute phase response (APR), accompanied by the synthesis of acute phase proteins (APPs), most importantly C-reactive protein (CRP) and serum amyloid A (SAA) (Gruys et al., 2005; Heinrich et al., 1990). The APR is a prominent systemic reaction and its purpose is to remove the initial cause of the disturbance and restore homeostasis (Slaviero et al., 2003). In some cases, this response persists and may lead to chronic or recurring inflammation (Balkwill and Mantovani, 2001).

### 1.2.1 The role of cytokines

Cytokines are well known mediators of the inflammatory response (Billingham, 1987). They are crucial pleiotropic elements in the immune response, acting locally or systemically, and they can exhibit both negative and positive effects on various target cells (Arai et al., 1990; Feghali and Wright, 1997). The group of cytokines comprises hundreds of small soluble proteins with molecular weights ranging from ~ 8 kDa to ~ 50 kDa (Cameron and Kelvin, 2000; Feghali and Wright, 1997). They are divided into groups according to their physical, functional, and/or receptor binding properties, dividing them broadly into interleukins, interferons, tumor necrosis factors, and chemokines.

Mostly hematopoietic growth factors make up the group of interleukins (IL) which are further divided into subgroups. The group of the IL-1-like cytokines comprises IL-1 $\alpha$ , IL-1 $\beta$ , IL-1 receptor antagonist (IL-1RA), and IL-18 (Dinarello, 1984). They are pro-inflammatory cytokines and are important mediators for the immune and AP response (Labow et al., 1997; Takeda et al., 1998). The common  $\beta$  and  $\gamma$  chain cytokine superfamilies are named according to their members' receptor binding properties and comprise IL-3 and IL-5, or IL-2, IL-4, IL-7, IL-9, IL-13, and IL-15, respectively (Cameron and Kelvin, 2000). They are mainly involved in leucocyte activation and differentiation, in which they show redundancy in function due to their common receptor (He and Malek, 1998; Hofmeister et al., 1999; Lantz et al., 1998). The IL-6-like cytokines such as IL-6, IL-11, LIF, OSM, G-CSF, and IL-12 are key mediators of various immune processes, demonstrating overlapping functions because they mostly utilize the glycoprotein 130 (gp130) or CD130 receptor (Cameron and Kelvin, 2000). Within this group of cytokines, IL-6 is an important pleiotropic factor which can act as a growth and differentiation factor in the hematopoietic and immune system, as well as induce and inhibit growth of leukemia, lymphoma, and breast carcinoma cells via autocrine feedback loops (Heinrich et al., 1990). Moreover, it is the major regulator of APP synthesis in human liver (Castell et al., 1989). While endothelial cells, fibroblasts, and monocytes are the major producers of IL-6, cancer cells were also shown to be a source (Grivennikov and Karin, 2008; Heinrich et al., 1990). Another related group of interleukins are the IL-10-like cytokines such as IL-10, IL-19, and IL-20, with IL-10 exerting anti-inflammatory functions, thereby suppressing the inflammatory response (Moore et al., 1993).

The interferons form another group of cytokines which were originally discovered as anti-viral peptides (Wheelock, 1965). This group is further divided into type I (IFN- $\alpha$  and IFN- $\beta$ )

and type II interferons (IFN- $\gamma$ ), signalling through different receptors (Boehm et al., 1997). Whereas IFN- $\alpha$  and - $\beta$  are key-players in modulating innate immune responses, IFN- $\gamma$  is a central player in pathogen defense by activating macrophages (De Maeyer and De Maeyer-Guignard, 1998).

The tumor necrosis factors represent a family of cytokines of importance in immune function and human disease (Ware, 2011). This steadily growing superfamily includes, among others, TNF- $\alpha$  and TNF- $\beta$  (Cameron and Kelvin, 2000). Originally identified as tumor killer cell, TNF- $\alpha$  (Pennica et al., 1984) is mainly produced by macrophages, natural killer cells, and T cells (Gruss and Dower, 1995). Its most potent inducer is lipopolysaccharide (LPS) and it plays a crucial role in acute and chronic inflammatory conditions (Gruss and Dower, 1995; Sedgwick et al., 2000).

Chemokines are a group of low molecular weight chemotactic cytokines that regulate leukocyte migration via a subset of seven-transmembrane, G-protein coupled receptors (Zlotnik and Yoshie, 2000). Through their receptors, chemokines activate multiple intracellular signaling pathways, leading to the generation of inositol triphosphate, release of calcium as well as activation of protein kinase C (PKC) and small guanosine triphosphate-binding proteins of the Ras and Rho families, thereby ultimately regulating leukocyte motility (Luster, 1998). Hence, chemokines play an important role in inflammatory diseases.

### **1.2.2 C-reactive protein: an exquisitely sensitive systemic marker of inflammation**

Named after its ability to precipitate the C-polysaccharide of *Streptococcus pneumoniae*, CRP was the first APP described (Tillett and Francis, 1930). It is an exquisitely sensitive and systemic marker of inflammation, and although nonspecific, it proved to be useful in clinical settings, including monitoring infections and postoperative complications, and assessing effectiveness of treatments on the course of disease (Macy et al., 1997; Pepys and Baltz, 1983). Whether CRP is a predictive marker in cardiovascular risk assessment, as demonstrated in several studies, remains controversial (Kaski and Garcia-Moll, 2000).

CRP is exclusively produced in hepatocytes, mainly under the transcriptional control of IL-6 (Castell et al., 1989; Heinrich et al., 1990). In healthy individuals, the median CRP serum concentration is usually less than 1 mg/l and can increase several hundred-fold to more than

500 mg/l within 48 hours after a single stimulus (Macy et al., 1997; Pepys and Hirschfield, 2003; Shine et al., 1981). CRP values that remain persistently over the generally accepted threshold of 10 mg/l indicate the presence of a significant APR and are associated with increased mortality (Lobo et al., 2003; Proctor et al., 2013; Salazar et al., 2014). Due to the short half-life of only 19 hours, its synthesis rate is the only significant determinant of CRP plasma concentration (Vigushin et al., 1993). CRP is stable during multiple freeze-thaw cycles, independent of anticoagulant type or individual, and displays no significant diurnal variation (Macy et al., 1997). Moreover, it is unaffected by diet (Pepys and Hirschfield, 2003).

CRP's major role is the regulation of clearance of abnormal materials from the plasma, whether of autologous or extrinsic origin (Pepys and Baltz, 1983). Its autologous ligands include modified plasma lipoproteins (Pepys et al., 1985), damaged cell membranes (Volanakis and Wirtz, 1979), and various phospholipids, most importantly phosphocholine (Du Clos, 1989). Extrinsic ligands include glycans and various other constituents of microorganisms (MOs) such as components of bacteria, fungi, and parasites (Pepys and Hirschfield, 2003). When aggregated or ligand-bound, CRP is a potent activator of the classical complement system, engaging the main adhesion molecule C3, the terminal membrane attack complex C5-C9, and the alternative pathway (C3b) via factor H (Mold et al., 1999). By providing mobilization of immune cells and enhancing opsonization, this complement activation helps to resolve the inflammatory response (Markiewski and Lambris, 2007).

### **1.3 Impact of inflammation and infection on drug metabolism**

It has long been known that inflammation modulates drug pharmacokinetics by downregulating expression and activity of hepatic P450s (Morgan, 1997; Renton, 2005). This includes important CYPs such as CYP1A2, 2B6, 2C8, 2C9, 2C19, and 3A4, as shown in multiple human and animal models of inflammation (Renton, 2005; Yang et al., 2012). Because of the vast number of xenobiotics and endogenous substrates of CYPs (Pelkonen et al., 2008), these changes largely contribute to effects on drug therapy (decreased clearance or toxicity) and alterations in physiological function (Renton, 2005). The mechanisms of regulation are complex and poorly understood. Post-translational regulation such as inhibition via nitric oxide (Minamiyama et al., 1997) or phosphorylation-dependent enzyme inactivation (Oesch-Bartlomowicz and Oesch, 2003) were previously proposed. However, transcriptional

suppression, mediated by cytokines such as IL-1 $\beta$ , IL-6, and TNF- $\alpha$ , is considered to be the primary mechanism leading to alterations in drug detoxification capacity (Aitken et al., 2006; Morgan et al., 2008). In this respect, special attention has been given to IL-6 which was shown to regulate various CYPs, including the important CYP3A4 (Aitken et al., 2006; Jover et al., 2002). Apart from CYPs, IL-6 was also shown to downregulate the mRNA expression of several phase II enzymes such as UGTs (Congiu et al., 2002; Richardson et al., 2006) and SULTs (Shimada et al., 1999), as well as the ABC drug transporters MDR1 (Sukhai et al., 2000) and MRP2 (Siewert et al., 2004), and various SLCs (Teng and Piquette-Miller, 2005; Yang et al., 2012). Whereas the regulatory mechanisms are not fully understood, these changes indicate much potential for inflammation-induced alterations in pharmacokinetic and pharmacodynamic disposition of drugs, especially in the case of ABC drug transporters that transport a large array of clinically important drugs (Petrovic et al., 2007; Vee et al., 2009). However, more clinical studies in this field are required, because findings from tissue and animal models cannot be fully translated to humans.

### 1.3.1 Clinical relevance

To date, many clinical studies have been conducted, investigating the influence of various infectious or inflammatory diseases on drug metabolism. It was more than 30 years ago when prolonged antipyrine half-lives were observed for the first time in patients with acute viral hepatitis (Burnett et al., 1976). Many more studies followed, demonstrating impaired antipyrine metabolism in patients with psoriasis (Marsden et al., 1984), pulmonary diseases (Laybourn et al., 1986; Sonne et al., 1985), acute viral infections (Brockmeyer et al., 1998), and sepsis (Carcillo et al., 2003). Since antipyrine is metabolized by at least six hepatic CYPs such as CYP1A2, 2B6, 2C8, 2C9, 2C18, and 3A4 (Engel et al., 1996), these observations indicated an impact on the P450 monooxygenase system *per se*. Such rather unspecific inhibition of P450-mediated drug metabolism was also shown in endotoxin (LPS)-administered volunteers ingesting a drug cocktail (Shedlofsky et al., 1994, 1997).

More specific findings were made in the late 70's, when significantly longer half-life of the drug theophylline was identified in children with chronic asthma and upper-respiratory-tract viral-illness (Chang et al., 1978). This was the first time a clinical study demonstrated altered functionality of a specific P450 isoenzyme, namely, CYP1A2 which is known to be responsible for the metabolism of theophylline (Fuhr et al., 1993). Various studies confirmed an impaired elimination of theophylline during various disease states such as viral infections

(Kraemer et al., 1982; Renton et al., 1980), bacterial infections (Gray et al., 1983), or sepsis (Toft et al., 1991). Moreover, a reduced activity of CYP1A2, as determined by altered caffeine metabolism, could be observed in AIDS patients with acute illness (Lee et al., 1993).

A variety of studies investigated the influence of infectious or inflammatory disease states on the activity of CYP2 family members. For instance, acute hepatitis A (HVA) infection in children and adults decreased the clearance of CYP2A6-metabolized coumarin (Pasanen et al., 1997). Helsby et al. found low CYP2C activity associated with severe psoriasis in a group of 82 patients (Helsby et al., 1998). In some HIV patients, CYP2D6 activity approached that of poor metabolizers despite having an extensive metabolizer genotype (O'Neil et al., 2000), and significantly lower CYP2D6 activity was observed in hepatitis C patients (Becquemont et al., 2002). Furthermore, Frye and colleagues found an inverse relationship between both TNF- $\alpha$  and IL-6 plasma concentration and the activity of CYP2C19 in congestive heart failure patients who received a probe drug cocktail (Frye et al., 2002).

A lot of attention has been given to metabolism of drugs by CYP3A family members, in particular CYP3A4. For example, altered clearance of the drugs midazolam and verapamil were observed in critically ill patients with septic shock and in patients with rheumatoid arthritis, respectively (Mayo et al., 2000; Shelly et al., 1987). The erythromycin breath test (ERMBT), a suitable test for *in vivo* assessment of CYP3A4 activity (Chiou et al., 2001), revealed compromised drug metabolism in cancer patients with significant APR, suggesting a reduction in CYP3A4 function (Rivory et al., 2002). Moreover, a study in healthy individuals found a negative correlation between influenza vaccine-induced IFN- $\gamma$  production and change in ERMBT, supporting *in vitro* findings of reduced CYP3A4 expression and activity upon IFN- $\gamma$  exposure (Abdel-Razzak et al., 1993; Hayney and Muller, 2003). Remarkably, alprazolam metabolism was inversely correlated with CRP plasma levels in hemodialysis patients with persistent inflammation, suggesting a downregulation of CYP3A4 activity (Molanaei et al., 2012).

Not only do disease conditions influence the drug detoxification capacity of the liver but also systemic stress induced by local insults such as an injury or surgery. The latter, for instance, was demonstrated in bone marrow transplant patients, where cyclosporine levels and metabolites were increased several-fold while IL-6 and CRP peaks were highest, indicating inhibition of CYP3A-dependent metabolism (Chen et al., 1994). Furthermore, it was

specifically shown for CYP3A4 that acute inflammation after surgery was associated with a decline in its activity (Haas et al., 2003).

In summary, acute and chronic infectious states, whether of septic or aseptic etiology, modulate the expression and activity of multiple P450 enzymes with potential clinical impact (e.g., adverse drug effects). There has been a bias towards the investigation of P450s, owing to their importance in metabolism of most clinically used drugs. Only little is known about the impact of inflammation on phase II DMEs and drug transporters. *In vitro* studies demonstrated that the regulation of phase II enzymes during inflammation exhibits similarities with P450 regulation (reviewed in Aitken et al., 2006). However, clinical studies in this field are scarce. Moreover, the impact of inflammation-induced changes in drug transporter expression on drug disposition is still poorly understood. Although transcriptional repression of drug transporters was demonstrated *in vitro*, only very few clinical studies showed altered drug transporter substrate pharmacokinetics because of the inflammatory response (reviewed in Petrovic et al., 2007). One reason for the slow advance of research in this field may be due to the broad substrate specificity of drug transporters which complicate targeted investigations (Mizuno et al., 2003).

### **1.3.2 Molecular mechanisms**

IL-6 is a pleiotropic cytokine that is involved in the activation of innate immunity and stimulation of the APR in the liver (Cameron and Kelvin, 2000). It also plays an important role in the downregulation of DMETs (Aitken et al., 2006), in which it was shown to be exceptionally potent (Morgan et al., 2008). Therefore, this chapter summarizes the current knowledge in cellular signaling downstream of the IL-6 receptor and its possible implication in the regulation of DMETs (**Figure 3**).

Classically, IL-6 signals through a receptor complex composed of glycoprotein 130 (gp130) and gp80 (IL-6R $\alpha$ ), or the soluble sIL-6R (Eulenfeld et al., 2012). Upon IL-6 binding to the receptor complex, protein-tyrosine kinases of the Jak family, Jak1, Jak2, and Tyk2 are activated of which Jak1 plays a major role (Guschin et al., 1995). Jak activation leads to phosphorylation of multiple tyrosine receptor motifs within the cytoplasmic region of gp130, recruiting signal transducer and activator of transcription 1 (STAT1), STAT3, and SH2-domain containing phosphatase 2 (SHP2), as well as the feedback inhibitor suppressor of cytokine signaling 3 (SOCS3) (Gerhartz et al., 1996; Schmitz et al., 2000). Both SHP2 and

SOCS3 contribute to Y759-dependent attenuation of IL-6 signaling through gp130 (Lehmann et al., 2003), by either dephosphorylation of STATs (Larsen and Röpke, 2002) or inhibition of Jak kinase activity (Wu et al., 2002), respectively. Upon successful phosphorylation at their critical motifs, STAT1 (Y701) and STAT3 (Y705) hetero- or homodimerize and translocate into the nucleus, where they exert their full transcriptional activity (Gerhartz et al., 1996).

Apart from STAT transcription factors, IL-6 also activates the mitogen activated protein kinase (MAPK)/extracellular regulated kinase 1 and 2 (ERK1/2) (MAPK/ERK)-cascade and the phosphatidyl-inositol-3-kinase (PI3K)-cascade (Eulenfeld et al., 2012). The activation of the MAPK/ERK pathway depends on the SHP2 recruitment site pY759 within gp130 (Fukada et al., 1996). Because this motif is also involved in the inhibition of STAT signaling, it controls the balance between the MAPK/ERK and STAT activation (Eulenfeld et al., 2012). Phosphorylated SHP2 binds to growth factor receptor bound protein 2 (Grb2), therefore acting as an adapter molecule to recruit the Grb2-SOS complex to the membrane. Subsequently, SOS activates the small GTPase Ras, which constitutes the initial step of the MAPK/ERK cascade (Fukada et al., 1996). GTP-bound Ras activates Raf which phosphorylates and activates MEK1 and MEK2 dual specificity kinases, which in turn phosphorylate and activate ERK1 and ERK2 MAPKs (Shields et al., 2000). Interestingly, MAPKs can phosphorylate Grb2-associated binder 1 (Gab1) protein which recruits SHP2 and PI3K, leading to enhanced MAPK activity and accumulation of PI3K-derived phosphatidyl-inositol-3-phosphate (PIP<sub>3</sub>), thus boosting the cytokine signaling as a positive feedback loop (Eulenfeld and Schaper, 2009). PI3K is also a well-known effector of Ras (Castellano and Downward, 2011). This leads to activation of AKT serine/threonine kinases (Cox and Der, 2002). AKT may then transiently associate with and induce the activation of I $\kappa$ B kinase (IKK) and thereby activate the canonical NF- $\kappa$ B pathway (Ozes et al., 1999; Romashkova and Makarov, 1999). IKK phosphorylates NF- $\kappa$ B-bound inhibitory molecules I $\kappa$ Bs, which leads to their degradation by the 26 S proteasome, thus allowing translocation of NF- $\kappa$ B to the nucleus (Baldwin, 1996). However, this mechanism has been neither confirmed nor validated since its original discovery and therefore remains controversial (Delhase et al., 2000).

The three major IL-6-activated signaling pathways, JAK/STAT, MAPK/ERK, and PI3K/AKT, are involved in the regulation of diverse physiological functions. JAK/STAT signaling activates the expression of many important APP (Gerhartz et al., 1996) and is involved in the regulation of cell growth, differentiation, and survival in an anti-apoptotic manner (Hirano et al., 2000). The MAPK/ERK cascade preferentially regulates cell growth

and differentiation but also controls several developmental programs (Schaeffer and Weber, 1999). Its concerted action with the JAK/STAT pathway is crucial for the balance of IL-6-dependent mitogenic and anti-apoptotic signaling (Fukada et al., 1996). PI3K/AKT signaling inactivates pro-apoptotic factors, but also initiates transcription of pro-apoptotic genes and can activate the proapoptotic NF- $\kappa$ B (Hennessy et al., 2005; Madrid et al., 2001). In contrast, AKT-mediated activation of mTOR stimulates cell proliferation (Wendel et al., 2004). Additionally, PI3K/AKT signaling controls cellular energy and glucose metabolism (Hardie et al., 2003), demonstrating the diverse functionality of this pathway. This complexity is further increased via its crosstalk with the MAPK/ERK cascade.

The mechanisms of transcriptional downregulation of DMET genes are very complex, relying on many different transcription factors such as CCAAT/enhancer binding proteins (C/EBPs), hepatic nuclear factors (HNFs), and diverse NRs (Aitken et al., 2006). How these transcription factors are affected during inflammation, is still scarcely understood. Several mechanisms have been proposed to interfere either with the basal or inducible expression of DMET genes, involving the aforementioned signaling events downstream of the IL-6 receptor (**Figure 3**).

The hepatic nuclear factor 4  $\alpha$  (HNF-4 $\alpha$ ) regulates the basal transcription of numerous DMET genes, particularly P450s (Jover et al., 2009). It directly activates the transcription of its target genes by interaction with factors such as the NRs PXR, CAR, and GR, as well as PGC-1 $\alpha$  and C/EBPs (Jover et al., 2009). Thus, downregulation of HNF-4 $\alpha$  expression or activity could contribute to suppression of DMETs (Aitken et al., 2006).

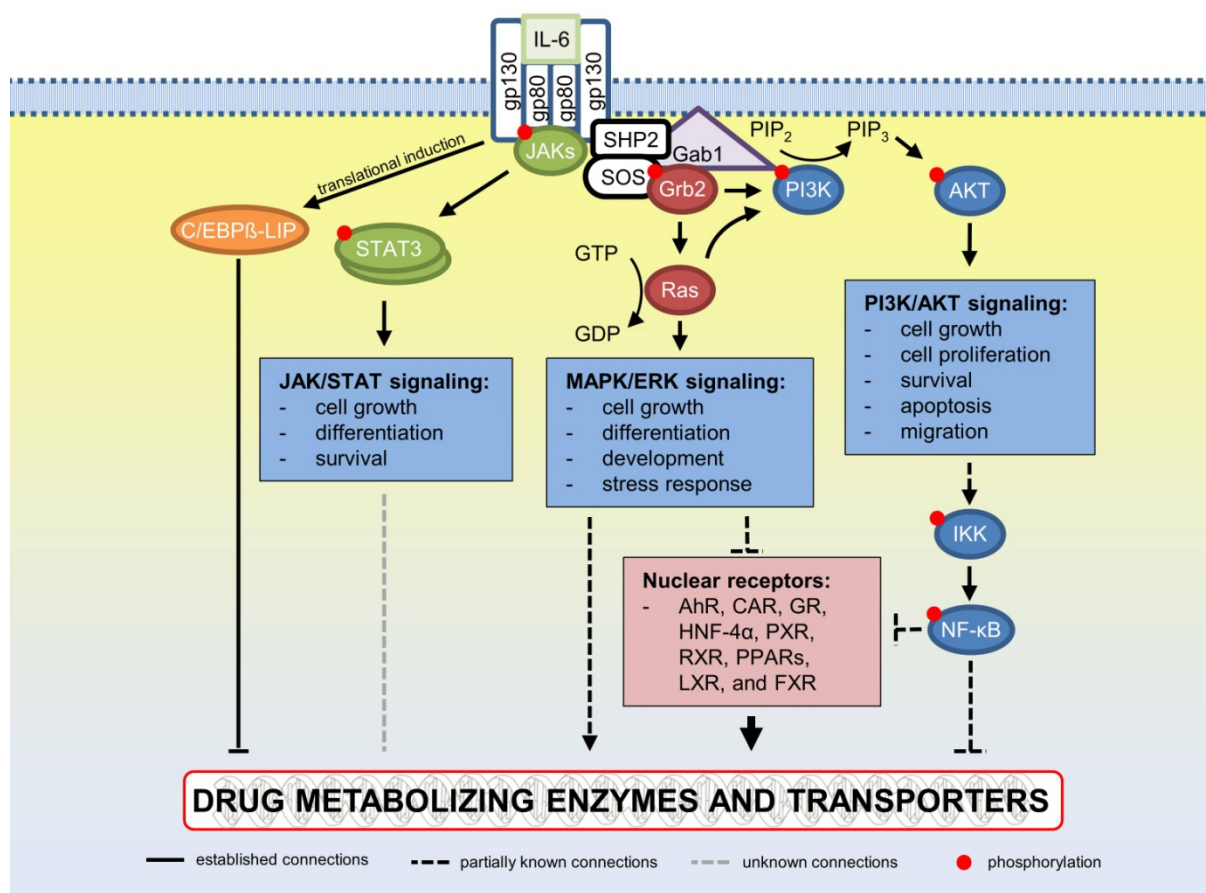


**Figure 3** Schematic of IL-6 signaling towards regulation of DMET genes. Multiple signaling cascades are activated downstream of the IL-6 receptor complex, indicated by different colors. Their predominant physiological roles are summarized in blue boxes. Arrows indicate (transcriptional) activation, whereas flat-ended arrows indicate inhibition or transcriptional repression. This figure was adapted and modified from Castellano and Downward, 2011; Eulenfeld et al., 2012; Jover et al., 2002.

The liver-enriched transcription factors C/EBPs are involved in the regulation of constitutive expression of P450s (Gonzalez and Lee, 1996). Jover and colleagues demonstrated an involvement of C/EBPβ in transcriptional repression of *CYP3A4* in response to inflammatory stimuli (Jover et al., 2002). They showed an IL-6-dependent increase in the truncated C/EBPβ-LIP (liver inhibitory protein) which antagonized transactivation of *CYP3A4* by full-length C/EBPβ-LAP (liver activating protein). A similar mechanism was shown to be involved in the transcriptional repression of *CYP2A6* (Pitarque et al., 2005). Whether this mechanism is of importance for the regulation of other P450s and DMEs remains to be investigated.

Several mechanisms for the suppression of inducible expression of DMETs have been proposed. For instance, upon inflammatory stimuli the action of the xenosensor PXR was antagonized via binding of the p65 subunit of NF- $\kappa$ B to RXR (Zhou et al., 2006). Thus, other RXR-dependent transcription factors such as CAR and PPAR can be antagonized in the same way (Zordoky and El-Kadi, 2009), potentially affecting expression of large gene batteries. Indeed, NF- $\kappa$ B appears to be very diverse in terms of its interaction capabilities. For instance, mutual repression between NF- $\kappa$ B and GR was shown to inhibit CAR expression (Pascucci et al., 2003). Moreover, the p65 subunit of NF- $\kappa$ B was shown to form an inactive complex with AhR, which is unable to translocate to the nucleus (Tian et al., 1999). Furthermore, several studies proposed a direct role of NF- $\kappa$ B in transcriptional regulation of CYPs through binding to their promoter regions, causing repression in most cases (reviewed Zordoky and El-Kadi, 2009). All these findings indicate that a broad spectrum of P450s and other DMETs are likely to be affected by the actions of NF- $\kappa$ B.

There is also increasing evidence that MAPK signaling interferes with the expression of various CYP genes by modulating the xenosensors AhR, PXR, and CAR. Apart from ERK, this involves Jun-N-terminal kinase (JNK) and p38 MAPK which exhibit extensive crosstalk with each other and non-MAPK pathways such as PKC and PI3K (Murray et al., 2010). Hence, it was shown that IL-1 $\beta$  activates JNK signaling which phosphorylates RXR, thereby suppressing transactivation of the Ntcp promoter (Li et al., 2002). More recently, similar observations were made by Ghose and colleagues, showing for the first time an increased JNK-dependent nuclear export of RXR- $\alpha$  (Ghose et al., 2004). In fact, MAPKs have been shown to translocate to the nucleus upon different stimuli (Raman et al., 2007), where similar docking motifs direct their site-specific association with NRs in order to effectively transduce the phosphorylation signal (Burgermeister et al., 2003). Moreover, this has been observed in the cytosol, as for instance, MAPK/ERK signaling impairs nuclear translocation of CAR (Koike et al., 2007). Apart from direct phosphorylation of NRs, MAPKs may also regulate recruitment or dissociation of coactivator or corepressor proteins via phosphorylation (Staudinger and Lichti, 2008). These findings indicate that MAPKs are important for the regulation of multiple proteins within NR-containing transcription complexes, thereby providing a broad-ranging mechanism for the suppression of NR-regulated genes during inflammation (Murray et al., 2010).

All this evidence indicates that transcriptional repression of DMETs may proceed through (a) liver-enriched C/EBPs independently of JAK/STAT signaling, (b) phosphorylation of NRs via the MAPK/ERK- or related MAPK-cascades, (c) or mutual repression between NF- $\kappa$ B and NRs as well as by direct binding of NF- $\kappa$ B to promoter regions (**Figure 3**). However, further research is needed to confirm the role of these pathways in the regulation of DMETs during inflammation. Particularly, studies in human models are required as findings from animal models cannot be fully translated to humans. Although many outstanding reviews in this field are available, there is a general lack in systematic studies investigating these mechanisms.

#### **1.4 *In vitro* test systems**

Although multiple clinical studies demonstrated adverse effects on drug metabolism in patients with infectious and inflammatory diseases, most functional studies in this field were conducted in mouse models. However, animal models poorly mimic the genomic response of humans, particularly during inflammatory conditions (Seok et al., 2013), demonstrating the need for more systematic analyses of these complex conditions in human *in vitro* models.

##### **1.4.1 Primary human hepatocytes**

Owing to species differences, human liver cells, such as PHH, are the model of choice for studying drug metabolism (Hewitt et al., 2001; Jemnitz et al., 2008). Liver tissue derived PHH (Ballet et al., 1984) are considered the “gold standard” for the investigation of various aspects of hepatic metabolism of drugs and other xenobiotics (Lecluyse and Alexandre, 2010). However, they are restricted in availability and have a limited life-span (Guillouzo et al., 1993). Furthermore, PHH exhibit marked interindividual functional variations, including variability in expression and corresponding activities of many genes related to drug metabolism (Morel et al., 1990; Rogue et al., 2012). Such variations are determined by the patient’s sex, age, liver diseases, pre-medication, nutritional status, or genetic background (Guillouzo et al., 1993). Hence, primary cells rather represent one individual rather than an entire population.

### 1.4.2 HepaRG cells

The HepaRG cell line was isolated from a hepatocellular carcinoma of a female patient suffering from chronic hepatitis C infection (Gripon et al., 2002). HepaRG cells are bi-potent progenitor cells and can differentiate into either biliary or hepatocyte lineages, representing the only example of complete differentiation *in vitro* (Cerec et al., 2007). Their gene expression profiles are more similar to PHH and human liver tissue than any other liver cell line, particularly among the drug processing genes (Hart et al., 2010). They demonstrate stable expression of key enzymes of the phase I (e.g., P450s) and phase II (e.g., UGTs and GSTs) drug metabolism, drug transporters (e.g., ABCs and SLCs), and NRs (e.g., CAR, PXR, and PPAR) (Andersson et al., 2012; Aninat et al., 2006; Rogue et al., 2012). In particular, major P450s were shown to be functionally expressed and selectively inhibited/induced by prototypical P450 inhibitors and inducers (Turpeinen et al., 2009). Thus, HepaRG cells are a useful *in vitro* model for drug metabolism and disposition studies and can, in many cases, replace the requirement for PHH (Andersson et al., 2012).

## 1.5 Objectives

One crucial objective of this thesis is a large-scale investigation of DMET gene expression changes in IL-6-stimulated PHH. This includes, apart from the major CYPs, genes coding for multiple phase II DMEs, drug transporters, and other important modifiers. Determination of protein expression and activity of important P450 enzymes should show whether transcriptional changes reflect changes in protein content and ultimately lead to impaired pharmacokinetics of probe drugs. Phosphoproteomic analysis should reveal the activation of signaling cascades downstream of the IL-6 receptor. The involvement of these signaling pathways in the regulation of DMET genes should be investigated by different perturbation approaches, such as pathway-specific chemical inhibition or gene-specific RNA-interference. Ultimately, this may help to better understand the underlying molecular mechanisms.

The inflammatory response and its impact on drug metabolism are poorly studied in HepaRG cells so far. Therefore, in a similar large-scale approach, expression patterns of DMET genes as well as P450 protein expression and activity in IL-6-exposed HepaRG cells should show how this model system compares to PHH. Furthermore, it should be investigated, whether the cytokines IL-1 $\beta$  and TNF- $\alpha$  are equally potent as IL-6.

Finally, a microarray study in IL-6-challenged PHH should be carried out in order to investigate inflammation-mediated changes in the drug detoxification system in an unbiased transcriptome-wide context. Microarray data from a large collection of well characterized liver samples was available for a retrospective analysis. From this collection, transcriptome-wide expression profiles obtained from livers of patients having undergone an APR should be analyzed in order to relate findings from cellular models to the *in vivo* organ level. This may help to pave the way towards a better understanding of how the liver organizes its many responsibilities.

## 2 MATERIALS

### 2.1 Chemical reagents

**Table 1** Chemical reagents.

Reagent	Supplier
[ <sup>2</sup> H <sub>3</sub> ] 4-Hydroxymephentoin	chemical synthesis (Richter et al., 2004)
[ <sup>2</sup> H <sub>3</sub> ] Hydroxybupropion hydrochloride	chemical synthesis (Richter et al., 2004)
[ <sup>2</sup> H <sub>4</sub> ] Acetaminophen	TRC, Toronto, CAN
[ <sup>2</sup> H <sub>5</sub> ] N-Desethylamodiaquin	TRC, Toronto, CAN
[ <sup>2</sup> H <sub>5</sub> ] o-/p-Hydroxyatorvastatin	TRC, Toronto, CAN
[ <sup>2</sup> H <sub>7</sub> ] 5-Hydroxypropafenone hydrochloride	Knoll, Ludwigshafen, GER
[ <sup>2</sup> H <sub>9</sub> ] Hydroxytolbutamid	TRC, Toronto, CAN
10 X TaqMan® RT Buffer	Applied, Foster City, USA
100 mM dNTP-Mix	Applied, Foster City, USA
2 X Assay Loading Reagent	Fluidigm, Amsterdam, NL
20 X GE Sample Loading Reagent	Fluidigm, Amsterdam, NL
2-Mercaptoethanol	Sigma-Aldrich, Steinheim, GER
4-Hydroxamephentoin	chemical synthesis (Richter et al., 2004)
5-Hydroxypropafenone hydrochloride	Knoll, Ludwigshafen, GER
740Y-P (PI3-Kinase activator)	Tocris, Minneapolis, USA
Acetaminophen	TRC, Toronto, CAN
Acetonitrile LC-MS	Riedel de Haen, Seelze, GER
Acrylamide/Bis (30:0.8)	Bio-Rad, Munich, GER
Ammoniumpersulfate (APS)	Merck, Darmstadt, GER
Amodiaquin	TRC, Toronto, CAN
Atorvastatin	TRC, Toronto, CAN
AZD6244 (Selumetinib)	Sellekchem, Houston, USA
Bovine serum albumine (BSA)	Sigma-Aldrich, Steinheim, GER
Bromophenolblue	Sigma-Aldrich, Steinheim, GER
Bupropion hydrochloride	chemical synthesis (Richter et al., 2004)
Chlorzoxazone	Sigma-Aldrich, Steinheim, GER
Dexamethasone (1 mM)	Sigma-Aldrich, Steinheim, GER
Dimethyl sulfoxide (DMSO)	Sigma-Aldrich, Steinheim, GER
Dulbecco's Phosphate Buffered Saline (DPBS)	GIBCO, Carlsbad, USA
Ethylenediaminetetraacetic acid (EDTA)	Sigma-Aldrich, Steinheim, GER
Fetal Bovine Serum (FBS) Gold	PAA Laboratories GmbH, Pasching, AT
Glycine	Serva, Heidelberg, GER
Hepes (1 M)	GIBCO, Carlsbad, USA
Human Insulin, INSUMAN Rapid (40 I.E.)	Sanofi, Frankfurt, GER
Hydrocortisone (50 mg/ml)	Pfizer Pharma GmbH, Karlsruhe, GER
Hydroxybupropion hydrochloride	chemical synthesis (Richter et al., 2004)
Hydroxytolbutamid	TRC, Toronto, CAN
Interleukin-1β (IL-1β)	Sigma-Aldrich, Steinheim, GER
Interleukin-6 (IL-6)	PromoCell GmbH, Heidelberg, GER
L-Glutamine (200 mM)	GIBCO, Carlsbad, USA
Lipofectamine® RNAiMax Reagent	Life Technologies, Carlsbad, USA
LY 294002 (PI3K inhibitor)	Merck, Darmstadt, GER

## MATERIALS

<b>Reagent</b>	<b>Supplier</b>
Mehtanol	Roth, Karlsruhe, GER
MEM non-essential amino acids 100 X (NEAA)	GIBCO, Carlsbad, USA
MgCl <sub>2</sub> (25 mM)	Applied, Foster City, USA
MultiScribe® Reverse Transcriptase (50 U/μl)	Applied, Foster City, USA
N-desethylamodiaquin	TRC, Toronto, CAN
NSC 74859, S3I-201 (STAT3 inhibitor)	Sellekchem, Houston, USA
Nuclease-free water	Ambion, Austin, USA
o-/p-Hydroxyatorvastatin	TRC, Toronto, CAN
Passive Lysis Buffer (5 X)	Promega, Madison, USA
Penicillin/Streptomycin (10,000 U/ml, 10 mg/ml)	GIBCO, Carlsbad, USA
Phenacetin	Sigma-Aldrich, Steinheim, GER
Ponceau S-solution	Sigma-Aldrich, Steinheim, GER
Potassium chloride (KCl)	Merck, Darmstadt, GER
Propafenone	Knoll, Ludwigshafen, GER
Random Hexamers	Applied, Foster City, USA
RNase Inhibitor (20 U/μl)	Applied, Foster City, USA
SC-514 (IKK-2 inhibitor)	Merck, Darmstadt, GER
Skim milk powder	Sigma-Aldrich, Steinheim, GER
S-Mephentoin	TRC, Toronto, CAN
Sodium chloride	Merck, Darmstadt, GER
Sodium dodecyl sulfate (SDS)	Sigma-Aldrich, Steinheim, GER
Sodium Pyruvate (100 mM)	GIBCO, Carlsbad, USA
Stattic (STAT3 inhibitor)	Sigma-Aldrich, Steinheim, GER
TaqMan® Universal PCR Master Mix (2 X)	Applied, Foster City, USA
TEMED	GIBCO, Carlsbad, USA
Tolbutamid	TRC, Toronto, CAN
Tris base	Roth, Karlsruhe, GER
Triton X-100	Sigma-Aldrich, Steinheim, GER
Trypsin 0.25%	GIBCO, Carlsbad, USA
Tumor necrosis factor-alpha (TNF-α)	Sigma-Aldrich, Steinheim, GER
Tween 20	Merck, Darmstadt, GER
U0126 (MEK1/2 inhibitor)	Promega, Madison, USA
William's E Medium (w/o L-Glutamine and Phenol Red)	GIBCO, Carlsbad, USA

## 2.2 Buffers and solutions

**Table 2** Buffers and solutions.

Buffer or solution	Component	Weight or volume
APS (10%)	Ammoniumpersulfate	1 g
	H <sub>2</sub> O <sub>millipore</sub>	ad 10 ml
Blotting buffer (Western blot)	Tris base	29 g
	Glycine	14.6 g
	SDS (20%)	9.25 ml
	Methanol	1000 ml
	H <sub>2</sub> O <sub>millipore</sub>	ad 5000 ml
DNA suspension buffer (T10E0.1)	Tris base	10 mM
	EDTA	0.1 mM
	pH 8.0	
Electrophoresis buffer (10 X)	Tris base	150 g
	Glycine	720 g
	SDS (20%)	250 ml
	H <sub>2</sub> O <sub>millipore</sub>	ad 5000 ml
Laemmli sample buffer (5 X)	SDS	10 g
	Tris-Cl pH 6.8 (1 M)	30.6 ml
	2-Mercaptoethanol	25 ml
	Bromophenolblue	
	H <sub>2</sub> O <sub>millipore</sub>	ad 75 ml
	Glycerin	25 ml
SDS (20%)	SDS	100 g
	H <sub>2</sub> O <sub>millipore</sub>	ad 500 ml
Skim milk (5%)	TBST (1 X)	100 ml
	skim milk	5 g
TBS (10 X)	Tris base	150 g
	NaCl	400 g
	KCl	10 g
	H <sub>2</sub> O <sub>millipore</sub>	ad 5000 ml
	pH adjusted to 7.4 by HCl	
TBST (1 X)	TBS (10 X)	500 ml
	H <sub>2</sub> O <sub>millipore</sub>	4500 ml
	Tween 20 (50%)	10 ml
Tris-HCL (0.5 M), pH 6.8	Tris base	30 g
	H <sub>2</sub> O <sub>millipore</sub>	ad 500 ml
	pH adjusted to 6.8 by HCl	
Tris-HCL (1.5 M), pH 8.8	Tris base	90.75 g
	H <sub>2</sub> O <sub>millipore</sub>	ad 500 ml
	pH adjusted to 8.8 by HCl	

## 2.3 Kits

**Table 3** Research kits.

<b>Kit</b>	<b>Supplier</b>
GeneChip® Eukaryotic Poly-A RNA Control Kit	Affymetrix, Santa Clara, USA
GeneChip® HuGene 2.0ST Array	Affymetrix, Santa Clara, USA
GeneChip® Hybridization, Wash & Stain Kit	Affymetrix, Santa Clara, USA
GeneChip® WT Terminal Expression, 3'-Amplification Reagent and Hybridization Controls	Affymetrix, Santa Clara, USA
GeneChip® WT Terminal Labeling	Affymetrix, Santa Clara, USA
Pierce™ BCA Protein Assay Kit	Thermo Scientific, Waltham, USA
QIASHredder™	Qiagen, Hilden, GER
RNA 6000 Nano Kit	Agilent Technologies, Waldbronn, GER
RNeasy Mini Kit	Qiagen, Hilden, GER
Rnase-Free Dnase Set	Qiagen, Hilden, GER
TaqMan® PreAmp Master Mix	Applied, Foster City, USA
TaqMan® Reverse Transcription Reagents	Applied, Foster City, USA
WT Expression Kit for Affymetrix® Whole Transcript Expression Arrays	Ambion, Austin, USA

## 2.4 Equipment

**Table 4** Devices and equipment.

<b>Device</b>	<b>Supplier</b>
2100 Bioanalyzer	Agilent Technologies, Waldbronn, GER
6460 triple quadrupole mass spectrometer	Agilent Technologies, Waldbronn, GER
Biofuge 22R/ Biofuge pico	Heraeus, Hanau, GER
Biomark® HD Reader	Fluidigm, Amsterdam, NL
Centrifuge 5424 R	Eppendorf, Hamburg, GER
EnSpire® Multimode Plate Reader	PerkinElmer, Waltham, USA
Fastblot B44	Biometra, Goettingen, GER
GeneChip® Fluidics Station 450	Affymetrix, Santa Clara, USA
GeneChip® Hybridation Oven 645	Affymetrix, Santa Clara, USA
GeneChip® Scanner 7G	Affymetrix, Santa Clara, USA
HERA cell 240	Heraeus, Hanau, GER
IFC Controller HX	Fluidigm, Amsterdam, NL
Millipore Water Purification System Milli Q	Millipore, Molsheim, FR
Mini-PROTEAN® Tetra Cell	Bio-Rad Laboratories GmbH, Munich, GER
ODYSSEY Infrared Imaging System	LI-COR Biosciences GmbH, Bad Homburg, GER
Olympus CKX 41	Olympus, Tokyo, JP
Power PAC 1000	Bio-Rad Laboratories GmbH, Munich, GER
Reaxtop Vortexer	Heidolph, Schwabach, GER
Thermocycler PTC-200	MJ Research, Waltham, USA
ThermoMixer Comfort	Eppendorf, Hamburg, GER
Universal 32 Centrifuge	Hettich Zentrifugen, Tuttlingen, GER
Universal 320 R Centrifuge	Hettich Zentrifugen, Tuttlingen, GER

## MATERIALS

<b>Device</b>	<b>Supplier</b>
Veriti 384-Well Thermal Cycler	Applied, Foster City, USA
Veriti 96-Well Thermal Cycler	Applied, Foster City, USA
Vibramax 100 Shaker	Heidolph, Schwabach, GER
Victor 1420 Multilabel Counter	Wallac / PerkinElmer, Waltham, USA

### 2.5 Consumables

**Table 5** Consumables.

<b>Material</b>	<b>Supplier</b>
384-Well PCR Plate Standard	Thermo Scientific, Waltham , USA
48.48 Dynamic Array™ IFC	Fluidigm, Amsterdam, NL
96-Well Polystyrol Microplate, transparent	Greiner Bio-One GmbH, Frickenhausen, GER
96.96 Dynamic Array™ IFC	Fluidigm, Amsterdam, NL
96-well PCR plate, non-skirted, clear	4titude Ltd, Berlin, GER
Tissue Culture Flask T-25 Vent Cap Red	Sarstedt Inc., Newton, USA
Tissue Culture Flask T-75 Vent Cap Red	Sarstedt Inc., Newton, USA
Nitrocellulose Membrane	NeoLab GmbH. Heidelberg, GER
Collagen I Cellware 12-Well Plate	Becton Dickinson, Bedford, USA
96-Well Cell Culture Plate	Greiner Bio-One GmbH, Frickenhausen, GER
Tube 15 ml	Sarstedt, Nuembrecht, GER
Tube 50 ml	Sarstedt, Nuembrecht, GER
C-Chip Neubauer improved hemocytometer	peqlab, Erlangen, GER
Safe-Lock Tubes 1.5 ml	Eppendorf, Hamburg, GER
Safe-Lock Tubes 2 ml	Eppendorf, Hamburg, GER
Safe-Lock Tubes 0.5 ml	Eppendorf, Hamburg, GER
MULTIWELL™ 24 well	Becton Dickinson, Bedford, USA

2.6 TaqMan® assays

**Table 6** TaqMan® assays used with the BioMark HD system (Fluidigm).

<b>Gene symbol</b>	<b>Cat.-number</b>	<b>Gene symbol</b>	<b>Cat.-number</b>
<i>ABCB1</i>	Hs01067802_m1	<i>HNF1A</i>	Hs00167041_m1
<i>ABCC2</i>	Hs00166123_m1	<i>HNF4A</i>	Hs01023298_m1
<i>ABCG2</i>	Hs00184979_m1	<i>INSIG1</i>	Hs01650977_g1
<i>ACOX1</i>	Hs01074241_m1	<i>INSIG2</i>	Hs00379223_m1
<i>ADH1A</i>	Hs00605167_g1	<i>JUN</i>	Hs00277190_s1
<i>AHR</i>	Hs00169233_m1	<i>NAT1</i>	Hs00265080_s1
<i>ALAS1</i>	Hs00167441_m1	<i>NAT2</i>	Hs00605099_m1
<i>ALDH2</i>	Hs00355914_m1	<i>NCOA1</i>	Hs00186661_m1
<i>ARNT</i>	Hs01121918_m1	<i>NCOA2</i>	Hs06197990_m1
<i>CCL2</i>	Hs00234140_m1	<i>NCOA3</i>	Hs01105248_m1
<i>CEBPA</i>	Hs00269971_s1	<i>NFKB1</i>	Hs00765730_m1
<i>CEBPB</i>	Hs00153133_m1	<i>NFKBIA</i>	Hs00153284_m1
<i>CEBPD</i>	Hs00270931_s1	<i>NR0B2</i>	Hs00222677_m1
<i>CPT1A</i>	Hs00912671_m1	<i>NR1H3</i>	Hs00172885_m1
<i>CREBBP</i>	Hs00231733_m1	<i>NR1H4</i>	Hs00231968_m1
<i>CRP</i>	Hs00265044_m1	<i>NR1I2</i>	Hs00243666_m1
<i>CYP1A1</i>	Hs00153120_m1	<i>NR1I3</i>	Hs00901571_m1
<i>CYP1A2</i>	Hs01070374_m1	<i>NR2F1</i>	Hs00818842_m1
<i>CYP2A6</i>	Hs00868409_s1	<i>NR2F2</i>	Hs01047078_m1
<i>CYP2B6</i>	Hs03044634_m1	<i>NR3C1</i>	Hs00230818_m1
<i>CYP2C19</i>	Hs00426380_m1	<i>PCK1</i>	Hs00159918_m1
<i>CYP2C8</i>	Hs00258314_m1	<i>PDK4</i>	Hs01037712_m1
<i>CYP2C9</i>	Hs00426397_m1	<i>POR</i>	Hs00287016_m1
<i>CYP2D6</i>	Hs00164385_m1	<i>PPARA</i>	Hs00231882_m1
<i>CYP2E1</i>	Hs00559367_m1	<i>PPARG</i>	Hs01115513_m1
<i>CYP3A4</i>	Hs00430021_m1	<i>RXRA</i>	Hs00172565_m1
<i>CYP3A5</i>	Hs01070905_m1	<i>SAAI/SAA2</i>	Hs00761949_s1
<i>CYP3A7</i>	Hs00426361_m1	<i>SCD</i>	Hs01682761_m1
<i>CYP7A1</i>	Hs00167982_m1	<i>SLC10A1</i>	Hs00161820_m1
<i>DPYD</i>	Hs00559279_m1	<i>SLC22A7</i>	Hs00198527_m1
<i>ELK1</i>	Hs00901847_m1	<i>SLCO1B1</i>	Hs00272374_m1
<i>FABP1</i>	Hs00155026_m1	<i>SOCS3</i>	Hs02330328_s1
<i>FDFT1</i>	Hs00926054_m1	<i>SOD2</i>	Hs00167309_m1
<i>FOS</i>	Hs00170630_m1	<i>SREBF1</i>	Hs00231674_m1
<i>FOXO1</i>	Hs00231106_m1	<i>SREBF2</i>	Hs00190237_m1
<i>G6PC</i>	Hs00609178_m1	<i>STAT3</i>	Hs00374280_m1
<i>GAPDH</i>	Hs99999905_m1	<i>SULT1A1</i>	Hs00738644_m1
<i>GSTA2</i>	Hs00747232_m1	<i>SULT1B1</i>	Hs00234899_m1
<i>GSTM1</i>	Hs01683722_gH	<i>TNFA</i>	Hs00174128_m1
<i>GSTP1</i>	Hs00168310_m1	<i>TPMT</i>	Hs00909011_m1
<i>HK2</i>	Hs00606086_m1	<i>UGT1A1</i>	Hs02511055_s1
<i>HMGCR</i>	Hs00168352_m1	<i>UGT2B7</i>	Hs00426591_m1
<i>HMGCS2</i>	Hs00985427_m1	<i>VDR</i>	Hs01045840_m1
<i>HMOX1</i>	Hs00157965_m1	<i>VEGFA</i>	Hs00900055_m1

All assays were purchased from Life Technologies, Carlsbad, USA

## 2.7 Antibodies

**Table 7** Antibodies for immunoblotting and their applied dilution in 1% skim milk-TBST.

Immunogen	Mol. weight	Host	Cat. #	Supplier	Dilution	Sec. ab. <sup>a</sup>
AKT pS473	60 kDa	rabbit	9271	CST	1:1,000	IRDye800
CYP1A2	58 kDa	mouse	-	custom	1:2,000	IRDye800
CYP2C8	56 kDa	rabbit	#Hu-A004	Puracyp	1:1,000	IRDye680
CYP2C9	56 kDa	rabbit	RDI-Cyp2C9abr	RDI	1:1,000	IRDye800
CYP3A4	57 kDa	rabbit	458234	BDGentest	1:1,000	IRDye680
ERK1/2-p Thr202/ Tyr204	42/44 kDa	rabbit	9101	CST	1:1,000	IRDye800
RXR- $\alpha$	52 kDa	mouse	PP-K8508-00	R&D	1:1,000	IRDye800
STAT1ph Tyr701	84/91 kDa	rabbit	9171	CST	1:1,000	IRDye800
STAT3ph Tyr705	79/86 kDa	rabbit	9145	CST	1:2,000	IRDye800
$\beta$ -Actin	42 kDa	mouse	A5441	Sigma- Aldrich	1:5,000	IRDye680/ 800

<sup>a</sup> dilution: 1:10,000

## 2.8 Primary cells and cell lines

### 2.8.1 Primary human hepatocytes

The use of PHH for research was approved by the local ethics committees of Berlin, Munich, Tuebingen, and Regensburg, and written informed consent was obtained from all patients. Hepatocytes were obtained from liver resection surgery and isolated as described elsewhere (Lee et al., 2013). Cells were delivered in an ice cold suspension.

### 2.8.2 HepaRG cells

HepaRG cells were obtained from a liver tumor of a female patient suffering from hepatocarcinoma. Frozen stocks of this cell line were purchased from Biopredic International and cultivated as described previously (Gripon et al., 2002). A working bank was created, strictly following the instructions.

### 2.8.3 Cell culture media

**Table 8** Composition of cell culture media.

Medium	Component	Volume
HepaRG differentiation medium (1%)	HepaRG growth medium	49.5 ml
	DMSO	0.5 ml
HepaRG differentiation medium (2%)	HepaRG growth medium	49 ml
	DMSO	1 ml
HepaRG growth medium	William's E Medium	500 ml
	FBS gold	50 ml
	L-Glutamine (200 mM)	5.6 ml
	Pen/Strep (10,000 U/ml)	5.6 ml
	Human Insulin (40 I.E.)	2 ml
	Hydrocortisone (50 mg/ml)	200 $\mu$ l
Hepatocyte cultivation medium	William's E Medium	450 ml
	FBS gold	50 ml
	Pen/Strep (10,000 U/ml)	5 ml
	L-Glutamine (200 mM)	5 ml
	Human Insulin (40 I.E.)	400 $\mu$ l
	DMSO	450 $\mu$ l
Hepatocyte full medium	Dexamethasone (1 mM)	50 $\mu$ l
	William's E Medium	450 ml
	FBS gold	50 ml
	Pen/Strep (10,000 U/ml)	5 ml
	L-Glutamine (200 mM)	5 ml
	Human Insulin (40 I.E.)	400 $\mu$ l
	Sodium Pyruvate (100 mM)	5 ml
	NEAA 100 X	5 ml
Hepes (1 M)	7.5 ml	
Hepatocyte starvation medium	Hydrocortisone (50 mg/ml)	8 $\mu$ l
	William's E Medium	500 ml
	Pen/Strep (10,000 U/ml)	5 ml
	L-Glutamine (200 mM)	5 ml

### 2.9 Liver samples

This study was approved by the ethics committees of the medical faculties of the Charité, Humboldt University, and of the University of Tuebingen and conducted in accordance with the Declaration of Helsinki. Written informed consent was obtained from each patient. Liver tissues and corresponding blood samples were previously collected from 150 patients of Caucasian ethnicity (71 males and 79 females) undergoing liver surgery at the Campus Virchow (University Medical Center Charité, Humboldt University, Berlin, Germany). The average age of the subjects was  $58 \pm 14$  years. All tissue samples were examined by a

pathologist and only histologically non-tumorous tissues were used and frozen at -80 °C. For each patient, detailed documentation of clinical parameters was available concerning age, sex, smoking habits, alcohol consumption, pre-surgical medication, pre-surgical liver serum parameters including CRP, as well as indication for liver resection, as previously described in detail (Klein et al., 2010; Nies et al., 2009). Patients who suffered from hepatitis, cirrhosis, or alcohol abuse were excluded.

## 2.10 Software and online tools

**Table 9** Software and online tools used for analyses.

<b>Software and online tools</b>	<b>Company or website</b>
Affymetrix Expression Console (Build 1.3.1.187)	Affymetrix, Santa Clara, USA
Analyst 8.0 software solution	Genedata, Basel, CH
CellDesigner 4.1	<a href="http://www.celldesigner.org/">http://www.celldesigner.org/</a>
DAVID Bioinformatics Database	<a href="http://david.abcc.ncifcrf.gov/">http://david.abcc.ncifcrf.gov/</a>
Enrichr	<a href="http://amp.pharm.mssm.edu/Enrichr/">http://amp.pharm.mssm.edu/Enrichr/</a>
Fluidigm Real-Time PCR Analysis	Fluidigm, Amsterdam, The Netherlands
GraphPad Prism 5.04	GraphPad Software, Inc., La Jolla, USA
Office 2010	Microsoft, Redmond, USA
REVIGO (Reduce + Visualize Gene Ontology)	<a href="http://revigo.irb.hr/">http://revigo.irb.hr/</a>
ODYSSEY Application Software 3.0 (3.0.30)	LI-COR Biosciences GmbH, Bad Homburg, GER
cell^F 3.2 (Build 1700)	Olympus, Tokyo, JP

### **3 METHODS**

#### **3.1 Cell culture**

##### **3.1.1 Cultivation of cells**

###### **3.1.1.1 Primary human hepatocytes**

PHH were received as cell suspension on ice. The cell suspension was washed twice in ice cold DPBS, centrifuged for 5 min at 80 x g and 4 °C. The cell pellet was resuspended in Hepatocyte full medium and cell number and viability were determined via trypan blue exclusion technique using the C-Chip Neubauer disposable hemocytometer.  $0.4 \times 10^6$  cells were plated on Collagen I Cellware 12-Well Plates (pre-coated with collagen) and cultivated at 37 °C (5% CO<sub>2</sub>) for 24 h. Subsequently, the medium was replaced by either Hepatocyte starvation medium or Hepatocyte cultivation medium and cells were incubated for another 24 h. For inflammatory gene expression and inhibition experiments (up to 24 h), cells were cultivated in Hepatocyte starvation medium, for long-term protein and P450 activity experiments (> 24 h) in Hepatocyte cultivation medium.

###### **3.1.1.2 HepaRG cells**

One cell vial (1.5 million cells) was thawed and cells transferred to HepaRG growth medium, and cultivated in 25 cm<sup>2</sup> (T-25) tissue culture flasks for two weeks. The medium was renewed every two or three days. Cells were passaged and transferred to MULTIWELL 24-well plates (50.000 cells per well) and cultivated for two more weeks. Growth medium was replaced by HepaRG differentiation medium (1%) for two days to adapt the cells to DMSO. Starting from the third day, cells were cultivated in HepaRG differentiation medium (2%) for another 12 days. At that stage, HepaRG cells reached a differentiated hepatocyte-like morphology and showed liver-specific functions. The cells were further maintained in HepaRG differentiation medium (2%) for the duration of the experiments.

### 3.1.2 Cytokine stimulation

For activation of the APR, PHH were treated with 10 ng/ml IL-6. This concentration was previously shown to sufficiently activate STAT3 as well as strongly induce *CRP* mRNA expression in cell model systems without being toxic (Campbell et al., 2001; Vee et al., 2009). For treatment, medium was aspirated and replaced by fresh Hepatocyte starvation or cultivation medium containing 10 ng/ml IL-6 in PBS (0.1% BSA) or vehicle only (PBS and 0.1% BSA). In chemical inhibition experiments, concentrated IL-6 was added to the medium to achieve a final concentration of 10 ng/ml.

In addition to IL-6 (10 ng/ml), HepaRG cells were treated with IL-1 $\beta$  (5 ng/ml) or tumor TNF- $\alpha$  (10 ng/ml). IL-1 $\beta$ , for example, showed the strongest suppressive capacity towards a member of the cytochrome P450 superfamily (*CYP2C11*) in rat hepatocytes in a concentration of 5 ng/ml (Chen et al., 1995). TNF- $\alpha$  was used in a concentration as suggested by the supplier (Sigma-Aldrich, Steinheim, Germany). For treatment, medium was aspirated and replaced by fresh HepaRG differentiation medium (2%) containing 5 ng/ml IL-1 $\beta$ , 10 ng/ml IL-6, or 10 ng/ml TNF- $\alpha$  in PBS (0.1% BSA) or vehicle only (PBS and 0.1% BSA).

Generally, for gene expression analysis cells were lysed and total RNA isolated (see 3.2.1) after 8 or 24 h. For long-term experiments (protein and activity), treatment was repeated every 24 h.

### 3.1.3 Chemical activation of signaling pathways

Chemical activation of PI3K was performed in PHH using a cell-permeable phosphopeptide activator 740Y-P (TOCRIS, Minneapolis, USA) with high affinity to the p85 subunit of the enzyme. 740Y-P stock solution (20 mM) was prepared in PBS. 740Y-P was previously applied in concentrations between approximately 10 and 20  $\mu$ M (Williams and Doherty, 1999). Here, a preliminary test in PHH showed that a concentration of 10  $\mu$ M is sufficient for causing a strong response in target gene expression (data not shown). Therefore, 740Y-P was applied in a concentration of 10  $\mu$ M in order to activate PI3K. For this purpose, medium was aspirated and replaced by fresh medium containing 740Y-P in the final concentration. PBS-treated cells served as control. Cells were lysed and total RNA isolated (see 3.2.1) after 24 h.

### 3.1.4 Chemical inhibition of signaling pathways

Three specific chemical inhibitors were applied, targeting three major signaling proteins: LY294002 for PI3K (upstream of AKT), U0126 for MEK1/2 (upstream of ERK1/2), and Stattic for STAT3. LY294002 was shown to be a potent inhibitor of PI3K in hepatocytes, where concentrations of  $> 20 \mu\text{M}$  inhibited the enzyme's activity by more than 90% (Blommaert et al., 1997). U0126 is a selective inhibitor for MEK-1 and -2 (Favata et al., 1998). It was shown to effectively inhibit wild-type MEK1 phosphorylation of ERK2 in concentrations between 20 and 100  $\mu\text{M}$  in *in vitro* experiments (Goueli et al., 1998). Stattic is a selective inhibitor of the activation, dimerization, and nuclear translocation of STAT3. It was previously shown to inhibit STAT3 *in vitro* with an  $\text{IC}_{50}$  value after one hour of incubation of  $5.1 \pm 0.8 \mu\text{M}$  (Schust et al., 2006). Here, chemical inhibition experiments were conducted in PHH. Inhibitor stock solutions (20 mM each) were prepared in DMSO. For inhibition, medium was aspirated and replaced by fresh medium containing one or a combination of chemical inhibitors in the final concentrations 1  $\mu\text{M}$ , 5  $\mu\text{M}$ , or 10  $\mu\text{M}$  (Stattic), and 20  $\mu\text{M}$  or 50  $\mu\text{M}$  (LY294002 and U0126). DMSO-treated cells served as control. After incubation for 1 h, cells were treated with IL-6 or vehicle as described above. Cells were lysed and total RNA isolated (see 3.2.1) after 24 h.

### 3.1.5 siRNA-mediated knock-down

KD of RXR- $\alpha$  via Silencer® Select Pre-designed siRNA (P/N4392420, #s12384; sense: UCGUCCUCUUUAACCCUGAtt, antisense: UCAGGGUUAAGAGGACGAtg; Applied Biosystems, Foster City, USA) was carried out in PHH, cultivated in Hepatocyte cultivation medium. The transfection mix was prepared as shown in **Table 10**. After incubation at RT for 20 min, the mix was added to one well (12-well plate), giving a total volume of 1.2 ml. Cells were then cultivated for 24 h at 37 °C until media was replaced by fresh Hepatocyte cultivation medium. After incubation for another 24 h at 37 °C, cells were treated with IL-6 or vehicle as described above (3.1.2).

**Table 10** Transfection mix.

Component	1 reaction ( $\mu\text{l}$ )
William's E Medium	195.8
Lipofectamine® RNAiMax Reagent	3
siRNA (20 $\mu\text{M}$ )	1.2 (24 pmol)
Total	200

## 3.2 Quantitative methods

### 3.2.1 RNA isolation and quantification

Total RNA was isolated from PHH using RNeasy Mini Kit including on column genomic DNA digestion with RNase free DNase Set, according to the manufacturer's instructions. In short, medium was aspirated and 350  $\mu$ l of RLT lysis buffer (+ 1% 2-mercaptoethanol) was added. Cells were harvested by rigorously scraping with a pipet tip and transferred to QIAshredder columns. After centrifugation for 2 min at 10.000 rpm in an Eppendorf table-top centrifuge the homogenized cell lysate was mixed with 1 volume of 70% ethanol. After on-column DNase digest for 15 min and several washing steps, total RNA was eluted with 30  $\mu$ l RNase-free water. The total isolated RNA was stored at -80 °C until further use. The RNA integrity and quantity was analyzed at the Agilent 2100 Bioanalyzer using the RNA 6000 Nano Kit, following the manufacturer's instructions. Only high quality samples with an integrity assignment > 7 were used for further experiments.

### 3.2.2 cDNA synthesis by reverse transcription

500 ng of total RNA were reverse transcribed to cDNA with TaqMan® Multiscribe Reverse Transcription Kit. One 50  $\mu$ l reaction contained 19.25  $\mu$ l of RNase-free water with 500 ng total RNA and 30.75  $\mu$ l reaction master mix (**Table 11**). The total reaction mixture was incubated in a Veriti 96-Well Thermal Cycler for 10 min at 25 °C, 30 min at 48 °C, and 5 min at 95 °C. Samples were stored at -20 °C until further use.

**Table 11** Components in the reverse transcription master mix.

Component	Final concentration	1 reaction ( $\mu$ l)
10 x TaqMan® RT buffer	1 x	5
MgCl <sub>2</sub> (25 mM)	5.5 mM	11
dNTP-Mix	500 $\mu$ M each	10
Random Hexamers	2.5 $\mu$ M	2.5
RNase inhibitor	0.4 U/ $\mu$ l	1
Multiscribe RT (50 U/ $\mu$ l)	1.25 U/ $\mu$ l	1.25
Total		30.75

### 3.2.3 Real-time PCR with the BioMark HD System

The BioMark HD system by Fluidigm is a high-throughput platform based on integrated fluidic circuits (IFCs) that allows for microarray-like gene expression studies by qPCR using commercially available TaqMan® gene expression assays (Spurgeon et al., 2008). Here we used 96.96 Dynamic Array IFCs to measure the mRNA expression of more than 80 selected genes (**Table 6**) simultaneously in up to 48 samples as duplicates.

#### 3.2.3.1 Specific target amplification

The specific target amplification (STA) was performed to increase target concentrations. Equal volumes of 20 X TaqMan® gene expression assays were combined up to a total of 100 assays. TaqMan® assays used in this study are listed in **Table 6**. The combined assays were diluted using DNA suspension buffer to a final concentration of 0.2 X. The STA reaction was prepared as shown in **Table 12** and the following thermal protocol was used: 95°C for 10 min, 95°C for 15 sec, 60°C for 4 min, 14 cycles. After cycling the reaction was diluted 1:5 by adding 20 µl DNA suspension buffer to the 5 µl STA volume. Samples were stored at -20°C until further use.

**Table 12** STA components.

Component	1 reaction (µl)
TaqMan® PreAmp Master Mix (2 X)	2.5
Pooled assay mix (0.2 X)	1.25
cDNA	1.25
Total	5

#### 3.2.3.2 qPCR using the BioMark HD System

10 X TaqMan® assays were prepared in 96-well PCR plates using the components described in **Table 13**. The sample pre-mix was prepared in 96-well PCR plates using the components described in **Table 14**.

**Table 13** 10 X assay mix components.

Components	1 reaction (µl)	1 reaction with overage (µl)
20 X TaqMan® gene expression assay	2.5	3.5
2 X Assay Loading Reagent	2.5	3.5
Total	5	7

**Table 14** Sample pre-mix components.

Components	1 reaction (µl)	1 reaction with overage (µl)
TaqMan® Universal PCR Master Mix (2 X)	2.5	3
20 X GE Sample Loading Reagent	0.25	0.3
cDNA (preamplified and diluted)	2.25	2.7
Total	5	6

The assay mix and sample pre-mix were vortexed thoroughly for 30 sec and centrifuged for 30 sec. Control line fluid was injected into the Dynamic Array IFC, which was subsequently primed in the IFC Controller HX. After priming, 5 µl of each assay and 5 µl of each sample were transferred into the respective inlets on the chip. The IFC Controller HX was used again to load the samples and assays into the chip. After loading, the chip was transferred to the Biomark HD Reader (thermal cycler) using the 96.96 specific protocol (GE 96x96 Standard v1): initial thermal mix step at 50 °C for 2 min, 70 °C for 30 min, and 25 °C for 10 min; 50 °C for 2 min; hot start at 95 °C for 10 min; PCR cycle 40 X denaturation at 95 °C for 15 sec and annealing at 60 °C for 1 min.

### 3.2.3.3 $\Delta\Delta\text{Ct}$ method for analysis of qPCR data

The delta delta Ct ( $\Delta\Delta\text{Ct}$ ) method is a convenient way to analyze the relative gene expression changes in real-time qPCR data (Livak and Schmittgen, 2001). Real-time qPCR results are usually expressed as cycle thresholds (Ct). Here, the thresholds were determined automatically for each detector (TaqMan® probe) by the Fluidigm Real-Time PCR Analysis Software. Delta Ct ( $\Delta\text{Ct}$ ) values were calculated by subtracting the mean Ct of the housekeeping gene (HKG) *GAPDH* from the mean Ct of the gene of interest. *GAPDH* was determined as the most stably expressed gene among a selection of HKGs (*ACTB*, *GUSB*, *HMBS*, *POLR2A*, *RPLP0*, *TBP*) by using the Normfinder Excel add-in as described by Andersen and colleagues (Andersen et al., 2004).  $\Delta\Delta\text{Ct}$  values were calculated by subtracting the  $\Delta\text{Ct}$  value of the calibrator sample (e.g., PBS, 0.1% BSA-treated) from the  $\Delta\text{Ct}$  of the experimental sample (e.g., IL-6-treated). As the Ct is on a log scale, base 2, linear fold changes (FCs) were calculated by the formula  $2^{(-\Delta\Delta\text{Ct})}$ .

### 3.2.3.4 Statistical analysis

For demonstration of gene expression changes, the mean of the FCs that were obtained from the  $\Delta\Delta\text{CT}$  method and their standard deviations are shown in bar graphs. Due to the considerably skewed symmetry of up- and downregulation in the linear fold change, all statistical analyses were carried out using the  $\Delta\text{Ct}$  values only. To determine the significance of gene expression changes, a paired t-test with pooled standard deviations and Bonferroni post-hoc-test for multiple comparisons was carried out using the GraphPad Prism 5.04 software.

### 3.2.4 Quantification of total protein content

Protein was isolated using the 5 x Passive Lysis Buffer (PLB), following the manufacturer's instruction. In short, medium was aspirated and washed with DPBS. Per well (12- or 24-well plate), 100  $\mu\text{l}$  of 1 x PLB were added and cells were harvested immediately by scraping vigorously with a pipet tip. The lysate was subjected to two freeze-thaw cycles and cleared by centrifugation for 30 sec at 4 °C. Total protein content was determined with the BCA Protein Assay Kit, according to the instructions. For each measurement, a standard curve had to be prepared. For this purpose, BSA was diluted in PBS (pH 7.2) to final concentrations of 1 mg/ml, 0.75 mg/ml, 0.6 mg/ml, 0.5 mg/ml, 0.3 mg/ml, 0.25 mg/ml, and 0.125 mg/ml. Standard curve and samples were then pipetted into a 96-well Polystyrole microplate with a sample to working reagent (WR) ratio of 1:10 (10  $\mu\text{l}$  sample and 90  $\mu\text{l}$  WR). The plate was incubated for 30 min at 37 °C and the absorbance measured at 570 nm with the Enspire Multimode Plate Reader.

### 3.2.5 Quantification of proteins by SDS-PAGE and immunoblotting

Relative protein quantification was performed by Western blot analysis. For this purpose, proteins were separated with sodium dodecyl sulfate (SDS) polyacrylamide gel electrophoresis (PAGE). **Table 15** shows all the components for the running and stacking gel solutions of a 10% polyacrylamide gel (approx. 5 X 8 cm in size).

**Table 15** SDS-PAGE running gel and stacking gel components.

Component	Running gel (10%)	Stacking gel (10%)
H <sub>2</sub> O <sub>millipore</sub>	4.98 ml	6.1 ml
1.5 M Tris-HCl, pH8.8	3.11 ml	-
0.5 M Tris-HCl, pH6.8	-	2.5 ml
Acrylamide/Bis (30:0.8)	4.15 ml	1.35 ml
10% SDS	125 µl	100 µl
TEMED	12.5 µl	10 µl
10% APS	125 µl	100 µl

Prior to loading, samples were mixed with 5 x Laemmli sample buffer and heated for 5 mins at 95 °C. Gels were run in a Mini-PROTEAN electrophoreses chamber at initial 80 V until samples entered the running gel, then at 100 V for 1 – 1.5 h.

Proteins were transferred by semidry-blotting onto a nitrocellulose membrane (2 mA/cm<sup>2</sup>, 15min), using a Fastblot 44 chamber. Membranes were blocked with 5% skim milk in TBST (1 X) for 1 h at room temperature. Primary antibodies were diluted in 1% skim milk-TBST as described in **Table 7**, and blots were incubated for 1 h at room temperature or overnight at 4 °C on a rocking platform. Membranes were washed three times in TBST and incubated under protection from light for 30 min at room temperature with the corresponding secondary antibody (see **Table 7**). Finally, membranes were washed again and the ODYSSEY infrared imaging system was used for detection.

### 3.2.6 Quantification of phosphoproteins by reverse phase protein array

For relative quantification of protein modifications, such as phosphorylations, reverse phase protein microarray (RPA) technology was used. In the RPA, tiny amounts of protein mixtures are immobilized in a microarray format and the presence of specific target proteins is screened by using highly selective antibodies (Poetz et al., 2005). This technology allowed for the simultaneous quantification of more than 100 proteins and protein modifications (phosphorylation) by direct two-step immunoassay using specific primary antibodies (Braeuning et al., 2011). Sample preparation and measurements were carried out at the Natural and Medical Sciences Institute (NMI) in Reutlingen (Dr. Thomas Joos, Dr. Markus Templin, and Dr. Ute Metzger), as described elsewhere (Braeuning et al., 2011). Experiments were planned and carried out at the IKP Stuttgart. Proteins were isolated using the CLB1 lysis buffer provided by the NMI. For this purpose, medium was aspirated and 60 µl CLB1 buffer

was added per well (12-well). Plates were subsequently sealed and immediately frozen at -80 °C until further use.

### 3.2.7 Quantification of P450 activities

Activities of seven cytochrome P450s were determined simultaneously with a Cocktail-Assay containing highly specific probe substrates for the respective P450 isoform, as described previously by Feidt et al., 2010. Here, the protocol was slightly modified. In short, the Cocktail-Assay was prepared in pre-warmed cultivation medium as described in **Table 16**. Medium was aspirated from the cells and replaced by 1 ml substrate cocktail. After incubation for 3 h at 37 °C (5% CO<sub>2</sub>), 50 µl culture supernatant was collected per well and mixed with 5 µl of 250 mM formic acid. Samples were stored at -20 °C until further use. Prior to measurement, 5 µl of appropriate deuterium-labeled internal standards (ISTD) for each drug metabolite were added to each sample. The mixture was vortexed and centrifuged at 16.000 g for 5 min and transferred into Eppendorf vials with glass inlets.

**Table 16** Composition of Cocktail-Assay (substrate cocktail).

P450	Substrate	Mol. weight (g/mol)	Stock conc. (mM)	Solvent	Final conc. (µM)
CYP1A2	Phenacetin	179	100	DMSO	50
CYP2B6	Bupropion	256	50	H <sub>2</sub> O	25
CYP2C8	Amodiaquin	465	10	H <sub>2</sub> O	5
CYP2C9	Tolbutamid	270	100	ACN	100
CYP2C19	S-Mephentoin	218	100	ACN	100
CYP2D6	Propafenone	378	10	MeOH	5
CYP3A4	Atorvastatin	559	5	1:1 ACN:H <sub>2</sub> O	35

#### 3.2.7.1 Internal standards and calibration

**Table 17** shows the stock solutions and solvents for the analytes and internal standards used for the Cocktail-Assay. Concentrations of the ISTDs were 5 µM for all substances except for [<sup>2</sup>H<sub>4</sub>] Acetaminophen (10 µM). For each analyte, a calibration curve in the concentration range from 0.005 to 5 µM was prepared using the ISTDs (0.01 to 10 µM for Acetaminophen). Via serial dilution, nine calibration points were prepared, starting with 50 µM of each analyte (100 µM for Acetaminophen). 5 µl of each calibration point were mixed with 40 µl cell culture medium, 10 µl ISTD and 6 µl of 250 mM formic acid to obtain the calibration samples. This was carried out prior to each measurement in parallel to samples preparation.

## METHODS

Additionally, several quality controls were used for verification of the calibration curve samples. Samples were measured using the Agilent 6460 triple quadrupole mass spectrometer coupled to an Agilent 1200 HPLC system as described by Feidt and colleagues (Feidt et al., 2010). Measurements were carried out by our institute's analytics department.

**Table 17** Stock solution of analytes and internal standards for the Cocktail-Assay.

Analyte	Internal standard (ISTD)	Stock conc. analyte / ISTD (mM)	Mol. weight analyte / ISTD (g/mol)	Solvent analyte / ISTD
Acetaminophen	[ <sup>2</sup> H <sub>4</sub> ] Acetaminophen	13.23 / 10	151 / 155	H <sub>2</sub> O
Hydroxybupropion-HCl	[ <sup>2</sup> H <sub>3</sub> ] Hydroxybupropion-HCl	6.84 / 3.39	292 / 295	H <sub>2</sub> O
N-Desethylamodiaquin	[ <sup>2</sup> H <sub>5</sub> ] N-Desethylamodiaquin	3.05 / 2.94	328 / 333	MeOH
Hydroxytolbutamid	[ <sup>2</sup> H <sub>9</sub> ] Hydroxytolbutamid	3.49 / 3.39	287 / 296	MeOH
4-Hydroxymephenoin	[ <sup>2</sup> H <sub>3</sub> ] 4-Hydroxymephenoin	8.54 / 4.21	234 / 237	MeOH
5-Hydroxypropafenone-HCl	[ <sup>2</sup> H <sub>7</sub> ] 5-Hydroxypropafenone-HCl	5.08 / 2.5	394 / 401	1:1 MeOH: H <sub>2</sub> O
<i>o</i> -Hydroxyatorvastatin	[ <sup>2</sup> H <sub>5</sub> ] <i>o</i> -Hydroxyatorvastatin	1.58 / 1.6	633 / 624	1:1 CAN: H <sub>2</sub> O

### 3.2.7.2 Statistical analysis

For demonstration of changes in P450 enzyme activities, the mean activities are shown as pmol/min/10<sup>6</sup> cells in bar graphs. To determine the significance of changes in activities, data was log<sub>2</sub> transformed and a paired t-test with pooled standard deviations and Bonferroni post-test for multiple comparisons was carried out using the GraphPad Prism 5.04 software.

### **3.3 Transcriptome analyses**

#### **3.3.1 Affymetrix *ex vivo* transcriptome study**

##### **3.3.1.1 Affymetrix Human Gene ST 2.0 array processing**

PHH from four female donors were treated with IL-6 as described in 3.1.2. RNA isolation and quantification for Affymetrix whole transcript analysis followed the same protocol as described in 3.2.1. Total RNA (100 ng) was spiked with Poly-A RNA from the Affymetrix® GeneChip® Eukaryotic Poly-A RNA Control Kit, according to the manufacturer's instructions. For further preparation of samples, the Ambion WT Expression Kit was used as described in the instructions. In short, first-strand and second-strand cDNA were synthesized and subsequently *in vitro* transcribed into cRNA. After purification of cRNA with magnetic Nucleic Acid Binding Beads, cRNA yield and quality was assessed and 2<sup>nd</sup>-cycle cDNA was synthesized using random hexamers. The cRNA template was hydrolyzed using RNase H and the single-strand (sense strand) 2<sup>nd</sup>-cycle cDNA was purified, and the yield was determined. The cDNA was subsequently fragmented and labeled with the GeneChip WT Terminal Labeling Kit, following the instructions. In short, single-strand cDNA was fragmented using Uracil-DNA Glycosylase and Human Apurinic Endonuclease 1 and subsequently labeled (Deoxynucleotidyl Transferase). For array hybridization, washing, and staining, the GeneChip Hybridization Control Kit and the GeneChip Hybridization, Wash and Stain Kit were used. The hybridization cocktail was prepared as described in the user's manual and the appropriate amount injected into the cartridge array (Affymetrix® GeneChip® HuGene 2.0ST Array) which was hybridized in the GeneChip® Hybridization Oven 645 at 45 °C and 60 rpm for 17 ± 1 h. Washing, staining, and scanning of the arrays was performed according to the GeneChip® Expression Wash, Stain and Scan Manual for Cartridge Arrays (P/N 702731) and the Affymetrix® GeneChip® Fluidics Station 450/250 user guide, using the GeneChip® Fluidics Station 450 and the Affymetrix® GeneChip® Scanner 7G.

##### **3.3.1.2 Data processing and statistical analysis**

Scanned GeneChip images were subjected to visual inspection and the Affymetrix® Expression Console was used for quality control of microarrays and preprocessing of expression data by log scale robust multi-array analysis (RMA; Gene Level - Default) (Irizarry et al., 2003). The filtered log<sub>2</sub> scale data derived from RMA analysis was mainly

processed using the Analyst 8.0 software solution. A total of 53,617 probe sets existed on each array. After combining synonymous probe sets and removal of probes that did not correspond to a mapped gene, 25,415 genes were selected for further analyses. Data was subjected to a 2 groups paired t-test and paired effect sizes were calculated to obtain log<sub>2</sub> fold changes (log<sub>2</sub>FC). Adjustment for multiple-testing was not carried out at this point.

### **3.3.2 Retrospective *in vivo* transcriptome study**

Whole genome gene expression profiles of the 150 particularly well-characterized liver samples were generated previously by using Human-WG-6v2 Expression BeadChips and are publically available (Schröder et al., 2013). Here, samples from patients with CRP plasma concentrations  $\leq 1$  mg/l (N = 98) and  $> 10$  mg/l (N = 7) were reanalyzed for a retrospective transcriptome study. Cut off values for acute phase and healthy control CRP levels were selected according to literature (Clark and Fraser, 1993; Macy et al., 1997; Pepys and Hirschfield, 2003; Shine et al., 1981). Hence, 45 samples were excluded. The log<sub>2</sub> scale data was also processed using the Analyst 8.0 software solution. A total of 48,804 probe sets existed on each array. After combining synonymous probe sets and removal of probes that did not correspond to a mapped gene, 24,754 genes were selected for further analyses. Data was subjected to a 2 groups Welch's t-test and paired effect sizes were calculated to obtain log<sub>2</sub> fold changes (log<sub>2</sub>FC). Adjustment for multiple-testing was not carried out at this point.

### **3.3.3 Annotation enrichment analyses**

#### **3.3.3.1 Gene Ontology**

Gene Ontology (GO) enrichment analysis was carried out in order to be able to biologically interpret transcriptome data. GO terms provide a controlled vocabulary for describing gene product annotation data from GO Consortium members (Ashburner et al., 2000) and characteristics of gene products. This helps to biologically interpret lists of genes obtained from transcriptome analyses. Here, lists of differentially regulated genes ( $p \leq 0.05$ ,  $FC \geq 1.5$  and  $\leq -1.5$ ) obtained from both transcriptome studies served as templates for GO term enrichment analyses, which were performed using Fisher's Exact Test in the Analyst 8.0 software. Bonferroni's multiple testing corrections were applied. To address the redundancy of GO terms, the online tool REVIGO (Reduce + Visualize Gene Ontology) was used for summarizing terms (Supek et al., 2011).

### **3.3.3.2 Kyoto Encyclopedia of Genes and Genomes**

The Kyoto Encyclopedia of Genes and Genomes (KEGG) pathway database is a collection of pathway maps representing current knowledge on molecular interaction and reaction networks for, e.g., metabolism, cellular processes, or human diseases (Kanehisa and Goto, 2000). For KEGG pathway enrichment analyses the DAVID Bioinformatics Database was used (Huang et al., 2009), based on a one-tail Fisher's exact test (Expression Analysis Systematic Explorer/EASE). Again, lists of differentially regulated genes ( $p \leq 0.05$ ,  $FC \geq 1.5$  and  $\leq -1.5$ ) served as templates. Bonferroni multiple testing adjustments were carried out by the online tool.

## 4 RESULTS

### 4.1 Impact of the inflammatory mediator interleukin-6 on the drug detoxification system in primary human hepatocytes

PHH are considered the gold standard for the investigation of hepatic drug and xenobiotic metabolism *in vitro* (Lecluyse and Alexandre, 2010). They have been used in our lab for several years and have been established as a reliable model for drug metabolism related studies. However, PHH exhibit marked interindividual variations and are restricted in availability. It is therefore crucial to maximize the read-out from experiments that are conducted in PHH. Here, a combined strategy was developed in order to efficiently investigate the impact of IL-6 on the drug detoxification system in PHH on different scales (**Figure 4**). IL-6-induced gene expression changes were determined by high-throughput TaqMan® quantitative real-time PCR based on microfluidic channels (BioMark HD system by Fluidigm). This technology allows for quantitation of up to 96 genes in 96 samples in a single run (approx. 2.5 hours), thus minimizing cost, experimental variability, sample usage, and working time. Preliminary time course experiments showed only moderately affected DMET gene expression during the first 4 hours after IL-6 stimulation, whereas after 24 hours pronounced effects were observed (data not shown). Hence, further gene expression analyses were carried out at the time points 8 and 24 hours. Signaling pathway activation upon IL-6 stimulation in PHH was determined by relative quantification of protein phosphorylations using RPA technology. This micro-scaled dot-blot platform allows for quantitative measurement of more than 100 proteins and protein modifications simultaneously with minimal sample usage. Since signal propagation via phosphorylation proceeds quickly, very early and consecutive time points were selected (0, 5, 10, 30, 60, and 180 minutes). The impact of IL-6 on protein expression and activity of major cytochrome P450s was determined in the same well after 24, 48, and 72 hours. Protein expression was determined by Western blot analysis. The activities of seven P450s were determined simultaneously with a Cocktail-Assay containing highly specific probe substrates for the respective isoform. Samples were measured using the Agilent 6460 triple quadrupole mass spectrometer coupled to an Agilent 1200 HPLC system. This combined approach of high-throughput technologies proved to be useful in order to obtain the maximum read-out from one experiment.

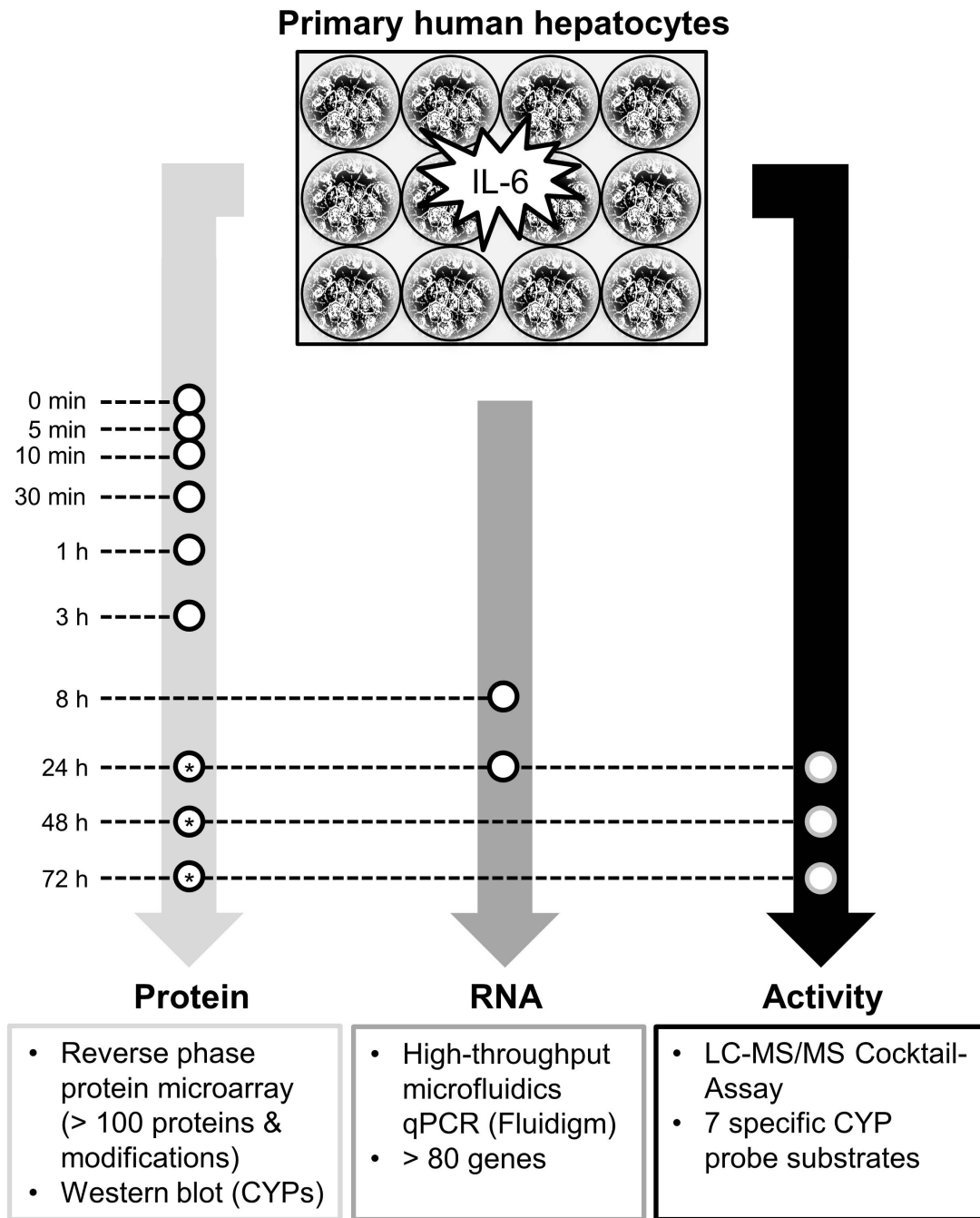


**Figure 4** Schematic experimental setup and timeline of the combined high-throughput approach. This strategy was developed in order to efficiently investigate the impact of IL-6 on the drug detoxification system in PHH. RPA technology was used for the identification of signaling pathway activation. Cytochrome P450 protein expression was determined via Western blot (time points indicated by \*). Gene expression changes of > 80 selected genes, AP genes, DMET genes (according to [www.pharmaadme.org](http://www.pharmaadme.org)), related regulatory genes and others, were measured using Fluidigm qPCR technology. Major 450 activities were investigated simultaneously by Liquid Chromatography-Tandem Mass Spectrometry (LC-MS/MS) Cocktail-Assay.

#### 4.1.1 Stimulation with interleukin-6

##### 4.1.1.1 Identification of differentially expressed genes

The APR was induced by stimulating PHH with 10 ng/ml of IL-6. The expression changes of a selected gene panel (**Table 6**) are displayed in a heat map (**Figure 5**). For illustrative purposes, the asymmetrical fold change was log<sub>2</sub>-transformed. The red cluster (on top) represents highly increased expression of AP genes which were identified as early as 8 hours after IL-6 stimulation, demonstrating the activation of the APR. The examined DMET gene panel (phase I/II metabolism, transporters, and modifiers) appeared to be moderately downregulated after 8 hours. A much stronger downregulation of these genes was observed 24 hours after the IL-6 challenge, showing very similar patterns in the different donors. In general, IL-6 elicited a profound transcriptional downregulation of many genes of interest that are associated with the drug detoxification system in PHH. The heat map clearly reflects the global character of this downregulation. Gene expression changes of genes coding for phase I DMEs and drug transporters appeared to be particularly robust across the different donors.

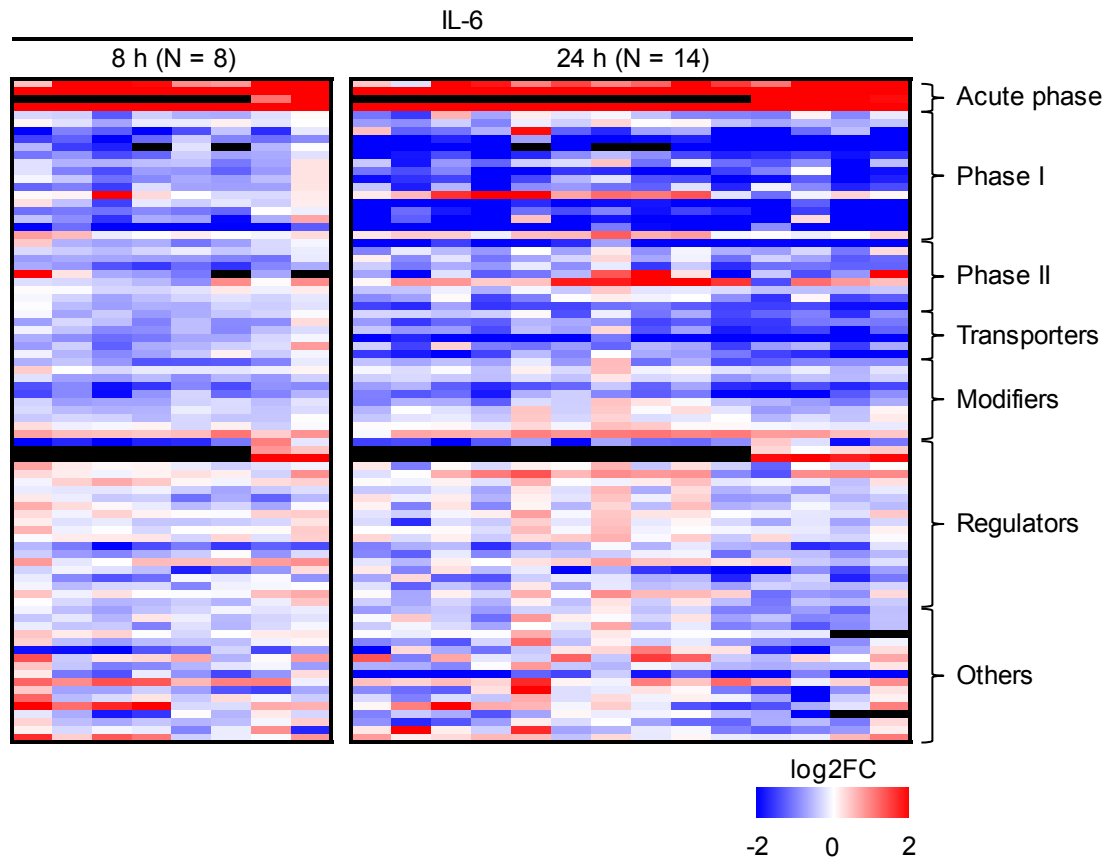


**Figure 5** Impact of IL-6 stimulation on gene expression in PHH. The heat map shows the relative log<sub>2</sub> gene expression changes (IL-6 vs. control) of 83 selected genes, including AP genes, DMET genes, related regulatory genes and others, 8 h and 24 h after IL-6 stimulation. Red and blue color indicates up- and downregulation, respectively, while black indicates lack of data. Columns represent the individual donors. Gene expression was normalized to *GAPDH*.

The mean fold changes of selected genes are presented as bar graphs. The full magnitude of AP activation is illustrated in **Figure 6**. Highly induced expression of the AP markers *CRP* (> 100-fold) and *SAA1/2* (> 4-fold) that code for C-reactive protein and Serum amyloid A, respectively, were observed upon IL-6 stimulation. The induction of the suppressor of cytokine signaling-coding *SOCS3* (> 6-fold) confirmed a positive IL-6 response. All observed effects were highly significant, as determined by grouped t-test with Bonferroni's post-hoc-test.

## RESULTS

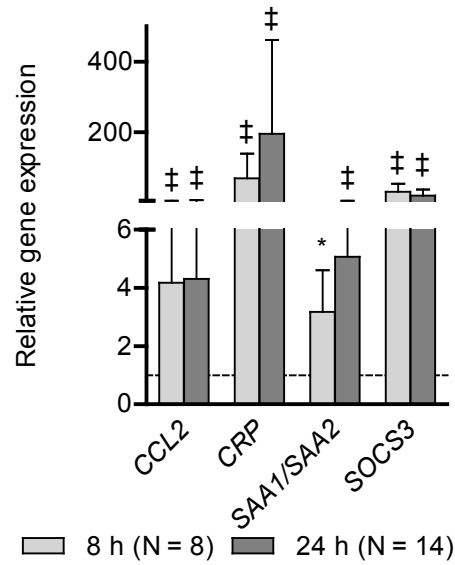


**Figure 6** Relative expression changes of AP genes in IL-6-challenged PHH. Bars represent the mean fold changes (IL-6 vs. control), 8 h (light grey) and 24 h (dark grey) after the stimulation. Error bars indicate standard deviations. Gene expression was normalized to the housekeeping gene *GAPDH*. Grouped t-test with Bonferroni's post-hoc test was carried out: \*,  $p < 0.05$ ; †,  $p < 0.01$ ; ‡,  $p < 0.001$ .

Among the phase I metabolism genes, most CYP isoforms were highly downregulated upon IL-6 stimulation in PHH (**Figure 7**). CYPs of major importance in drug metabolism were transcriptionally downregulated by more than 50%, compared to controls. On average, the expression of *CYP1A2* was decreased by > 75%, *CYP3A4* by > 80%, *CYP2C9* by > 60%, and *CYP2D6* by  $\approx 50\%$  after 24 hours, which was statistically significant. *CYP7A1* was significantly downregulated by > 80% as early as 8 hours after the IL-6 challenge. Interestingly, *CYP2E1* was the only phase I metabolism gene that was significantly upregulated with an almost 2-fold induction. There was no significant impact on mRNA expression of *ADH1A*, *ALDH2*, and *DPYD*.

## RESULTS

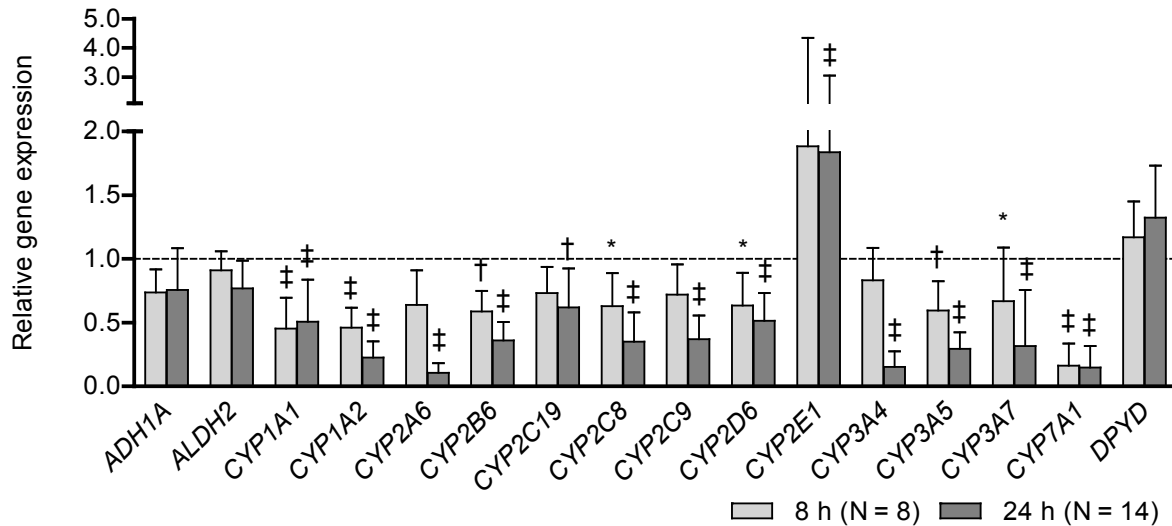


**Figure 7** Relative expression changes of phase I metabolism genes in IL-6-challenged PHH. Bars represent the mean fold changes (IL-6 vs. control), 8 h (light grey) and 24 h (dark grey) after the stimulation. Error bars indicate standard deviations. Gene expression was normalized to *GAPDH*. Grouped t-test with Bonferroni's post-hoc test was applied: \*,  $p < 0.05$ ; †,  $p < 0.01$ ; ‡,  $p < 0.001$ .

The relative gene expression changes of phase II metabolism, transporter, and DMET modifier genes are shown in **Figure 8**. The effects on phase II metabolism genes were rather diverse with only *GSTA2*, *NAT2*, and *UGT2B7* being significantly downregulated by 50% or more. The relative changes of *SULT1A1* expression appeared to be highly variable between the donors, whereas *SULT1B1* was significantly induced (> 2-fold) after 24 hours of IL-6 stimulation. All three examined *ABC* and *SLC* transporters were significantly downregulated on the transcript level. *ABCB1/MDR1* was downregulated by > 35%, *ABCC2/MRP2* by > 50%, and *SLC10A1/NTCP* by > 75% after challenging the cells with IL-6 for 24 hours. Among the major DMET modifiers, only *NR1I2/PXR* and *NR1I3/CAR* were identified as significantly downregulated (> 50%).

Overall, many important DMET genes were downregulated in response to IL-6 stimulation in PHH. The most significant impact was found on the expression of genes that code for P450s, ABCs, and SLCs. Almost all of their major isoforms were transcriptionally downregulated. The suppressive potency of IL-6 towards CYPs, in particular, was extraordinary. However, the average phase II metabolism gene expression appeared to be not as strongly affected by IL-6. A much stronger variability in gene expression could be observed in this group of genes with some showing a trend towards upregulation.

## RESULTS

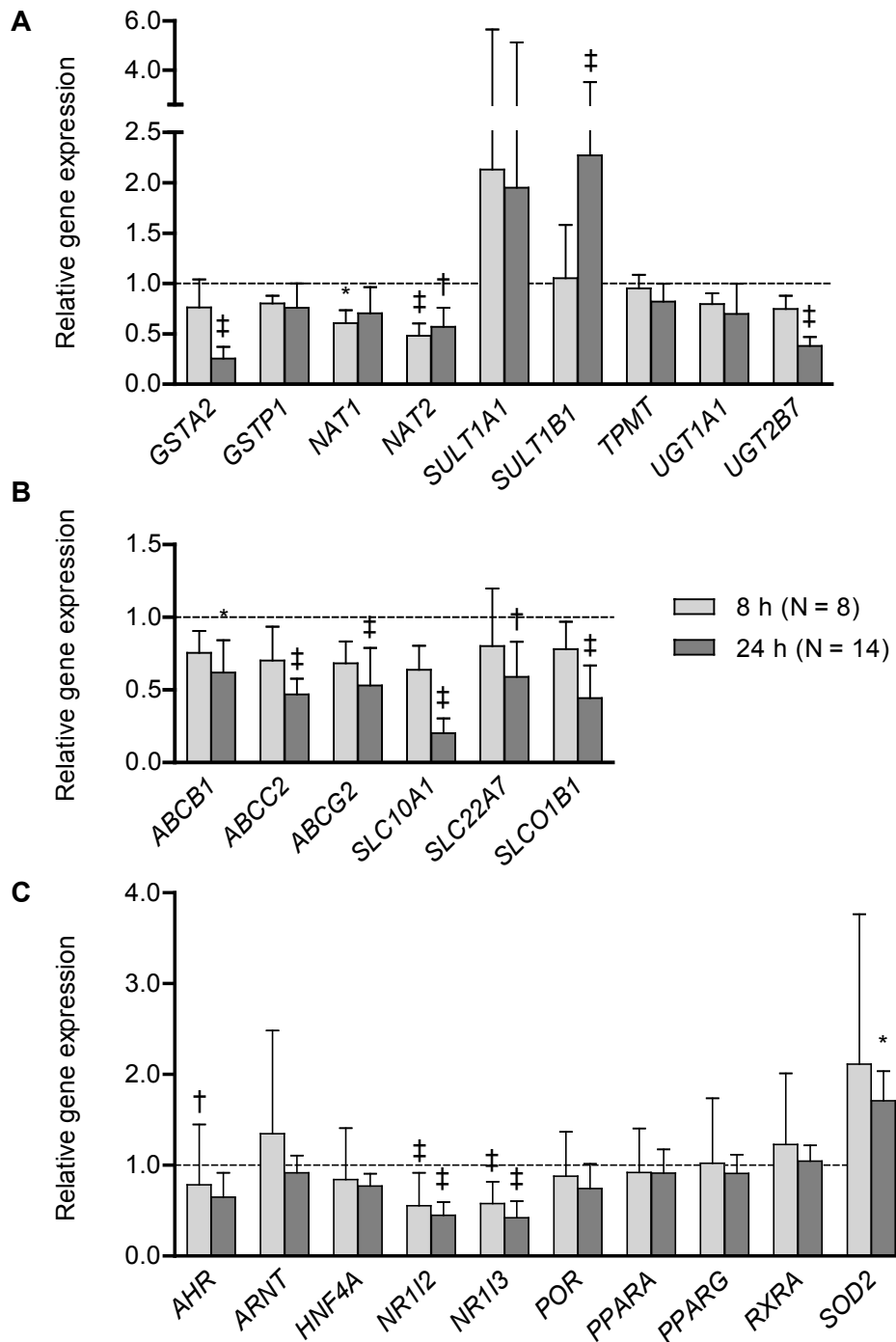


**Figure 8** Relative expression changes of (A) phase II metabolism, (B) transporter, and (C) DMET modifier genes in IL-6-challenged PHH. Bars represent the mean fold changes (IL-6 vs. control), 8 h (light grey) and 24 h (dark grey) after the stimulation. Error bars indicate standard deviations. Gene expression was normalized to *GAPDH*. Grouped t-test with Bonferroni's post-hoc test was carried out: \*,  $p < 0.05$ ; †,  $p < 0.01$ ; ‡,  $p < 0.001$ .

#### 4.1.1.2 Cytochrome P450 protein expression

Western blot analysis was carried out in order to analyze whether the IL-6-mediated transcriptional changes lead to reduced P450 protein. **Figure 9** shows one representative immunoblot of the CYP isoforms 1A2 and 3A4. The  $\beta$ -Actin staining confirmed equal protein content in each lane. The protein expression of the examined CYP isoenzymes did not appear to be significantly reduced after IL-6 exposure for 24 or 48 hours. After 72 hours, CYP1A2 was clearly reduced in IL-6-challenged cells. Remarkably, CYP3A4 protein was almost completely absent in response to IL-6.

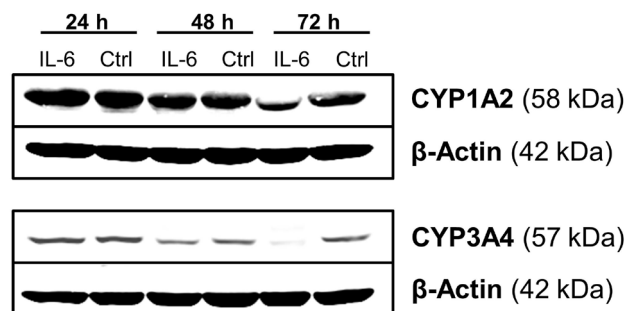


**Figure 9** Western blot analysis of P450 isoenzymes in IL-6-challenged PHH. Shown are immunostainings of CYP1A2 and CYP3A4 in total protein lysates from PHH exposed to IL-6.  $\beta$ -Actin staining served as loading control.

#### 4.1.1.3 Cytochrome P450 activities

IL-6 stimulation in PHH was shown to cause many transcriptional changes of DMET genes, in particular of P450 isoforms. However, lacking correlations between gene expression and protein level or activity are frequently observed. For instance, factors such as the half-life of proteins play an important role. Hence, it was investigated whether IL-6 also had an impact on the activities of major P450s. For this purpose, metabolite formation rates of the CYP isoforms 1A2, 2B6, 2C19, 2C8, 2C9, and 3A4 were determined in PHH from one donor that were exposed to IL-6 for up to 72 hours (**Figure 10**). Cells with the control treatment indicated a stable formation of most metabolites during the length of the experiment. Only acetaminophen formation was reduced by more than 50% within the first 48 hours, indicating a loss of basal CYP1A2 activity. In cells exposed to IL-6 for 48 hours, a decreased formation rate of all examined metabolites was observed. After 72 hours, the formation rates of

## RESULTS

acetaminophen, 4'-OH-mephenytoin, and OH-tolbutamide were reduced by more than 50%, indicating decreased activities of the P450s CYP1A2, 2C19, and 2C9, respectively. The activities of CYP2B6, 2C8, and 3A4 appeared to be reduced by more than 75%, as determined by lower formation rates of OH-bupropion, N-DE-amodiaquine, and *o*-OH-atorvastatin, respectively. The formation rate of 5'-OH-propafenone (CYP2D6) was barely measurable in this particular donor (data not shown). Contrary to all others, OH-chlorzoxazone formation was increased by 100% in PHH exposed to IL-6 for 24 and 48 hours (data not shown). All these findings could be replicated with similar outcome in several donors, with CYP2D6 usually demonstrating highest variability (data not shown). Therefore, apart from transcriptional downregulation of major P450 isoforms, IL-6 impaired their metabolic functionality as early as 48 hours after the stimulation.

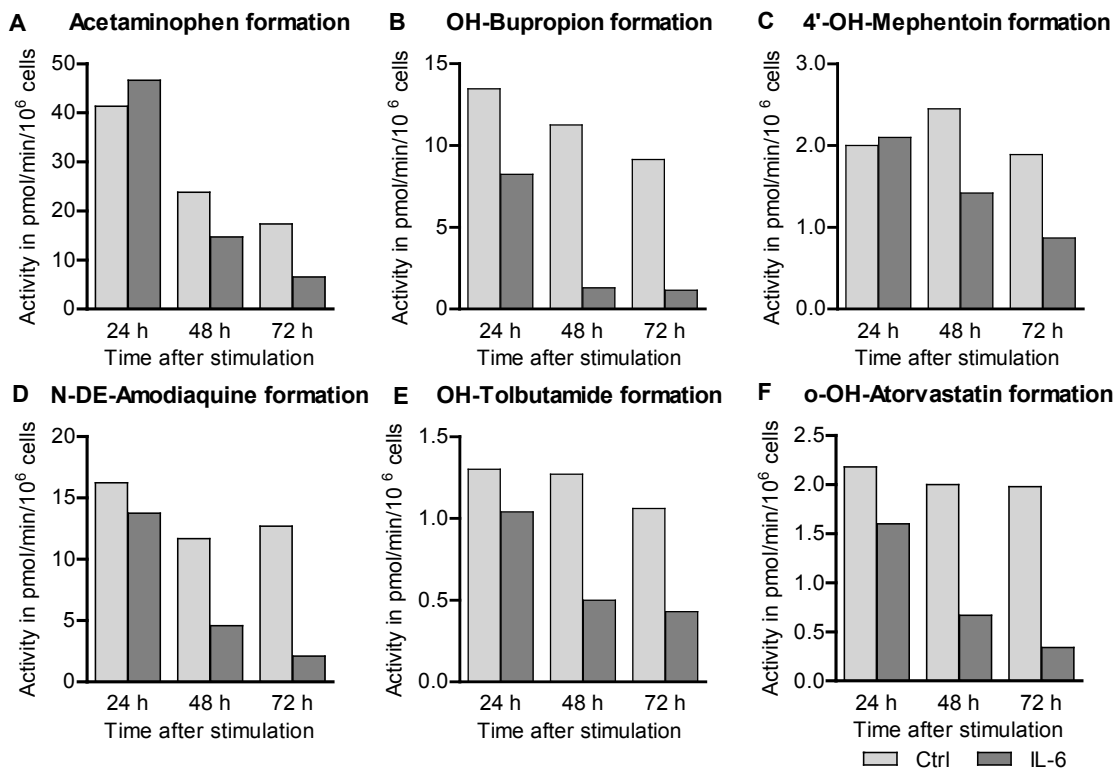


**Figure 10** Activities of P450 isoenzymes in PHH, as determined by the formation rate of (A) acetaminophen (CYP1A2), (B) OH-bupropion (CYP2B6), (C) 4'-OH-mephenytoin (CYP2C19), (D) N-DE-amodiaquine (CYP2C8), (E) OH-tolbutamide (CYP2C9), and (F) *o*-OH-atorvastatin (CYP3A4). Graphs show the formation rate of the respective metabolite in cells treated with IL-6 (dark grey, N = 1) and control (Ctrl, light grey, N = 1) at different time points (24 h, 48 h, and 72 h).

### **4.1.2 Interleukin-6 response pathways**

Only a few IL-6 response pathways are known and their relevance in the regulation of the drug detoxification system is not clear. Here we aim to investigate the major pathways that are activated upon IL-6 stimulation in PHH and if or to which extent they are involved in the regulation of the drug detoxification system.

#### **4.1.2.1 Major signaling pathways activated by interleukin-6**

Signaling pathway activation upon IL-6 stimulation in PHH was determined by relative quantification of a large panel of phosphoproteins (PP) using RPA technology. The heat map in **Figure 11 (A)** shows the relative changes in PP content in IL-6-challenged PHH compared to the respective controls in one donor. Among the 32 detected PP, induced phosphorylations of AKT S473, ERK1/2 T202/Y204, STAT1 Y701, and STAT3 Y705 were observed (**Figure 11, B –E**). Whereas ERK1/2 and STAT3 phosphorylations occurred within 5 minutes after IL-6 stimulation, AKT and STAT1 phosphorylation was induced after 10 – 30 minutes. The highest increase in phosphorylation (> 20-fold) was observed for STAT3.

## RESULTS

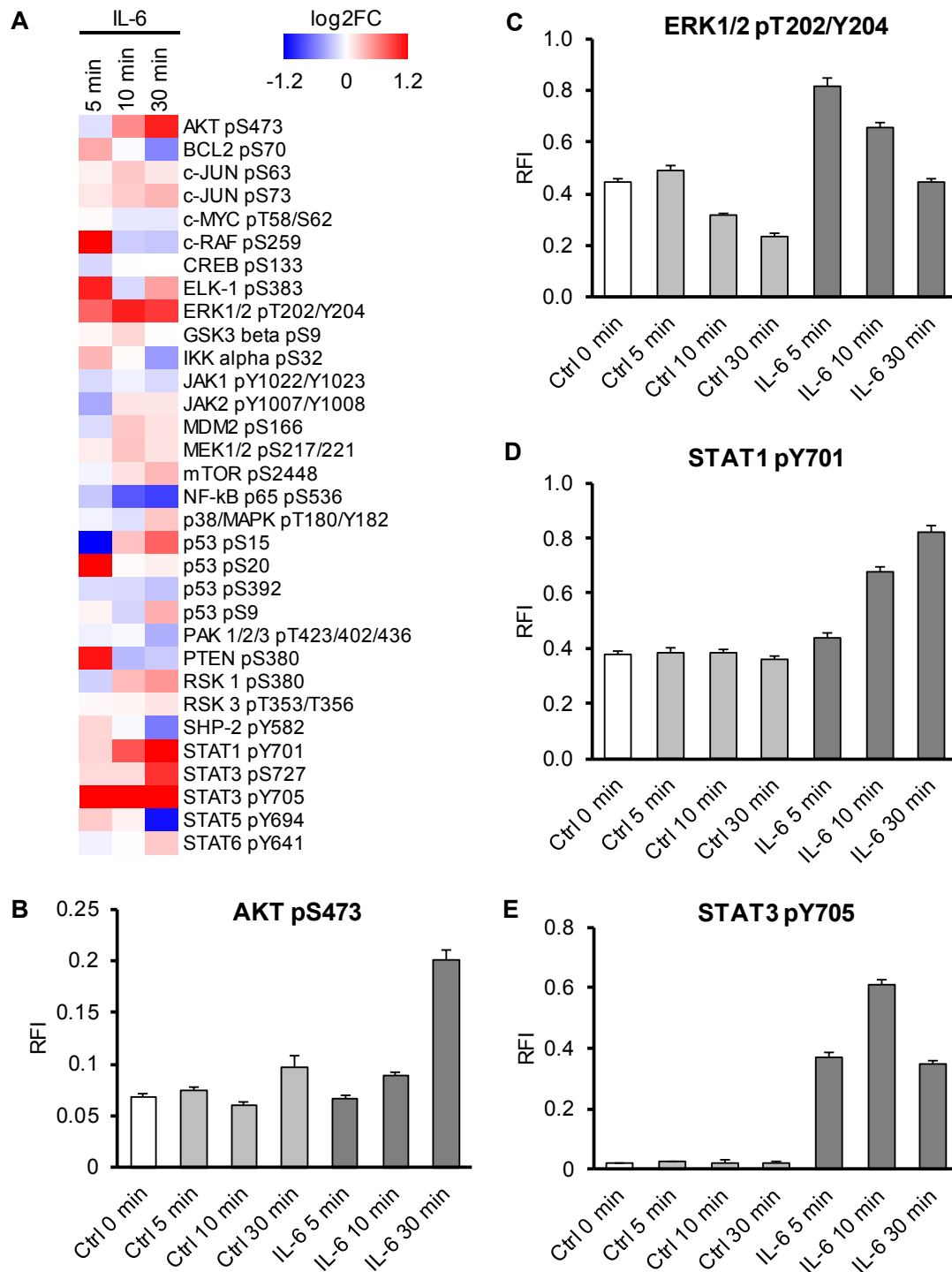


**Figure 11** Phosphoprotein activation upon IL-6 stimulation in PHH. (A) A heat map revealed the relative changes (IL-6 vs. control) in PP levels, of which 32 were detected in total by using phosphospecific antibodies. Red represents an increase, and blue a decrease on a log<sub>2</sub> scale. Relative fluorescent intensities (RFIs) of (B) AKT pS473, (C) ERK1/2 pT202/Y204, (D) STAT1 pY701, and (E) STAT3 pY705 are shown at different time points after IL-6 stimulation (dark grey) with their respective controls (Ctrl, vehicle; light grey). RFIs were obtained from the RPA and background-normalized. Error bars represent standard deviations, which were calculated from four technical replicates in serial dilutions. These measurements were carried out by the NMI in Reutlingen.

## RESULTS

Western blot analyses were carried out for the validation and confirmation of the RPA findings (**Figure 12**). Increased phosphorylation of AKT S473 was detected 10 minutes after IL-6 treatment. However, a basal activity of AKT was observed (**Figure 12, A**). ERK1/2 also showed a moderate basal activity but its phosphorylation was strongly induced by IL-6 treatment. STAT1 phosphorylation was slightly increased. A very prominent STAT3 activation confirmed the array results and therefore the role of IL-6 as a known activator of the STAT3 pathway (**Figure 12, B**).

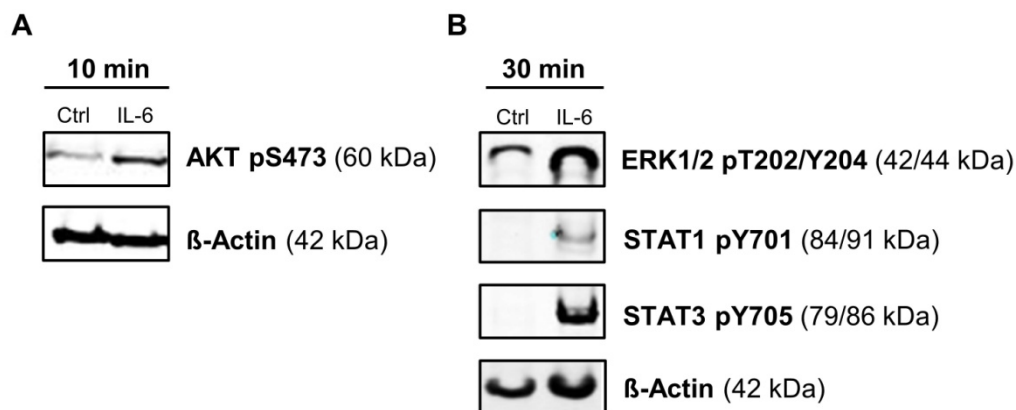


**Figure 12** Western blot of total cell lysate from PHH, 10 min and 30 min after stimulation with IL-6. Two blots were stained with specific antibodies against (**A**) AKT pS473 and (**B**) ERK1/2 pT202/Y204, STAT1 pY701, and STAT3 pY705.  $\beta$ -Actin staining is shown for each blot. 20  $\mu$ g of protein were loaded per lane. Detection was performed with the Odyssey infrared imaging system. These measurements were carried out by the NMI in Reutlingen.

### 4.1.2.2 Chemical inhibition of major signaling pathways

Analyses in 4.1.2.1 had shown that IL-6 stimulation of PHH activated several major response pathways. To elucidate the involvement of these signaling pathways in the regulation of the drug detoxification system, chemical inhibition experiments were carried out. Three specific chemical inhibitors were applied, targeting three major signaling proteins: LY294002 for PI3K (upstream of AKT), U0126 for MEK1/2 (upstream of ERK1/2), and Stattic for STAT3. Their specificity was previously shown in the literature (refer to 3.1.4). Here, their ability to block signal propagation downstream of the IL-6 receptor in PHH was validated by using the RPA technology. For this purpose, PHH from one donor were treated with IL-6 to induce the activation of AKT, ERK1/2, and STAT3, as shown in **Figure 13**. Inhibitors were applied

## RESULTS

---

prior to IL-6 stimulation and their impact on PP activation was investigated. A minor early induction of AKT S473 phosphorylation could be identified in IL-6-challenged PHH (**A**), however, the magnitude of induction was not as high as could be observed in other donors. The inhibitor LY294002 caused a general decrease in AKT S473 phosphorylation, demonstrating its effectiveness. An IL-6-mediated activation of ERK1/2 (**B**) was confirmed and could be completely abolished by using the inhibitor U0126. Furthermore, IL-6-induced STAT3 Y705 phosphorylation (**C**) was effectively inhibited by Stattic.

Taken together, the inhibitors LY294002, U0126, and Stattic effectively prevented IL-6-induced signaling through the major pathways AKT/PI3K, MAPK/ERK, and STAT3, respectively. Thus, chemical inhibition analyses on the gene expression level could be carried out to investigate the involvement of major IL-6 response pathways in DMET gene regulation.

## RESULTS

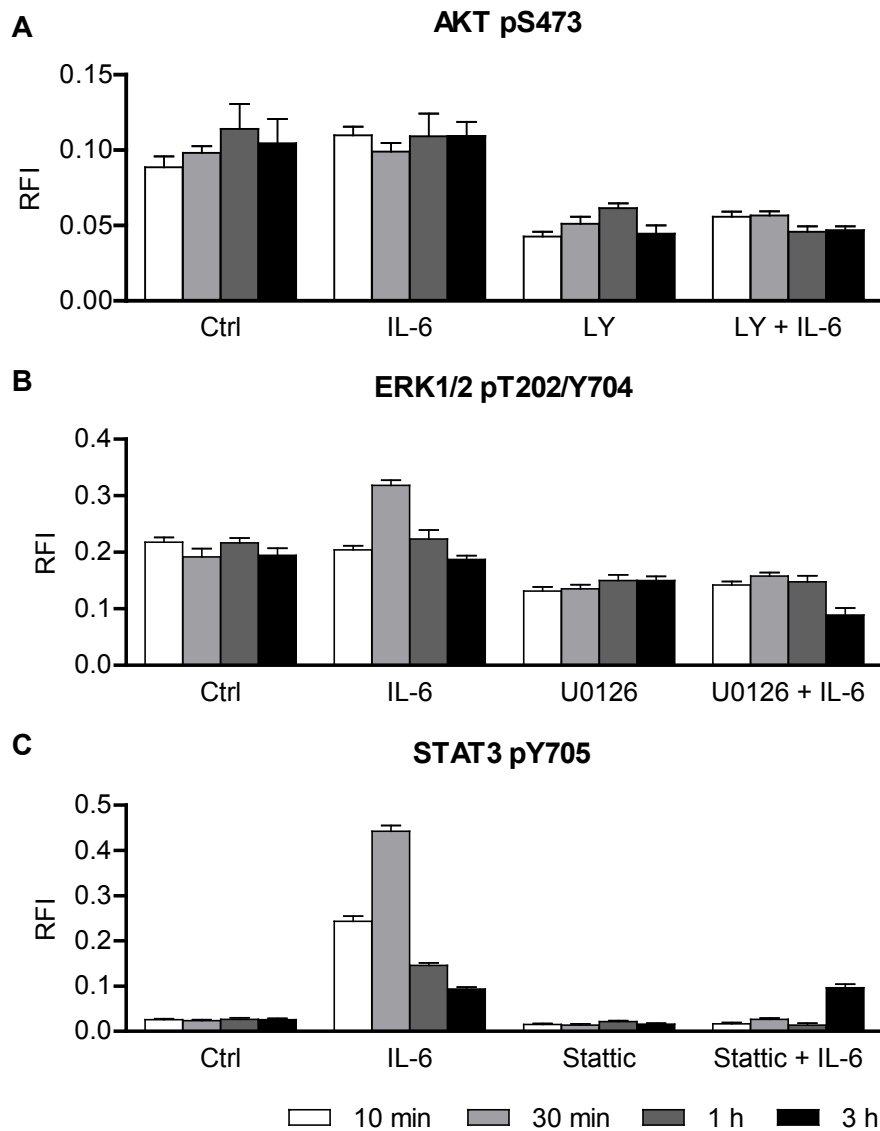


**Figure 13** Phosphoprotein activation upon IL-6 stimulation and signal inhibition in PHH. Shown are relative fluorescent intensities (RFI) of (A) AKT pSer473, (B) ERK1/2 pT202/Y204, and (C) STAT3 pY705. Treatments are indicated on the x-axis and time points by color code. The inhibitors LY(294002) and U0126 were applied in a concentration of 50  $\mu$ M each, Stattic in 10  $\mu$ M, 1 h prior to IL-6 stimulation. RFIs were obtained from the RPA and background-normalized. Standard deviations shown were calculated from four technical replicates in serial dilutions. Abbreviations: Ctrl, control. These measurements were carried out by the NMI in Reutlingen.

## RESULTS

Individual inhibition of IL-6 response pathways was performed to elucidate the contribution of each pathway. For this purpose, PHH from one representative donor were incubated with a chemical inhibitor, one hour prior to stimulation with IL-6. Relative gene expression changes, as determined by Fluidigm qPCR, are shown in **Figure 14**. IL-6 treatment alone (indicated as Ctrl) caused highly induced expression of AP markers and downregulation of many important DMET genes.

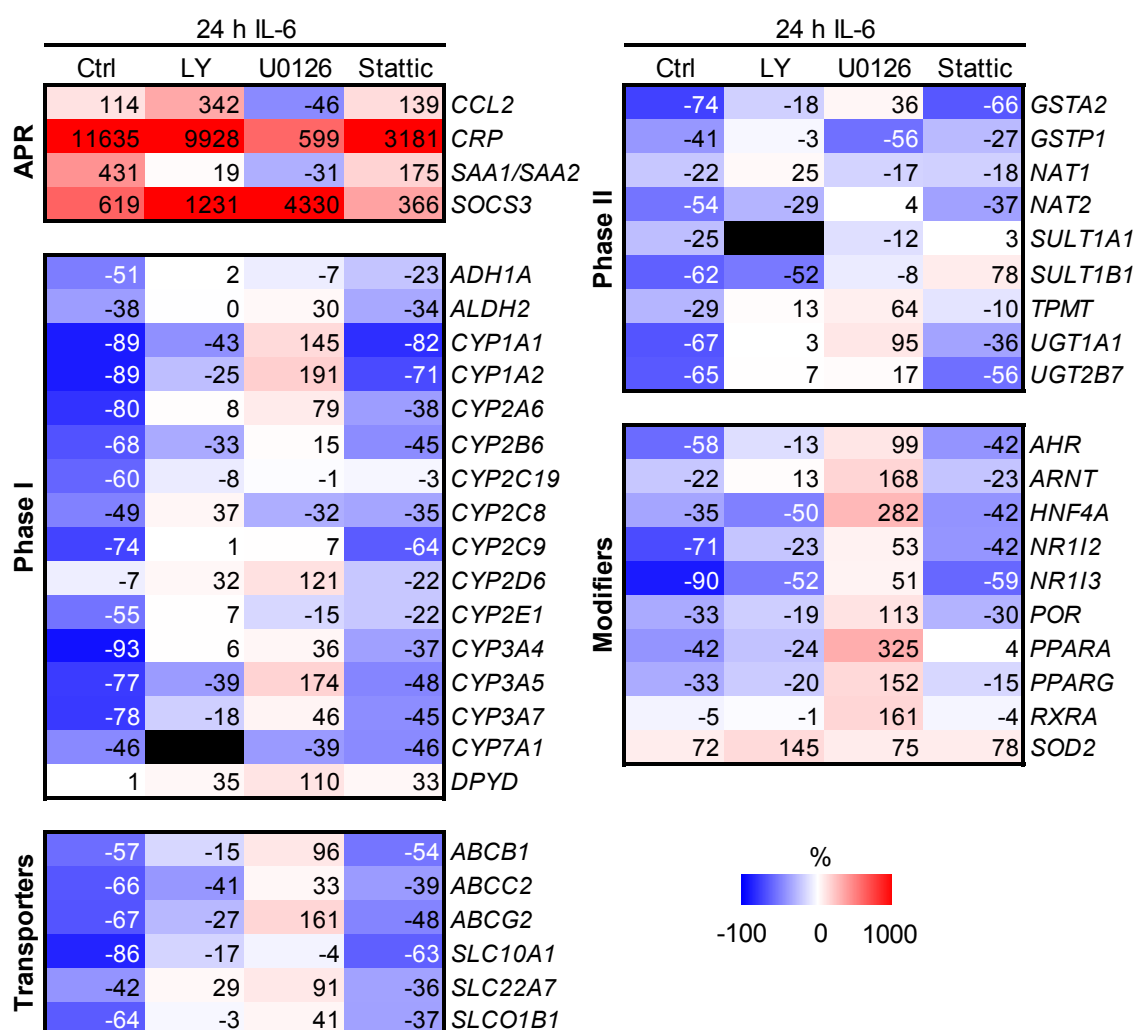


**Figure 14** Individual inhibition of major IL-6 response pathways. The heat maps show the relative changes in gene expression (in %) for APR and DMET genes upon individual chemical inhibition and IL-6 stimulation. Red represents up- and blue downregulation. Black indicates lack of data. The inhibitors LY(294002) and U0126 were applied at a concentration of 50  $\mu$ M each (Stattic at 10  $\mu$ M) 1 h prior to IL-6 stimulation. Gene expression was normalized to *GAPDH*. Ctrl represents IL-6-mediated gene expression changes (IL-6 vs. DMSO), whereas LY, U0126, and Stattic represent IL-6-mediated gene expression changes observed after inhibition (inhibitor + IL-6 vs. inhibitor).

## RESULTS

---

The PI3K/AKT pathway inhibitor LY effectively inhibited the IL-6-mediated induction of *SAA1/SAA2* and attenuated many IL-6-mediated effects on DMET genes, in particular *CYPs*. Only *CYP1A1*, *1A2*, *2B6*, and *3A5* were still downregulated, however, to a lesser extent. Downregulation of transporter genes by IL-6 was mostly attenuated by the inhibition with LY, with more pronounced effects on *SLCs* compared to *ABCs*. Among the phase II metabolism genes, *GSTA2*, *NAT2*, and *SULT1B1* were still downregulated by IL-6. Not much impact of the inhibition with LY on IL-6-mediated effects on modifier genes was observed.

MEK1/2 inhibition by U0126 abolished almost all IL-6-induced effects on phase I/II metabolism and transporter genes with many being reversed. For instance, *CYP1A1*, *1A2*, *2A6*, *2D6*, and *3A5* were upregulated whereas *CYP2C8* and *CYP7A1* were still downregulated by IL-6 after MAPK/ERK inhibition. The expression of transporter genes was rather upregulated than downregulated, which was also observed in the group of modifier genes. Among the phase II metabolism genes, IL-6-mediated downregulation of *GSTP1* was not inhibited. However, U0126 effectively prevented an IL-6-mediated upregulation of the AP markers *CCL2* and *SAA1/2*.

Inhibition by Stattic negatively influenced IL-6-induced expression of *SOCS3*, however, did not completely abolish it. The IL-6-mediated downregulation of DMET genes was only attenuated by Stattic in the case of a few phase I (*CYP2* & *3* family) and phase II metabolism genes (*SULTs*).

These findings indicated an involvement of all three tested IL-6 response pathways in the regulation of DMET genes. The potency and extent of inhibition, however, differed between pathways. Generally, the PI3K/AKT and MAPK/ERK pathways appeared to play more prominent roles than the STAT3 pathway.

For further investigation, combinatorial inhibitions (co-inhibitions) were performed. For this purpose PHH from one representative donor were incubated with a combination of two inhibitors, one hour prior to IL-6 stimulation. Relative gene expression changes, as determined by qPCR, are shown in **Figure 15**. IL-6 treatment (indicated as Ctrl) caused a global downregulation of the examined DMET genes, as observed before. This coordinated IL-6-mediated downregulation could be almost completely abolished by using a combination of the MAPK/ERK pathway inhibitor U0126 and the STAT3 inhibitor Stattic (only PI3K signaling was assumed to be active). Only a few *CYPs* (*1A1*, *1A2*, *3A7*, and *7A1*) were still downregulated by more than 10%, whereas the mRNA expression of *SULT1A1* was increased

## RESULTS

upon IL-6 stimulation after the co-inhibition. The IL-6-induced upregulation of the AP marker *CRP* was attenuated by the co-inhibition but not completely inhibited. Furthermore, an increased expression of *SOCS3* was observed in IL-6-challenged PHH after the inhibition.

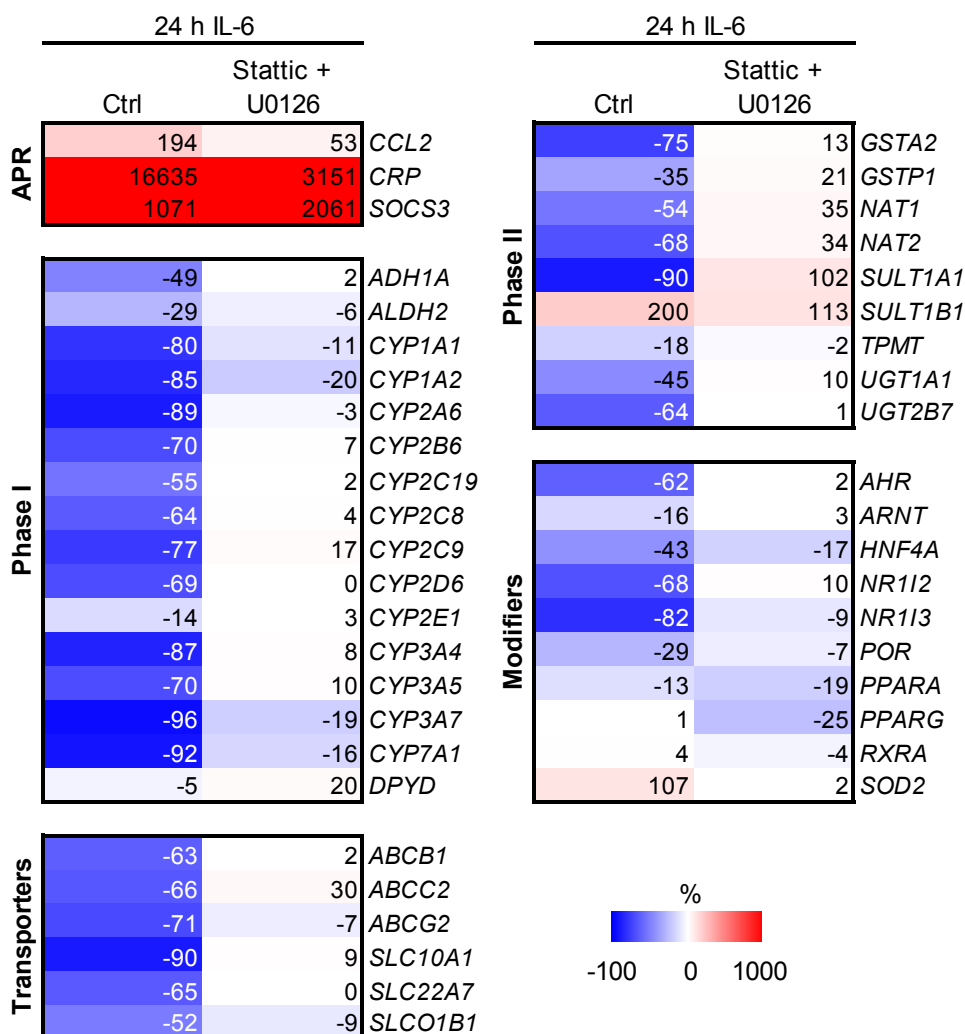


**Figure 15** Combinatorial inhibition of the major IL-6 response pathways STAT3 and MAPK/ERK. The heat maps show the relative changes in gene expression (in %) for APR and DMET genes upon combinatorial chemical inhibition with U0126 + Stattic and IL-6 stimulation. Red represents up- and blue downregulation. The inhibitors Stattic and U0126 were applied in the concentrations 10  $\mu$ M and 50  $\mu$ M, respectively, 1 h prior to IL-6 stimulation. Gene expression was normalized to *GAPDH*. Ctrl represents IL-6-mediated gene expression changes (IL-6 vs. DMSO), whereas U0126 + Stattic represents IL-6-mediated gene expression changes observed after co-inhibition (inhibitors + IL-6 vs. inhibitors).

## RESULTS

Co-inhibition of the IL-6 response pathways MAPK/ERK and PI3K/AKT (only STAT3 was assumed to be active) was carried out in PHH, obtained from another donor. Relative gene expression changes, as determined by qPCR, are shown in **Figure 16**. A downregulation of almost all major DMET genes upon IL-6 stimulation (indicated as Ctrl) was observed and confirmed the previous findings.

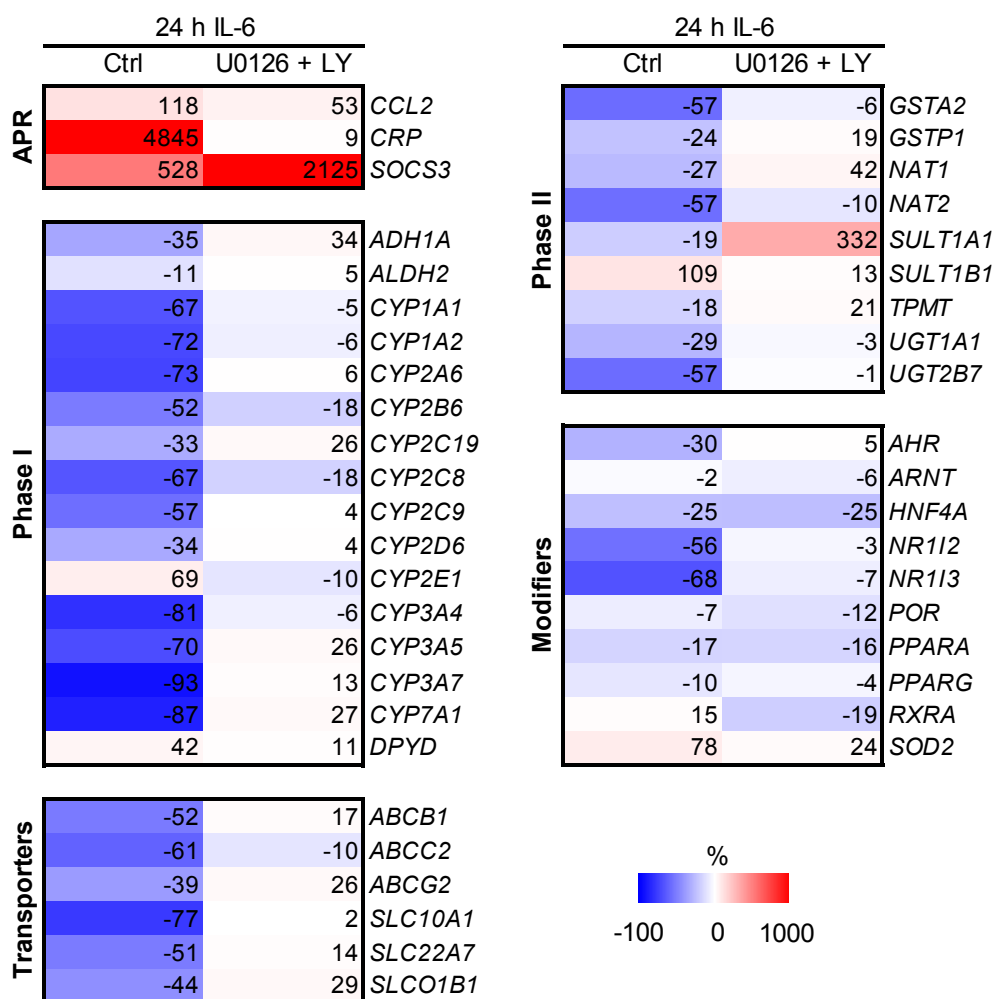


**Figure 16** Combinatorial inhibition of the major IL-6 response pathways MAPK/ERK and PI3K/AKT. The heat maps show the relative changes in gene expression (in %) for APR and DMET genes upon combinatorial chemical inhibition with U0126 + LY and IL-6 stimulation. Red represents up- and blue downregulation. The inhibitors LY(294002) and U0126 were applied in a concentration of 50  $\mu$ M each, 1 h prior to IL-6 stimulation. Gene expression was normalized to *GAPDH*. Ctrl represents IL-6-mediated gene expression changes (IL-6 vs. DMSO), whereas U0126 + LY represents IL-6-mediated gene expression changes observed after co-inhibition (inhibitors + IL-6 vs. inhibitors).

MAPK/ERK and PI3K/AKT co-inhibition by U0126 and Stattic almost completely abolished the coordinated IL-6-mediated downregulation of DMET genes. Only *CYP2B6* and *CYP2C8* appeared to be still marginally downregulated, whereas *SULT1A1* was highly upregulated by IL-6 after the co-inhibition. The expression of *HNF4A* did not show any change. Interestingly, the IL-6-induced upregulation of the AP marker *CRP* was completely inhibited while that of *SOCS3* was even enhanced.

Unfortunately, a combinatorial inhibition of the PI3K/AKT and STAT3 pathways repeatedly caused cell death of PHH, as determined by phase contrast microscopy and analysis of integrity and quantity of total RNA using the Agilent 2100 Bioanalyzer (data not shown). Nevertheless, the co-inhibition experiments indicated that both PI3K/AKT and STAT3 signaling play minor roles in the IL-6-mediated regulation of DMET genes. Almost no gene expression changes upon IL-6 stimulation were observed if only one of the pathways (PI3K/AKT or STAT3) remained active, which supposedly was the case when the other two major pathways were inhibited. Consequently, the data suggested that the MAPK/ERK pathway plays a major role. Whenever this signaling cascade was inhibited, IL-6 could not exert its effects anymore. Contrary, individual inhibition experiments indicated that the PI3K/AKT pathway is involved in IL-6 signaling towards DMET gene regulation. According to literature (1.3.2), this hypothesis remains conceivable. Hence, this pathway was investigated in a different approach.

#### **4.1.2.3 Chemical activation of the PI3K/AKT pathway**

Analyses in 4.1.2.2 had shown a possible role of the PI3K/AKT pathway in IL-6-mediated regulation of DMET genes. However, contrary observations were made in co-inhibition experiments. In order to investigate this caveat, the cell-permeable phosphopeptide 740Y-P was applied in PHH to activate PI3K and thus the PI3K/AKT signaling cascade. **Figure 17** shows the gene expression changes in 740Y-P-stimulated PHH. For comparison, relative gene expression upon IL-6 stimulation, observed in the same donor, are illustrated.

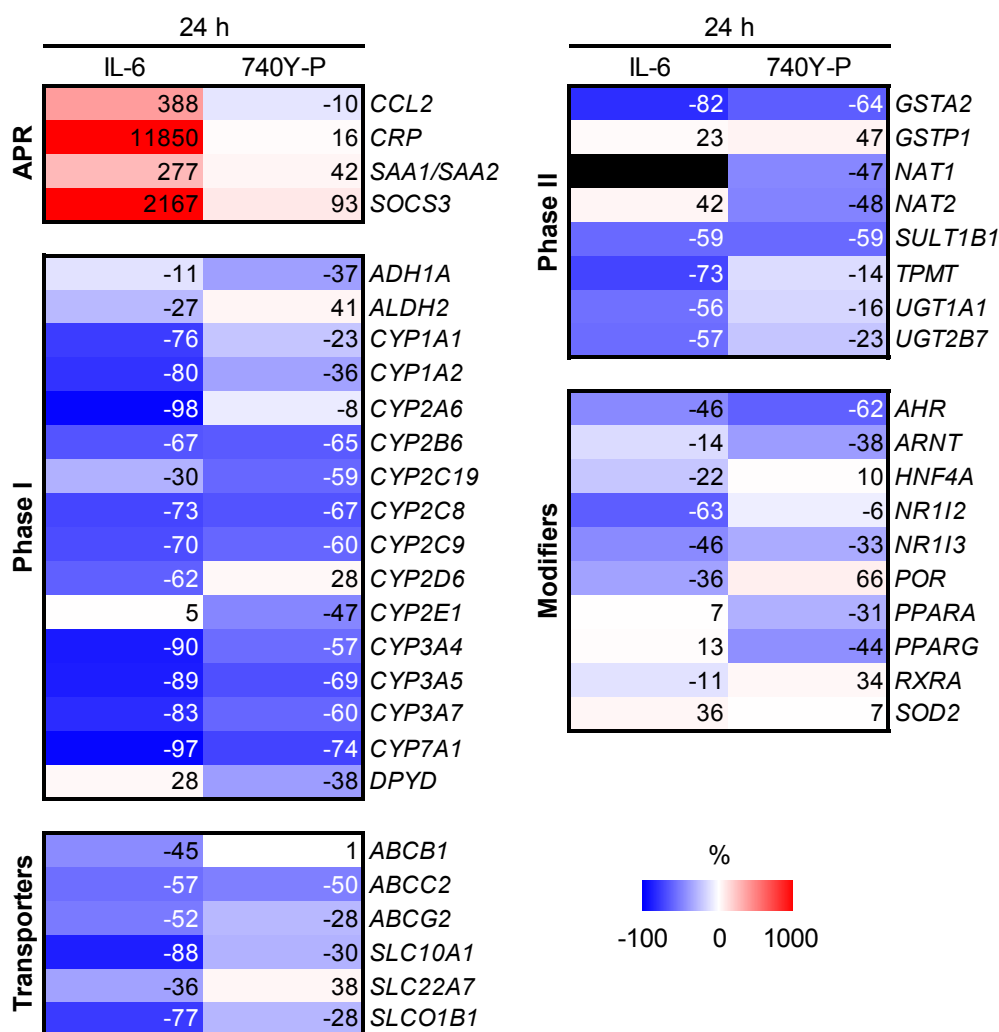


**Figure 17** PI3K activation in PHH. The heat maps show the relative changes in gene expression (in %) for APR and DMET genes upon IL-6 stimulation (IL-6 vs. control) or PI3K activation via 740Y-P (740Y-P vs. control). Red represents up- and blue downregulation. Black indicates lack of data. 740Y-P was applied in a concentration of 10  $\mu$ M. Gene expression was normalized to *GAPDH*.

740Y-P caused a strong downregulation of many phase I/II metabolism and transporter genes, but no significant upregulation of AP markers. Interestingly, the patterns of downregulation were highly similar to those observed in IL-6-challenged cells, showing almost a global downregulation of the examined DMET genes. Whereas *CYP1A1* and *IA2* were marginally affected, *CYP2A6* and *2D6* were not downregulated at all by 740Y-P. The mRNA expression of *CYP2E1* and *DPYD* appeared to be downregulated in contrast to their IL-6-mediated regulation. The mRNA expression of the transporters *ABCC2*, *ABCG2*, *SLC10A1*, and *SLCO1B1* was also decreased upon activation of PI3K, however, to a lesser extent than by IL-6 stimulation. Gene expression changes of *GSTA2*, *GSTP1*, and *SULT1B1* in 740Y-P-

stimulated PHH were comparable to those observed in IL-6-challenged cells. *NAT1* and *2* were downregulated by approximately 50%. The effects of 740Y-P on *UGTs* appeared to be of less magnitude. Interestingly, *NR1I2/PXR* expression was not influenced by 740Y-P but was impaired by IL-6 stimulation.

These results demonstrated that the activation of PI3K negatively affected the mRNA expression of important DMET genes in a coordinated fashion. These negative effects were highly similar to those observed upon IL-6 stimulation, supporting the role of PI3K/AKT as an IL-6 response pathway.

#### **4.1.2.4 Knock-down of the central nuclear receptor RXR- $\alpha$**

The nuclear hormone receptor RXR is a known DMET modifier and plays a central role in the regulation of many genes due to its ability to form heterodimers with orphan receptors (Germain et al., 2006; Mangelsdorf and Evans, 1995; Wang and LeCluyse, 2003). AKT may activate NF- $\kappa$ B whose p65 subunit directly interacts with RXR, thus antagonizing its ability to heterodimerize with other NRs (Gu et al., 2006; Romashkova and Makarov, 1999). Here, the impact of a siRNA-mediated RXR- $\alpha$  KD on the gene expression of major DMET genes was investigated. The results were compared with the effects elicited on the expression of DMET genes by IL-6 treatment or PI3K activation.

The success of the siRNA-mediated KD of RXR- $\alpha$  was evaluated by gene expression and Western blot analysis. The former confirmed a transcriptional downregulation of *RXR $\alpha$*  by more than 90% after 72 hours (see **Figure 19**). Western blot analysis revealed an almost complete loss of RXR- $\alpha$  protein as early as 48 hours after the KD (**Figure 18**). The  $\beta$ -Actin staining confirmed equal protein content in each lane. RXR- $\alpha$  was therefore successfully knocked down.

## RESULTS

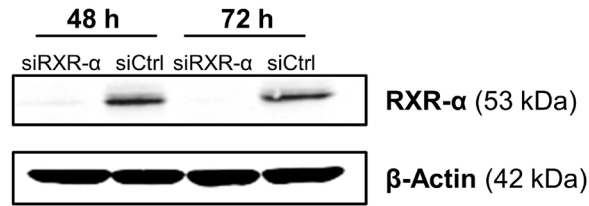


**Figure 18** Western blot analysis of RXR- $\alpha$  after KD in PHH. Shown are immunostainings of RXR- $\alpha$  in total protein lysates from PHH transfected with siCtrl (control) and siRXR- $\alpha$ .  $\beta$ -Actin staining served as loading control.

**Figure 19** illustrates the IL-6 and RXR- $\alpha$  KD-induced gene expression changes in PHH from one representative donor. This particular donor showed a transcriptional response to IL-6 stimulation comparable to the above described results. AP markers were highly upregulated whereas a global downregulation of major DMET genes was observed. A successful RXR- $\alpha$  KD was confirmed by a more than 90% downregulation of *RXR $\alpha$*  mRNA. The KD did not cause a significant induction of the acute phase. However, the impact on the gene expression of phase I/II metabolism, transporter, and modifier genes was very pronounced. The patterns of downregulation appeared very similar to those obtained in IL-6-challenged PHH. Among the phase I metabolism genes, only *CYP1A1* was not negatively affected by the KD. The transporters *ABCC2*, *ABCG2*, *SLC22A7*, and *SLCO1B1* were downregulated, almost to the same extent as by IL-6. The negative impact on the mRNA expression of phase II metabolism genes was not very distinct. Among the DMET modifiers, *AHR*, *HNF4A*, *NR1I2/PXR*, and *NR1I3/CAR* expression was strongly impaired after the KD of RXR- $\alpha$ , which was in agreement with the IL-6-induced effects.

It could therefore be shown that a KD of the important nuclear receptor RXR- $\alpha$  in PHH elicited many pronounced effects on the gene expression of major DMET genes, similar to those observed in IL-6-challenged PHH. More interestingly, the patterns of downregulation were akin to the gene expression patterns in PHH with an activated PI3-kinase (4.1.2.3).

RESULTS

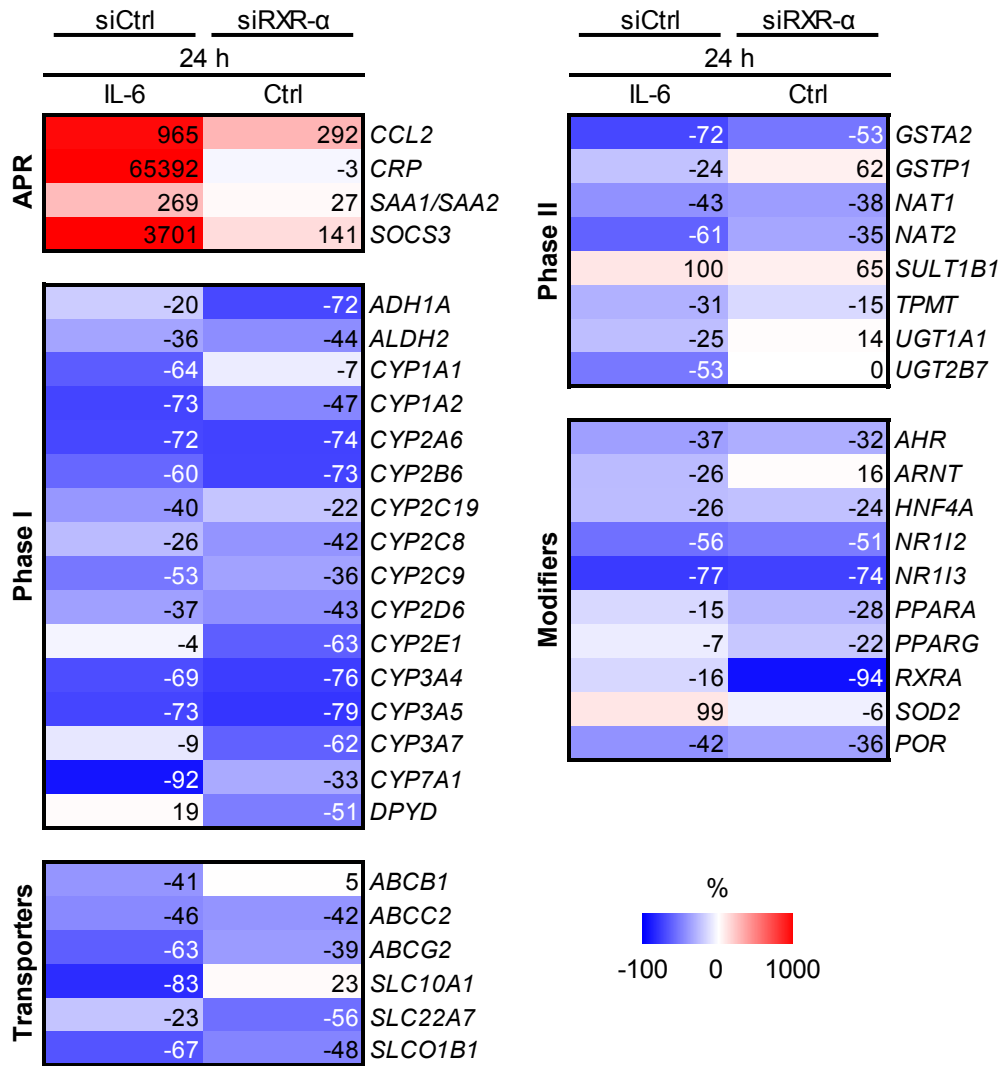


**Figure 19** siRNA-mediated RXR- $\alpha$  KD in PHH. The heat maps show the relative changes in gene expression (in %) for APR and DMET genes upon IL-6 stimulation (IL-6 vs. control) or siRNA-mediated KD of RXR- $\alpha$  (siRXR- $\alpha$  vs. siControl). Red represents up- and blue downregulation. IL-6-treated cells were transfected with siControl (siCtrl). Cells, transfected with siRXR- $\alpha$ , were treated with vehicle (Ctrl = PBS + 0.1% BSA). Gene expression was normalized to *GAPDH*.

## **4.2 Impact of inflammatory mediators on the drug detoxification system in HepaRG cells**

PHH are not a model of choice for the study of sensitive regulatory mechanisms due to their high interindividual variability. Furthermore, they are limited in availability and replication capability. Therefore, a more robust model system that would serve the needs, namely, provide more reproducible results in a metabolically complete system, was used. The human hepatocellular carcinoma derived HepaRG cell line has been shown to retain many functional characteristics of PHH, including the expression of key DMETs and NRs (Andersson et al., 2012). The influence of inflammatory mediators, however, has been poorly studied in HepaRG cells so far. Here, in a first part, a systematic comparison of IL-6-mediated effects on drug detoxification in PHH and HepaRG cells is presented. Additionally, more detailed studies with different cytokines were carried out.

### **4.2.1 HepaRG cells as a model for interleukin-6-induced effects**

HepaRG cells were stimulated with IL-6 and relative gene expression of AP markers and major DMET genes, as determined by qPCR, were compared to PHH. A scatter plot displays the relative gene expression in HepaRG cells and PHH upon IL-6 stimulation, as calculated with the  $\Delta\Delta\text{CT}$  method (**Figure 20**). A Pearson's parametric correlation analysis was performed to determine the relationship between both datasets. A very strong positive correlation ( $r = 0.91$ ,  $N = 43$ ,  $p < 0.001$ ) confirmed that the observed effects on gene expression of major DMET genes in PHH were highly similar to those in HepaRG cells. HepaRG cells therefore appeared to be a suitable model for the investigation of IL-6-mediated expression changes of major DMET genes.

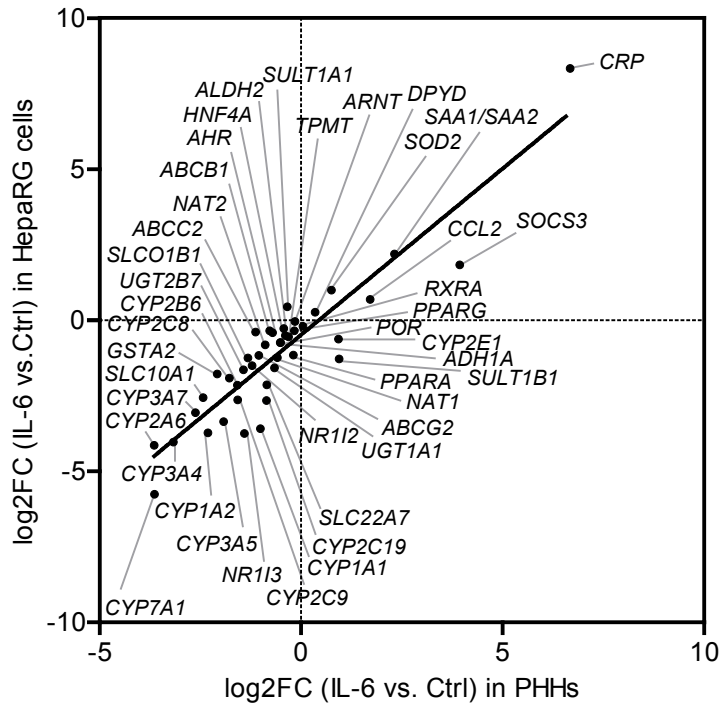


**Figure 20** Correlation of gene expression changes from PHH (N = 14) and HepaRG cells (N = 5). The log<sub>2</sub> fold changes (IL-6 vs. Ctrl) as determined by qPCR in PHH (x-axis) and HepaRG cells (y-axis) are plotted to visualize the correlation of relative expression of 43 genes. These genes include AP markers involved in the IL-6 response and major DMET genes. Pearson parametric correlation analysis was performed ( $r = 0.91$ ;  $p < 0.0001$ ).

#### 4.2.1.1 Identification of differentially expressed genes

Heat maps illustrate the gene expression changes in IL-6-challenged HepaRG cells, as determined by qPCR (**Figure 21**). The activation of the APR was confirmed by highly increased expression of AP genes as early as 8 hours after the IL-6 stimulation. A very early impact could also be observed on some phase I metabolism genes. After 24 hours, strongly impaired mRNA expression was identified, in particular of phase I metabolism, transporter, and specific modifier genes. Phase II metabolism gene expression was also negatively affected by IL-6, however, to a lesser extent. In general, IL-6 elicited a profound transcriptional downregulation of many genes of interest that are associated with the drug detoxification system in HepaRG cells. The heat map reflects the global character of this downregulation. These results were highly reproducible in repeated experiments.

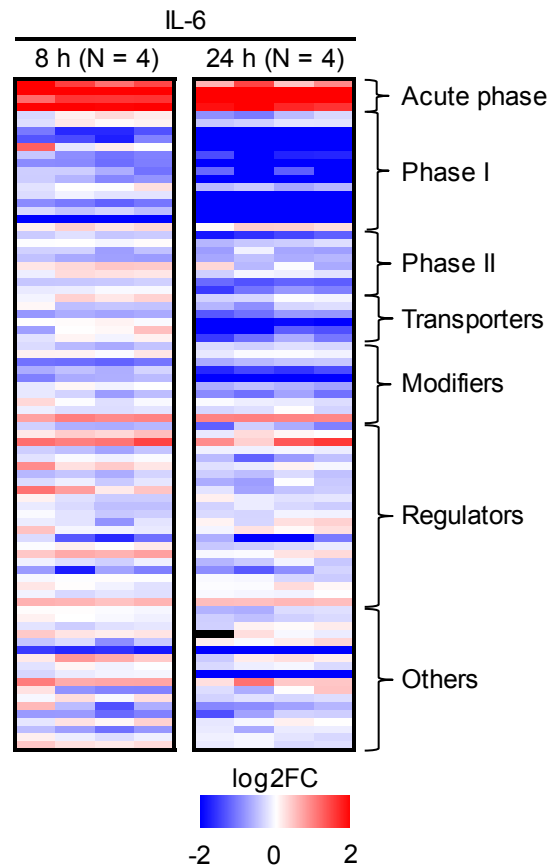


**Figure 21** Impact of IL-6 stimulation on gene expression in HepaRG cells. The heat map shows the relative log<sub>2</sub> gene expression changes (IL-6 vs. control) of 84 selected genes, including AP, DMET and related regulatory genes, 8 h and 24 h after IL-6 stimulation. Red represents up- and blue downregulation. Black indicates lack of data. Columns represent individual experiments. Gene expression was normalized to *GAPDH*.

The mean fold changes of selected genes are presented as bar graphs. The mean fold changes of AP genes upon IL-6 stimulation in HepaRG cells are illustrated in **Figure 22**. Highly increased expression of the AP markers *CRP* (> 100-fold) and *SAAI/2* (> 4-fold) could be observed. The induction of *SOCS3* ( $\approx$  4-fold) confirmed the positive IL-6 response. All observed effects were highly significant and their magnitude was very similar to those observed in IL-6-challenged PHH (4.1.1.1).

## RESULTS

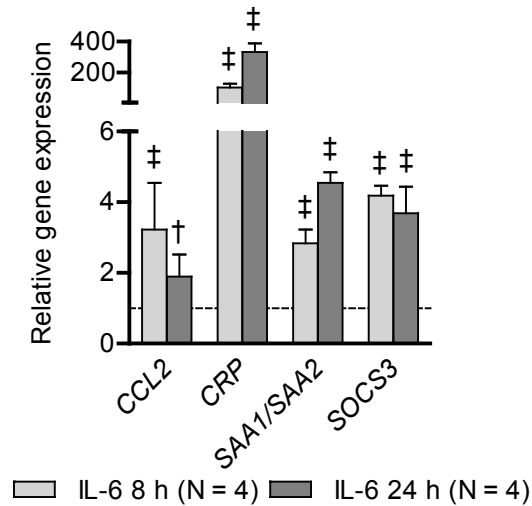


**Figure 22** Relative expression changes of AP genes in IL-6-challenged HepaRG cells. Bars represent the mean fold changes (IL-6 vs. control), 8 h (light grey) and 24 h (dark grey) after the stimulation. Error bars indicate standard deviations. Gene expression was normalized to *GAPDH*. Grouped t-test with Bonferroni's post-hoc test was carried out: \*,  $p < 0.05$ ; †,  $p < 0.01$ ; ‡,  $p < 0.001$ .

IL-6 stimulation of HepaRG cells strongly impaired the mRNA expression of all major CYP isoforms, as demonstrated in **Figure 23, A**. With the exception of *CYP2E1*, a statistically highly significant transcriptional downregulation by at least 60% was observed for all CYP isoforms. The IL-6-mediated effects on phase II metabolism gene expression was not very pronounced in HepaRG cells, comparable to the findings in PHH (**Figure 23, B**). 24 hours after IL-6 stimulation, only *GSTA2*, *UGT1A1*, and *UGT2B7* were significantly downregulated by 65%, 55%, and 45%, respectively. Among the transporter genes, the expression of the three major *SLCs* (*SLC10A1/NTCP* > 80%, *SLC22A7* > 70%, and *SLCO1B1* > 50%) and *ABCG2* ( $\approx 50\%$ ) was significantly impaired, whereas *ABCB1* and *ABCC2* expression showed only a tendency towards a lower expression (**Figure 23, C**).

## RESULTS

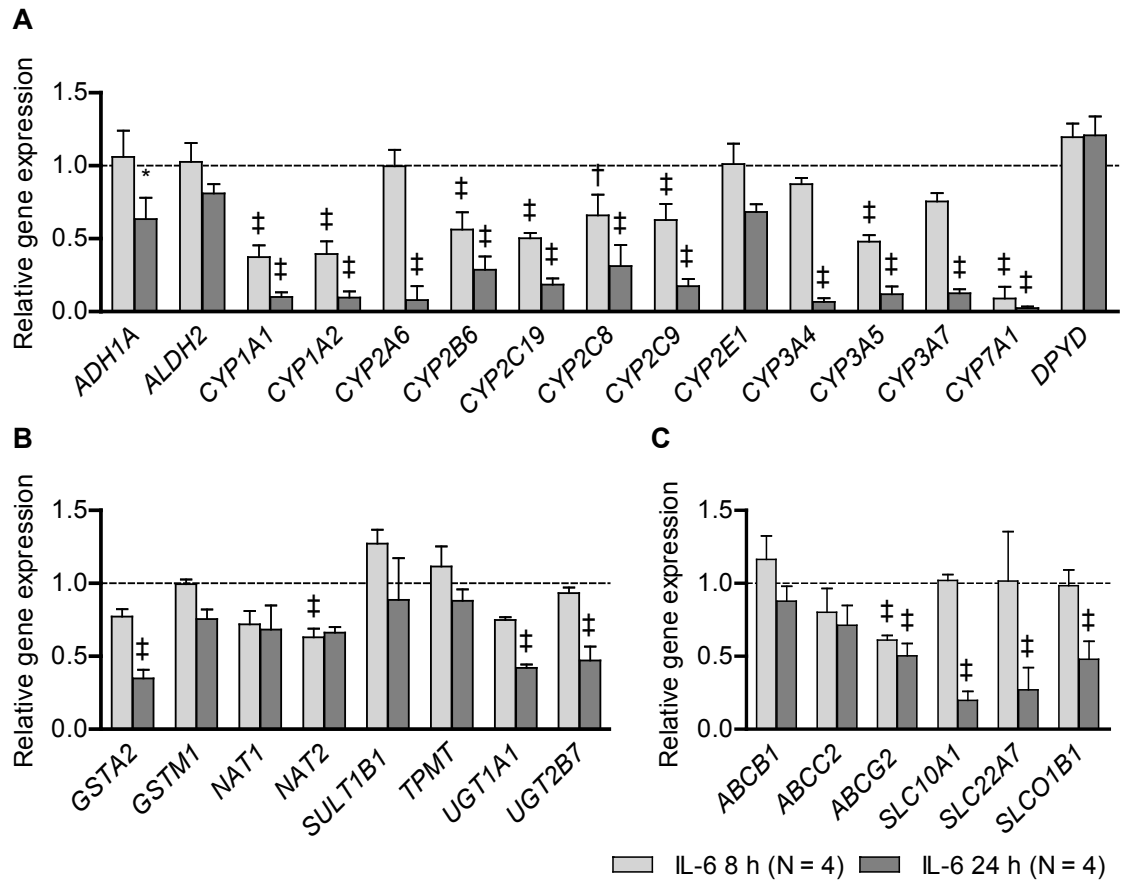


**Figure 23** Relative expression changes of (A) phase I metabolism, (B) phase II metabolism, and (C) transporter genes in IL-6-challenged HepaRG cells. Bars represent the mean fold changes (IL-6 vs. control), 8 h (light grey) and 24 h (dark grey) after the stimulation. Error bars indicate standard deviations. Gene expression was normalized to *GAPDH*. Grouped t-test with Bonferroni's post-hoc test was carried out: \*,  $p < 0.05$ ; †,  $p < 0.01$ ; ‡,  $p < 0.001$ .

Among the major DMET modifiers, *NR1I2/PXR* and *NR1I3/CAR* were identified as significantly downregulated on transcriptional level, both by at least 60% (**Figure 24**), which was in agreement with the findings in PHH. Interestingly, the mRNA expression of *HNF4A* and *PPARA* was significantly impaired in IL-6-challenged HepaRG cells, which could not be observed in PHH.

## RESULTS

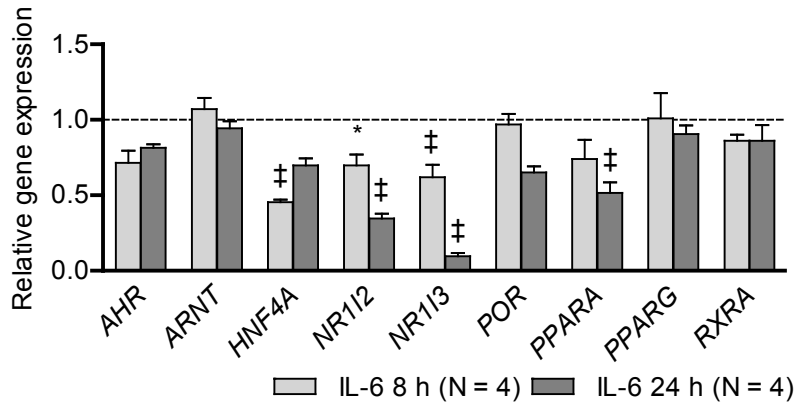


**Figure 24** Relative expression changes of DMET modifier genes in IL-6-challenged HepaRG cells. Bars represent the mean fold changes (IL-6 vs. control), 8 h (light grey) and 24 h (dark grey) after the stimulation. Error bars indicate standard deviations. Gene expression was normalized to *GAPDH*. Grouped t-test with Bonferroni's post-hoc test was carried out: \*,  $p < 0.05$ ; †,  $p < 0.01$ ; ‡,  $p < 0.001$ .

### 4.2.1.2 Cytochrome P450 protein expression

IL-6 caused a global transcriptional downregulation of all P450 isoforms examined in HepaRG cells. Whether this translated into reduced isoenzyme protein expression was investigated via Western blot analyses. **Figure 25** shows one representative immunoblot of the CYP isoforms 3A4, 2C8, and 2C9. The  $\beta$ -Actin staining confirmed equal protein content in each lane. The protein expression of the examined P450 isoenzymes did not appear to be significantly reduced after IL-6 exposure for 24 hours. After 48 hours, markedly reduced expression of all examined CYP isoenzymes by more than 50% was observed, as determined by signal intensity counts. Remarkably, CYP3A4 and CYP2C8 protein contents declined by > 90% in IL-6-challenged cells, compared to controls. A suppression of approximately 80% was observed for CYP2C9.

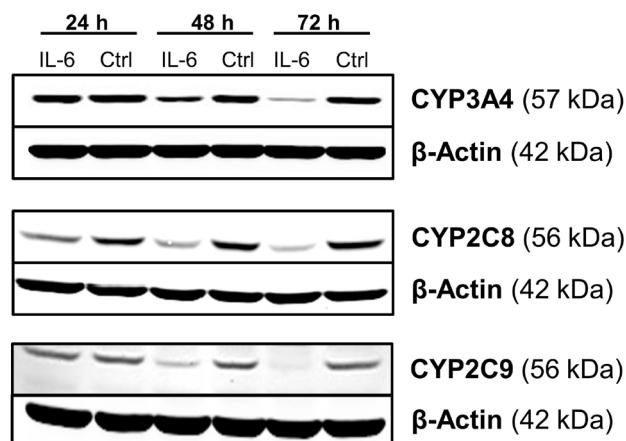


**Figure 25** Western blot analysis of P450 isoenzymes in IL-6-challenged HepaRG cells. Shown are immunostainings of CYP3A4, CYP2C8, and CYP2C9 in total protein lysates from HepaRG cells exposed to IL-6.  $\beta$ -Actin staining served as loading control.

#### 4.2.1.3 Cytochrome P450 activities

The activities of the major CYP isoenzymes 1A2, 2B6, 2C19, 2C8, 2C9, and 3A4 were determined in IL-6-challenged HepaRG cells using the Cocktail-Assay. **Figure 26** summarizes the formation of their respective metabolites, as determined in four independent experiments. The controls indicated a very stable activity of all isoenzymes over a time span of 72 hours. In IL-6-exposed cells, a decreased formation rate of all examined metabolites could be observed. As early as 24 hours after the stimulation, formation rates of acetaminophen, OH-bupropion, 4'-OH-mephentoin, and OH-tolbutamide were significantly lower compared to the controls indicating reduced activities of CYP1A2, CYP2B6, CYP2C19, and CYP2C9, respectively. After 48 hours, the activities of all examined P450s were significantly reduced by at least 60%, as determined by their metabolite formation rate. 72 hours after IL-6 stimulation, the formation rates of acetaminophen (CYP1A2) and OH-tolbutamide (CYP2C9) were reduced by > 70%, of 4'-OH-mephentoin (CYP2C19) and *o*-OH-atorvastatin (CYP3A4) by > 80%, and of OH-bupropion (CYP2B6) and N-DE-amodiaquine (CYP2C8) by > 90%. The formation rate of 5'-OH-propafenone (CYP2D6) was not measurable in HepaRG cells.

In summary, an IL-6-mediated transcriptional downregulation of many major DMET genes in HepaRG cells could be shown. For major P450 isoenzymes, this also translated into reduced protein expression and metabolic activities.

## RESULTS

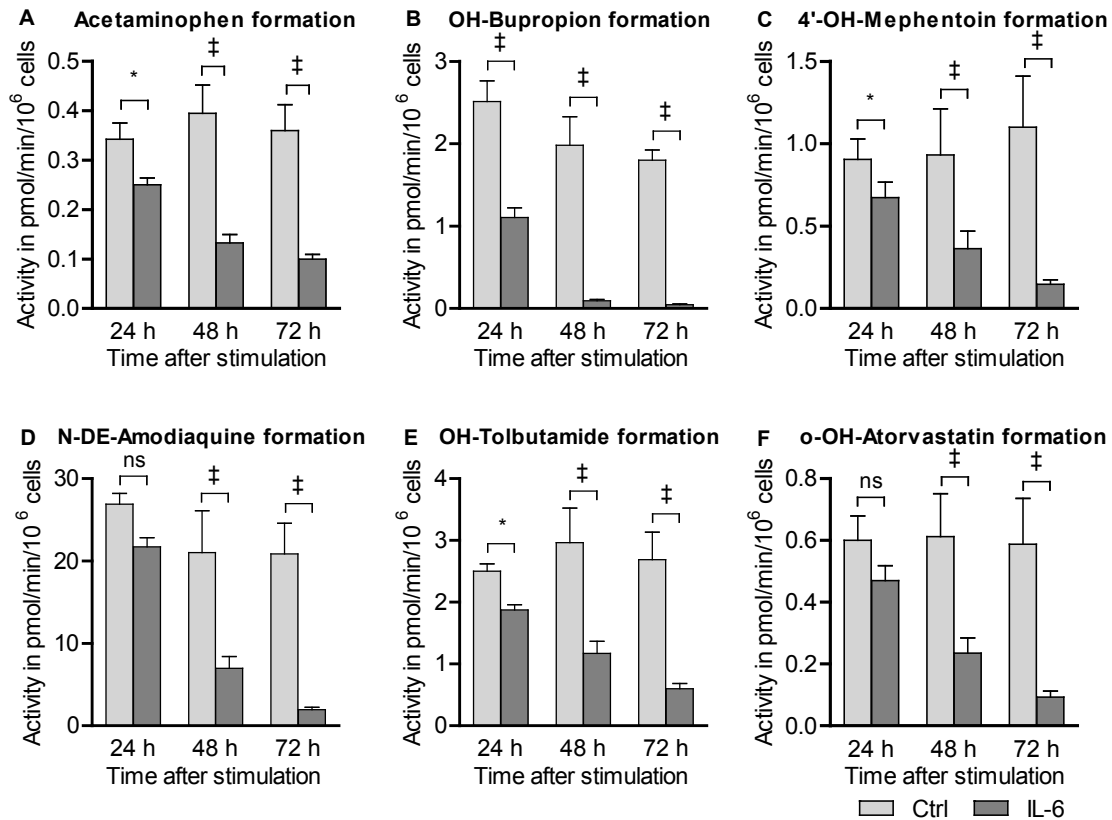


**Figure 26** Activities of P450 isoenzymes in HepaRG cells, as determined by the formation rate of (A) acetaminophen (CYP1A2), (B) OH-bupropion (CYP2B6), (C) 4'-OH-mephenytoin (CYP2C19), (D) N-DE-amodiaquine (CYP2C8), (E) OH-tolbutamide (CYP2C9), and (F) *o*-OH-atorvastatin (CYP3A4). Graphs show the formation rate of the respective metabolite in cells treated with IL-6 (dark grey, N = 4) and control (Ctrl, light grey, N = 4) at different time points (24 h, 48 h and 72 h). Grouped t-test with Bonferroni's post-hoc test was carried out: \*,  $p < 0.05$ ; †,  $p < 0.01$ ; ‡,  $p < 0.001$ .

### 4.2.2 Stimulation with interleukin-1 $\beta$ and tumor necrosis factor- $\alpha$

IL-6 stimulation of HepaRG cells caused an extensive downregulation of many DMET genes while also affecting protein expression and activities of major P450 isoenzymes. The question arose whether such coordinated effects can also be induced by other inflammatory mediators. For this purpose, interleukin-1 $\beta$  (IL-1 $\beta$ ) and tumor necrosis factor- $\alpha$  (TNF- $\alpha$ ) were applied to HepaRG cells.

#### 4.2.2.1 Identification of differentially expressed genes

Gene expression changes in IL-1 $\beta$  and TNF- $\alpha$ -challenged HepaRG cells, as determined by qPCR, are illustrated in **Figure 27**. AP markers were highly increased upon stimulation with IL-1 $\beta$  or TNF- $\alpha$ . A few phase I metabolism genes appeared to be downregulated as early as 8 hours after both stimulations. After 24 hours, strongly impaired mRNA expression of almost all phase I/II metabolism, transporter, and modifier genes were observed in IL-1 $\beta$ -challenged HepaRG cells. The heat map patterns demonstrate the global downregulation, in particular by IL-1 $\beta$ . The effects elicited by TNF- $\alpha$  were not as pronounced, in particular among phase II metabolism and transporter genes.

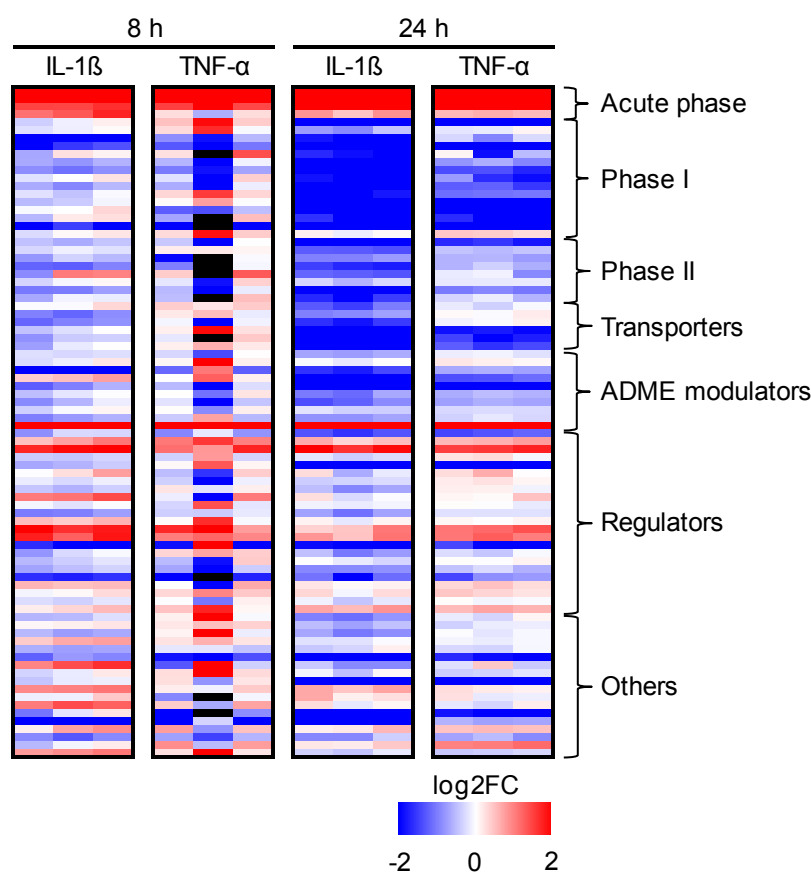


**Figure 27** Impact of IL-1 $\beta$  and TNF- $\alpha$  stimulation on gene expression in HepaRG cells. The heat map shows the relative log<sub>2</sub> gene expression changes (IL-1 $\beta$ /TNF- $\alpha$  vs. control) of 84 genes, including AP, DMET and related regulatory genes, 8 h and 24 h after stimulation. Red represents up- and blue downregulation. Black indicates lack of data. Columns represent individual experiments (N = 3). Gene expression was normalized to *GAPDH*.

## RESULTS

A strong induction of the AP marker *CRP* (> 200-fold) and *SAAI/2* (> 5-fold) could be observed upon IL-1 $\beta$  stimulation in HepaRG cells. TNF- $\alpha$  only caused a > 20-fold induction of *CRP* expression. A minor induction of *SOCS3* ( $\approx$  2-fold) was observed upon both treatments (data not shown).

**Figure 28 (A)** shows the phase I metabolism gene expression changes in HepaRG cells, caused by IL-1 $\beta$  treatment. After 24 hours, the mRNA expression of all *CYPs* was downregulated by 70% or more, as was the expression of *ADH1A*. These effects were statistically highly significant. TNF- $\alpha$  demonstrated less potency towards downregulation of *CYP* expression, but effects were still significant (**Figure 28, B**).

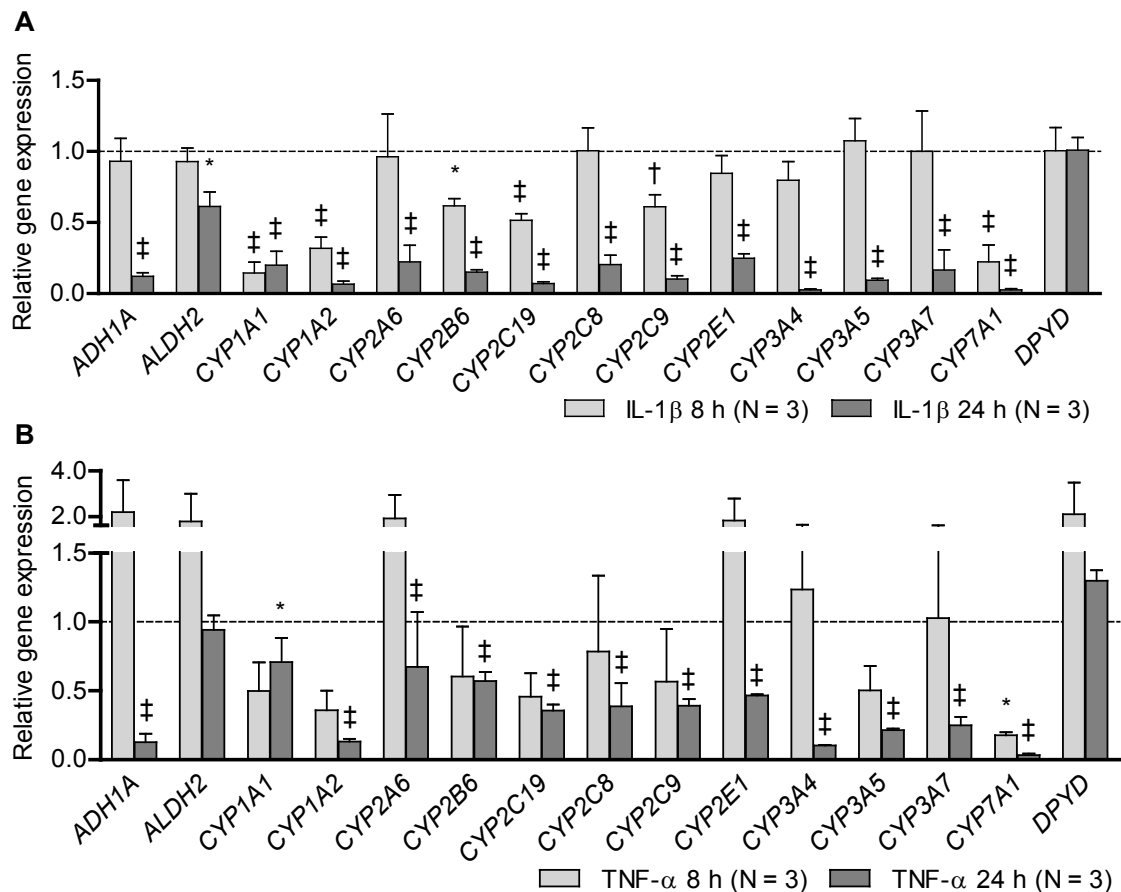


**Figure 28** Relative expression changes of phase I metabolism genes in (A) IL-1 $\beta$ - and (B) TNF- $\alpha$ -challenged HepaRG cells. Bars represent the mean fold changes (IL-1 $\beta$ /TNF- $\alpha$  vs. control), 8 h (light grey) and 24 h (dark grey) after the stimulation. Error bars indicate standard deviations. Gene expression was normalized to *GAPDH*. Grouped t-test with Bonferroni's post-hoc test was carried out: \*,  $p < 0.05$ ; †,  $p < 0.01$ ; ‡,  $p < 0.001$ .

## RESULTS

As shown in **Figure 29**, all major phase II metabolism genes, except *TPMT*, were significantly downregulated (> 50%, each) in IL-1 $\beta$ -challenged HepaRG cells (**A**). Upon TNF- $\alpha$  stimulation (**B**), only a significant downregulation of *GSTA2* ( $\approx$  70%), *NAT1* (> 30%), *NAT2* (> 30%), and *UGT1A1* (> 50%) was identified. IL-1 $\beta$  caused a significant transcriptional downregulation of all analyzed *ABC* ( $\approx$  50%, each) and *SLC* transporters (> 80%, each)(**Figure 29, A**). TNF- $\alpha$  stimulation, on the other hand, did not affect *ABC* expression, however, did lead to significant downregulation of *SLC10A1* (> 70%), *SLC22A7* (> 70%), and *SLC01B1* ( $\approx$  70%)( **Figure 29, B**).

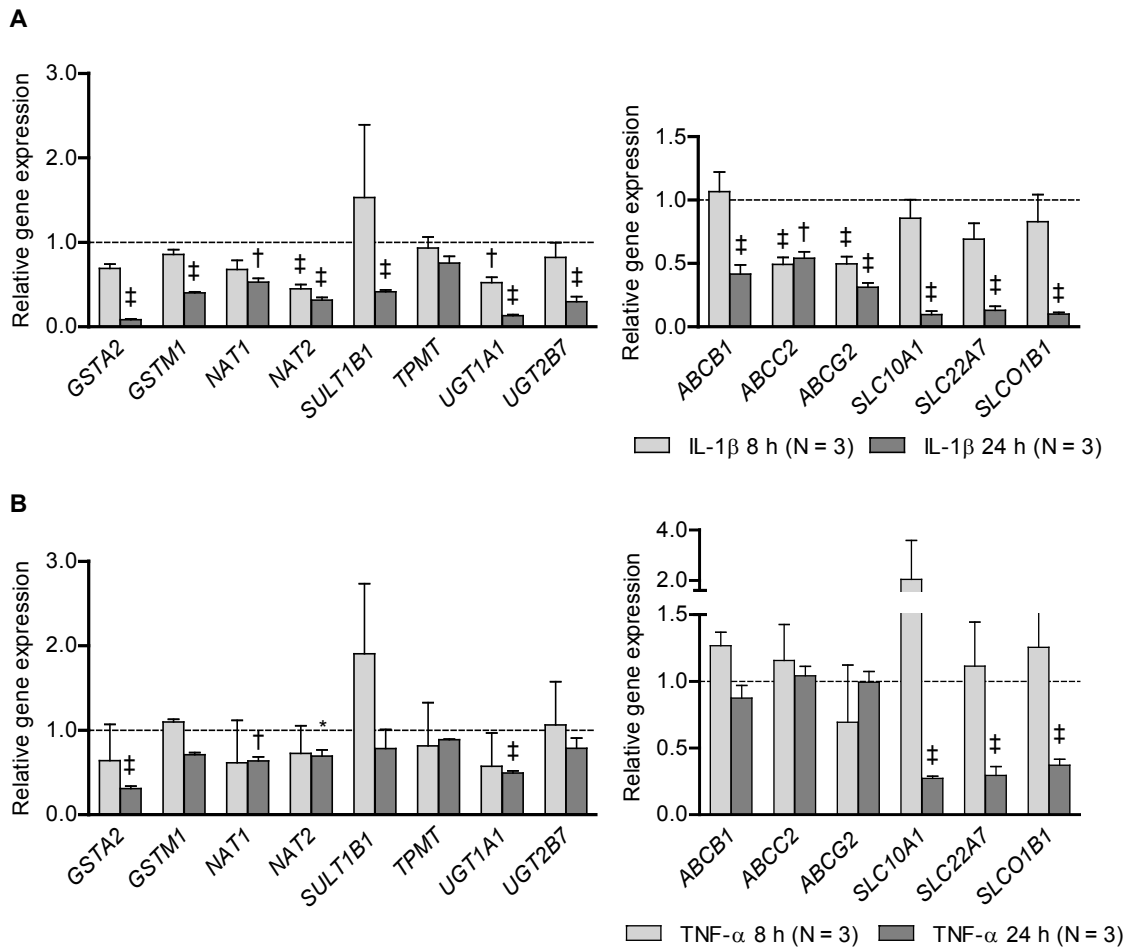


**Figure 29** Relative expression changes of phase II metabolism and transporter genes in (**A**) IL-1 $\beta$ - and (**B**) TNF- $\alpha$ -challenged HepaRG cells. Bars represent the mean fold changes (IL-1 $\beta$ /TNF- $\alpha$  vs. control), 8 h (light grey) and 24 h (dark grey) after the stimulation. Error bars indicate standard deviations. Grouped t-test with Bonferroni's post-hoc-test was carried out: \*,  $p < 0.05$ ; †,  $p < 0.01$ ; ‡,  $p < 0.001$ .

Among the DMET modifier genes, both cytokines caused significant transcriptional downregulation of *HNF4A*, *NR1I2/PXR*, *NR1I3/CAR*, *POR*, and *PPARA*. IL-1 $\beta$  treatment led to significant suppression of *RXR $\alpha$*  gene expression. Remarkably, mRNA expression of *NR1I2/PXR* and *NR1I3/CAR* was downregulated by > 90%, each, upon IL-1 $\beta$  stimulation and by 60% and 80% upon TNF- $\alpha$  stimulation, respectively (data not shown).

Taken together, exposure of HepaRG cells to IL-1 $\beta$  and TNF- $\alpha$  for 24 hours caused an analogous coordinated downregulation of important DMET genes, in particular of CYP isoforms. However, the potency of these two inflammatory mediators and the extent of suppression varied among the examined genes.

#### 4.2.2.2 Cytochrome P450 activities

The activities of the major CYP isoenzymes 1A2, 2B6, 2C19, 2C8, 2C9, and 3A4 were also determined in HepaRG exposed to IL-1 $\beta$  and TNF- $\alpha$  for up to 72 hours. **Table 18** summarizes the metabolite formation rates of acetaminophen (CYP1A2), OH-bupropion (CYP2B6), 4'-OH-mephentoin (CYP2C19), N-DE-amodiaquine (CYP2C8), OH-tolbutamide (CYP2C9), and *o*-OH-atorvastatin (CYP3A4), as determined in two independent experiments. The formation rates of acetaminophen, OH-bupropion, N-DE-amodiaquin, and OH-tolbutamide were reduced as early as 24 hours after exposure of cells to IL-1 $\beta$  and TNF- $\alpha$ , indicating suppression of CYP1A2, CYP2B6, CYP2C8, and CYP2C9. After 72 hours, both treatments caused suppressions of all examined P450 activities by more than 80%, as determined by metabolite formation rates. Therefore, IL-1 $\beta$  and TNF- $\alpha$  demonstrated a similar repressive potency towards P450 activities.

## RESULTS

**Table 18** Time dependent metabolite formation by P450s in IL-1 $\beta$ - and TNF- $\alpha$ -treated HepaRG cells. Shown are the mean values from two repeated experiments. Corresponding P450 enzymes are shown in square brackets.

Timepoints (h)	Ctrl	IL-1 $\beta$	TNF- $\alpha$
<b>acetaminophen formation in pmol/min/10<sup>6</sup> cells [CYP1A2]</b>			
24	0.38	0.26	0.29
48	0.48	0.14	0.15
72	0.45	0.07	0.06
<b>OH-bupropion formation in pmol/min/10<sup>6</sup> cells [CYP2B6]</b>			
24	2.90	1.84	2.67
48	2.39	0.08	0.54
72	1.69	0.03	0.09
<b>4'-OH-mephentoin formation in pmol/min/10<sup>6</sup> cells [CYP2C19]</b>			
24	1.11	0.98	0.77
48	1.37	0.35	0.33
72	1.62	0.00	0.04
<b>N-DE-amodioquine formation pmol/min/10<sup>6</sup> cells [CYP2C8]</b>			
24	29.08	22.66	24.96
48	28.70	5.57	6.29
72	26.62	0.62	0.67
<b>OH-tolbutamide formation in pmol/min/10<sup>6</sup> cells [CYP2C9]</b>			
24	2.65	1.73	1.97
48	3.85	0.82	0.97
72	3.45	0.13	0.20
<b><i>o</i>-OH-atorvastatin formation in pmol/min/10<sup>6</sup> cells [CYP3A4]</b>			
24	0.71	0.72	0.77
48	0.83	0.30	0.29
72	0.84	0.06	0.07

### 4.3 Transcriptome-wide impact of inflammatory mediators

Comprehensive studies addressing the impact of a systemic acute phase response on the liver transcriptome in humans have not yet been reported. Here, an Affymetrix microarray study in IL-6-challenged PHH was carried out in order to investigate inflammation-mediated changes in the drug detoxification system in an unbiased transcriptome-wide context. Gene annotation analyses were carried out in order to elucidate the major influenced biological processes and pathways. Transcriptome-wide expression profiles obtained from livers of patients having undergone an APR were analyzed retrospectively. Findings were subjected to combined and comparative analyses in order to relate findings from cellular models to the *in vivo* organ level.

### 4.3.1 Affymetrix microarray study in primary human hepatocytes treated with interleukin-6

Transcriptome-wide gene expression profiles of primary human hepatocytes from four donors treated with IL-6 were generated by using Affymetrix GeneChip HuGene 2.0ST arrays. After combining synonymous probe sets and removal of probes that did not correspond to a mapped gene, 25,415 genes were used for further analyses.

#### 4.3.1.1 Identification of differentially expressed genes

Among the 25,415 genes used for the analyses, 508 genes were differentially expressed with a p value cut-off of  $\leq 0.05$  and a fold change cut-off of  $\geq 1.5$  and  $\leq -1.5$ . The 248 upregulated and 260 downregulated genes are shown in **Supplement Table 1**. The ten top differentially expressed genes in IL-6-challenged PHH are summarized in **Table 19**.

The highest fold induction was observed for the metalloreductase *STEAP4*, followed by the major AP marker *CRP*. Additionally, the AP markers *SAA2* and *PLA2G2A* were found among the ten most strongly upregulated genes. As expected, the expression of the suppressors of cytokine signaling *SOCS1* and *SOCS3* was highly increased in response to the IL-6 stimulation.

Among the ten most strongly downregulated genes, six DMET genes were found (according to [www.pharmaadme.org](http://www.pharmaadme.org)). The *CYP* isoforms *2C8*, *3A4*, and *2A6* were identified as the strongest negatively affected genes on the transcriptome level. A very strong downregulation was also observed for the *CYPs* *2C9* and *4A11* as well as for the transporter *SLC10A1*.

## RESULTS

**Table 19** Top differentially expressed genes in IL-6-challenged PHH.

Gene symbol <sup>a</sup>	Gene name	Log2 FC	SD	P value <sup>b</sup>
<i>Upregulated genes</i>				
<i>STEAP4</i>	STEAP Family Member 4	4.70	± 1.53	8.63E-03
<i>CRP</i>	C-reactive protein	3.71	± 1.50	1.58E-02
<i>ADAMTS1</i>	ADAM metalloproteinase with thrombospondin type 1 motif, 1	3.04	± 0.63	2.35E-03
<i>AVPR1A</i>	Arginine Vasopressin Receptor 1A	2.53	± 0.46	1.58E-03
<i>SOCS1</i>	Suppressor of cytokine signaling 1	2.47	± 0.18	1.14E-04
<i>DHODH</i>	Dihydroorotate dehydrogenase (quinone)	2.40	± 0.26	3.60E-04
<i>SAA2</i>	Serum Amyloid 2	2.28	± 0.77	9.52E-03
<i>CFHR3</i>	Complement factor H-related 3	2.25	± 0.97	1.89E-02
<i>CREB3L3</i>	cAMP responsive element binding protein 3-like 3	2.22	± 0.66	6.80E-03
<i>PLA2G2A</i>	Phospholipase A2, group IIA	2.10	± 0.43	2.31E-03
<i>Downregulated genes</i>				
<i>CYP2C8</i>	Cytochrome P450, family 2, subfamily C, polypeptide 8	-2.34	± 0.57	3.73E-03
<i>CYP3A4</i>	Cytochrome P450, family 3, subfamily A, polypeptide 4	-2.26	± 0.90	1.51E-02
<i>CYP2A6</i>	Cytochrome P450, family 2, subfamily A, polypeptide 6	-2.26	± 0.74	8.72E-03
<i>GLYAT</i>	Glycine-N-acyltransferase	-2.25	± 0.57	4.19E-03
<i>CYP2B7P1</i>	Cytochrome P450, family 2, subfamily B, polypeptide 7 pseudogene 1	-2.08	± 1.29	4.88E-02
<i>OTC</i>	Ornithine carbamoyltransferase	-1.97	± 0.33	1.27E-03
<i>CYP2C9</i>	Cytochrome P450, family 2, subfamily C, polypeptide 9	-1.82	± 0.84	2.22E-02
<i>SLC10A1</i>	Solute Carrier Family 10 (Sodium/Bile Acid Cotransporter Family), Member 1	-1.82	± 0.43	3.49E-03
<i>CYP4A11</i>	Cytochrome P450, family 4, subfamily A, polypeptide 11	-1.80	± 0.74	1.65E-02
<i>AKR1B10</i>	Aldo-keto reductase family 1, member B10 (aldose reductase)	-1.77	± 0.67	1.32E-02

Log2FC = log2 fold change, IL-6 compared to control. Values represent mean ± SD for N = 4 gene chips per group.

<sup>a</sup> miRNAs, lncRNAs, and LOCs excluded

<sup>b</sup> Two groups paired t-test

All DMET genes that were identified as differentially expressed in IL-6-treated PHH are shown in **Table 20**. A total of ten DMET genes showed an increased expression including *CYP2E1* which was more than 2-fold induced. Remarkably, 30 DMET genes were downregulated including many important phase I metabolism genes (e.g., *CYPs* and *ADHs*), phase II metabolism genes (e.g., *GSTs*, *SULTs* and *UGTs*), transporter genes (e.g., *ABCs* and *SLCs*), and one gene coding for a DMET modifier (*NR1I2/PXR*). The latter is known to be involved in the inducible expression of many DMET genes.

## RESULTS

**Table 20** Differentially expressed DMET genes in IL-6-challenged PHH.

Gene symbol	Log2FC	SD	P-value <sup>a</sup>	Gene symbol	Log2FC	SD	P-value <sup>a</sup>
<b>Upregulated genes</b>				<i>CYP1A2</i>	-1.25	± 0.26	2.38E-03
<i>DHRS13</i>	1.61	± 0.68	1.79E-02	<i>CYP3A5</i>	-1.14	± 0.30	4.91E-03
<i>SLC5A6</i>	1.50	± 0.26	1.38E-03	<i>CYP39A1</i>	-1.12	± 0.08	9.48E-05
<i>NNMT</i>	1.48	± 0.40	7.96E-03	<i>GSTA2</i>	-1.11	± 0.36	8.53E-03
<i>CYP21A2</i>	1.14	± 0.28	3.59E-03	<i>CYP2B6</i>	-1.06	± 0.23	2.81E-03
<i>SULT1B1</i>	1.07	± 0.44	1.64E-02	<i>SLC22A10</i>	-0.97	± 0.52	3.26E-02
<i>CYP2E1</i>	1.05	± 0.58	3.61E-02	<i>NR1I2</i>	-0.95	± 0.37	1.40E-02
<i>SERPINA7</i>	0.91	± 0.20	2.60E-03	<i>SLC22A1</i>	-0.94	± 0.23	3.92E-03
<i>ABCA1</i>	0.80	± 0.10	5.75E-04	<i>FMO5</i>	-0.92	± 0.13	6.99E-04
<i>GPX2</i>	0.77	± 0.35	2.16E-02	<i>UGT2B10</i>	-0.88	± 0.30	9.00E-03
<i>PLGLB1</i>	0.61	± 0.32	3.25E-02	<i>ABCG2</i>	-0.83	± 0.10	4.58E-04
<b>Downregulated genes</b>				<i>SULT2A1</i>	-0.83	± 0.38	2.22E-02
<i>CYP2C8</i>	-2.34	± 0.57	3.73E-03	<i>ABCC2</i>	-0.81	± 0.20	3.68E-03
<i>CYP3A4</i>	-2.26	± 0.90	1.51E-02	<i>SLCO1B3</i>	-0.77	± 0.35	2.21E-02
<i>CYP2A6</i>	-2.26	± 0.74	8.72E-03	<i>UGT2B11</i>	-0.77	± 0.88	4.92E-02
<i>CYP2C9</i>	-1.82	± 0.84	2.22E-02	<i>CYP2C19</i>	-0.71	± 0.13	1.69E-03
<i>SLC10A1</i>	-1.82	± 0.43	3.49E-03	<i>GSTA1</i>	-0.71	± 0.34	2.47E-02
<i>CYP4A11</i>	-1.80	± 0.74	1.65E-02	<i>ALDH5A1</i>	-0.65	± 0.18	5.72E-03
<i>ADH1C</i>	-1.52	± 0.63	1.72E-02	<i>SLC22A3</i>	-0.63	± 0.20	8.03E-03
<i>ADH4</i>	-1.44	± 0.89	4.86E-02	<i>ADH6</i>	-0.62	± 0.22	1.08E-02
<i>SULT1E1</i>	-1.36	± 0.47	1.02E-02	<i>CYP2A7</i>	-0.60	± 0.32	3.38E-02

Log2FC = log2 fold change, IL-6 compared to control. Values represent mean ± SD for N = 4 gene chips per group.

<sup>a</sup> Two groups paired t-test

### 4.3.1.2 Validation of microarray data by qPCR

Variability in microarray results occurs not only from lab to lab and user to user but also due to their small dynamic range which limits sensitivity and specificity. For technical and biological validation, 32 differentially expressed genes were selected including 28 genes that code for core DMETs (according to [www.pharmaadme.org](http://www.pharmaadme.org)), and four inflammation related genes involved in the IL-6 response to validate microarray data using TaqMan® gene expression assays, the gold standard in microarray quality control. **Supplement Table 2** summarizes the gene expression changes (indicated as log2FC) in IL-6-treated PHH measured with microarrays and qPCR. The latter was performed in the same set of donors that was used for microarray analysis (discovery set, N = 4) for technical validation and an independent set (validation set, N = 11) for cross-validation of biological effects. QPCR analysis in the discovery set confirmed the IL-6-induced changes in hepatocyte gene expression for almost all genes. The biggest discrepancy was found for *GSTM1* which was downregulated according to qPCR and only marginally differentially regulated according to microarray analysis. The

## RESULTS

---

fold changes obtained from qPCR analysis were higher than those from microarray analysis in most cases (27 genes).

When comparing microarray results with qPCR analysis in the validation set, only the expression change of one gene (*GSTM1*) did not coincide with the microarray results, similar to the findings in the discovery set. The expression change of this gene was, however, not significant after Bonferroni-Holm adjustment for multiple testing ( $p=0.095$ ). Interestingly, qPCR analysis showed significant expression changes of all *ABC*- and *SLC*-transporters and all major *CYP* genes except *CYP1A1*, *2C19*, and *2E1*. Four of the phase II metabolism genes showed significant changes (*GSTA2*, *NAT2*, *SULT1B1*, and *UGT2B7*). Among the inflammation related genes only *SOD2* was significantly affected, possibly due to the generally high variance in this group of genes. The fold changes obtained from qPCR analysis were also higher than those from microarray analysis in many cases (24 genes).

A significant correlation of gene expression changes from microarray and qPCR analysis of the validation set is shown in **Figure 30** (Pearson  $r=0.93$ ,  $p < 0.0001$ , 95% CI=0.86 – 0.97). The correlation between gene expression changes from microarray and qPCR analysis of the discovery set was even higher (Pearson  $r=0.96$ ,  $p < 0.0001$ , 95% CI=0.93 – 0.98; figure not shown).

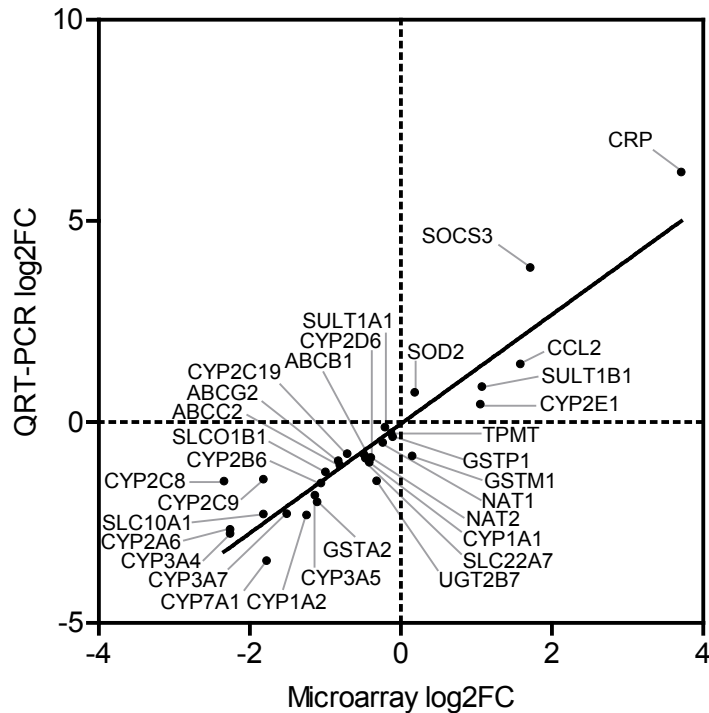


**Figure 30** Correlation of gene expression changes from microarray and qPCR analysis. QPCR assays were used in an independent donor set (validation set,  $N = 11$ ) for biological cross-validation of DNA microarray results ( $N = 4$ ). The log<sub>2</sub> fold changes (IL-6 vs. control) as determined by microarray (x-axis) and qPCR (y-axis) are plotted to visualize the correlation of relative expression of 32 genes. These genes include major AP markers involved in the IL-6 response and essential phase I/II metabolism, and transporter genes. Pearson parametric correlation analysis was performed ( $p = 0.93$ ;  $p < 0.0001$ ).

#### 4.3.1.3 Identification of over-represented annotation terms

To be able to interpret the differentially expressed genes in a biological context, over-represented gene ontologies (GO) were identified using Fisher's Exact Test in the category "biological process". 413 of the 508 differentially expressed genes in IL-6-challenged PHH were assigned to 74 GO terms with a Bonferroni adjusted p-value  $\leq 0.05$  (**Supplement Table 3**). The top GO terms in the category "biological process" are shown in **Figure 31**.

## RESULTS

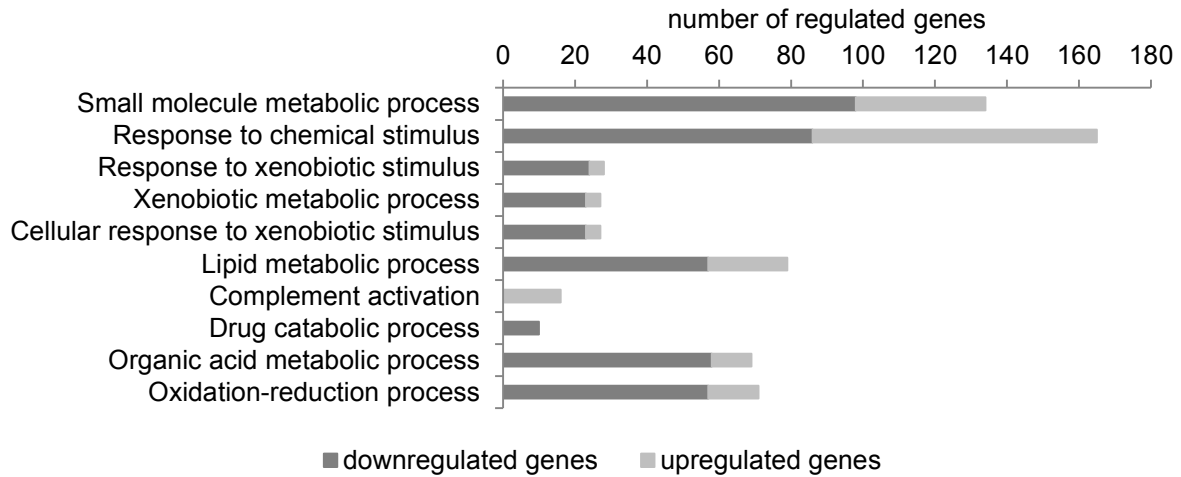


**Figure 31** Top ten significantly over-represented GO terms in the category “*biological process*” in IL-6-challenged PHH. The numbers of up- and downregulated genes within the terms are indicated by bars. Terms are ranked by Bonferroni-adjusted p-value from top ( $p = 7.48E-15$ ) to bottom ( $p = 5.43E-10$ ). For GO IDs and p-values refer to **Supplement Table 3**.

Most of these terms contained a higher proportion of downregulated genes compared to upregulated genes. The two top terms did not provide much biological information due to their high level in ontology hierarchy. The terms “*Response to xenobiotic stimulus*”, “*Xenobiotic metabolic process*”, “*Cellular response to xenobiotic stimulus*”, and “*Drug catabolic process*” contained mostly downregulated genes. The enriched term “*Complement activation*”, however, contained only upregulated genes. Among the other top significantly enriched GO terms, many redundancies were found. This is a common appearance in gene annotation analyses. Here, this issue was addressed by summarizing all significantly over-represented terms with the REVIGO online tool, based on their p-value. This analysis not only broke down the long list of enriched (and repetitive) GO terms, but also indicated the “core” biological processes that were influenced in IL-6-challenged PHH. Here, only three major representative processes were found: “*Lipid metabolism*”, “*Xenobiotic metabolism*”, and “*Defense response*”.

#### 4.3.1.4 Identification of over-represented regulatory pathways

Molecular interaction networks were identified by applying DAVID gene term enrichment analysis on the 508 differentially expressed genes in IL-6-challenged PHH, using the network database KEGG. 91 of the 508 differentially expressed genes were assigned to 26 KEGG pathways with an EASE Score  $< 0.1$ . After Bonferroni-adjustment for multiple testing, eight significantly enriched KEGG pathways remained (**Figure 32**).

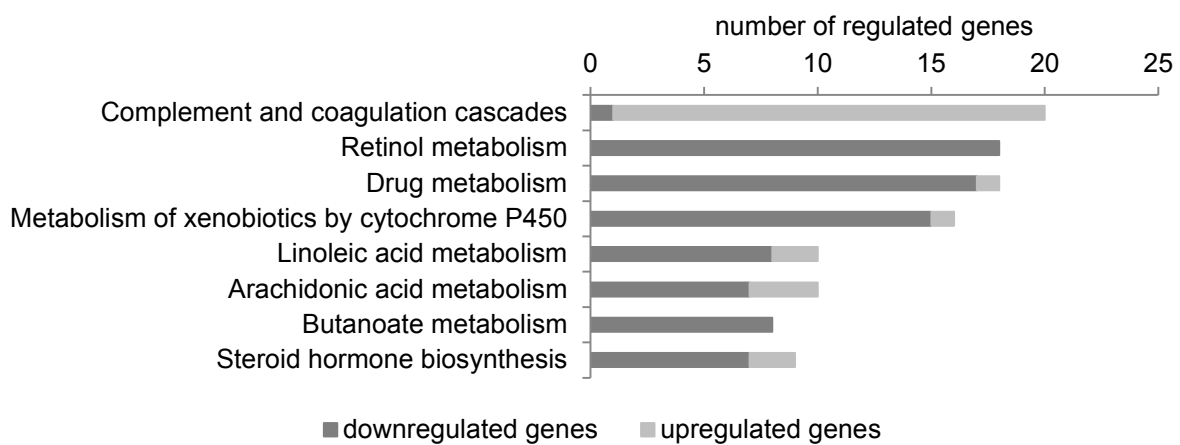


**Figure 32** Significantly over-represented KEGG pathways in IL-6-challenged PHH. The numbers of up- and downregulated genes within the terms are indicated by bars. Terms are ranked by Bonferroni-adjusted p-value from top ( $p = 7.46E-10$ ) to bottom ( $p = 0.044$ ).

The top enriched pathway was “*Complement and coagulation cascades*”. The three pathways “*Retinol metabolism*”, “*Drug metabolism*”, and “*Metabolism of xenobiotics by cytochrome P450*” showed a large overlap in their gene sets, including many major downregulated DMET genes. All other over-represented pathways also contained mainly DMET genes. The pathways “*Drug metabolism*” and “*Metabolism of xenobiotics by cytochrome P450*” contained solely one upregulated gene, *CYP2E1*.

Overall, IL-6 appeared to influence mostly xenobiotic metabolism related interaction networks in a negative manner. This is in agreement with the enriched biological processes as determined in the GO term analyses.

### 4.3.2 Retrospective transcriptome study in patients with elevated CRP

Transcriptome-wide gene expression profiles of 105 liver samples, generated previously by using Human-WG-6v2 Expression BeadChips (Schröder et al., 2013), were reanalyzed for a retrospective transcriptome study. After combining synonymous probe sets and removal of probes that did not correspond to a mapped gene, 24,754 genes were selected for further analyses.

#### 4.3.2.1 Identification of differentially expressed genes

In livers of patients with elevated CRP ( $> 10\text{mg/l}$ ;  $N = 7$ ) compared to normal CRP ( $\leq 1\text{mg/l}$ ;  $N = 98$ ), 559 genes were differentially expressed with a p value cut-off of  $\leq 0.05$  and a fold change cut-off of  $\geq 1.5$  and  $\leq -1.5$ . All probe sets representing the differentially expressed genes are illustrated in heat maps (**Figure 33**). Complete hierarchical clustering categorized samples and probe sets into distinct clusters. The heat maps revealed clusters of highly increased and decreased gene expression in patients with elevated CRP plasma concentrations (columns on the right, indicated by orange bar). Among all differentially expressed genes that met the above mentioned criteria, up- and downregulated genes were evenly distributed (**Figure 33, A**). DMET genes are summarized in **Figure 33, B**. Remarkably, in patients with elevated CRP plasma concentration, complete hierarchical clustering of probe sets via Pearson correlation revealed a disproportionate fraction of downregulated DMET genes. Similar findings were reported in the Affymetrix transcriptome study in IL-6-challenged PHH. Therefore, transcriptome data from liver samples were subjected to further analyses.

Detailed analysis via Analyst 8.0 software solution revealed 272 upregulated and 287 downregulated genes (**Supplement Table 4**). The most strongly up- and downregulated genes are shown in **Table 21**.

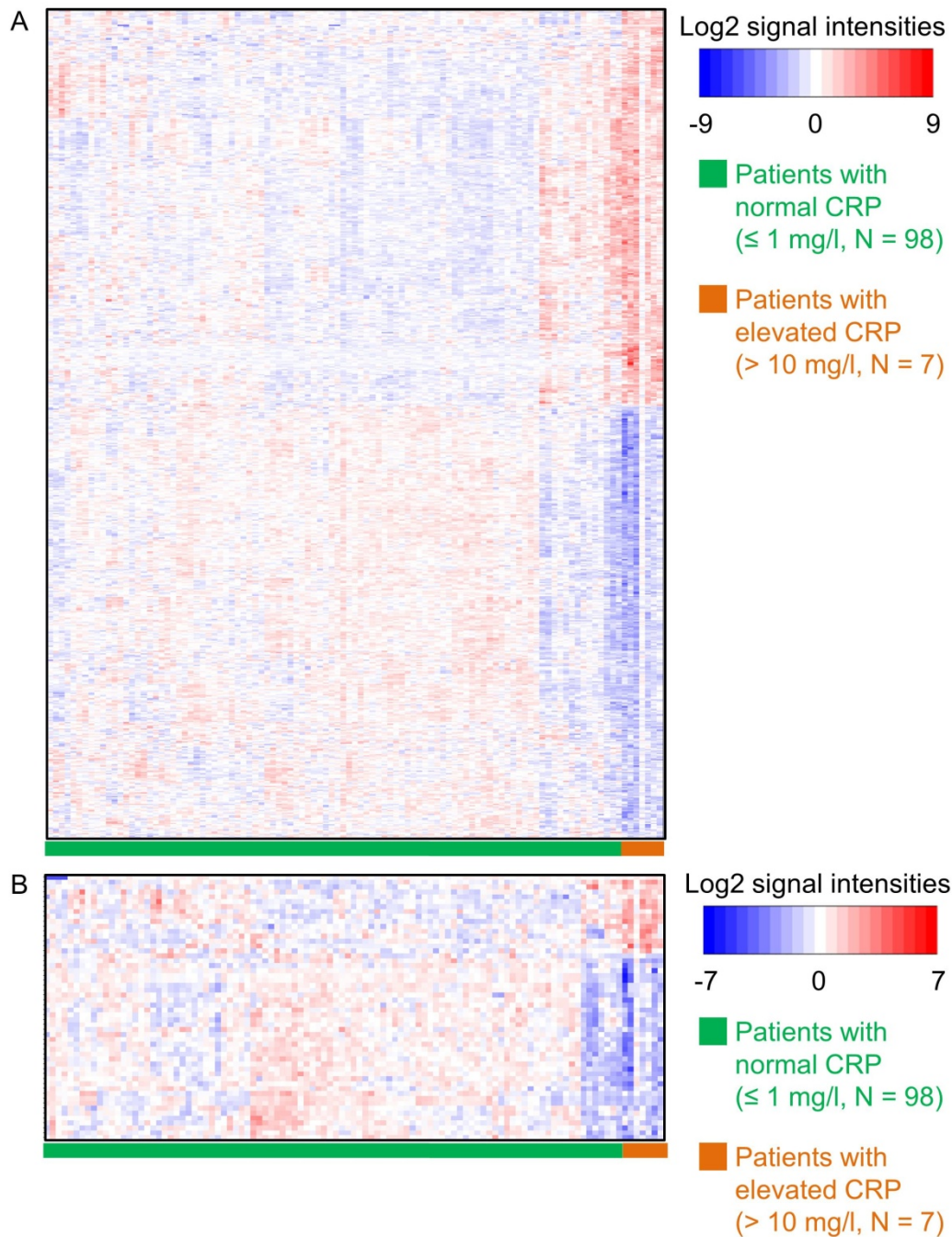


**Figure 33** Heat maps of differentially expressed genes in patients with normal CRP (N = 98) compared to elevated CRP plasma concentrations (N = 7). Data was obtained with Human-WG-6v2 Expression BeadChips and 559 differentially expressed genes with a Welch's t-test p value < 0.05 and a fold change  $\geq 1.5$  were revealed. These genes were represented by 649 probe sets. Columns and rows in heat maps were ordered using complete hierarchical clustering of samples by euclidean distance and complete hierarchical clustering of probe sets via Pearson correlation, respectively. Normalized log<sub>2</sub> signal intensities, centered and standardized per probe set, are shown in color code (blue = low, white = mid, red = high). Heat map **A** shows all 559 probe sets described above, whereas only probe sets representing DMET genes are shown in **B**.

## RESULTS

**Table 21** Top differentially expressed genes in livers of patients with elevated CRP (> 10 mg/l) compared to normal CRP (≤ 1 mg/l).

Gene symbol	Gene name	log <sub>2</sub> FC	SD	P-Value <sup>a</sup>
<i>Upregulated genes</i>				
<i>SPINK1</i>	Serine Peptidase Inhibitor, Kazal Type 1	5.43	± 2.91	6.24E-04
<i>PLA2G2A</i>	Phospholipase A2, Group IIA	4.49	± 2.39	3.77E-04
<i>SAA2</i>	Serum amyloid A2	4.46	± 1.85	1.34E-06
<i>SAA1</i>	Serum amyloid A1	4.42	± 1.78	2.74E-05
<i>CCL20</i>	Chemokine Ligand 20	3.14	± 2.60	1.01E-02
<i>GPX2</i>	Glutathione Peroxidase 2	2.89	± 1.55	2.80E-05
<i>LCN2</i>	Lipocalin 2	2.88	± 1.79	2.32E-03
<i>CSAG3A</i>	CSAG Family, Member 3	2.40	± 1.31	2.56E-03
<i>UBD</i>	Ubiquitin D	2.20	± 1.95	3.77E-03
<i>RASD1</i>	RAS, Dexamethasone-Induced 1	2.20	± 1.90	7.86E-03
<i>Downregulated genes</i>				
<i>HSD17B13</i>	Hydroxysteroid (17-Beta) Dehydrogenase 13	-2.26	± 1.30	2.07E-03
<i>BBOX1</i>	Butyrobetaine (Gamma), 2-Oxoglutarate Dioxygenase 1	-2.13	± 1.70	5.96E-03
<i>GSTA5</i>	Glutathione S-Transferase Alpha 5	-2.10	± 1.62	6.64E-03
<i>HEPACAM</i>	Hepatic And Glial Cell Adhesion Molecule	-2.07	± 1.83	1.07E-02
<i>BCHE</i>	Butyrylcholinesterase	-2.07	± 1.16	9.79E-04
<i>GSTA2</i>	Glutathione S-Transferase Alpha 2	-2.06	± 1.66	1.41E-02
<i>PFKFB1</i>	Fructose-2,6-Biphosphatase 1	-2.02	± 1.10	2.07E-03
<i>CYP2C19</i>	Cytochrome P450, Family 2, Subfamily C, Polypeptide 19	-1.99	± 1.80	1.11E-02
<i>GSTA1</i>	Glutathione S-Transferase Alpha 1	-1.97	± 1.70	1.91E-02
<i>SRD5A2</i>	Steroid-5-Alpha-Reductase, Alpha Polypeptide 2	-1.92	± 1.34	5.52E-03

Log<sub>2</sub>FC = log<sub>2</sub> fold change, elevated CRP compared to normal. Values represent mean for for N = 7 (CRP hi.) and N = 98 (CRP norm.) arrays per group

<sup>a</sup> Two groups Welch's t

The serine peptidase inhibitor *SPINK1* was the most upregulated gene in liver samples from patients with elevated CRP plasma levels. The AP markers *PLA2G2A*, *SAA1*, and *SAA2* also showed a strong fold induction, so did the chemokine *CCL20*. Interestingly, the DMET gene *GPX2* was highly upregulated.

*HSD17B13* was identified as the most downregulated gene in patients with elevated CRP plasma levels. Furthermore, the four DMET genes *GSTA1*, *GSTA2*, *GSTA5*, and *CYP2C19* showed a decreased expression. Notably, *CYP3A4* was more than 3-fold repressed (data not shown) with a borderline significance (p = 0.07).

All differentially regulated DMET genes in patients with elevated CRP plasma levels are summarized in **Table 22**. In total, 13 DMET genes were upregulated. 29 DMET genes were identified with a decreased expression. These included important phase I metabolism (e.g.,

## RESULTS

*CYPs* and *ADHs*), phase II metabolism (e.g., *GSTs* and *UGTs*), and transporter genes (e.g., *ABCs* and *SLCs*).

**Table 22** Differentially expressed DMET genes in livers of patients with elevated CRP (> 10mg/l) compared to normal CRP (≤ 1mg/l).

Gene symbol	log2FC	SD	P-value <sup>a</sup>	Gene symbol	log2FC	SD	P-value <sup>a</sup>
<b>Upregulated genes</b>							
<i>GPX2</i>	2.89	± 1.55	2.80E-05	<i>ADH4</i>	-1.43	± 1.39	2.82E-02
<i>SLC5A6</i>	1.49	± 1.12	4.03E-03	<i>CYP2A6</i>	-1.40	± 1.03	3.84E-03
<i>GPX3</i>	1.13	± 0.61	1.57E-04	<i>ADH6</i>	-1.17	± 0.93	5.29E-03
<i>SOD2</i>	1.03	± 1.01	6.65E-04	<i>UGT2B17</i>	-1.11	± 0.55	4.89E-03
<i>SLC7A5</i>	0.81	± 0.95	2.81E-02	<i>CYP2A7</i>	-1.10	± 1.41	4.11E-02
<i>SLCO4A1</i>	0.79	± 0.88	2.15E-02	<i>SLCO1B1</i>	-1.00	± 0.66	1.20E-03
<i>SULT2A1</i>	0.78	± 1.59	1.18E-04	<i>ABCG2</i>	-0.98	± 0.70	4.63E-03
<i>CYP21A2</i>	0.77	± 0.96	1.70E-02	<i>CYP39A1</i>	-0.92	± 1.01	4.10E-02
<i>NNMT</i>	0.70	± 0.86	7.03E-03	<i>UGT2B10</i>	-0.91	± 1.00	3.18E-02
<i>DHRS13</i>	0.68	± 0.54	5.78E-03	<i>XDH</i>	-0.91	± 0.65	3.33E-03
<i>ALDH4A1</i>	0.67	± 0.55	1.95E-02	<i>SLC22A1</i>	-0.89	± 1.00	3.32E-02
<i>SLC7A7</i>	0.65	± 0.59	4.61E-03	<i>CYP4A11</i>	-0.85	± 0.91	4.60E-02
<i>CYP8B1</i>	0.61	± 0.72	4.16E-02	<i>NR1I3</i>	-0.82	± 0.77	2.19E-02
<b>Downregulated genes</b>							
<i>GSTA5</i>	-2.10	± 1.62	6.64E-03	<i>UGT2B11</i>	-0.78	± 0.73	1.43E-02
<i>GSTA2</i>	-2.06	± 1.66	1.41E-02	<i>PON1</i>	-0.73	± 0.83	3.14E-02
<i>CYP2C19</i>	-1.99	± 1.80	1.11E-02	<i>CYP2C18</i>	-0.71	± 0.63	1.05E-02
<i>GSTA1</i>	-1.97	± 1.70	1.91E-02	<i>ALDH5A1</i>	-0.69	± 0.74	3.57E-02
<i>CYP1A2</i>	-1.90	± 2.08	4.06E-02	<i>ALDH7A1</i>	-0.65	± 0.65	2.69E-02
<i>SLC22A10</i>	-1.66	± 1.09	1.72E-05	<i>UGT2B15</i>	-0.65	± 0.91	3.83E-02
<i>CYP3A43</i>	-1.59	± 1.58	2.19E-02	<i>PDE3B</i>	-0.62	± 0.46	6.10E-04
				<i>PON3</i>	-0.61	± 0.60	1.66E-02
				<i>CAT</i>	-0.60	± 0.58	1.47E-02

Log2FC = log2 fold change, elevated CRP compared to normal. Values represent mean for for N = 7 (CRP hi.) and N = 98 (CRP norm.) arrays per group

<sup>a</sup> Two groups Welch's t

### 4.3.2.2 Identification of over-represented annotation terms and regulatory pathways

The 24 significantly over-represented annotation terms in the category “*biological process*” in patients with elevated CRP plasma levels are shown in **Supplement Table 5**. The top ten GO terms are illustrated in **Figure 34**. Many of these terms belonged to higher hierarchical levels, meaning that they were rather unspecific. Remarkably, the terms “*Xenobiotic metabolic process*” and “*Cellular response to xenobiotic stimulus*” were identified as highly enriched and contained mostly downregulated genes. Other interesting findings were the enrichments of the terms “*Cellular amino acid metabolic process*”, “*Carboxylic acid catabolic process*”, and “*Monocarboxylic acid metabolic process*”, hinting at an influence on amino acid

## RESULTS

metabolic processes in general. REVIGO summary analysis revealed the major term “*Organic acid metabolism*” as a broad representative process which is influenced in patients with elevated CRP plasma levels.

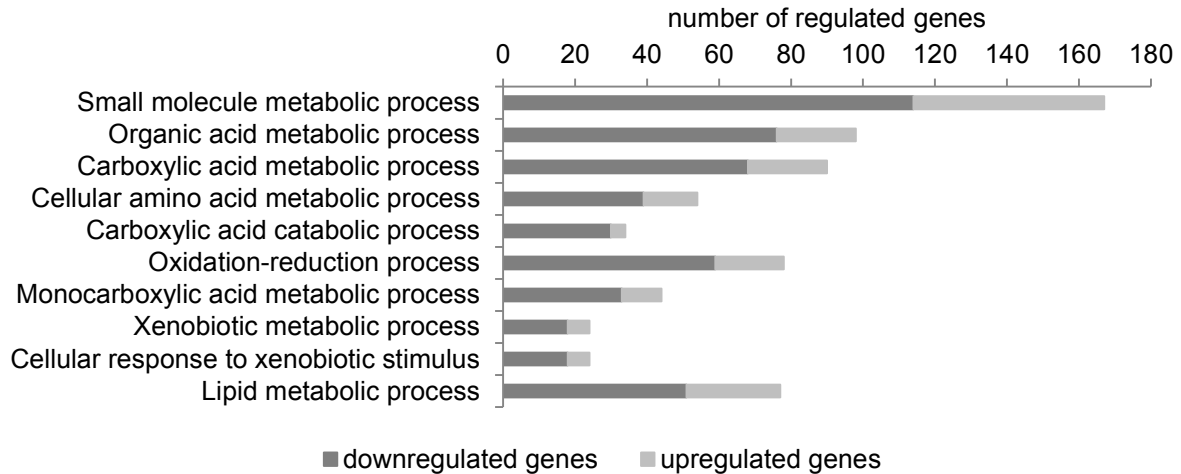


**Figure 34** Top ten significantly over-represented GO terms in the category “*biological process*” in patients with elevated CRP plasma levels. The numbers of up- and downregulated genes within the terms are indicated by bars. Terms are ranked by Bonferroni-adjusted p-value from top ( $p = 8.01E-24$ ) to bottom ( $p = 3.86E-7$ ). For GO IDs and p-values refer to **Supplement Table 5**.

DAVID’s KEGG enrichment analysis revealed six significantly enriched pathways, which are shown in **Figure 35**. The most significantly enriched pathway was “*Glycine, serine and threonine metabolism*” with 11 out of 12 genes downregulated. The enriched pathways “*Retinol metabolism*”, “*Drug metabolism*”, and “*Metabolism of xenobiotics by cytochrome P450s*” contained only downregulated DMET genes.

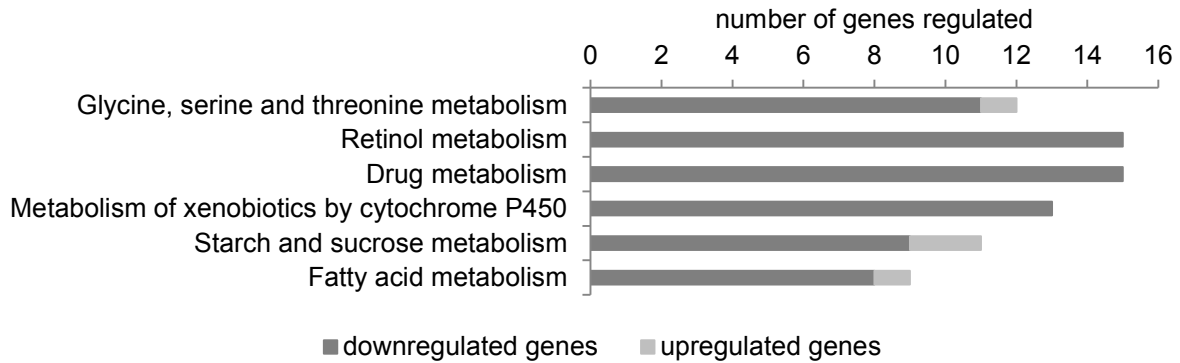


**Figure 35** Significantly over-represented KEGG pathways in patients with elevated CRP plasma levels. The numbers of up- and downregulated genes within the terms are indicated by bars. Terms are ranked by Bonferroni-adjusted p-value from top ( $p = 5.41E-6$ ) to bottom ( $p = 0.042$ ).

Taken together, mainly processes and interaction networks related to xenobiotic and amino acid metabolism appeared to be affected in livers of patients with elevated CRP plasma levels (*in vivo*). All enriched xenobiotic related processes and interaction networks mainly contained downregulated genes. This is in good agreement with the findings in IL-6-challenged PHH (*ex vivo*). However, a broader spectrum of metabolic processes appeared to be affected *in vivo*, as indicated by the enriched core biological process “*Organic acid metabolism*”.

### 4.3.3 Combined and comparative analyses

For a combined analysis of microarray data, obtained from IL-6-challenged PHH and liver samples from patients with elevated CRP plasma levels, an intersection between all mapped genes was created, resulting in 16,684 genes. Among these common genes, an overlap of 44 upregulated ( $p \leq 0.05$  and  $FC \geq -1.5$ ) and 55 downregulated genes ( $p \leq 0.05$  and  $FC \leq -1.5$ ) was identified (**Figure 36**). Among the commonly upregulated genes, the AP genes *CCL20*, *CRP*, *LBP*, and *SAA2* were found. Furthermore, five upregulated DMET genes were identified, as indicated by bold letters. Among the commonly downregulated genes, a total of 16 DMET genes were found.

## RESULTS

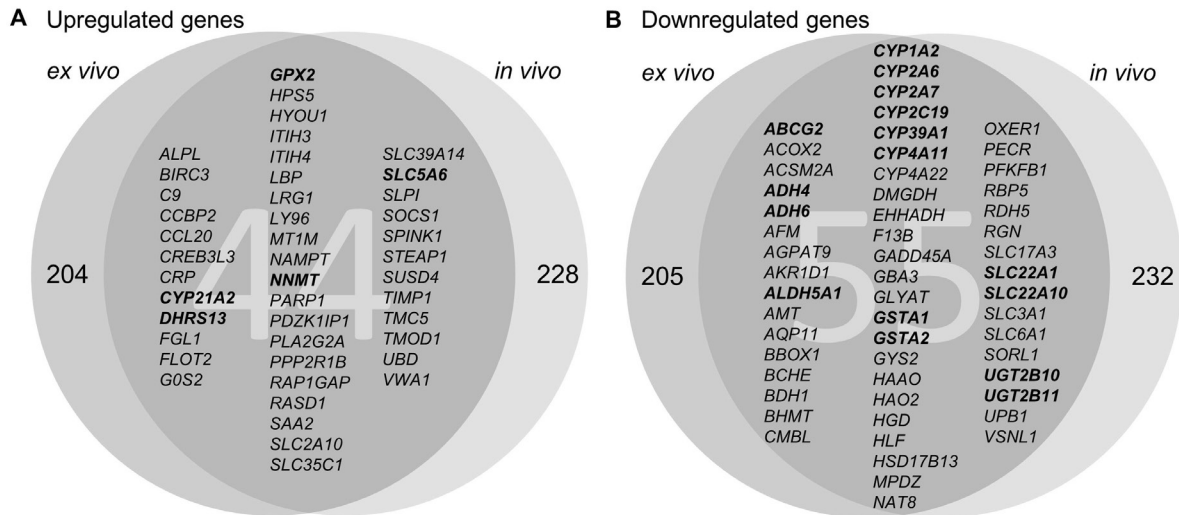


**Figure 36** Overlapping genes between IL-6-challenged PHH (*ex vivo*) and liver samples with elevated CRP plasma levels (*in vivo*). Shown are the significantly (**A**) upregulated and (**B**) downregulated genes with a p-value cut-off of  $\leq 0.05$  and a fold change cut-off of  $\geq 1.5$  and  $\leq -1.5$ , respectively. Numbers represent the number of genes in each group. DMET genes are indicated in **bold** letters.

The commonly up- and downregulated genes were combined to a union group (N = 99).

Fisher's exact test revealed 15 over-represented GO terms in the category "biological process" with a Bonferroni adjusted p-value  $\leq 0.05$  (**Supplement Table 6**). The three most significantly enriched GO terms were "Xenobiotic metabolic process", "Cellular response to xenobiotic stimulus", and "Response to xenobiotic stimulus". These redundant terms contained the same set of twelve downregulated genes which were almost exclusively DMET genes (e.g., *ADHs* and *CYPs*). REVIGO summarized all enriched GO terms to "Xenobiotic metabolism" as a major representative and "Drug metabolism" as a minor representative process.

According to DAVID gene term enrichment analysis, four KEGG pathways were significantly enriched with a Bonferroni adjusted p-value  $\leq 0.05$ : "Retinol metabolism", "Drug metabolism", "Metabolism of xenobiotics by cytochrome P450s", and "Fatty acid metabolism". They mainly contained downregulated genes.

Here, the commonly influenced biological processes and regulatory networks in IL-6-challenged PHH and liver samples from patients with elevated CRP plasma levels were identified. A negative impact on xenobiotic metabolic related processes appeared to be of major importance.

## 5 DISCUSSION

It has long been known that the inflammatory response results in downregulation of many DMETs (Aitken et al., 2006; Morgan, 1997). This can lead to decreased microsomal metabolism and reduced drug clearance, in particular by cytochrome P450s, as could be shown in several clinical studies using specific probe drugs (Becquemont et al., 2002; Carcillo et al., 2003; Jakob et al., 2002; Molanaei et al., 2012). Yet, the reason for this pathophysiological consequence is still a major question. The mechanisms leading to alterations in drug clearance during the host response to inflammation or infection can be explained in part by transcriptional suppression but also by post-transcriptional mechanisms (Aitken and Morgan, 2007; Jover et al., 2002; Morgan, 2001). However, a recent symposium report, summarizing the advances in regulation showed that the current knowledge in this field is still scarce (Morgan et al., 2008). Furthermore, the use of animal models is complicated due to interspecies differences in expression and regulation of, e.g., P450s and the inflammatory response in general (Morgan, 1997; Seok et al., 2013). Hence, human models are required for reliable studies, yet costly and limited in availability. Only one study investigated the effects of an inflammatory mediator on the expression of a large panel of DMETs in a systematic way, however, the implication of their findings in the context of drug metabolism was lacking (Yang et al., 2012). Other studies in this field were rather focused on, e.g., specific drug transporters (Vee et al., 2009) or P450s (Siewert et al., 2000). Furthermore, mechanistic aspects of the regulation of drug metabolizing enzymes and transporters in infection and inflammation have not been investigated in a systematic manner.

Therefore, in a first part of this thesis, PHH, the gold standard for the investigation of hepatic drug and xenobiotic metabolism *in vitro* (Lecluyse and Alexandre, 2010), were challenged with the pro-inflammatory cytokine IL-6. This particular cytokine was selected because it was shown to be a major cytokine responsible for the hepatic P450 downregulation (Siewert et al., 2000). Changes in gene expression of a large panel of DMETs were investigated as well as the impact on P450 activities. PP analyses were carried out to identify the IL-6 responsive signaling pathways. Their roles in the regulation of DMET genes during inflammatory conditions were investigated by chemical activation/inhibition and siRNA-mediated KD of signaling molecules.

The interindividual variability of PHH complicates the investigation of sensitive regulatory mechanisms. Therefore, in the second part of this thesis it was investigated, whether the

HepaRG cell line is a useful model for studying the impact of inflammatory mediators on human drug metabolism. This cell line has previously been shown to retain many functional characteristics of PHH including the expression of key metabolic enzymes, drug transporters, and NRs (Andersson et al., 2012).

The last part of this thesis focused on the impact of inflammatory mediators on the drug metabolism system in an unbiased genome-wide context, addressing the question, why the previously observed effects could be advantageous for the organism. For this purpose, genome-wide mRNA expression was analyzed in IL-6-challenged PHH. The findings were compared to a retrospective genome-wide analysis in liver samples from patients having undergone an APR in order to relate findings from cellular models to the *in vivo* organ level.

### **5.1 Influence of the inflammatory mediator interleukin-6 on drug metabolizing enzymes and transporters**

CRP is a sensitive and systemic marker of inflammation and is only produced in hepatocytes under the transcriptional control of IL-6 (Pepys and Baltz, 1983; Pepys and Hirschfield, 2003). Here, IL-6 stimulation of PHH led to highly increased mRNA expression (up to 200-fold) of *CRP*, confirming an activation of the APR. The expression of the AP gene *SAAI/2*, for which IL-6 was shown to play a critical role in induction, was also upregulated (Hagihara et al., 2004). Furthermore, increased expression of *SOCS3*, a negative feedback regulator, supported the activation of the IL-6 signaling cascade (Starr et al., 1997).

Gene expression changes of a total of 83 genes were determined by high-throughput TaqMan® qPCR in IL-6-challenged PHH. The profiles revealed a concerted downregulation of many, but not all, DMETs upon IL-6 stimulation. These effects appeared to be very conservative among the different donors despite the extraordinarily large interindividual variability of drug metabolism among humans (Zanger, 2012). In the following, not all examined genes will be discussed. The focus will be primarily on changes in drug metabolism and drug transporter related genes.

In various models, inflammation and infection were associated with decreased hepatic expression and activity of P450s (Aitken et al., 2006; Morgan, 2009), with some (e.g., 2B6, 2C9, 2C19, and 3A4) more strongly affected by IL-6 than by other inflammatory agents (Aitken and Morgan, 2007). Here, in IL-6-challenged PHH, a coordinated transcriptional

suppression of the *CYP* isoforms *1A1*, *1A2*, *2A6*, *2B6*, *2C8*, *2C9*, *2C19*, *2D6*, *3A4*, *3A5*, *3A7*, and *7A1* was observed after 24 hours. The mRNA of some *CYPs* (e.g., *1A1*, *1A2*, and *7A1*) was strongly suppressed as early as 8 hours after the stimulation. In fact, time course experiments showed a strong suppression (> 80%) of *CYP7A1* after only 2 hours (data not shown). This is in agreement with observations that were previously made in primary rat hepatocytes during inflammatory conditions (Gupta et al., 2001). *CYP7A1* encodes for cholesterol 7 $\alpha$ -hydroxylase, the rate-limiting enzyme in bile acid synthesis. Under physiological conditions it is feedback inhibited by Kupffer cell-derived cytokines in response to bile acids returning to the liver via enterohepatic circulation (Chiang, 2009). Because bile acids in the enterohepatic circulation play an important role in whole-body lipid homeostasis (Chiang, 2009), a rapid regulation of *CYP7A1* may be favorable for the organism. Here, the IL-6 stimulation appeared to trigger this important feedback mechanism.

Remarkably, the suppression of mRNA levels was also shown to translate into reduced enzyme activities of six examined *CYPs*. Metabolite formation rates 72 hours after IL-6 exposure indicated decreased activities of the *CYP* isoenzymes *1A2*, *2B6*, *2C8*, *2C9*, *2C19*, and *3A4*. All were decreased by at least 50%. The activity of *CYP3A4*, which is known to be responsible for the oxidative metabolism of > 30% of all known drugs (Zanger et al., 2008), was repeatedly shown to be suppressed by more than 70%. Since *CYPs* of the families 1, 2, and 3 (with major contributors *2C9*, *2D6*, *2C19*, *2C8*, and *2B6*) are responsible for catalyzing three quarters of all known drug oxidations (Anzenbacher and Anzenbacherová, 2012; Zanger et al., 2008), potential adverse clinical impacts are evident. Indeed, reduced clearance of specific drugs/selected probe drugs in patients with acute and chronic infectious states of aseptic or septic etiology were previously shown (**1.3.1**).

Interestingly, unlike most major *CYP* isoforms, *CYP2E1* expression was induced upon IL-6 stimulation and translated into an approximately 2-fold increased enzyme activity in some donors. This is contrary to previous observations in human and rodent models where pro-inflammatory cytokines usually caused a repression of *CYP2E1* (Abdel-Razzak et al., 1993; Hakkola et al., 2003; Siewert et al., 2000). The constitutive expression of hepatic *CYP2E1* is known to be mainly regulated by HNF-1 $\alpha$  (Gonzalez, 2007). However, the mechanisms of induction or suppression of the *CYP2E1* enzyme are still poorly understood due to their complexity, involving transcriptional, translational, and post-translational effects (Gonzalez, 2007). A recent report by Lee and colleagues demonstrated an involvement of the PI3K pathway in *CYP2E1* induction in PHH (Lee et al., 2014). This very interesting observation

will be discussed in the following chapter of this thesis in the context of signaling pathways that are involved in DMET gene regulation (5.2). Regardless, it remains to be elucidated why the rather highly expressed *CYP2E1* (Zanger and Schwab, 2013) is upregulated whereas all other major CYP isoforms are downregulated during the inflammatory response. One possibility may be that an increased activity of CYP2E1 leads to elevated oxidative stress (Thurman et al., 1999) that aggravates the inflammatory response, therefore sensitizing the liver to pro-inflammatory cytokines (Cederbaum et al., 2012).

To date, only little is known about the impact of inflammatory signaling on phase II drug metabolizing enzymes. Several studies in humans and rodents showed only minor decrease in *UGT* expression (Aitken et al., 2006). IL-6 suppressed *UGT1A1* mRNA expression in primary rat hepatocytes (Strasser et al., 1998) and a study in human liver revealed a correlation between decreased gene expression of *UGT2B7* and inflammation (Congiu et al., 2002). These findings could be confirmed in this work in PHH exposed to IL-6, where *UGT1A1* expression showed a negative trend and *UGT2B7* was significantly downregulated by > 50%. *SULT1A1* and *IBI* mRNA expression appeared to be highly variable with a tendency towards upregulation during inflammatory conditions in PHH. This is, at least in parts, in accordance with data showing enhanced activity of SULT1A1 in patients with hepatocellular carcinoma (Wang et al., 2010) and in patients with active Crohn's disease (Waring et al., 2013). Contrary, previous studies in livers of rats with increased IL-6 sera levels showed decreased mRNA levels of *SULT1A1* and *IBI* (Shimada et al., 1999). These findings indicate that the variability of SULTs during inflammation is species specific. Studies in rat hepatocytes demonstrated interleukin-dependent suppression of mRNA expression of *GSTA2* while *GSTP1* expression was not decreased (Maheo et al., 1997), which is consistent with the findings in PHH exposed to IL-6. *NAT1* and 2 mRNA expression was also decreased which in case of the former has been shown to be cytokine dependent (Buranrat et al., 2007). Despite this apparently selective rather than coordinated suppression of phase II metabolizing enzymes by IL-6, adverse clinical impacts are possible. However, due to a lack of human studies in this field, this remains speculative.

The drug transporters MDR1 (encoded by *ABCB1*) and MRP2 (*ABCC2*) are key transporters in hepatic biliary secretion (Petrovic et al., 2007). Both were significantly downregulated in PHH exposed to IL-6, consistent with previous findings in rodents (Siewert et al., 2004; Sukhai et al., 2000) and human hepatocytes (Vee et al., 2009; Yang et al., 2012). Apart from the effects on hepatic-biliary efflux transporters, the amounts of mRNA from several

members of the SLC transporter families were shown to be decreased in livers of LPS-treated rodents and in IL-6-treated human hepatocytes (Cherrington et al., 2004; Teng and Piquette-Miller, 2005; Yang et al., 2012). Here, the mRNA expression of the bile acid uptake transporter *SLC10A1* (coding for NTCP) was significantly decreased by more than 70%, consistent with previous findings (Vee et al., 2009). The organic anion transporters *SLC22A7* (OAT2) and *SLCO1B1* (OATP2) were not as strongly, however significantly suppressed. Such coordinated downregulation of drug transporters involved in secretion and clearance of bile acids as well as other compounds during inflammatory conditions may be clinically relevant. Future studies in human tissues are required for elucidating the clinical impacts of these inflammation-related drug transporter changes.

Major P450s and drug transporters are not only expressed in the liver but also in the gastrointestinal tract (Pond and Tozer, 1984; Shen et al., 1997). There they contribute to the so-called first-pass effect by absorption and metabolism of orally administered drugs in their transit to the systemic circulation and thereby limit their bioavailability (Shen et al., 1997). It was previously shown in rats that endotoxin-induced inflammation imposes a reduction in expression and activity of MDR1, MRP2, and CYP3A4 in the intestine (Kalitsky-Szirtes et al., 2004), similar to observations in the liver. Here, the impact of inflammatory signaling on DMETs in the human intestine was not addressed. Therefore, it remains to be investigated whether the first-pass metabolism is also negatively affected during inflammation in humans.

Only a few studies, primarily in rodents, addressed the regulation of gene expression of NRs and other modifiers of DMETs in the liver. For instance, reduced P450 enzyme expression was associated with repression of CAR (*NR1I3*) and PXR (*NR1I2*) mRNA levels in mouse liver during the APR (Beigneux et al., 2002). Interestingly, both NRs were shown to be significantly downregulated in PHH exposed to IL-6. In the case of PXR, this is consistent with previous findings of others which have observed lower PXR levels in IL-6-treated human hepatocytes (Pascussi et al., 2000). Since CAR and PXR are major regulators of DMET genes (Tolson and Wang, 2010), their reduced basal levels may cause decreases in transcription and expression of these genes. However, it is unlikely that a reduced mRNA expression of CAR and PXR strongly affected the abundance of the respective functional NR within only 24 hours. Hence, this route of action could have only partially contributed to the short-term downregulation of DMET genes but may be important for a sustained response.

Interestingly, the enzymatic antioxidant superoxide dismutase 2 (*SOD2*) was upregulated in IL-6-stimulated PHH. *SOD2* is primarily responsible for detoxification of ROS (Rahman, 2007). P450-catalyzed reactions are known to generate ROS and *CYP2E1* is particularly active in this respect (Guengerich, 2012). Since *CYP2E1* was found to be induced in IL-6-challenged PHH, a concomitant upregulation of *SOD2* may be a protective mechanism. In fact, it was shown that ROS activates NF- $\kappa$ B (Gilmore, 2006), and NF- $\kappa$ B induces the expression of *SOD2* (Storz et al., 2005). Conversely, it was previously discussed that ROS and their related factors may be involved in downregulation of P450s to prevent further deleterious effects (Morgan, 2001). However, the mechanisms are not well understood and often contradictory. Collectively, in this study, the gene expression of other important NRs (e.g., FXR, LXR, PPARs, and RXR) as well as hepatic nuclear factors HNF-1 $\alpha$  and HNF-4 $\alpha$  was not significantly affected in IL-6-treated PHH.

Taken together, stimulation of PHH with IL-6 led to highly increased gene expression of major APPs and a concomitant downregulation of major DMETs in a coordinated fashion. Most prominently affected was the mRNA expression of major P450s, which also translated into highly reduced activities of some isoforms. Some major phase II metabolizing enzymes (*GSTs* and *UGTs*) were significantly suppressed by IL-6, whereas some were induced (*SULTs*). Important multidrug and organic anion transporters were coordinately downregulated. Such global repression caused by inflammation in humans is very likely to contribute to the known alterations of pharmacokinetic features of drugs.

## **5.2 Inflammatory signaling pathways involved in the regulation of drug metabolizing enzymes and transporters**

This part of the thesis targeted the identification of IL-6 response pathways and how they may contribute to the coordinated downregulation of DMETs. Whereas post-transcriptional regulation may play a role, transcriptional suppression was suggested to be the primary mechanism for the decline of CYP and drug transporter mRNAs in liver (Aitken et al., 2006; Petrovic et al., 2007). Molecular mechanisms that may or may not be involved are summarized in chapter 1.3.2.

First, major IL-6 responsive signaling pathways were identified by PP analyses. Only a few major signaling molecules demonstrated increased phosphorylation status, namely AKT (S473), ERK1/2 (T202/Y204), STAT1 (Y701), and STAT3 (Y705). These findings were also

confirmed by Western blot analyses. Indeed, STAT1 and STAT3 are well established APR factors that are activated by IL-6 and undergo critical tyrosine phosphorylation of Y701 or Y705, respectively, in order to hetero- or homodimerize (Gerhartz et al., 1996). Their activation thereby confirms a positive IL-6 receptor complex response. However, STAT1 response upon IL-6 stimulation was proposed to be very inefficient (Haan et al., 2005) and was therefore not included in further analyses. Activation of mitogen activated protein kinase ERK1/2 upon IL-6 stimulation was demonstrated to be Gab1-mediated, involving Grb2, Ras, and SHP2 (Eulenfeld et al., 2012; Takahashi-Tezuka et al., 1998). MAPK activation was further shown to be crucial for the balance of IL-6-dependent mitogenic and anti-apoptotic signaling together with STAT3 (Fukada et al., 1996). ERK1/2 activation in PHH exposed to IL-6 was demonstrated. Interestingly, the aforementioned Ras acts as a critical relay switch and is known to activate PI3K, which activates AKT serine/threonine kinases (Cox and Der, 2002). Phosphorylation at S473 is thereby considered to be crucial for full activation of AKT (Franke et al., 1997). In IL-6-challenged PHH, a moderate AKT phosphorylation was repeatedly shown, however, was variable in its magnitude. Western blot data suggested that AKT was already basally present in its phosphorylated state in some donors. This is not surprising since AKT is involved in cell-cycle progression and apoptosis (Chang et al., 2003), and donors of PHH often suffer from liver cancer. Nevertheless, IL-6 led to induction of phosphorylation of AKT at S473. In fact, this can lead to NF- $\kappa$ B activation, as shown previously (Madrid et al., 2001; Ozes et al., 1999; Romashkova and Makarov, 1999). As summarized in chapter 1.3.2, NF- $\kappa$ B may play a central role in the regulation of DMETs during inflammation due to its capability to interfere with NR signaling. So far, there are no studies available that systematically addressed this interesting hypothesis.

By performing chemical pathway inhibition and activation as well as RNA silencing, the role of the PI3K/AKT, MAPK/ERK, and STAT3 pathways in regulation of DMETs was elucidated. Inhibition of STAT3 by Stattic led to repression of IL-6-mediated induction of *SOCS3* mRNA expression. It has previously been shown that cytokines, in particular IL-6, quickly induce the expression of *SOCS3* via STATs, thereby inhibiting the function of JAK by binding to the cytokine receptor (Larsen and Röpke, 2002). Since some cytokine receptors have been shown to induce SOCS independently of STAT (Cassatella et al., 1999), it is not surprising that STAT3 inhibition did not completely abolish *SOCS3* expression. STAT3 inhibition also repressed *CRP* mRNA induction via IL-6. STAT3 has been shown to be involved in transcriptional regulation of *CRP* (Zhang et al., 1996). However, the transcription

factors C/EBP- $\beta$  and NF- $\kappa$ B also play a role (Agrawal et al., 2001; Voleti and Agrawal, 2005). Interestingly, the IL-6-mediated effect on DMET mRNA expression was not largely affected by STAT3 inhibition. This is supported by previous studies, showing that ,e.g., CYP3A4 downregulation by IL-6 is independent of JAK/STAT signaling (Jover et al., 2002). However, some CYP genes of the *CYP2* and *CYP3* families and *SULTs* were moderately attenuated in their downregulation. Since there is no evidence that STAT3 can directly bind to promoter elements of DMET genes and regulate their expression, extensive crosstalks (Eulenfeld et al., 2012) and unspecificity of chemical inhibitors *per se* (Karaman et al., 2008) may be explanations for these observations. It is therefore suggested that STAT3 is not involved in IL-6-mediated downregulation of DMETs.

Inhibition of MEK1/2 (upstream of ERK1/2) by U0126 repressed IL-6-induced *CRP* mRNA expression whereas *SOCS3* expression was increased. The latter was previously observed when SHP2-dependent signaling events (such as MAPK) at the IL-6 receptor complex were inhibited (Schmitz et al., 2000). Among DMET genes, MAPK inhibition strongly affected almost all IL-6-induced effects. In some cases, gene expression changes were actually reversed. Indeed, it has been shown that MAPK signaling is frequently implicated in the regulation of ,e.g., P450s (Murray et al., 2010). Modulation of phosphorylation status of NRs is one of the proposed mechanisms. For instance, LPS stimulation and interleukin signaling have been demonstrated to activate JNK, leading to phosphorylation-dependent nuclear export of RXR- $\alpha$  and therefore interfering with NR signaling (Ghose et al., 2004). RXR- $\alpha$  is of central importance in the regulation of not only CYPs but also many other DMET genes (**see 1.1.2**) and may well be a central player in the coordinated response to IL-6. Available studies in this field are usually very specific. Systematic studies are non-existent. Here, with the help of high-throughput technologies, a broad-scale implication of MAPK signaling events is indicated.

PI3K inhibition moderately interfered with IL-6-mediated induction of *CRP* expression. Downstream NF- $\kappa$ B activity may be responsible for that, since *CRP* expression is in parts also regulated by this TF (see above). *SOCS3* mRNA expression was increased, which can be explained by the SHP2 dependent balance of signaling (see above). Among DMET genes, PI3K inhibition caused a repression of all IL-6-mediated effects. In particular, the downregulation of CYPs was sometimes completely abolished. The mRNA expression of *ABC* transporters and DMET modifier genes was, however, not as strongly affected. As described previously (**1.3.2**), PI3K/AKT signaling can activate NF- $\kappa$ B which was shown to

interfere with NR signaling. This could explain the coordinated effects on DMET genes expression upon IL-6 stimulation. An important role in this regard is thereby also attributed to PI3K/AKT signaling.

Co-inhibition analyses of PI3K and MAPK abolished almost all IL-6-mediated effects on DMET gene expression, supporting previous findings of individual inhibitions. Since STAT3 signaling is anticipated to remain active during this co-inhibition, its negligible role is further emphasized. Contrary to these findings, co-inhibition of STAT3 and MAPK signaling abolished the IL-6-mediated effects on DMET gene expression in a very similar manner. This would attribute less importance to the PI3K/AKT signaling pathway which, according to individual inhibition of this pathway, is not the case. Extensive crosstalk between pathways, in particular MAPK and PI3K/AKT, may explain such contradictory findings (Eulenfeld et al., 2012). It should also be kept in mind that chemical inhibitors, depending on their concentration, can act unspecifically (Karaman et al., 2008) and have, e.g., also been shown to activate NRs (Harmsen et al., 2013).

Stimulations of PHH with a specific PI3K activator revealed patterns of gene expression changes that were highly similar to those observed in IL-6-challenged cells. The majority of DMET genes were drastically downregulated whereas no significant activation of the APR could be determined. These novel findings highlight the importance of PI3K/AKT signaling in the regulation of DMET genes. It was previously discussed that signaling events downstream of the IL-6 receptor complex, such as PI3K/AKT and NF- $\kappa$ B, may converge at NRs, in particular RXR- $\alpha$  (see above). Hence, KD of this central NR was performed in PHH. As expected, the patterns of DMET gene expression changes showed striking similarities to those observed in IL-6-stimulated cells. Together with the effects exerted by PI3K activation, an important role of NF- $\kappa$ B as an antagonistic factor in NR signaling is therefore strongly suggested. Needless to say, detailed mechanistic analyses are required in this area of research.

Taken together, this rather broad approach investigating expression changes of major DMET genes upon IL-6 exposure in PHH in combination with pathway inhibition or activation emphasizes the roles of MAPK and PI3K/AKT signaling. Both pathways appeared to largely contribute to the regulation of DMET genes during inflammation. A detailed analysis by hand, however, is almost impossible due to the large amounts of data created with high-throughput technologies. Crosstalk and feedback events further complicate things. To overcome this challenge, these data are currently being implemented in a systems biology

approach for identifying underlying biological mechanisms contributing to the complex processes of DMET regulation during inflammation in liver. This work is carried out in cooperation with Prof. Dr. Andreas Zell and Roland Keller at the Center for Bioinformatics Tübingen (ZBIT), within the framework of the BMBF project “Virtual Liver”.

### **5.3 HepaRG cells as a model for studying the influence of inflammatory mediators on human drug metabolism**

PHH have become the “gold standard” for the investigation of hepatic metabolism of drugs and other xenobiotics (Lecluyse and Alexandre, 2010). However, primary cells are limited in availability and often costly. Furthermore, many hepatic genes can quantitatively vary among individuals (Rogue et al., 2012). This makes primary cells unpredictable, particularly when investigating sensitive regulatory mechanisms. Therefore, in terms of reliability and reproducibility, the choice of the most suitable cell model remains a matter of debate. The human hepatocellular carcinoma derived HepaRG cell line has been shown to retain many functional characteristics of PHH including the expression of key drug metabolizing enzymes, drug transporters, and nuclear receptors (Andersson et al., 2012; Aninat et al., 2006; Rogue et al., 2012). They are bi-potent progenitor cells and can differentiate into either biliary or hepatocyte lineages (Cerec et al., 2007). HepaRG cells represent the only example of complete differentiation of liver progenitor cells *in vitro* (Andersson et al., 2012), and the gene expression profiles of the differentiated cells are more similar to PHH and human liver tissue than any other liver cell line, particularly among the drug processing genes (Hart et al., 2010). In particular, major P450s were shown to be functionally expressed and selectively inhibited/induced by prototypical P450 inhibitors and inducers (Turpeinen et al., 2009). Thus, HepaRG cells are a useful *in vitro* model for drug metabolism and disposition studies and can, in many cases, replace the requirement for PHH (Andersson et al., 2012).

This work was aimed at evaluating the robustness and the suitability of the highly differentiated human HepaRG cell line in the investigation of the impact of inflammatory processes on drug detoxification capacity. Until now, only little work has been presented in this respect, and systematic studies in this field of research are lacking.

Relative expression changes of human-relevant drug metabolism as well as APR marker genes in IL-6-challenged HepaRG cells and PHH demonstrated a very strong correlation. The APR was strongly induced by IL-6 in HepaRG cells with a several hundred-fold increase in

*CRP* mRNA expression, very similar to PHH. *SOCS3* induction appeared to be of less magnitude, however still highly significant. Hence, it was demonstrated that HepaRG cells retained responsiveness to the pro-inflammatory cytokine IL-6.

Remarkably, HepaRG cells exposed to IL-6 demonstrated a global transcriptional downregulation of major *CYP* genes which has not been shown before in such a systematic approach. Only IL-6-mediated repression of *CYP3A4* expression upon LPS stimulation was previously demonstrated in HepaRG cells (Aninat et al., 2008). *CYP2D6* was excluded from the analysis because it is known to be very low expressed in HepaRG cells compared to PHH (Aninat et al., 2006). The overall effects were highly similar to those observed in PHH. Accordingly, mRNA expression of *ADH1A*, *ALDH2*, and *DPYD* was only moderately affected. Interestingly, *CYP2E1* expression was not upregulated by IL-6 in HepaRG cells but rather appeared to be repressed. This is in accordance with previous results, reporting abnormal expression and activity of CYP2E1 in HepaRG cells, probably due to culture conditions (Hegarath et al., 2010; Kanebratt and Andersson, 2008). The *CYP2E1* gene is also known to be polymorphic, which may also play a role (Neafsey et al., 2009). IL-6 exposure of HepaRG cells caused profoundly reduced protein levels of CYP isoenzymes CYP3A4, 2C8, and 2C9, also strongly impairing their activities along with 1A2, 2B6, and 2C19. Supporting the relevance of these findings, intrinsic clearance rates of common reference drugs generally show good correlations between PHH and HepaRG cells (Lübberstedt et al., 2011). Furthermore, P450 activities were much better preserved in HepaRG cells over the investigated culture period of 72 hours. Moreover, IL-1 $\beta$  and TNF- $\alpha$  treatment of HepaRG cells globally suppressed CYP mRNA expression with the former causing much stronger effects. Both treatments led to remarkably decreased activities of six major CYP isoenzymes (CYP1A2, 2B6, 2C19, 2C8, 2C9, and 3A4). Since these major P450s are responsible for the breakdown of approximately 75% of all commonly prescribed drugs (Zanger and Schwab, 2013), these findings emphasize the usefulness of the HepaRG model for preclinical *in vitro* studies.

Not much attention has been credited to phase II drug metabolism in HepaRG cells. Whereas major *GSTs* and *UGTs* were shown to be expressed similarly to PHH (Aninat et al., 2006; Kanebratt and Andersson, 2008), the impact of pro-inflammatory cytokines on regulation of phase II drug metabolizing enzymes has not been addressed so far. The expression changes in HepaRG cells exposed to IL-6 were almost analog to those observed in PHH. The mRNA expression of *GSTs*, *NATs*, and *UGTs* was suppressed whereas *SULT1B1* and *TPMT* were not

largely affected. IL-1 $\beta$  stimulation of HepaRG cells caused a much stronger suppression of *GST*, *NAT*, and *UGT* isoforms, compared to IL-6. Moreover, *SULT1B1* was significantly downregulated. TNF- $\alpha$ -induced expression changes of phase II metabolism genes were comparable to those observed in IL-6-exposed HepaRG cells.

The major drug transporters *ABCG2*, *SLC10A1* (coding for NTCP), *SLC22A7*, and *SLCO1B1* (OATP2) were transcriptionally repressed by IL-6. *ABCB1* (MDR1) and *ABCC2* (MRP2) were only moderately affected, comparably to findings in PHH. IL-1 $\beta$  exposure suppressed mRNA expression of all the aforementioned transporters, confirming previous findings (Le Vee et al., 2008). TNF- $\alpha$  stimulation of HepaRG cells for 24 hours impaired mRNA expression of *SLC* transporters but not *ABCs*. Indeed, TNF- $\alpha$  is known to be responsible for the transcriptional downregulation of the hepatic bile acid transporter NTCP (Cherrington et al., 2013) but rather leads to increased mRNA expression of MDR1 (Poller et al., 2010).

As shown in PHH, IL-6 stimulation of HepaRG cells significantly suppressed mRNA expression of CAR and PXR. The same held true for IL-1 $\beta$  and TNF- $\alpha$  stimulation. A previous study in HepaRG cells demonstrated functionality of major NRs by inducing CYP gene expression with prototypical inducers (Aninat et al., 2006). Possible implications of altered NR gene expression were discussed in 5.1. Interestingly, transcription of *HNF4A* and *PPARA* was significantly repressed in HepaRG cells exposed to either IL-1 $\beta$ , IL-6, or TNF- $\alpha$ . In fact, HNF-4 $\alpha$  (*HNF4A*) is particularly involved in constitutive expression of CYPs and a key transcription factor in NR-mediated response to xenobiotics (Lim and Huang, 2008; Zanger and Schwab, 2013). The NR PPAR- $\alpha$ , for instance, was shown to directly regulate the transcription of *CYP3A4* in human liver (Thomas et al., 2013). However, in contrast to their regulatory role, little is known about how NRs are regulated (Sharma et al., 2014), and more detailed analyses are required in this field.

Taken together, striking similarities in DMET gene expression upon IL-6 stimulation were discovered in HepaRG cells compared to PHH. Major phase I/II drug metabolizing enzymes, drug transporters, and modifier genes were significantly repressed. Only few genes were differentially regulated (e.g., *CYP2E1*), however, no major contradictory observations were made. Decreased protein expression and activity of major P450s could be determined. Exposure of HepaRG cells to different cytokines resulted in moderately different gene expression patterns, indicating specific responsiveness to particular pro-inflammatory cytokines. HepaRG cells are therefore suggested to be a good model for studying

inflammation-mediated changes in human drug metabolic processes. Moreover, they may well serve as a model for studying regulatory mechanisms which are easily affected by interindividual variability.

#### **5.4 The hepatic transcriptome during inflammation**

Only a few studies have investigated the impact of a systemic APR on a genomic level. Coulouarn and colleagues, for example, analyzed liver tissue samples from AP patients with a custom array covering large parts of the human liver transcriptome (Coulouarn et al., 2004). However, their study mainly focused on APR-related factors. An impact on drug metabolism – one major function of the liver – was not reported. Other studies investigated AP-induced changes in transcriptomes of non-liver cells such as macrophages or leukocytes (Jura et al., 2008; Xiao et al., 2011). A comprehensive un-biased study, addressing the impact of a systemic APR on the liver transcriptome in humans, has not yet been reported.

An earlier transcriptome-wide study in our group has shown in liver samples from patients with elevated CRP levels, significant downregulation of the important *CYP3A4* and effects on numerous other DMET genes, as shown by complete hierarchical clustering (data unpublished). CRP is a sensitive and systemic marker of inflammation and is only produced in hepatocytes, mainly under the transcriptional control by the cytokine IL-6 (Castell et al., 1989; Pepys and Baltz, 1983). Therefore, in order to determine the impact of inflammation on liver specific functions, in particular the drug detoxification system, in a genome-wide context, IL-6-challenged PHH were used as an *ex vivo* model. A retrospective study of transcriptome-wide gene expression profiles from 105 human liver samples, including samples with elevated CRP plasma levels ( $N = 7$ ), was performed for *in vivo* verification. The differences and similarities between both studies are discussed in the context of drug metabolism.

In PHH exposed to IL-6 for 24 hours, approximately 2% of all examined genes on the microarray were differentially regulated ( $p \leq 0.05$ ,  $FC \geq 1.5$  and  $\leq -1.5$ ). The most strongly upregulated gene was *STEAP4*, a metalloredutase involved in iron transport. Its expression in mice liver was shown to be regulated by C/EBP- $\alpha$  and STAT3 in the presence of IL-6 (Ramadoss et al., 2010). Not surprisingly, *CRP* was the second most upregulated gene. Furthermore, the IL-6-regulated serum amyloid *SAA2* and phospholipase *PLA2G2A* were identified among the top upregulated genes (Crowl et al., 1991; Hagihara et al., 2004). GO

enrichment analyses revealed an activation of the complement system, a part of the innate immune system, in which IL-6 plays an important role (Naugler and Karin, 2008). These findings confirmed the responsiveness of PHH to the IL-6 stimulus. In livers of patients with elevated CRP, a similar amount of differentially regulated genes, as in IL-6-challenged PHH, was identified. Increased mRNA expression of *CRP*, *PLA2G2A*, and *SAA2* were shown. The most strongly upregulated gene was *SPINK1*, an IL-6-inducible AP reactant (Stenman, 2011). A *bona fide* IL-6 response can therefore be anticipated. However, no enriched acute phase or immune response related processes were found by GO term analyses. This observation may be explained by unknown time schedules of blood sampling for determination of APPs (e.g., CRP) and execution of surgery. In other words, the APR may not have been as “acute” anymore by the time the liver material was extracted from the patients.

Remarkably, major human-relevant CYPs dominated the top list of most strongly downregulated genes in IL-6-challenged PHH. The mRNA expression of the CYP isoforms *CYP2C8*, *3A4*, and *2A6* was more than 4-fold repressed. A total of 40 DMET genes were identified as significantly altered. 30 of these genes were downregulated, including almost all transcripts of major CYPs of importance in humans (e.g., *1A2*, *2A6*, *2B6*, *2C8*, *2C9*, *2C19*, *3A4*, and *3A5*), phase II drug metabolizing enzymes (e.g., *GSTAs*, *SULTs*, and *UGTs*) and drug transporters (*ABCs* and *SLCs*). Some DMET genes were upregulated including *CYP2E1* and *SULT1B1*. QPCR analyses confirmed the authenticity of most of these gene expression changes. In liver samples from patients with elevated CRP, 29 DMET genes were downregulated including important genes coding for phase I/II drug metabolizing enzymes (e.g., *ADHs*, *ALDHs*, *CYPs*, *GSTs*, and *UGTs*) and drug transporters (e.g., *ABCG2* and *SLCs*). Only few DMET genes were upregulated. In both studies, gene term enrichment analyses indicated a very strong influence on xenobiotic metabolic and related processes, containing mostly downregulated DMET genes. Moreover, KEGG pathway analyses revealed that drug and xenobiotic metabolic signaling pathways were the most strongly impacted reaction networks. These findings clearly demonstrate that the drug detoxification system in the liver is largely affected during inflammation. Previous investigations in this thesis showed that, at least for P450s, changes in mRNA expression reflect changes in protein expression and activity, emphasizing the clinical relevance of these findings.

Gene annotation analysis furthermore identified enriched processes related to lipid metabolism. IL-6, for instance, was shown to play a pleiotropic role in hepatic lipid metabolism (Hassan et al., 2014). A variety of lipids are involved in these processes

including, e.g., bile acids, ketone bodies, fatty acids, steroids, and triacylglycerols. Here, for instance, peroxisomal beta-oxidation appeared to be specifically impaired in both models, as indicated by suppressed *EHHADH* and *ACOX2* which code for peroxisomal L-bifunctional enzyme and acyl-CoA oxidase 2, respectively. These enzymes are involved in the first, second, and third step of peroxisomal beta-oxidation which is believed to be important in the initial breakdown of very long-chain fatty acids (Houten et al., 2012). Impaired peroxisomal beta-oxidation can lead to hypertriglyceridemia which was previously associated with systemic inflammation (Jonkers et al., 2002; Sammalkorpi et al., 1988) but also with accumulation of harmful metabolites of arachidonic acid which further induce the inflammatory response (Schrader and Fahimi, 2006). However, decreased ROS generation due to loss of peroxisomal function could be an anti-inflammatory feature of this complex regulation.

Moreover, differentially expressed genes in PHH exposed to IL-6 and livers from patients with elevated CRP indicated an impact on another important lipid metabolic process, namely, steroid metabolism. In this respect, significantly less expressed *HSD17B13*, *GSTA1*, and *GSTA2* was identified. The 17 $\beta$ -hydroxysteroid dyhydrogenase *HSD17B13* was previously characterized in liver (Liu et al., 2007) and was the strongest downregulated gene in livers from patients with elevated CRP. Interestingly, 17 $\beta$ -HSDs and GSTA family members are major steroid regulators in mammals (Baker, 2001; Matsumura et al., 2013). The CYP2C19, for instance, is involved in the oxidation of (Yamazaki and Shimada, 1997) and was shown to be regulated by steroids (Mwinyi et al., 2010). Here, its expression was downregulated. These findings demonstrate the large scale impact on diverse lipid metabolic processes during inflammation in the human liver.

Remarkably, combined enrichment analysis revealed that the strongest influenced biological processes and molecular interaction networks in PHH exposed to IL-6 and livers from patients with elevated CRP were associated with metabolism of xenobiotics and fatty acids. Indeed, such major metabolic reorganization is a known response of the hepatic transcriptome in human liver disease (Shackel et al., 2006). Suppression of DMETs in response to inflammatory stimuli has been known for decades (Renton, 2005). Yet, it continues to be a major question what the reason for this global downregulation may be. In this context, the transcriptome data indicated that processes and regulatory pathways related to amino acid metabolism are part of the metabolic reorganization. This was, however, more prominently the case in livers from patients with elevated CRP. Due to the artificial environment, these

characteristics may have been changed or lost in IL-6-challenged PHH. In fact, it was proposed earlier by Morgan and colleagues that during infection or inflammation the liver sacrifices its drug detoxification capacity in favor of APP synthesis (Morgan, 2001). These APPs are mainly CRP and SAA, released by hepatocytes after cytokine stimulation (Heinrich et al., 1990). They are of utmost importance for the initiation of the innate immunity and can rapidly increase up to 1,000-fold (Gruys et al., 2005). Such metabolic challenge would require not only the reduction of processes that consume amino acids (e.g., synthesis of DMETs), but also changes in amino acid household such as conversion and redirection of supply. Indeed, modifications of the amino acid metabolism during immune system activation could be observed previously (Le Floc'h et al., 2004). Interestingly, CRP and SAA contain disproportionate amounts of essential aromatic amino acids, most importantly phenylalanine (Reeds et al., 1994). Since these amino acids are not readily available in the liver, they need to be recovered. In the long term, this is achieved by the brake down of mixed muscle protein (Kurpad, 2006), however for immediate availability amino acids need to be recovered from liver protein. This idea is supported by significantly upregulated ubiquitin D (*UBD*) and downregulated homogentisate 1,2-dioxygenase (*HGD*) in both microarray studies. The former actively breaks down P450s (Correia et al., 2005) and the latter is responsible for catabolism of phenylalanine and tyrosine. Gene expression patterns in livers from patients with elevated CRP indicated that many more amino acid metabolic pathways are affected. Serine conversion from glycine appeared to be favored, as indicated by downregulated ( $\downarrow$ ) *GATM*, whereas its *de novo* synthesis was impaired ( $\downarrow$  *PHGDH*). Proline degradation appeared to be inhibited ( $\downarrow$  *PRODH*) and glutamate synthesis favored ( $\uparrow$  *ALDH4A1*). Remarkably, decreased expression of the rate-limiting enzyme (*GCL*) in glutathione (GSH) synthesis was detected. GSH is present in all mammalian tissues and defends against oxidative stress (Lu, 2013). Its precursor cysteine may be more readily available if synthesis of GSH is inhibited. Cystein supplementation, for example, has been shown to improve GSH synthesis in infected patients (Kurpad, 2006). These findings indicate major changes in protein and amino acid metabolism, probably in favor of allocating important precursors for the synthesis of APPs in the liver while sacrificing the drug detoxification capacity.

Taken together, these findings highlight the scale on which the human liver transcriptome is affected during inflammation. Major genomic reorganization related to xenobiotic, lipid and, amino acid metabolism takes place. It appears that the liver devotes its transcriptional machinery to the immune response while other major liver functions are shut down. Here,

examination of the whole liver transcript helped to define patterns of gene expression and gene relationships which is ultimately very useful in understanding liver pathophysiology. However, there are several caveats to be aware of and disease and technical discrepancies need to be considered in functional genomic studies. The normal liver transcriptome, for example, is highly complex and shows significant individual variability in transcript expression. Its complexity can increase several-fold during disease (Shackel et al., 2006). Moreover, microarrays – if not specifically designed for their purpose – are very restricted in terms of gene coverage, rather sampling than profiling the transcriptome (Shackel et al., 2006). Studies in liver tissues, using probes that were not specifically selected for this organ, resulted in informative genes representing only a fraction of those expressed in any given vertebrate tissue sample (Coulouarn et al., 2004; Yano et al., 2001). Custom designed tissue-targeting microarrays could help to overcome these problems and considerable efforts have been made in this field (Coulouarn et al., 2004). Additionally, the relationship between gene transcripts and the corresponding protein expression is an unknown variable. Many examples have shown that ,e.g., post-translational modifications control protein expression and function independently of the corresponding mRNA expression (Cloos and Christgau, 2004). Nevertheless, microarrays provide a powerful tool for the detection of alterations in mRNA expression which accompanies and may regulate physiological and pathological changes.

## 5.5 Conclusions

The studies conducted in this thesis largely aimed at the drug detoxification system in human liver and how it is affected during infection and inflammation. It was hypothesized that signaling pathways that converge at NR signaling may play prominent roles during such conditions. Since current knowledge in this field is patchy at best, systematic and comprehensive studies were required. Finally, the question was posed whether the observed changes are merely a pathophysiological consequence or may be due to a general compensatory response.

This work showed that IL-6 exposure of PHH causes pronounced and coordinated alterations of mRNA expression of numerous genes of importance for metabolism and transport of drugs, including important regulators. Major CYPs such as CYP1A2 and 3A4 demonstrated decreased protein expression and activity. IL-6-challenged HepaRG cells showed highly similar gene expression patterns. Major phase I/II drug metabolizing enzymes, drug transporters, and modifier genes were significantly repressed. Decreased protein expression and activity of major CYPs (e.g., CYP2C8, 2C9, and 3A4) were determined. Exposure of HepaRG cells to IL-1 $\beta$  and TNF- $\alpha$  resulted in moderately different gene expression patterns, indicating specific responsiveness to particular pro-inflammatory cytokines. HepaRG cells proved to be responsive to pro-inflammatory stimuli and appear to retain regulatory networks leading to AP-related changes in drug metabolism capacity.

In PHH, several signaling cascades were activated upon IL-6 stimulation. The major IL-6 response pathway STAT3 appeared to be of minor relevance in the downregulation of DMET genes. In fact, the data indicated a contribution of the MAPK and PI3K/AKT signaling pathways. An interaction of these pathways with NR signaling, most importantly RXR- $\alpha$ , is very likely and may explain the coordinated effects observed on the transcriptional level.

Microarray analyses in IL-6-treated PHH and liver samples from patients with elevated CRP revealed most prominent effects on xenobiotic metabolism. Furthermore, major metabolic reorganization takes place, including lipid and amino acid metabolic processes. There is reason to believe that the liver fully devotes its metabolic capability to the activation of the innate immune system while other functions are reduced. These findings provide novel aspects of understanding the acute phase response and its impact on drug detoxification in human liver, thereby contributing to explain the huge interindividual variability in susceptibility to drugs and other environmental factors.

## 5.6 Future directions

To be able to handle the sheer amount of data generated in this study, a systems biology approach is currently used in collaboration with the Virtual Liver Network ([www.virtual-liver.de](http://www.virtual-liver.de)), a major national initiative funded by the German Federal Ministry of Education and Research (BMBF). In the subproject “B5: Cell-cell communication influences detoxifying functions in human liver”, PP and gene expression data acquired from perturbation studies (inhibition, KD, etc.) are implemented into signaling networks and gene expression models (in collaboration with Prof. Dr. Andreas Zell and Roland Keller at the Center for Bioinformatics, Tübingen). The signaling networks consist of Boolean models, representing possible signaling cascades including also crosstalks. So called pre-knowledge (PKN) models are optimized by training them against different data sets. During this process, optimal network structures are determined. The gene expression model is comprised in another module, based on Fuzzy Logistics, describing gene expression of DMET genes in true values between 0 and 1. The combined model is again optimized and fitted to the data sets. However, highly interconnected networks that include non-linear motifs like feedforward and feedback loops cannot be accurately described by logical models. Approaches using differential models are mandatory in this case. Therefore, the model is compiled into a dynamic model using ordinary differential equations (ODE) systems based on specialized rate laws. This model should ultimately describe the impact of IL-6 on the drug detoxification system in human liver and allow for predictions of the effects of IL-6 on intracellular signaling cascades that are involved in the regulation of DMET genes.

Physiologically based pharmacokinetic (PBPK) models for disease-drug interactions during inflammation may also be conceivable. In fact, such an approach was just recently shown for the suppression of CYP3A by IL-6 (Machavaram et al., 2013). Although this is still an emerging field, such simulations provide the first step in the extrapolation of *in vitro* information to *in vivo* events. Since batteries of DMET genes appear to be affected by inflammatory mediators such as IL-6, systematic approaches would be required.

A lot more work is required in order to understand the detailed molecular mechanisms leading to the observed effects. The involvement of many different transcription factors (liver enriched transcriptions factors, NRs, and cofactors) and extensive pathway crosstalks further complicate the research and may be daunting. The disadvantages of primary cells were discussed previously, and results from HepaRG cells were promising. They likely retain

functional molecular mechanisms that cause downregulation of DMETs during inflammation. However, this will need to be addressed in detailed mechanistic studies, such as combinatorial KDs of key kinases or NRs in order to find major players in signal propagation and regulation and thus unravel the molecular interaction networks. Particularly, the involvement of NF- $\kappa$ B remains intriguing. Nuclear translocation and molecular interaction studies may help to elucidate its role in the coordinated downregulation of DMET genes.

The work of this thesis was also decisive for the planning of a clinical study that investigates the impact of malaria infection on the expression and function of DMET genes relevant for metabolism of common anti-malaria drugs. For this purpose, the pharmacokinetics of these drugs as well as the contributions of various metabolic enzymes (P450s and UGTs) and drug transporters (ABCs and SLCs) are systematically assessed in a controlled clinical study. Since increased levels of pro-inflammatory cytokines and abrupt increase in CRP during onset of fever were previously observed in malaria patients (Harpaz et al., 1992), this clinical study may provide novel aspects of regulation of the drug detoxification system during inflammation. This study was recently submitted to the Deutsche Forschungsgemeinschaft (DFG) and is currently under review.

## 6 REFERENCES

- Abdel-Razzak, Z., Loyer, P., Fautrel, A., Gautier, J.C., Corcos, L., Turlin, B., Beaune, P., and Guillouzo, A. (1993). Cytokines down-regulate expression of major cytochrome P-450 enzymes in adult human hepatocytes in primary culture. *Mol. Pharmacol.* *44*, 707–715.
- Agrawal, A., Cha-Molstad, H., Samols, D., and Kushner, I. (2001). Transactivation of C-reactive protein by IL-6 requires synergistic interaction of CCAAT/enhancer binding protein beta (C/EBP beta) and Rel p50. *J. Immunol. Baltim. Md 1950* *166*, 2378–2384.
- Aitken, A.E., and Morgan, E.T. (2007). Gene-specific effects of inflammatory cytokines on cytochrome P450 2C, 2B6 and 3A4 mRNA levels in human hepatocytes. *Drug Metab. Dispos. Biol. Fate Chem.* *35*, 1687–1693.
- Aitken, A.E., Richardson, T.A., and Morgan, E.T. (2006). Regulation of drug-metabolizing enzymes and transporters in inflammation. *Annu. Rev. Pharmacol. Toxicol.* *46*, 123–149.
- Andersen, C.L., Jensen, J.L., and Ørntoft, T.F. (2004). Normalization of real-time quantitative reverse transcription-PCR data: a model-based variance estimation approach to identify genes suited for normalization, applied to bladder and colon cancer data sets. *Cancer Res.* *64*, 5245–5250.
- Andersson, T.B., Kanebratt, K.P., and Kenna, J.G. (2012). The HepaRG cell line: a unique in vitro tool for understanding drug metabolism and toxicology in human. *Expert Opin. Drug Metab. Toxicol.* *8*, 909–920.
- Aninat, C., Piton, A., Glaise, D., Le Charpentier, T., Langouët, S., Morel, F., Guguen-Guillouzo, C., and Guillouzo, A. (2006). Expression of cytochromes P450, conjugating enzymes and nuclear receptors in human hepatoma HepaRG cells. *Drug Metab. Dispos. Biol. Fate Chem.* *34*, 75–83.
- Aninat, C., Seguin, P., Descheemaeker, P.-N., Morel, F., Malledant, Y., and Guillouzo, A. (2008). Catecholamines induce an inflammatory response in human hepatocytes. *Crit. Care Med.* *36*, 848–854.
- Anzenbacher, P., and Anzenbacherová, E. (2012). Drug-Metabolizing Enzymes - An Overview. In *Metabolism of Drugs and Other Xenobiotics*, (Weinheim, Germany: Wiley-VCH), pp. 3–25.
- Arai, K.I., Lee, F., Miyajima, A., Miyatake, S., Arai, N., and Yokota, T. (1990). Cytokines: coordinators of immune and inflammatory responses. *Annu. Rev. Biochem.* *59*, 783–836.
- Ashburner, M., Ball, C.A., Blake, J.A., Botstein, D., Butler, H., Cherry, J.M., Davis, A.P., Dolinski, K., Dwight, S.S., Eppig, J.T., et al. (2000). Gene ontology: tool for the unification of biology. The Gene Ontology Consortium. *Nat. Genet.* *25*, 25–29.
- Baker, M.E. (2001). Evolution of 17 $\beta$ -hydroxysteroid dehydrogenases and their role in androgen, estrogen and retinoid action. *Mol. Cell. Endocrinol.* *171*, 211–215.
- Baldwin, A.S., Jr (1996). The NF-kappa B and I kappa B proteins: new discoveries and insights. *Annu. Rev. Immunol.* *14*, 649–683.
- Balkwill, F., and Mantovani, A. (2001). Inflammation and cancer: back to Virchow? *Lancet* *357*, 539–545.
- Ballet, F., Bouma, M.E., Wang, S.R., Amit, N., Marais, J., and Infante, R. (1984). Isolation, culture and characterization of adult human hepatocytes from surgical liver biopsies. *Hepatology* *4*, 849–854.
- Becquemont, L., Chazouilleres, O., Serfaty, L., Poirier, J.M., Broly, F., Jaillon, P., Poupon, R., and Funck-Brentano, C. (2002). Effect of interferon alpha-ribavirin bitherapy on cytochrome P450 1A2 and 2D6 and N-acetyltransferase-2 activities in patients with chronic active hepatitis C. *Clin. Pharmacol. Ther.* *71*, 488–495.
- Beierle, I., Meibohm, B., and Derendorf, H. (1999). Gender differences in pharmacokinetics and pharmacodynamics. *Int. J. Clin. Pharmacol. Ther.* *37*, 529–547.

- Beigneux, A.P., Moser, A.H., Shigenaga, J.K., Grunfeld, C., and Feingold, K.R. (2002). Reduction in cytochrome P-450 enzyme expression is associated with repression of CAR (constitutive androstane receptor) and PXR (pregnane X receptor) in mouse liver during the acute phase response. *Biochem. Biophys. Res. Commun.* *293*, 145–149.
- Beutler, B. (2004). Innate immunity: an overview. *Mol. Immunol.* *40*, 845–859.
- Billingham, M.E. (1987). Cytokines as inflammatory mediators. *Br. Med. Bull.* *43*, 350–370.
- Van Bladeren, P.J. (2000). Glutathione conjugation as a bioactivation reaction. *Chem. Biol. Interact.* *129*, 61–76.
- Blommaert, E.F., Krause, U., Schellens, J.P., Vreeling-Sindelárová, H., and Meijer, A.J. (1997). The phosphatidylinositol 3-kinase inhibitors wortmannin and LY294002 inhibit autophagy in isolated rat hepatocytes. *Eur. J. Biochem. FEBS* *243*, 240–246.
- Boehm, U., Klamp, T., Groot, M., and Howard, J.C. (1997). Cellular responses to interferon-gamma. *Annu. Rev. Immunol.* *15*, 749–795.
- Braeuning, A., Heubach, Y., Knorpp, T., Kowalik, M.A., Templin, M., Columbano, A., and Schwarz, M. (2011). Gender-Specific Interplay of Signaling through  $\beta$ -Catenin and CAR in the Regulation of Xenobiotic-Induced Hepatocyte Proliferation. *Toxicol. Sci.* *123*, 113–122.
- Brockmeyer, N.H., Barthel, B., Mertins, L., and Goos, M. (1998). Changes of antipyrine pharmacokinetics during influenza and after administration of interferon-alpha and -beta. *Int. J. Clin. Pharmacol. Ther.* *36*, 309–311.
- Buranrat, B., Prawan, A., Sripa, B., and Kukongviriyapan, V. (2007). Inflammatory cytokines suppress arylamine N-acetyltransferase 1 in cholangiocarcinoma cells. *World J. Gastroenterol. WJG* *13*, 6219–6225.
- Burgermeister, E., Lanzendoerfer, M., and Scheuer, W. (2003). Comparative analysis of docking motifs in MAP-kinases and nuclear receptors. *J. Biomol. Struct. Dyn.* *20*, 623–634.
- Burnett, D.A., Barak, A.J., Tuma, D.J., and Sorrell, M.F. (1976). Altered elimination of antipyrine in patients with acute viral hepatitis. *Gut* *17*, 341–344.
- Cameron, M.J., and Kelvin, D.J. (2000). Cytokines, Chemokines and Their Receptors - Madame Curie Bioscience Database - NCBI Bookshelf.
- Campbell, J.S., Prichard, L., Schaper, F., Schmitz, J., Stephenson-Famy, A., Rosenfeld, M.E., Argast, G.M., Heinrich, P.C., and Fausto, N. (2001). Expression of suppressors of cytokine signaling during liver regeneration. *J. Clin. Invest.* *107*, 1285–1292.
- Carcillo, J.A., Doughty, L., Kofos, D., Frye, R.F., Kaplan, S.S., Sasser, H., and Burckart, G.J. (2003). Cytochrome P450 mediated-drug metabolism is reduced in children with sepsis-induced multiple organ failure. *Intensive Care Med.* *29*, 980–984.
- Cassatella, M.A., Gasperini, S., Bovolenta, C., Calzetti, F., Vollebregt, M., Scapini, P., Marchi, M., Suzuki, R., Suzuki, A., and Yoshimura, A. (1999). Interleukin-10 (IL-10) selectively enhances CIS3/SOCS3 mRNA expression in human neutrophils: evidence for an IL-10-induced pathway that is independent of STAT protein activation. *Blood* *94*, 2880–2889.
- Castell, J.V., Gómez-Lechón, M.J., David, M., Andus, T., Geiger, T., Trullenque, R., Fabra, R., and Heinrich, P.C. (1989). Interleukin-6 is the major regulator of acute phase protein synthesis in adult human hepatocytes. *FEBS Lett.* *242*, 237–239.
- Castellano, E., and Downward, J. (2011). RAS Interaction with PI3K. *Genes Cancer* *2*, 261–274.
- Cederbaum, A.I., Yang, L., Wang, X., and Wu, D. (2012). CYP2E1 Sensitizes the Liver to LPS- and TNF  $\alpha$ -Induced Toxicity via Elevated Oxidative and Nitrosative Stress and Activation of ASK-1 and JNK Mitogen-Activated Kinases. *Int. J. Hepatol.* *2012*, 582790.
- Cerec, V., Glaise, D., Garnier, D., Morosan, S., Turlin, B., Drenou, B., Gripon, P., Kremisdorf, D., Guguen-Guillouzo, C., and Corlu, A. (2007). Transdifferentiation of hepatocyte-like

- cells from the human hepatoma HepaRG cell line through bipotent progenitor. *Hepatology*. Baltimore, Md 45, 957–967.
- Chang, F., Lee, J.T., Navolanic, P.M., Steelman, L.S., Shelton, J.G., Blalock, W.L., Franklin, R.A., and McCubrey, J.A. (2003). Involvement of PI3K/Akt pathway in cell cycle progression, apoptosis, and neoplastic transformation: a target for cancer chemotherapy. *Leukemia* 17, 590–603.
- Chang, K.C., Bell, T.D., Lauer, B.A., and Chai, H. (1978). Altered theophylline pharmacokinetics during acute respiratory viral illness. *Lancet* 1, 1132–1133.
- Chen, J.Q., Ström, A., Gustafsson, J.A., and Morgan, E.T. (1995). Suppression of the constitutive expression of cytochrome P-450 2C11 by cytokines and interferons in primary cultures of rat hepatocytes: comparison with induction of acute-phase genes and demonstration that CYP2C11 promoter sequences are involved in the suppressive response to interleukins 1 and 6. *Mol. Pharmacol.* 47, 940–947.
- Chen, Y.L., Vraux, V.L., Leneveu, A., Dreyfus, F., Stheneur, A., Florentin, I., Sousa, M.D., Giroud, J.P., Flouvat, B., and Chauvelot-Moachon, L. (1994). Acute-phase response, interleukin-6, and alteration of cyclosporine pharmacokinetics. *Clin. Pharmacol. Ther.* 55, 649–660.
- Cherrington, N.J., Slitt, A.L., Li, N., and Klaassen, C.D. (2004). Lipopolysaccharide-mediated regulation of hepatic transporter mRNA levels in rats. *Drug Metab. Dispos. Biol. Fate Chem.* 32, 734–741.
- Cherrington, N.J., Estrada, T.E., Frisk, H.A., Canet, M.J., Hardwick, R.N., Dvorak, B., Lux, K., and Halpern, M.D. (2013). The hepatic bile acid transporters Ntcp and Mrp2 are downregulated in experimental necrotizing enterocolitis. *Am. J. Physiol. Gastrointest. Liver Physiol.* 304, G48–56.
- Chiang, J.Y.L. (2009). Bile acids: regulation of synthesis. *J. Lipid Res.* 50, 1955–1966.
- Chiou, W.L., Jeong, H.Y., Wu, T.C., and Ma, C. (2001). Use of the erythromycin breath test for in vivo assessments of cytochrome P4503A activity and dosage individualization. *Clin. Pharmacol. Ther.* 70, 305–310.
- Clark, G.H., and Fraser, C.G. (1993). Biological Variation of Acute Phase Proteins. *Ann. Clin. Biochem. Int. J. Biochem. Med.* 30, 373–376.
- Claro da Silva, T., Polli, J.E., and Swaan, P.W. (2013). The solute carrier family 10 (SLC10): beyond bile acid transport. *Mol. Aspects Med.* 34, 252–269.
- Cloos, P.A.C., and Christgau, S. (2004). Post-translational modifications of proteins: implications for aging, antigen recognition, and autoimmunity. *Biogerontology* 5, 139–158.
- Du Clos, T.W. (1989). C-reactive protein reacts with the U1 small nuclear ribonucleoprotein. *J. Immunol. Baltimore, Md* 143, 2553–2559.
- Congiu, M., Mashford, M.L., Slavin, J.L., and Desmond, P.V. (2002). UDP glucuronosyltransferase mRNA levels in human liver disease. *Drug Metab. Dispos. Biol. Fate Chem.* 30, 129–134.
- Correia, M.A., Sadeghi, S., and Mundo-Paredes, E. (2005). CYTOCHROME P450 UBIQUITINATION: Branding for the Proteolytic Slaughter? *Annu. Rev. Pharmacol. Toxicol.* 45, 439–464.
- Cotreau, M.M., von Moltke, L.L., and Greenblatt, D.J. (2005). The influence of age and sex on the clearance of cytochrome P450 3A substrates. *Clin. Pharmacokinet.* 44, 33–60.
- Coulouarn, C., Lefebvre, G., Derambure, C., Lequerre, T., Scotte, M., Francois, A., Cellier, D., Daveau, M., and Salier, J.-P. (2004). Altered gene expression in acute systemic inflammation detected by complete coverage of the human liver transcriptome. *Hepatology* 39, 353–364.
- Cox, A.D., and Der, C.J. (2002). Ras family signaling: therapeutic targeting. *Cancer Biol. Ther.* 1, 599–606.

- Crowl, R.M., Stoller, T.J., Conroy, R.R., and Stoner, C.R. (1991). Induction of phospholipase A2 gene expression in human hepatoma cells by mediators of the acute phase response. *J. Biol. Chem.* 266, 2647–2651.
- David Josephy, P., Peter Guengerich, F., and Miners, J.O. (2005). “Phase I and Phase II” drug metabolism: terminology that we should phase out? *Drug Metab. Rev.* 37, 575–580.
- Delhase, M., Li, N., and Karin, M. (2000). Signalling pathways: Kinase regulation in inflammatory response. *Nature* 406, 367–368.
- Dinareello, C.A. (1984). Interleukin-1. *Rev. Infect. Dis.* 6, 51–95.
- Duanmu, Z., Weckle, A., Koukouritaki, S.B., Hines, R.N., Falany, J.L., Falany, C.N., Kocarek, T.A., and Runge-Morris, M. (2006). Developmental expression of aryl, estrogen, and hydroxysteroid sulfotransferases in pre- and postnatal human liver. *J. Pharmacol. Exp. Ther.* 316, 1310–1317.
- Engel, G., Hofmann, U., Heidemann, H., Cosme, J., and Eichelbaum, M. (1996). Antipyrine as a probe for human oxidative drug metabolism: identification of the cytochrome P450 enzymes catalyzing 4-hydroxyantipyrine, 3-hydroxymethylantipyrine, and norantipyrine formation. *Clin. Pharmacol. Ther.* 59, 613–623.
- Eulenfeld, R., and Schaper, F. (2009). A new mechanism for the regulation of Gab1 recruitment to the plasma membrane. *J. Cell Sci.* 122, 55–64.
- Eulenfeld, R., Dittrich, A., Khouri, C., Müller, P.J., Mütze, B., Wolf, A., and Schaper, F. (2012). Interleukin-6 signalling: more than Jaks and STATs. *Eur. J. Cell Biol.* 91, 486–495.
- Favata, M.F., Horiuchi, K.Y., Manos, E.J., Daulerio, A.J., Stradley, D.A., Feeser, W.S., Dyk, D.E.V., Pitts, W.J., Earl, R.A., Hobbs, F., et al. (1998). Identification of a Novel Inhibitor of Mitogen-activated Protein Kinase Kinase. *J. Biol. Chem.* 273, 18623–18632.
- Feghali, C.A., and Wright, T.M. (1997). Cytokines in acute and chronic inflammation. *Front. Biosci. J. Virtual Libr.* 2, d12–26.
- Feidt, D.M., Klein, K., Hofmann, U., Riedmaier, S., Knobloch, D., Thasler, W.E., Weiss, T.S., Schwab, M., and Zanger, U.M. (2010). Profiling induction of cytochrome p450 enzyme activity by statins using a new liquid chromatography-tandem mass spectrometry cocktail assay in human hepatocytes. *Drug Metab. Dispos. Biol. Fate Chem.* 38, 1589–1597.
- Le Floch, N., Melchior, D., and Oblad, C. (2004). Modifications of protein and amino acid metabolism during inflammation and immune system activation. *Livest. Prod. Sci.* 87, 37–45.
- Franke, T.F., Kaplan, D.R., Cantley, L.C., and Toker, A. (1997). Direct regulation of the Akt proto-oncogene product by phosphatidylinositol-3,4-bisphosphate. *Science* 275, 665–668.
- Frye, R.F., Schneider, V.M., Frye, C.S., and Feldman, A.M. (2002). Plasma levels of TNF-alpha and IL-6 are inversely related to cytochrome P450-dependent drug metabolism in patients with congestive heart failure. *J. Card. Fail.* 8, 315–319.
- Fuhr, U., Doehmer, J., Battula, N., Wölfel, C., Flick, I., Kudla, C., Keita, Y., and Staib, A.H. (1993). Biotransformation of methylxanthines in mammalian cell lines genetically engineered for expression of single cytochrome P450 isoforms. Allocation of metabolic pathways to isoforms and inhibitory effects of quinolones. *Toxicology* 82, 169–189.
- Fukada, T., Hibi, M., Yamanaka, Y., Takahashi-Tezuka, M., Fujitani, Y., Yamaguchi, T., Nakajima, K., and Hirano, T. (1996). Two signals are necessary for cell proliferation induced by a cytokine receptor gp130: involvement of STAT3 in anti-apoptosis. *Immunity* 5, 449–460.
- Gandhi, M., Aweeka, F., Greenblatt, R.M., and Blaschke, T.F. (2004). Sex differences in pharmacokinetics and pharmacodynamics. *Annu. Rev. Pharmacol. Toxicol.* 44, 499–523.
- George, G., Wynne, H.A., and Woodhouse, K.W. (1990). The association of age with the induction of drug-metabolizing enzymes in human monocytes. *Age Ageing* 19, 364–367.

- Gerhartz, C., Heesel, B., Sasse, J., Hemmann, U., Landgraf, C., Schneider-Mergener, J., Horn, F., Heinrich, P.C., and Graeve, L. (1996). Differential Activation of Acute Phase Response Factor/STAT3 and STAT1 via the Cytoplasmic Domain of the Interleukin 6 Signal Transducer gp130. *J. Biol. Chem.* *271*, 12991–12998.
- Germain, P., Chambon, P., Eichele, G., Evans, R.M., Lazar, M.A., Leid, M., Lera, A.R.D., Lotan, R., Mangelsdorf, D.J., and Gronemeyer, H. (2006). International Union of Pharmacology. LXIII. Retinoid X Receptors. *Pharmacol. Rev.* *58*, 760–772.
- Ghose, R., Zimmerman, T.L., Thevananther, S., and Karpen, S.J. (2004). Endotoxin leads to rapid subcellular re-localization of hepatic RXRalpha: A novel mechanism for reduced hepatic gene expression in inflammation. *Nucl. Recept.* *2*, 4.
- Gilmore, T.D. (2006). Introduction to NF-kappaB: players, pathways, perspectives. *Oncogene* *25*, 6680–6684.
- Gonzalez, F.J. (2007). The 2006 Bernard B. Brodie Award Lecture. Cyp2e1. *Drug Metab. Dispos. Biol. Fate Chem.* *35*, 1–8.
- Gonzalez, F.J., and Lee, Y.H. (1996). Constitutive expression of hepatic cytochrome P450 genes. *FASEB J.* *10*, 1112–1117.
- Gonzalez, F.J., and Tukey, R.H. (2005). Drug Metabolism. In Goodman & Gilman's The Pharmacological Basis of Therapeutics, (New York: McGraw-Hill), pp. 71–91.
- Goueli, S.A., Hsiao, K., Lu, T., and Simposn, D. (1998). U0126: A Novel, Selective and Potent Inhibitor of MAP Kinase Kinase (MEK). *Promega Notes* *6*.
- Gray, J.D., Renton, K.W., and Hung, O.R. (1983). Depression of theophylline elimination following BCG vaccination. *Br. J. Clin. Pharmacol.* *16*, 735–737.
- Gripon, P., Rumin, S., Urban, S., Le Seyec, J., Glaise, D., Cannie, I., Guyomard, C., Lucas, J., Trepo, C., and Guguen-Guillouzo, C. (2002). Infection of a human hepatoma cell line by hepatitis B virus. *Proc. Natl. Acad. Sci. U. S. A.* *99*, 15655–15660.
- Grivennikov, S., and Karin, M. (2008). Autocrine IL-6 signaling: a key event in tumorigenesis? *Cancer Cell* *13*, 7–9.
- Gruss, H.J., and Dower, S.K. (1995). The TNF ligand superfamily and its relevance for human diseases. *Cytokines Mol. Ther.* *1*, 75–105.
- Gruys, E., Toussaint, M.J.M., Niewold, T.A., and Koopmans, S.J. (2005). Acute phase reaction and acute phase proteins. *J. Zhejiang Univ. Sci. B* *6*, 1045–1056.
- Gu, X., Ke, S., Liu, D., Sheng, T., Thomas, P.E., Rabson, A.B., Gallo, M.A., Xie, W., and Tian, Y. (2006). Role of NF-kappaB in regulation of PXR-mediated gene expression: a mechanism for the suppression of cytochrome P-450 3A4 by proinflammatory agents. *J. Biol. Chem.* *281*, 17882–17889.
- Guengerich, P.F. (2012). Cytochromes P450. In *Metabolism of Drugs and Other Xenobiotics*, (Weinheim, Germany: Wiley-VCH), pp. 27–66.
- Guillouzo, A., Morel, F., Fardel, O., and Meunier, B. (1993). Use of human hepatocyte cultures for drug metabolism studies. *Toxicology* *82*, 209–219.
- Gupta, S., Stravitz, R.T., Dent, P., and Hylemon, P.B. (2001). Down-regulation of Cholesterol 7 $\alpha$ -Hydroxylase (CYP7A1) Gene Expression by Bile Acids in Primary Rat Hepatocytes Is Mediated by the c-Jun N-terminal Kinase Pathway. *J. Biol. Chem.* *276*, 15816–15822.
- Guschin, D., Rogers, N., Briscoe, J., Witthuhn, B., Watling, D., Horn, F., Pellegrini, S., Yasukawa, K., Heinrich, P., and Stark, G.R. (1995). A major role for the protein tyrosine kinase JAK1 in the JAK/STAT signal transduction pathway in response to interleukin-6. *EMBO J.* *14*, 1421–1429.
- Haan, S., Keller, J.F., Behrmann, I., Heinrich, P.C., and Haan, C. (2005). Multiple reasons for an inefficient STAT1 response upon IL-6-type cytokine stimulation. *Cell. Signal.* *17*, 1542–1550.
- Haas, C.E., Kaufman, D.C., Jones, C.E., Burstein, A.H., and Reiss, W. (2003). Cytochrome P450 3A4 activity after surgical stress. *Crit. Care Med.* *31*, 1338–1346.

- Hagihara, K., Nishikawa, T., Isobe, T., Song, J., Sugamata, Y., and Yoshizaki, K. (2004). IL-6 plays a critical role in the synergistic induction of human serum amyloid A (SAA) gene when stimulated with proinflammatory cytokines as analyzed with an SAA isoform real-time quantitative RT-PCR assay system. *Biochem. Biophys. Res. Commun.* *314*, 363–369.
- Hakkola, J., Hu, Y., and Ingelman-Sundberg, M. (2003). Mechanisms of down-regulation of CYP2E1 expression by inflammatory cytokines in rat hepatoma cells. *J. Pharmacol. Exp. Ther.* *304*, 1048–1054.
- Hardie, D.G., Scott, J.W., Pan, D.A., and Hudson, E.R. (2003). Management of cellular energy by the AMP-activated protein kinase system. *FEBS Lett.* *546*, 113–120.
- Harmsen, S., Meijerman, I., Maas-Bakker, R.F., Beijnen, J.H., and Schellens, J.H.M. (2013). PXR-mediated P-glycoprotein induction by small molecule tyrosine kinase inhibitors. *Eur. J. Pharm. Sci. Off. J. Eur. Fed. Pharm. Sci.* *48*, 644–649.
- Harpaz, R., Edelman, R., Wasserman, S.S., Levine, M.M., Davis, J.R., and Sztein, M.B. (1992). Serum cytokine profiles in experimental human malaria. Relationship to protection and disease course after challenge. *J. Clin. Invest.* *90*, 515–523.
- Hart, S.N., Li, Y., Nakamoto, K., Subileau, E., Steen, D., and Zhong, X. (2010). A comparison of whole genome gene expression profiles of HepaRG cells and HepG2 cells to primary human hepatocytes and human liver tissues. *Drug Metab. Dispos. Biol. Fate Chem.* *38*, 988–994.
- Hassan, W., Ding, L., Gao, R.-Y., Liu, J., and Shang, J. (2014). Interleukin-6 signal transduction and its role in hepatic lipid metabolic disorders. *Cytokine* *66*, 133–142.
- Hayney, M.S., and Muller, D. (2003). Effect of influenza immunization on CYP3A4 activity in vivo. *J. Clin. Pharmacol.* *43*, 1377–1381.
- He, Y.W., and Malek, T.R. (1998). The structure and function of gamma c-dependent cytokines and receptors: regulation of T lymphocyte development and homeostasis. *Crit. Rev. Immunol.* *18*, 503–524.
- Hegarat, L.L., Dumont, J., Josse, R., Huet, S., Lancelur, R., Mourot, A., Poul, J.-M., Guguen-Guillouzo, C., Guillouzo, A., and Fessard, V. (2010). Assessment of the genotoxic potential of indirect chemical mutagens in HepaRG cells by the comet and the cytokinesis-block micronucleus assays. *Mutagenesis* *25*, 555–560.
- Heinrich, P.C., Castell, J.V., and Andus, T. (1990). Interleukin-6 and the acute phase response. *Biochem. J.* *265*, 621–636.
- Helsby, N.A., Ward, S.A., Parslew, R.A., Friedmann, P.S., and Rhodes, L.E. (1998). Hepatic cytochrome P450 CYP2C activity in psoriasis: studies using proguanil as a probe compound. *Acta Derm. Venereol.* *78*, 81–83.
- Hennessy, B.T., Smith, D.L., Ram, P.T., Lu, Y., and Mills, G.B. (2005). Exploiting the PI3K/AKT pathway for cancer drug discovery. *Nat. Rev. Drug Discov.* *4*, 988–1004.
- Hewitt, N.J., Bühring, K.U., Dasenbrock, J., Haunschild, J., Ladstetter, B., and Utesch, D. (2001). Studies comparing in vivo:in vitro metabolism of three pharmaceutical compounds in rat, dog, monkey, and human using cryopreserved hepatocytes, microsomes, and collagen gel immobilized hepatocyte cultures. *Drug Metab. Dispos. Biol. Fate Chem.* *29*, 1042–1050.
- Hirano, T., Ishihara, K., and Hibi, M. (2000). Roles of STAT3 in mediating the cell growth, differentiation and survival signals relayed through the IL-6 family of cytokine receptors. *Oncogene* *19*, 2548–2556.
- Hofmeister, R., Khaled, A.R., Benbernou, N., Rajnavolgyi, E., Muegge, K., and Durum, S.K. (1999). Interleukin-7: physiological roles and mechanisms of action. *Cytokine Growth Factor Rev.* *10*, 41–60.
- Holm, S. (1979). A simple sequentially rejective multiple test procedure. *Scand. J. Stat.* *6*, 65–70.

- Honkakoski, P., and Negishi, M. (2000). Regulation of cytochrome P450 (CYP) genes by nuclear receptors. *Biochem. J.* *347*, 321–337.
- Houten, S.M., Denis, S., Argmann, C.A., Jia, Y., Ferdinandusse, S., Reddy, J.K., and Wanders, R.J.A. (2012). Peroxisomal L-bifunctional enzyme (Ehhadh) is essential for the production of medium-chain dicarboxylic acids. *J. Lipid Res.* *53*, 1296–1303.
- Huang, D.W., Sherman, B.T., and Lempicki, R.A. (2009). Bioinformatics enrichment tools: paths toward the comprehensive functional analysis of large gene lists. *Nucleic Acids Res.* *37*, 1–13.
- International Transporter Consortium, Giacomini, K.M., Huang, S.-M., Tweedie, D.J., Benet, L.Z., Brouwer, K.L.R., Chu, X., Dahlin, A., Evers, R., Fischer, V., et al. (2010). Membrane transporters in drug development. *Nat. Rev. Drug Discov.* *9*, 215–236.
- Irizarry, R.A., Bolstad, B.M., Collin, F., Cope, L.M., Hobbs, B., and Speed, T.P. (2003). Summaries of Affymetrix GeneChip probe level data. *Nucleic Acids Res.* *31*, e15–e15.
- Jakob, S.M., Ruokonen, E., Rosenberg, P.H., and Takala, J. (2002). Effect of dopamine-induced changes in splanchnic blood flow on MEGX production from lidocaine in septic and cardiac surgery patients. *Shock Augusta Ga* *18*, 1–7.
- Jancova, P., Anzenbacher, P., and Anzenbacherova, E. (2010). Phase II drug metabolizing enzymes. *Biomed. Pap. Med. Fac. Univ. Palacký Olomouc Czechoslov.* *154*, 103–116.
- Jemnitz, K., Veres, Z., Monostory, K., Kóbori, L., and Vereczkey, L. (2008). Interspecies differences in acetaminophen sensitivity of human, rat, and mouse primary hepatocytes. *Toxicol. Vitro Int. J. Publ. Assoc. BIBRA* *22*, 961–967.
- Jonkers, I.J., Mohrschladt, M.F., Westendorp, R.G., van der Laarse, A., and Smelt, A.H. (2002). Severe hypertriglyceridemia with insulin resistance is associated with systemic inflammation: reversal with bezafibrate therapy in a randomized controlled trial. *Am. J. Med.* *112*, 275–280.
- Jover, R., Bort, R., Gómez-Lechón, M.J., and Castell, J.V. (2002). Down-regulation of human CYP3A4 by the inflammatory signal interleukin-6: molecular mechanism and transcription factors involved. *FASEB J. Off. Publ. Fed. Am. Soc. Exp. Biol.* *16*, 1799–1801.
- Jover, R., Moya, M., and Gómez-Lechón, M.J. (2009). Transcriptional regulation of cytochrome p450 genes by the nuclear receptor hepatocyte nuclear factor 4-alpha. *Curr. Drug Metab.* *10*, 508–519.
- Jura, J., Wegrzyn, P., Korostyński, M., Guzik, K., Oczko-Wojciechowska, M., Jarzab, M., Kowalska, M., Piechota, M., Przewłocki, R., and Koj, A. (2008). Identification of interleukin-1 and interleukin-6-responsive genes in human monocyte-derived macrophages using microarrays. *Biochim. Biophys. Acta* *1779*, 383–389.
- Kalgutkar, A.S., Obach, R.S., and Maurer, T.S. (2007). Mechanism-based inactivation of cytochrome P450 enzymes: chemical mechanisms, structure-activity relationships and relationship to clinical drug-drug interactions and idiosyncratic adverse drug reactions. *Curr. Drug Metab.* *8*, 407–447.
- Kalitsky-Szirtes, J., Shayeganpour, A., Brocks, D.R., and Piquette-Miller, M. (2004). Suppression of Drug-Metabolizing Enzymes and Efflux Transporters in the Intestine of Endotoxin-Treated Rats. *Drug Metab. Dispos.* *32*, 20–27.
- Kanebratt, K.P., and Andersson, T.B. (2008). Evaluation of HepaRG cells as an in vitro model for human drug metabolism studies. *Drug Metab. Dispos. Biol. Fate Chem.* *36*, 1444–1452.
- Kanehisa, M., and Goto, S. (2000). KEGG: Kyoto Encyclopedia of Genes and Genomes. *Nucleic Acids Res.* *28*, 27–30.
- Karaman, M.W., Herrgard, S., Treiber, D.K., Gallant, P., Atteridge, C.E., Campbell, B.T., Chan, K.W., Ciceri, P., Davis, M.I., Edeen, P.T., et al. (2008). A quantitative analysis of kinase inhibitor selectivity. *Nat. Biotechnol.* *26*, 127–132.

- Kaski, J.C., and Garcia-Moll, X. (2000). C-Reactive Protein as a Clinical Marker of Risk. *Circulation* 102, e63–e64.
- Kinirons, M.T., and O'Mahony, M.S. (2004). Drug metabolism and ageing. *Br. J. Clin. Pharmacol.* 57, 540–544.
- Klein, K., Winter, S., Turpeinen, M., Schwab, M., and Zanger, U.M. (2010). Pathway-Targeted Pharmacogenomics of CYP1A2 in Human Liver. *Front. Pharmacol.* 1.
- Kmiec, Z. (2001). *Cooperation of Liver Cells in Health and Disease: With 18 Tables* (Springer).
- Koike, C., Moore, R., and Negishi, M. (2007). Extracellular signal-regulated kinase is an endogenous signal retaining the nuclear constitutive active/androstane receptor (CAR) in the cytoplasm of mouse primary hepatocytes. *Mol. Pharmacol.* 71, 1217–1221.
- Koukouritaki, S.B., Manro, J.R., Marsh, S.A., Stevens, J.C., Rettie, A.E., McCarver, D.G., and Hines, R.N. (2004). Developmental expression of human hepatic CYP2C9 and CYP2C19. *J. Pharmacol. Exp. Ther.* 308, 965–974.
- Kraemer, M.J., Furukawa, C.T., Koup, J.R., Shapiro, G.G., Pierson, W.E., and Bierman, C.W. (1982). Altered Theophylline Clearance During an Influenza B Outbreak. *Pediatrics* 69, 476–480.
- Kurpad, A.V. (2006). The requirements of protein & amino acid during acute & chronic infections. *Indian J. Med. Res.* 124, 129–148.
- Labow, M., Shuster, D., Zetterstrom, M., Nunes, P., Terry, R., Cullinan, E.B., Bartfai, T., Solorzano, C., Moldawer, L.L., Chizzonite, R., et al. (1997). Absence of IL-1 signaling and reduced inflammatory response in IL-1 type I receptor-deficient mice. *J. Immunol. Baltim. Md* 159, 2452–2461.
- Lantz, C.S., Boesiger, J., Song, C.H., Mach, N., Kobayashi, T., Mulligan, R.C., Nawa, Y., Dranoff, G., and Galli, S.J. (1998). Role for interleukin-3 in mast-cell and basophil development and in immunity to parasites. *Nature* 392, 90–93.
- Larsen, L., and Röpke, C. (2002). Suppressors of cytokine signalling: SOCS. *APMIS Acta Pathol. Microbiol. Immunol. Scand.* 110, 833–844.
- Laybourn, C., Tønnesen, P., Loft, S., Sonne, J., and Døssing, M. (1986). Pulmonary disease and antipyrine clearance. *Clin. Pharmacol. Ther.* 40, 415–419.
- Lecluyse, E.L., and Alexandre, E. (2010). Isolation and culture of primary hepatocytes from resected human liver tissue. *Methods Mol. Biol. Clifton NJ* 640, 57–82.
- Lee, B.L., Wong, D., Benowitz, N.L., and Sullam, P.M. (1993). Altered patterns of drug metabolism in patients with acquired immunodeficiency syndrome. *Clin. Pharmacol. Ther.* 53, 529–535.
- Lee, J.K., Chung, H.J., Fischer, L., Fischer, J., Gonzalez, F.J., and Jeong, H. (2014). Human Placental Lactogen Induces CYP2E1 Expression via PI 3-Kinase Pathway in Female Human Hepatocytes. *Drug Metab. Dispos. Biol. Fate Chem.* 42, 492–499.
- Lee, S.M.L., Schelcher, C., Demmel, M., Hauner, M., and Thasler, W.E. (2013). Isolation of human hepatocytes by a two-step collagenase perfusion procedure. *J. Vis. Exp. JoVE.*
- Lehmann, U., Schmitz, J., Weissenbach, M., Sobota, R.M., Hortner, M., Friederichs, K., Behrmann, I., Tsiaris, W., Sasaki, A., Schneider-Mergener, J., et al. (2003). SHP2 and SOCS3 contribute to Tyr-759-dependent attenuation of interleukin-6 signaling through gp130. *J. Biol. Chem.* 278, 661–671.
- Leslie, E.M., Deeley, R.G., and Cole, S.P.C. (2005). Multidrug resistance proteins: role of P-glycoprotein, MRP1, MRP2, and BCRP (ABCG2) in tissue defense. *Toxicol. Appl. Pharmacol.* 204, 216–237.
- Li, D., Zimmerman, T.L., Thevananther, S., Lee, H.-Y., Kurie, J.M., and Karpen, S.J. (2002). Interleukin-1 beta-mediated suppression of RXR:RAR transactivation of the Ntcp promoter is JNK-dependent. *J. Biol. Chem.* 277, 31416–31422.

- Lim, Y.-P., and Huang, J. (2008). Interplay of pregnane X receptor with other nuclear receptors on gene regulation. *Drug Metab. Pharmacokinet.* 23, 14–21.
- Liu, S., Huang, C., Li, D., Ren, W., Zhang, H., Qi, M., Li, X., and Yu, L. (2007). Molecular cloning and expression analysis of a new gene for short-chain dehydrogenase/reductase 9. *Acta Biochim. Pol.* 54, 213–218.
- Livak, K.J., and Schmittgen, T.D. (2001). Analysis of relative gene expression data using real-time quantitative PCR and the 2(-Delta Delta C(T)) Method. *Methods San Diego Calif* 25, 402–408.
- Lobo, S.M.A., Lobo, F.R.M., Bota, D.P., Lopes-Ferreira, F., Soliman, H.M., Mélot, C., and Vincent, J.-L. (2003). C-reactive protein levels correlate with mortality and organ failure in critically ill patients. *Chest* 123, 2043–2049.
- Lonard, D.M., and O'Malley, B.W. (2006). The expanding cosmos of nuclear receptor coactivators. *Cell* 125, 411–414.
- Lu, S.C. (2013). Glutathione synthesis. *Biochim. Biophys. Acta* 1830, 3143–3153.
- Lübberstedt, M., Müller-Vieira, U., Mayer, M., Biemel, K.M., Knöspel, F., Knobloch, D., Nüssler, A.K., Gerlach, J.C., and Zeilinger, K. (2011). HepaRG human hepatic cell line utility as a surrogate for primary human hepatocytes in drug metabolism assessment in vitro. *J. Pharmacol. Toxicol. Methods* 63, 59–68.
- Luster, A.D. (1998). Chemokines — Chemotactic Cytokines That Mediate Inflammation. *N. Engl. J. Med.* 338, 436–445.
- Machavaram, K.K., Almond, L.M., Rostami-Hodjegan, A., Gardner, I., Jamei, M., Tay, S., Wong, S., Joshi, A., and Kenny, J.R. (2013). A Physiologically Based Pharmacokinetic Modeling Approach to Predict Disease-Drug Interactions: Suppression of CYP3A by IL-6. *Clin. Pharmacol. Ther.* 94, 260–268.
- Mackenzie, P.I., Bock, K.W., Burchell, B., Guillemette, C., Ikushiro, S., Iyanagi, T., Miners, J.O., Owens, I.S., and Nebert, D.W. (2005). Nomenclature update for the mammalian UDP glycosyltransferase (UGT) gene superfamily. *Pharmacogenet. Genomics* 15, 677–685.
- Macy, E.M., Hayes, T.E., and Tracy, R.P. (1997). Variability in the measurement of C-reactive protein in healthy subjects: implications for reference intervals and epidemiological applications. *Clin. Chem.* 43, 52–58.
- Madrid, L.V., Mayo, M.W., Reuther, J.Y., and Baldwin, A.S., Jr (2001). Akt stimulates the transactivation potential of the RelA/p65 Subunit of NF-kappa B through utilization of the Ikappa B kinase and activation of the mitogen-activated protein kinase p38. *J. Biol. Chem.* 276, 18934–18940.
- De Maeyer, E., and De Maeyer-Guignard, J. (1998). Type I interferons. *Int. Rev. Immunol.* 17, 53–73.
- Maheo, K., Antras-Ferry, J., Morel, F., Langouët, S., and Guillouzo, A. (1997). Modulation of glutathione S-transferase subunits A2, M1, and P1 expression by interleukin-1beta in rat hepatocytes in primary culture. *J. Biol. Chem.* 272, 16125–16132.
- Mangelsdorf, D.J., and Evans, R.M. (1995). The RXR heterodimers and orphan receptors. *Cell* 83, 841–850.
- Markiewski, M.M., and Lambris, J.D. (2007). The Role of Complement in Inflammatory Diseases From Behind the Scenes into the Spotlight. *Am. J. Pathol.* 171, 715–727.
- Marsden, J.R., Williams, F.M., Keys, B., Rawlins, M.D., and Shuster, S. (1984). Reduction of antipyrine clearance in psoriasis. *Br. J. Clin. Pharmacol.* 17, 331–333.
- Matsumura, T., Imamichi, Y., Mizutani, T., Ju, Y., Yazawa, T., Kawabe, S., Kanno, M., Ayabe, T., Katsumata, N., Fukami, M., et al. (2013). Human glutathione S-transferase A (GSTA) family genes are regulated by steroidogenic factor 1 (SF-1) and are involved in steroidogenesis. *FASEB J. Off. Publ. Fed. Am. Soc. Exp. Biol.* 27, 3198–3208.

- Mayo, P.R., Skeith, K., Russell, A.S., and Jamali, F. (2000). Decreased dromotropic response to verapamil despite pronounced increased drug concentration in rheumatoid arthritis. *Br. J. Clin. Pharmacol.* *50*, 605–613.
- Mikkaichi, T., Suzuki, T., Tanemoto, M., Ito, S., and Abe, T. (2004). The organic anion transporter (OATP) family. *Drug Metab. Pharmacokinet.* *19*, 171–179.
- Minamiyama, Y., Takemura, S., Imaoka, S., Funae, Y., Tanimoto, Y., and Inoue, M. (1997). Irreversible inhibition of cytochrome P450 by nitric oxide. *J. Pharmacol. Exp. Ther.* *283*, 1479–1485.
- Mizuno, N., Niwa, T., Yotsumoto, Y., and Sugiyama, Y. (2003). Impact of Drug Transporter Studies on Drug Discovery and Development. *Pharmacol. Rev.* *55*, 425–461.
- Molanaei, H., Stenvinkel, P., Qureshi, A.R., Carrero, J.J., Heimbürger, O., Lindholm, B., Diczfalusy, U., Odar-Cederlöf, I., and Bertilsson, L. (2012). Metabolism of alprazolam (a marker of CYP3A4) in hemodialysis patients with persistent inflammation. *Eur. J. Clin. Pharmacol.* *68*, 571–577.
- Mold, C., Gewurz, H., and Du Clos, T.W. (1999). Regulation of complement activation by C-reactive protein. *Immunopharmacology* *42*, 23–30.
- Moore, K.W., O’Garra, A., de Waal Malefyt, R., Vieira, P., and Mosmann, T.R. (1993). Interleukin-10. *Annu. Rev. Immunol.* *11*, 165–190.
- Morel, F., Beaune, P.H., Ratanasavanh, D., Flinois, J.P., Yang, C.S., Guengerich, F.P., and Guillouzo, A. (1990). Expression of cytochrome P-450 enzymes in cultured human hepatocytes. *Eur. J. Biochem. FEBS* *191*, 437–444.
- Morgan, E.T. (1997). Regulation of cytochromes P450 during inflammation and infection. *Drug Metab. Rev.* *29*, 1129–1188.
- Morgan, E.T. (2001). Regulation of cytochrome p450 by inflammatory mediators: why and how? *Drug Metab. Dispos. Biol. Fate Chem.* *29*, 207–212.
- Morgan, E.T. (2009). Impact of infectious and inflammatory disease on cytochrome P450-mediated drug metabolism and pharmacokinetics. *Clin. Pharmacol. Ther.* *85*, 434–438.
- Morgan, E.T., Goralski, K.B., Piquette-Miller, M., Renton, K.W., Robertson, G.R., Chaluvadi, M.R., Charles, K.A., Clarke, S.J., Kacevska, M., Liddle, C., et al. (2008). Regulation of Drug-Metabolizing Enzymes and Transporters in Infection, Inflammation, and Cancer. *Drug Metab. Dispos.* *36*, 205–216.
- Murray, M., Cui, P.H., and Zhou, F. (2010). Roles of mitogen-activated protein kinases in the regulation of CYP genes. *Curr. Drug Metab.* *11*, 850–858.
- Mwinyi, J., Cavaco, I., Pedersen, R.S., Persson, A., Burkhardt, S., Mkrтчian, S., and Ingelman-Sundberg, M. (2010). Regulation of CYP2C19 expression by estrogen receptor  $\alpha$ : implications for estrogen-dependent inhibition of drug metabolism. *Mol. Pharmacol.* *78*, 886–894.
- Naugler, W.E., and Karin, M. (2008). The wolf in sheep’s clothing: the role of interleukin-6 in immunity, inflammation and cancer. *Trends Mol. Med.* *14*, 109–119.
- Neafsey, P., Ginsberg, G., Hattis, D., Johns, D.O., Guyton, K.Z., and Sonawane, B. (2009). Genetic polymorphism in CYP2E1: Population distribution of CYP2E1 activity. *J. Toxicol. Environ. Health B Crit. Rev.* *12*, 362–388.
- Nies, A.T., Koepsell, H., Winter, S., Burk, O., Klein, K., Kerb, R., Zanger, U.M., Keppler, D., Schwab, M., and Schaeffeler, E. (2009). Expression of organic cation transporters OCT1 (SLC22A1) and OCT3 (SLC22A3) is affected by genetic factors and cholestasis in human liver. *Hepatology* *50*, 1227–1240.
- Nigam, S.K., Bush, K.T., and Bhatnagar, V. (2007). Drug and toxicant handling by the OAT organic anion transporters in the kidney and other tissues. *Nat. Clin. Pract. Nephrol.* *3*, 443–448.
- O’Neil, W.M., Gilfix, B.M., Markoglou, N., Di Girolamo, A., Tsoukas, C.M., and Wainer, I.W. (2000). Genotype and phenotype of cytochrome P450 2D6 in human

- immunodeficiency virus-positive patients and patients with acquired immunodeficiency syndrome. *Eur. J. Clin. Pharmacol.* *56*, 231–240.
- Oesch-Bartlomowicz, B., and Oesch, F. (2003). Cytochrome-P450 phosphorylation as a functional switch. *Arch. Biochem. Biophys.* *409*, 228–234.
- Ozes, O.N., Mayo, L.D., Gustin, J.A., Pfeffer, S.R., Pfeffer, L.M., and Donner, D.B. (1999). NF-kappaB activation by tumour necrosis factor requires the Akt serine-threonine kinase. *Nature* *401*, 82–85.
- Pasanen, M., Rannala, Z., Tooming, A., Sotaniemi, E.A., Pelkonen, O., and Rautio, A. (1997). Hepatitis A impairs the function of human hepatic CYP2A6 in vivo. *Toxicology* *123*, 177–184.
- Pascussi, J.M., Gerbal-Chaloin, S., Pichard-Garcia, L., Daujat, M., Fabre, J.M., Maurel, P., and Vilarem, M.J. (2000). Interleukin-6 negatively regulates the expression of pregnane X receptor and constitutively activated receptor in primary human hepatocytes. *Biochem. Biophys. Res. Commun.* *274*, 707–713.
- Pascussi, J.M., Busson-Le Coniat, M., Maurel, P., and Vilarem, M.-J. (2003). Transcriptional Analysis of the Orphan Nuclear Receptor Constitutive Androstane Receptor (NR1I3) Gene Promoter: Identification of a Distal Glucocorticoid Response Element. *Mol. Endocrinol.* *17*, 42–55.
- Pascussi, J.-M., Gerbal-Chaloin, S., Duret, C., Daujat-Chavanieu, M., Vilarem, M.-J., and Maurel, P. (2008). The tangle of nuclear receptors that controls xenobiotic metabolism and transport: crosstalk and consequences. *Annu. Rev. Pharmacol. Toxicol.* *48*, 1–32.
- Pelkonen, O., Turpeinen, M., Hakkola, J., Honkakoski, P., Hukkanen, J., and Raunio, H. (2008). Inhibition and induction of human cytochrome P450 enzymes: current status. *Arch. Toxicol.* *82*, 667–715.
- Penaloza, C.G., Estevez, B., Han, D.M., Norouzi, M., Lockshin, R.A., and Zakeri, Z. (2014). Sex-dependent regulation of cytochrome P450 family members Cyp1a1, Cyp2e1, and Cyp7b1 by methylation of DNA. *FASEB J. Off. Publ. Fed. Am. Soc. Exp. Biol.* *28*, 966–977.
- Pennica, D., Nedwin, G.E., Hayflick, J.S., Seeburg, P.H., Derynck, R., Palladino, M.A., Kohr, W.J., Aggarwal, B.B., and Goeddel, D.V. (1984). Human tumour necrosis factor: precursor structure, expression and homology to lymphotoxin. *Nature* *312*, 724–729.
- Pepys, M.B., and Baltz, M.L. (1983). Acute phase proteins with special reference to C-reactive protein and related proteins (pentaxins) and serum amyloid A protein. *Adv. Immunol.* *34*, 141–212.
- Pepys, M.B., and Hirschfield, G.M. (2003). C-reactive protein: a critical update. *J. Clin. Invest.* *113*, 1805–1812.
- Pepys, M.B., Rowe, I.F., and Baltz, M.L. (1985). C-reactive protein: binding to lipids and lipoproteins. *Int. Rev. Exp. Pathol.* *27*, 83–111.
- Petrovic, V., Teng, S., and Piquette-Miller, M. (2007). REGULATION OF DRUG TRANSPORTERS: DURING INFECTION AND INFLAMMATION. *Mol. Interv.* *7*, 99–111.
- Pitarque, M., Rodríguez-Antona, C., Oscarson, M., and Ingelman-Sundberg, M. (2005). Transcriptional Regulation of the Human CYP2A6 Gene. *J. Pharmacol. Exp. Ther.* *313*, 814–822.
- Poetz, O., Schwenk, J.M., Kramer, S., Stoll, D., Templin, M.F., and Joos, T.O. (2005). Protein microarrays: catching the proteome. *Mech. Ageing Dev.* *126*, 161–170.
- Poller, B., Drewe, J., Krähenbühl, S., Huwyler, J., and Gutmann, H. (2010). Regulation of BCRP (ABCG2) and P-glycoprotein (ABCB1) by cytokines in a model of the human blood-brain barrier. *Cell. Mol. Neurobiol.* *30*, 63–70.
- Pond, S.M., and Tozer, T.N. (1984). First-pass elimination. Basic concepts and clinical consequences. *Clin. Pharmacokinet.* *9*, 1–25.

- Proctor, M.J., Horgan, P.G., Talwar, D., Fletcher, C.D., Morrison, D.S., and McMillan, D.C. (2013). Optimization of the systemic inflammation-based Glasgow Prognostic Score. *Cancer* 119, 2325–2332.
- Rahman, K. (2007). Studies on free radicals, antioxidants, and co-factors. *Clin. Interv. Aging* 2, 219–236.
- Ramadoss, P., Chiappini, F., Bilban, M., and Hollenberg, A.N. (2010). Regulation of Hepatic Six Transmembrane Epithelial Antigen of Prostate 4 (STEAP4) Expression by STAT3 and CCAAT/Enhancer-binding Protein  $\alpha$ . *J. Biol. Chem.* 285, 16453–16466.
- Raman, M., Chen, W., and Cobb, M.H. (2007). Differential regulation and properties of MAPKs. *Oncogene* 26, 3100–3112.
- Reeds, P.J., Fjeld, C.R., and Jahoor, F. (1994). Do the Differences between the Amino Acid Compositions of Acute-Phase and Muscle Proteins Have a Bearing on Nitrogen Loss in Traumatic States? *J. Nutr.* 124, 906–910.
- Renton, K.W. (2005). Regulation of drug metabolism and disposition during inflammation and infection. *Expert Opin. Drug Metab. Toxicol.* 1, 629–640.
- Renton, K.W., Gray, J.D., and Hall, R.I. (1980). Decreased elimination of theophylline after influenza vaccination. *Can. Med. Assoc. J.* 123, 288–290.
- Richardson, T.A., Sherman, M., Kalman, D., and Morgan, E.T. (2006). Expression of UDP-glucuronosyltransferase isoform mRNAs during inflammation and infection in mouse liver and kidney. *Drug Metab. Dispos. Biol. Fate Chem.* 34, 351–353.
- Riches, Z., Stanley, E.L., Bloomer, J.C., and Coughtrie, M.W.H. (2009). Quantitative evaluation of the expression and activity of five major sulfotransferases (SULTs) in human tissues: the SULT “pie.” *Drug Metab. Dispos. Biol. Fate Chem.* 37, 2255–2261.
- Richter, T., Mürdter, T.E., Heinkele, G., Pleiss, J., Tatzel, S., Schwab, M., Eichelbaum, M., and Zanger, U.M. (2004). Potent mechanism-based inhibition of human CYP2B6 by clopidogrel and ticlopidine. *J. Pharmacol. Exp. Ther.* 308, 189–197.
- Rivory, L.P., Slaviero, K.A., and Clarke, S.J. (2002). Hepatic cytochrome P450 3A drug metabolism is reduced in cancer patients who have an acute-phase response. *Br. J. Cancer* 87, 277–280.
- Rogue, A., Lambert, C., Spire, C., Claude, N., and Guillouzo, A. (2012). Interindividual variability in gene expression profiles in human hepatocytes and comparison with HepaRG cells. *Drug Metab. Dispos. Biol. Fate Chem.* 40, 151–158.
- Romashkova, J.A., and Makarov, S.S. (1999). NF-kappaB is a target of AKT in anti-apoptotic PDGF signalling. *Nature* 401, 86–90.
- Salazar, J., Martínez, Nez, M., Sofía, A., a, Ch&#xe1, Vez, M., Toledo, A., A&#xf1, Ez, R., et al. (2014). C-Reactive Protein: Clinical and Epidemiological Perspectives. *Cardiol. Res. Pract.* 2014.
- Sammalkorpi, K., Valtonen, V., Kerttula, Y., Nikkilä, E., and Taskinen, M.R. (1988). Changes in serum lipoprotein pattern induced by acute infections. *Metabolism.* 37, 859–865.
- Scandlyn, M.J., Stuart, E.C., and Rosengren, R.J. (2008). Sex-specific differences in CYP450 isoforms in humans. *Expert Opin. Drug Metab. Toxicol.* 4, 413–424.
- Schaeffer, H.J., and Weber, M.J. (1999). Mitogen-Activated Protein Kinases: Specific Messages from Ubiquitous Messengers. *Mol. Cell. Biol.* 19, 2435–2444.
- Schinkel, A.H., and Jonker, J.W. (2003). Mammalian drug efflux transporters of the ATP binding cassette (ABC) family: an overview. *Adv. Drug Deliv. Rev.* 55, 3–29.
- Schmitz, J., Weissenbach, M., Haan, S., Heinrich, P.C., and Schaper, F. (2000). SOCS3 exerts its inhibitory function on interleukin-6 signal transduction through the SHP2 recruitment site of gp130. *J. Biol. Chem.* 275, 12848–12856.
- Schrader, M., and Fahimi, H.D. (2006). Peroxisomes and oxidative stress. *Biochim. Biophys. Acta* 1763, 1755–1766.

- Schröder, A., Klein, K., Winter, S., Schwab, M., Bonin, M., Zell, A., and Zanger, U.M. (2013). Genomics of ADME gene expression: mapping expression quantitative trait loci relevant for absorption, distribution, metabolism and excretion of drugs in human liver. *Pharmacogenomics J.* *13*, 12–20.
- Schust, J., Sperl, B., Hollis, A., Mayer, T.U., and Berg, T. (2006). Stattic: a small-molecule inhibitor of STAT3 activation and dimerization. *Chem. Biol.* *13*, 1235–1242.
- Scotto, K.W. (2003). Transcriptional regulation of ABC drug transporters. *Oncogene* *22*, 7496–7511.
- Sedgwick, J.D., Riminton, D.S., Cyster, J.G., and Körner, H. (2000). Tumor necrosis factor: a master-regulator of leukocyte movement. *Immunol. Today* *21*, 110–113.
- Seok, J., Warren, H.S., Cuenca, A.G., Mindrinos, M.N., Baker, H.V., Xu, W., Richards, D.R., McDonald-Smith, G.P., Gao, H., Hennessy, L., et al. (2013). Genomic responses in mouse models poorly mimic human inflammatory diseases. *Proc. Natl. Acad. Sci.* *110*, 3507–3512.
- Shackel, N.A., Seth, D., Haber, P.S., Gorrell, M.D., and McCaughan, G.W. (2006). The hepatic transcriptome in human liver disease. *Comp. Hepatol.* *5*, 6.
- Sharma, Y., Chilamakuri, C.S.R., Bakke, M., and Lenhard, B. (2014). Computational Characterization of Modes of Transcriptional Regulation of Nuclear Receptor Genes. *PLoS ONE* *9*.
- Shedlofsky, S.I., Israel, B.C., McClain, C.J., Hill, D.B., and Blouin, R.A. (1994). Endotoxin administration to humans inhibits hepatic cytochrome P450-mediated drug metabolism. *J. Clin. Invest.* *94*, 2209–2214.
- Shedlofsky, S.I., Israel, B.C., Tosheva, R., and Blouin, R.A. (1997). Endotoxin depresses hepatic cytochrome P450-mediated drug metabolism in women. *Br. J. Clin. Pharmacol.* *43*, 627–632.
- Shelly, M.P., Mendel, L., and Park, G.R. (1987). Failure of critically ill patients to metabolise midazolam. *Anaesthesia* *42*, 619–626.
- Shen, Kunze, and Thummel (1997). Enzyme-catalyzed processes of first-pass hepatic and intestinal drug extraction. *Adv. Drug Deliv. Rev.* *27*, 99–127.
- Shields, J.M., Pruitt, K., McFall, A., Shaub, A., and Der, C.J. (2000). Understanding Ras: “it ain’t over ‘til it’s over”. *Trends Cell Biol.* *10*, 147–154.
- Shimada, M., Watanabe, E., Iida, Y., Nagata, K., and Yamazoe, Y. (1999). Alteration of hepatic sulfation by endotoxin. *Jpn. J. Pharmacol.* *80*, 371–373.
- Shine, B., de Beer, F.C., and Pepys, M.B. (1981). Solid phase radioimmunoassays for human C-reactive protein. *Clin. Chim. Acta* *117*, 13–23.
- Siewert, E., Bort, R., Kluge, R., Heinrich, P.C., Castell, J., and Jover, R. (2000). Hepatic Cytochrome P450 Down-regulation During Aseptic Inflammation in the Mouse Is Interleukin 6 Dependent. *Hepatology* *32*, 49–55.
- Siewert, E., Dietrich, C.G., Lammert, F., Heinrich, P.C., Matern, S., Gartung, C., and Geier, A. (2004). Interleukin-6 regulates hepatic transporters during acute-phase response. *Biochem. Biophys. Res. Commun.* *322*, 232–238.
- Slaviero, K.A., Clarke, S.J., and Rivory, L.P. (2003). Inflammatory response: an unrecognised source of variability in the pharmacokinetics and pharmacodynamics of cancer chemotherapy. *Lancet Oncol.* *4*, 224–232.
- Sonne, J., Døssing, M., Loft, S., and Andreasen, P.B. (1985). Antipyrine clearance in pneumonia. *Clin. Pharmacol. Ther.* *37*, 701–704.
- Sonoda, J., Rosenfeld, J.M., Xu, L., Evans, R.M., and Xie, W. (2003). A nuclear receptor-mediated xenobiotic response and its implication in drug metabolism and host protection. *Curr. Drug Metab.* *4*, 59–72.
- Spurgeon, S.L., Jones, R.C., and Ramakrishnan, R. (2008). High throughput gene expression measurement with real time PCR in a microfluidic dynamic array. *PloS One* *3*, e1662.

- Starr, R., Willson, T.A., Viney, E.M., Murray, L.J., Rayner, J.R., Jenkins, B.J., Gonda, T.J., Alexander, W.S., Metcalf, D., Nicola, N.A., et al. (1997). A family of cytokine-inducible inhibitors of signalling. *Nature* *387*, 917–921.
- Staudinger, J.L., and Lichti, K. (2008). Cell signaling and nuclear receptors: new opportunities for molecular pharmaceuticals in liver disease. *Mol. Pharm.* *5*, 17–34.
- Stenman, U.-H. (2011). SPINK1: A New Therapeutic Target in Cancer? *Clin. Chem.* *57*, 1474–1475.
- Storz, P., Döppler, H., and Toker, A. (2005). Protein kinase D mediates mitochondrion-to-nucleus signaling and detoxification from mitochondrial reactive oxygen species. *Mol. Cell. Biol.* *25*, 8520–8530.
- Strasser, S.I., Mashford, M.L., and Desmond, P.V. (1998). Regulation of uridine diphosphate glucuronosyltransferase during the acute-phase response. *J. Gastroenterol. Hepatol.* *13*, 88–94.
- Sukhai, M., Yong, A., Kalitsky, J., and Piquette-Miller, M. (2000). Inflammation and interleukin-6 mediate reductions in the hepatic expression and transcription of the *mdr1a* and *mdr1b* Genes. *Mol. Cell Biol. Res. Commun. MCBRC* *4*, 248–256.
- Supek, F., Bošnjak, M., Škunca, N., and Šmuc, T. (2011). REVIGO Summarizes and Visualizes Long Lists of Gene Ontology Terms. *PLoS ONE* *6*, e21800.
- Takahashi-Tezuka, M., Yoshida, Y., Fukada, T., Ohtani, T., Yamanaka, Y., Nishida, K., Nakajima, K., Hibi, M., and Hirano, T. (1998). Gab1 acts as an adapter molecule linking the cytokine receptor gp130 to ERK mitogen-activated protein kinase. *Mol. Cell. Biol.* *18*, 4109–4117.
- Takeda, K., Tsutsui, H., Yoshimoto, T., Adachi, O., Yoshida, N., Kishimoto, T., Okamura, H., Nakanishi, K., and Akira, S. (1998). Defective NK cell activity and Th1 response in IL-18-deficient mice. *Immunity* *8*, 383–390.
- Teng, S., and Piquette-Miller, M. (2005). The involvement of the pregnane X receptor in hepatic gene regulation during inflammation in mice. *J. Pharmacol. Exp. Ther.* *312*, 841–848.
- Thomas, M., Burk, O., Klumpp, B., Kandel, B.A., Damm, G., Weiss, T.S., Klein, K., Schwab, M., and Zanger, U.M. (2013). Direct Transcriptional Regulation of Human Hepatic Cytochrome P450 3A4 (CYP3A4) by Peroxisome Proliferator-Activated Receptor Alpha (PPAR $\alpha$ ). *Mol. Pharmacol.*
- Thummel, K.E., and Lin, Y.S. (2014). Sources of interindividual variability. *Methods Mol. Biol. Clifton NJ* *1113*, 363–415.
- Thurman, R.G., Bradford, B.U., Iimuro, Y., Frankenberg, M.V., Knecht, K.T., Connor, H.D., Adachi, Y., Wall, C., Arteel, G.E., Raleigh, J.A., et al. (1999). Mechanisms of alcohol-induced hepatotoxicity: studies in rats. *Front. Biosci. J. Virtual Libr.* *4*, e42–46.
- Tian, Y., Ke, S., Denison, M.S., Rabson, A.B., and Gallo, M.A. (1999). Ah receptor and NF-kappaB interactions, a potential mechanism for dioxin toxicity. *J. Biol. Chem.* *274*, 510–515.
- Tillett, W.S., and Francis, T. (1930). Serological Reactions in Pneumonia with a Non-Protein Somatic Fraction of Pneumococcus. *J. Exp. Med.* *52*, 561–571.
- Toft, P., Heslet, L., Hansen, M., and Klitgaard, N.A. (1991). Theophylline and ethylenediamine pharmacokinetics following administration of aminophylline to septic patients with multiorgan failure. *Intensive Care Med.* *17*, 465–468.
- Tolson, A.H., and Wang, H. (2010). Regulation of drug-metabolizing enzymes by xenobiotic receptors: PXR and CAR. *Adv. Drug Deliv. Rev.* *62*, 1238–1249.
- Turpeinen, M., Tolonen, A., Chesne, C., Guillouzo, A., Uusitalo, J., and Pelkonen, O. (2009). Functional expression, inhibition and induction of CYP enzymes in HepaRG cells. *Toxicol. Vitro Int. J. Publ. Assoc. BIBRA* *23*, 748–753.

- Vee, M.L., Lecureur, V., Stieger, B., and Fardel, O. (2009). Regulation of Drug Transporter Expression in Human Hepatocytes Exposed to the Proinflammatory Cytokines Tumor Necrosis Factor- $\alpha$  or Interleukin-6. *Drug Metab. Dispos.* *37*, 685–693.
- Le Vee, M., Gripon, P., Stieger, B., and Fardel, O. (2008). Down-regulation of organic anion transporter expression in human hepatocytes exposed to the proinflammatory cytokine interleukin 1beta. *Drug Metab. Dispos. Biol. Fate Chem.* *36*, 217–222.
- Vigushin, D.M., Pepys, M.B., and Hawkins, P.N. (1993). Metabolic and scintigraphic studies of radioiodinated human C-reactive protein in health and disease. *J. Clin. Invest.* *91*, 1351–1357.
- Volanakis, J.E., and Wirtz, K.W. (1979). Interaction of C-reactive protein with artificial phosphatidylcholine bilayers. *Nature* *281*, 155–157.
- Voleti, B., and Agrawal, A. (2005). Regulation of basal and induced expression of C-reactive protein through an overlapping element for OCT-1 and NF-kappaB on the proximal promoter. *J. Immunol. Baltim. Md 1950* *175*, 3386–3390.
- Wang, H., and LeCluyse, E.L. (2003). Role of orphan nuclear receptors in the regulation of drug-metabolising enzymes. *Clin. Pharmacokinet.* *42*, 1331–1357.
- Wang, X.-R., Qu, Z.-Q., Li, X.-D., Liu, H.-L., He, P., Fang, B.-X., Xiao, J., Huang, W., and Wu, M.-C. (2010). Activity of sulfotransferase 1A1 is dramatically upregulated in patients with hepatocellular carcinoma secondary to chronic hepatitis B virus infection. *Cancer Sci.* *101*, 412–415.
- Ware, C.F. (2011). The TNF receptor super family in immune regulation. *Immunol. Rev.* *244*, 5–8.
- Waring, R.H., Harris, R.M., Hunter, J.O., and Mitchell, S.C. (2013). Xenobiotic sulphation and its variability during inflammation: a factor in adverse drug reactions? *Curr. Drug Metab.* *14*, 361–365.
- Waxman, D.J., and Holloway, M.G. (2009). Sex differences in the expression of hepatic drug metabolizing enzymes. *Mol. Pharmacol.* *76*, 215–228.
- Wendel, H.-G., De Stanchina, E., Fridman, J.S., Malina, A., Ray, S., Kogan, S., Cordon-Cardo, C., Pelletier, J., and Lowe, S.W. (2004). Survival signalling by Akt and eIF4E in oncogenesis and cancer therapy. *Nature* *428*, 332–337.
- Wheeler, J.B., Stourman, N.V., Thier, R., Dommermuth, A., Vuilleumier, S., Rose, J.A., Armstrong, R.N., and Guengerich, F.P. (2001). Conjugation of haloalkanes by bacterial and mammalian glutathione transferases: mono- and dihalomethanes. *Chem. Res. Toxicol.* *14*, 1118–1127.
- Wheelock, E.F. (1965). Interferon-Like Virus-Inhibitor Induced in Human Leukocytes by Phytohemagglutinin. *Science* *149*, 310–311.
- Williams, E.J., and Doherty, P. (1999). Evidence for and against a pivotal role of PI 3-kinase in a neuronal cell survival pathway. *Mol. Cell. Neurosci.* *13*, 272–280.
- Wolbold, R., Klein, K., Burk, O., Nüssler, A.K., Neuhaus, P., Eichelbaum, M., Schwab, M., and Zanger, U.M. (2003). Sex is a major determinant of CYP3A4 expression in human liver. *Hepatology. Baltim. Md* *38*, 978–988.
- Wu, T.R., Hong, Y.K., Wang, X.-D., Ling, M.Y., Dragoi, A.M., Chung, A.S., Campbell, A.G., Han, Z.-Y., Feng, G.-S., and Chin, Y.E. (2002). SHP-2 Is a Dual-specificity Phosphatase Involved in Stat1 Dephosphorylation at Both Tyrosine and Serine Residues in Nuclei. *J. Biol. Chem.* *277*, 47572–47580.
- Xiao, W., Mindrinos, M.N., Seok, J., Cuschieri, J., Cuenca, A.G., Gao, H., Hayden, D.L., Hennessy, L., Moore, E.E., Minei, J.P., et al. (2011). A genomic storm in critically injured humans. *J. Exp. Med.* *208*, 2581–2590.
- Xu, C., Li, C.Y.-T., and Kong, A.-N.T. (2005). Induction of phase I, II and III drug metabolism/transport by xenobiotics. *Arch. Pharm. Res.* *28*, 249–268.

- Yamazaki, H., and Shimada, T. (1997). Progesterone and testosterone hydroxylation by cytochromes P450 2C19, 2C9, and 3A4 in human liver microsomes. *Arch. Biochem. Biophys.* *346*, 161–169.
- Yang, Q., Doshi, U., Li, N., and Li, A.P. (2012). Effects of Culture Duration on Gene Expression of P450 Isoforms, Uptake and Efflux Transporters in Primary Hepatocytes Cultured in the Absence and Presence of Interleukin-6: Implications for Experimental Design for the Evaluation of Downregulatory Effects of Biotherapeutics. *Curr. Drug Metab.*
- Yano, N., Habib, N.A., Fadden, K.J., Yamashita, H., Mitry, R., Jauregui, H., Kane, A., Endoh, M., and Rifai, A. (2001). Profiling the adult human liver transcriptome: analysis by cDNA array hybridization. *J. Hepatol.* *35*, 178–186.
- Zanger, U.M. (2012). Introduction to Drug Metabolism. In *Metabolism of Drugs and Other Xenobiotics*, (Weinheim, Germany: Wiley-VCH), pp. 287–300.
- Zanger, U.M., and Schwab, M. (2013). Cytochrome P450 enzymes in drug metabolism: Regulation of gene expression, enzyme activities, and impact of genetic variation. *Pharmacol. Ther.*
- Zanger, U.M., Turpeinen, M., Klein, K., and Schwab, M. (2008). Functional pharmacogenetics/genomics of human cytochromes P450 involved in drug biotransformation. *Anal. Bioanal. Chem.* *392*, 1093–1108.
- Zanger, U.M., Klein, K., Thomas, M., Rieger, J.K., Tremmel, R., Kandel, B.A., Klein, M., and Magdy, T. (2014). Genetics, epigenetics, and regulation of drug-metabolizing cytochrome p450 enzymes. *Clin. Pharmacol. Ther.* *95*, 258–261.
- Zhang, D., Sun, M., Samols, D., and Kushner, I. (1996). STAT3 participates in transcriptional activation of the C-reactive protein gene by interleukin-6. *J. Biol. Chem.* *271*, 9503–9509.
- Zhang, L., Zhang, Y.D., Zhao, P., and Huang, S.-M. (2009). Predicting drug-drug interactions: an FDA perspective. *AAPS J.* *11*, 300–306.
- Zhou, C., Tabb, M.M., Nelson, E.L., Grün, F., Verma, S., Sadatrafiei, A., Lin, M., Mallick, S., Forman, B.M., Thummel, K.E., et al. (2006). Mutual repression between steroid and xenobiotic receptor and NF-kappaB signaling pathways links xenobiotic metabolism and inflammation. *J. Clin. Invest.* *116*, 2280–2289.
- Zlotnik, A., and Yoshie, O. (2000). Chemokines: a new classification system and their role in immunity. *Immunity* *12*, 121–127.
- Zordoky, B.N.M., and El-Kadi, A.O.S. (2009). Role of NF-kappaB in the regulation of cytochrome P450 enzymes. *Curr. Drug Metab.* *10*, 164–178.

## 7 PUBLICATIONS

### 7.1 Publications in peer reviewed journals

Zanger UM, Klein K, Thomas M, Rieger JK, Tremmel R, Kandel BA, **Klein M**, Magdy T. Genetics, epigenetics and regulation of drug metabolizing cytochrome P450 enzymes. *Clinical Pharmacology and Therapeutics*. 2014. 95 (3):258-61.

Trusch F, **Klein M**, Finsterbusch T, Kuehn J, Hofmann J, Ehlers B. Seroprevalence of human polyomavirus 9 and cross-reactivity to African green monkey-derived lymphotropic polyomavirus. *Journal of General Virology*. 2012. 93 (4): 698-705.

### 7.2 Posters presented at national and international meetings

**Klein M**, Rieger JK, Thomas M, Hofmann U, Damm G, Zanger UM. Influence of the acute phase response on the drug detoxification system: A systematic comparison of primary human hepatocytes and HepaRG cells. 2014. Poster presented at 20<sup>th</sup> International Symposium on Microsomes and Drug Oxidations, Stuttgart.

Keller M, **Klein M**, Thomas M, Metzger U, Templin MF, Joos TO, Hoffmann S, Kandel BA, Dräger A, Zanger UM, Zell A. Modelling IL-6-mediated regulation of ADME genes. 2014. Poster presented at 20<sup>th</sup> International Symposium on Microsomes and Drug Oxidations, Stuttgart.

**Klein M**, Kandel BA, Thomas M, Hofmann U, Metzger U, Templin M, Damm G, Zanger UM. Signaling pathways of IL-6-mediated down-regulation of drug detoxification capacity in human hepatocytes. 2013. Poster presented at 10<sup>th</sup> International ISSX Meeting, Toronto.

**Klein M**, Keller R, Thomas M, Tscherneck S, Hofmann U, Metzger U, Templin M, Joos T, Bode J, Timmer J, Draeger A, Zell A, Zanger UM. B5: Cell-cell communication influences detoxifying functions in hepatocytes. 2013. Poster presented at Virtual Liver Mid-term Evaluation, Berlin.

**Klein M**, Draeger A, Joos T, Kandel BA, Keller R, Metzger U, Templin M, Thomas M, Tscherneck S, Zell A, Zanger UM. Elucidation of signalling pathways involved in IL-6-mediated downregulation of drug detoxification capacity. 2012. Poster presented at Systems Biology of Mammalian Cells (SBMC), Leipzig.

Zanger UM, **Klein M**, Keller R, Thomas M, Tscherneck S, Hofmann U, Metzger U, Templin M, Joos T, Bode J, Timmer J, Draeger A, Zell A. B5: Cell-cell communication influences detoxifying functions in hepatocytes. 2012. Poster presented at Virtual Liver Scientific Advisory Board Meeting, Leipzig.

**Klein M**, Kandel BA, Klein K, Thomas M, Thasler W, Schwab M, Zanger UM. Influences of inflammatory processes on ADME gene expression in human liver and hepatocytes. 2011. Poster presented at 17<sup>th</sup> North American Regional ISSX Meeting, Atlanta.

### 7.3 Other publications

Zanger UM, Thomas M, Kerb R, Hofmann U, Kandel BA, **Klein M**, Schwab M. Biotransformation von Fremdstoffen in der Leber: Systembiologische Ansätze zur Vorhersage von Arzneimittelwirkungen. *Systembiologie.de Magazine*. 2012. 5: 65-68.

## 8 ACKNOWLEDGEMENTS

Without the support, patience and guidance of the following people, this study would not have been completed. It is to them that I owe my deepest gratitude.

First, I would like to thank my supervisor Prof. Dr. Ulrich Zanger for giving me the opportunity to work in this interesting field of research. I am grateful for the many valuable discussions throughout the course of my studies and his personal and scientific advice.

I also thank Prof. Dr. Matthias Schwab, the head of the Dr. Margarete Fischer-Bosch-Institute of Clinical Pharmacology (IKP), for giving me the opportunity to pursue my dissertation in this great research environment.

I wish to thank Prof. Dr. Monilola Olayioye for her kind willingness to supervise and review my Ph.D. thesis.

I am grateful to Dr. Maria Thomas for her scientific ideas as well as the many encouraging discussions I had with her.

I particularly thank Dr. Kathrin Klein for her support, guidance, and helpful suggestions throughout the past years.

Special thanks to Benjamin Kandel, who first introduced me to the IKP and always supported me with scientific and practical advice.

My thank also go to Dr. Jessica Rieger for the extensive scientific discussions and her assistance in experimental questions and Roman Tremmel for his support as a fellow Ph.D. student in the Zanger group.

I thank my collaborators, Prof. Dr. Andreas Zell, Dr. Andreas Dräger, and Roland Keller from the Center for Bioinformatics Tübingen (ZBIT) for the interesting interdisciplinary discussions and their contribution to our joint project within the framework of the Virtual Liver Network, a major national initiative funded by the German Federal Ministry of Education and Research (BMBF).

I also wish to acknowledge my collaborators, Dr. Thomas Joos, Dr. Markus Templin, and Dr. Ute Metzger from the Natural and Medical Sciences Institute (NMI) in Reutlingen. I particularly thank Dr. Ute Metzger for coordinating and carrying out proteomics

## ACKNOWLEDGEMENTS

---

measurements for our joint project and for the fruitful scientific discussions.

I gratefully acknowledge the excellent technical assistance of Igor Liebermann and Britta Klumpp. I further wish to thank Dr. Ute Hofmann, Sonja Seefried, and all colleagues from the analytics department for performing LC-MS/MS measurements and their assistance in analyzing the data.

Many thanks go to my friends and colleagues at the IKP, for the pleasant working environment and their constant helpfulness.

Last, but not least, I would like to thank my wife for her understanding and love during the past few years. Her faithful support and encouragement made this dissertation possible. My parents receive my deepest gratitude for their dedication and the many years of support during my undergraduate studies that provided the foundation for this work.

This study was supported by the German Federal Ministry of Education and Research (Virtual Liver grant 0315755) and by the Robert Bosch Stiftung, Stuttgart, Germany.

## **9 DECLARATION/ERKLÄRUNG**

I hereby declare that I have written this dissertation myself using no other sources or materials than those indicated. I furthermore declare that this dissertation has not yet been submitted to any other official commission, neither in this nor in equal form.

Hiermit erkläre ich, dass ich diese Dissertation eigenständig und nur unter Verwendung der angegebenen Materialien und Hilfsmittel angefertigt habe. Des Weiteren erkläre ich, dass diese Dissertation weder in dieser noch in ähnlicher Form einer anderen Prüfungsbehörde vorgelegt wurde.

Marcus Klein, 18.06.2014

10 SUPPLEMENTS

**Supplement Table 1**  
Differentially regulated genes ( $p \leq 0.05$ ,  $FC \geq 1.5$  and  $\leq -1.5$ ) in IL-6-challenged PHH.

Gene symbol	log <sub>2</sub> FC	P-value <sup>a</sup>
STEAP4	4.70	8.63E-03
CRP	3.71	1.58E-02
ADAMTS1	3.04	2.35E-03
AVPR1A	2.53	1.58E-03
SOCS1	2.47	1.14E-04
DHODH	2.40	3.60E-04
SAI2	2.28	9.52E-03
CFHR3	2.25	1.89E-02
CREB3L3	2.22	6.80E-03
LOC100124692	2.20	8.69E-03
PLA2G2A	2.10	2.31E-03
SGK1	1.97	8.40E-03
PKD1L3	1.95	8.63E-03
MIR4661	1.93	3.81E-04
MT1M	1.93	2.07E-02
FLJ45139	1.92	5.82E-03
SOCS3	1.88	3.26E-03
SLC17A2	1.88	1.66E-05
LRG1	1.86	5.73E-04
DUOXA2	1.79	4.68E-02
CHI3L1	1.73	6.89E-04
ASCL1	1.72	4.00E-02
SPINK1	1.67	8.68E-03
DHRS13	1.61	1.79E-02
CCL2	1.58	1.48E-02
CCBP2	1.52	3.42E-03
SLC5A6	1.50	1.38E-03
NNMT	1.48	7.96E-03
ALPL	1.44	6.73E-03
OSMR	1.37	8.02E-04
EPO	1.35	3.07E-02
MT1X	1.33	1.85E-02
CD38	1.29	2.74E-03
NAMPT	1.28	4.27E-02
IGF1	1.28	4.73E-03
FAM20A	1.25	2.45E-04
TMC5	1.25	3.34E-04
CEBPD	1.20	9.89E-04
HPR	1.20	3.73E-02
DTX4	1.19	1.99E-03
ORM1	1.17	1.62E-03
RARRES3	1.17	1.26E-03
LIMK2	1.16	2.84E-03
SERPINA10	1.16	6.29E-03
SLC13A5	1.16	8.43E-03
IFITM1	1.15	4.77E-02
STS	1.14	7.91E-03
CYP21A2	1.14	3.59E-03
TRIM40	1.14	6.15E-03
AHNAK2	1.13	7.95E-04
C8A	1.12	8.63E-05
CPN1	1.11	1.58E-03
SLC1A4	1.09	2.26E-02
UBD	1.08	1.81E-02
GALNT2	1.08	4.25E-03
MT1L	1.08	3.54E-02
FNIP2	1.08	5.38E-03
HIF1A-AS2	1.07	1.84E-02
SULT1B1	1.07	1.64E-02
GFPT2	1.06	3.00E-02
VNN3	1.06	2.88E-02
CYP2E1	1.05	3.61E-02

Gene symbol	log <sub>2</sub> FC	P-value <sup>a</sup>
VWAI	1.05	4.96E-03
PDZK1IP1	1.04	1.94E-03
STEAP1	1.03	1.69E-02
BCL6	1.02	3.44E-03
TEAD4	1.01	1.16E-02
C10orf10	1.01	6.22E-03
C9	1.01	1.25E-02
C5orf27	1.00	9.32E-04
CISH	1.00	7.23E-03
UNC5CL	1.00	2.31E-05
SLC35C1	0.98	1.17E-03
C5	0.98	3.67E-03
TACSTD2	0.97	3.86E-02
MIR3118-5	0.96	8.19E-03
IFNA13	0.96	2.96E-02
ILIRN	0.95	3.13E-02
EFNA1	0.95	2.70E-02
C8B	0.95	9.31E-05
ICAM1	0.95	2.53E-05
TSPAN15	0.94	2.08E-03
SERPINF2	0.94	2.22E-02
CXCL2	0.94	5.40E-04
FGG	0.94	1.17E-02
KCTD14	0.93	4.32E-03
FAM198A	0.93	3.46E-03
CXCL5	0.93	8.92E-03
OR5L2	0.93	8.73E-03
RN5S191	0.92	3.23E-03
SERPINA7	0.91	2.60E-03
CARHSP1	0.90	2.10E-02
SUSD4	0.90	2.89E-02
MIR494	0.89	3.29E-02
WDR72	0.89	6.24E-03
MIR151B	0.88	1.23E-03
TRBV6-1	0.88	3.11E-03
IL18BP	0.88	6.29E-03
APOL1	0.87	2.86E-02
CP	0.87	6.08E-03
MEIS2	0.87	3.63E-03
LOC100287562	0.87	1.22E-02
FAM46C	0.87	2.09E-02
PIMI	0.86	2.98E-02
LOC100507419	0.86	8.16E-03
CFHR1	0.85	1.77E-02
TIMP1	0.85	4.67E-03
RN5S404	0.84	4.60E-02
FAM169B	0.84	5.15E-03
FGL1	0.83	1.95E-03
CIR	0.83	7.95E-03
IL24	0.83	3.87E-02
SMA5	0.83	4.67E-02
IFITM4P	0.82	3.09E-02
ENOX2	0.81	2.87E-02
TTPA	0.81	1.25E-04
DOC2B	0.81	3.75E-02
SLC7A2	0.80	1.31E-02
RND1	0.80	2.55E-03
ABCA1	0.80	5.75E-04
LY96	0.80	3.63E-02
ACTBL2	0.80	1.45E-02
SNX10	0.79	6.21E-03
PDE11A	0.79	7.27E-03
TLCD2	0.79	3.43E-02
ELF3	0.79	2.30E-03
PREB	0.79	4.93E-03
HIF1A	0.79	3.27E-04
LPCAT1	0.77	5.78E-03
C4A	0.77	1.51E-03
GPX2	0.77	2.16E-02

Gene symbol	log <sub>2</sub> FC	P-value <sup>a</sup>
C4B	0.77	2.04E-03
TNFSF14	0.76	4.23E-02
HPS5	0.76	3.37E-02
IL1R1	0.76	9.34E-03
GK	0.75	1.11E-02
C4BPA	0.75	2.31E-03
RN5S422	0.75	1.10E-02
C6	0.75	2.47E-02
BIRC3	0.75	2.67E-03
RNU6-81	0.75	8.73E-03
BLNK	0.75	5.91E-03
CASP4	0.74	5.75E-03
TPST1	0.74	7.12E-03
AGTR1	0.73	1.04E-03
RAP1GAP	0.73	5.04E-03
SERPINA1	0.73	4.20E-03
RASD1	0.73	4.30E-02
PC	0.72	3.81E-02
MIR1227	0.72	1.88E-02
PRAMEF11	0.72	2.51E-02
CFB	0.72	1.95E-04
C9orf106	0.71	2.73E-02
GOS2	0.71	4.01E-02
IGSF9	0.71	4.11E-03
PDIA4	0.71	1.43E-02
MIR3907	0.71	1.56E-02
GK-AS1	0.71	2.58E-02
CFH	0.70	8.10E-04
GUSBP9	0.70	2.31E-02
NUCB2	0.70	1.90E-02
STARD5	0.70	4.66E-02
PLSCR1	0.70	7.90E-03
HYOU1	0.70	1.23E-02
SLP1	0.70	1.92E-02
ETV6	0.70	5.42E-04
NFKBIZ	0.70	5.46E-05
FGA	0.70	1.22E-02
CPHL1P	0.70	1.18E-02
STEAP2	0.69	4.27E-02
PELI1	0.69	3.39E-02
ITIH4	0.69	4.32E-03
KHK	0.69	4.63E-03
NRP1	0.68	1.28E-02
PDIA3	0.68	3.44E-02
ETS2	0.68	1.90E-03
C17orf62	0.68	1.71E-02
KRTAP5-2	0.68	1.30E-02
CADPS2	0.68	1.13E-02
ITIH3	0.68	1.94E-02
IFITM2	0.67	1.48E-03
CYP21A1P	0.67	1.33E-02
DNAJC3	0.67	1.19E-02
LOC100507603	0.67	5.81E-03
PPAPDC1B	0.67	4.33E-02
C4A-AS1	0.67	5.55E-03
ST6GALNAC6	0.67	7.31E-03
SLC39A14	0.67	1.89E-04
JUNB	0.67	1.01E-02
HPX	0.67	1.55E-02
BHLHA15	0.67	2.02E-02
SLC10A7	0.66	3.31E-02
LOC152225	0.66	3.94E-02
CIS	0.66	3.78E-02
STEAP3	0.66	6.33E-03
ARL14	0.66	2.77E-02
SDF2L1	0.65	2.56E-02
B3GNT3	0.65	1.49E-02
ERO1LB	0.65	4.18E-02
MLXIP	0.65	2.98E-06
AQP3	0.65	2.87E-02

SUPPLEMENTS

Gene symbol	log <sub>2</sub> FC	P-value <sup>a</sup>
<i>ADRA1A</i>	0.65	8.34E-03
<i>SLC2A10</i>	0.64	3.95E-02
<i>PTGFR</i>	0.64	1.82E-02
<i>FLOT2</i>	0.64	1.57E-03
<i>CCL20</i>	0.64	3.34E-02
<i>CRELD2</i>	0.64	3.69E-03
<i>TRIM15</i>	0.64	1.01E-02
<i>CD14</i>	0.64	1.48E-02
<i>LBP</i>	0.64	1.82E-03
<i>BCAM</i>	0.63	1.35E-02
<i>GK-IT1</i>	0.63	1.34E-02
<i>PCMI</i>	0.63	1.73E-02
<i>SPP1</i>	0.63	2.89E-02
<i>TC2N</i>	0.63	1.15E-02
<i>TSPYL2</i>	0.63	4.53E-02
<i>PLIN1</i>	0.63	4.46E-02
<i>TMEM163</i>	0.63	1.20E-02
<i>CCDC109B</i>	0.63	6.52E-03
<i>MUC1</i>	0.63	4.19E-02
<i>MIR622</i>	0.62	7.71E-03
<i>CCDC71L</i>	0.62	7.32E-04
<i>RASL11A</i>	0.62	7.31E-03
<i>LOC100505536</i>	0.62	1.27E-02
<i>TRIM51GP</i>	0.61	1.67E-02
<i>EDEM3</i>	0.61	2.77E-02
<i>C4BPB</i>	0.61	1.83E-02
<i>MIR548AK</i>	0.61	1.28E-02
<i>PLGLB1</i>	0.61	3.25E-02
<i>ANG</i>	0.61	5.49E-03
<i>MLEC</i>	0.60	3.11E-03
<i>SEMA4B</i>	0.60	1.96E-04
<i>SNORD19B</i>	0.60	1.89E-02
<i>APCS</i>	0.60	1.33E-02
<i>MTSS1L</i>	0.60	1.17E-02
<i>FGB</i>	0.60	3.68E-04
<i>MTUS1</i>	0.59	2.52E-03
<i>MANF</i>	0.59	1.82E-02
<i>PDGFRL</i>	0.59	1.36E-02
<i>PPP2R1B</i>	0.59	1.56E-02
<i>PARP1</i>	0.59	4.45E-03
<i>RUFY3</i>	0.59	4.78E-02
<i>SLC25A28</i>	0.59	1.21E-02
<i>MIR3148</i>	0.59	1.23E-02
<i>ARRDC3</i>	0.59	6.32E-03
<i>TMOD1</i>	0.59	2.70E-03
<i>ZNF295</i>	0.59	5.70E-03
<i>CYP2C8</i>	-2.34	3.73E-03
<i>CYP3A4</i>	-2.26	1.51E-02
<i>CYP2A6</i>	-2.26	8.72E-03
<i>GLYAT</i>	-2.25	4.19E-03
<i>CYP2B7P1</i>	-2.08	4.88E-02
<i>OTC</i>	-1.97	1.27E-03
<i>CYP2C9</i>	-1.82	2.22E-02
<i>SLC10A1</i>	-1.82	3.49E-03
<i>CYP4A11</i>	-1.80	1.65E-02
<i>AKR1B10</i>	-1.77	1.32E-02
<i>PFKFB1</i>	-1.69	3.69E-03
<i>HSD17B13</i>	-1.66	1.20E-02
<i>CXCL11</i>	-1.62	1.29E-02
<i>GBA3</i>	-1.59	6.12E-03
<i>CYP4A22</i>	-1.57	8.15E-03
<i>ACE2</i>	-1.55	3.21E-03
<i>ADH1C</i>	-1.52	1.72E-02
<i>SLC16A4</i>	-1.52	3.11E-03
<i>CYP3A7</i>	-1.51	5.07E-03
<i>CXCL10</i>	-1.50	6.91E-03
<i>ADH4</i>	-1.44	4.86E-02
<i>LOC100507511</i>	-1.44	3.74E-02
<i>F13B</i>	-1.42	2.49E-03
<i>HMGCS2</i>	-1.36	6.87E-03
<i>SULT1E1</i>	-1.36	1.02E-02
<i>TAT</i>	-1.33	2.34E-02
<i>DCDC2</i>	-1.33	9.52E-03
<i>TSKU</i>	-1.32	2.88E-02

Gene symbol	log <sub>2</sub> FC	P-value <sup>a</sup>
<i>DSG1</i>	-1.32	4.11E-02
<i>BBOX1</i>	-1.27	1.91E-03
<i>CYP1A2</i>	-1.25	2.38E-03
<i>PEG10</i>	-1.23	1.94E-02
<i>BHMT</i>	-1.22	1.09E-02
<i>AFM</i>	-1.21	1.57E-02
<i>DIO1</i>	-1.20	7.49E-03
<i>FETUB</i>	-1.17	2.34E-04
<i>RTP3</i>	-1.15	3.48E-02
<i>CPS1</i>	-1.15	7.50E-04
<i>ARG1</i>	-1.14	1.88E-02
<i>CYP3A5</i>	-1.14	4.91E-03
<i>NPR3</i>	-1.14	4.76E-02
<i>CYP39A1</i>	-1.12	9.48E-05
<i>GSTA2</i>	-1.11	8.53E-03
<i>IFIT1</i>	-1.11	1.44E-02
<i>EGOT</i>	-1.08	5.25E-04
<i>LECT2</i>	-1.07	2.80E-02
<i>SLC17A4</i>	-1.07	5.43E-03
<i>CYP2B6</i>	-1.06	2.81E-03
<i>KCNJ8</i>	-1.05	3.36E-02
<i>IFIT2</i>	-1.04	2.18E-02
<i>EDN1</i>	-1.04	5.10E-04
<i>SOX4</i>	-1.04	2.95E-02
<i>ANXA13</i>	-1.03	1.20E-02
<i>SPP2</i>	-1.03	1.18E-02
<i>PRAMEF10</i>	-1.02	4.74E-03
<i>ANO1</i>	-1.01	7.01E-03
<i>SESN3</i>	-1.00	4.59E-05
<i>ZCCHC16</i>	-1.00	4.27E-02
<i>THBS1</i>	-0.99	1.01E-02
<i>HLF</i>	-0.99	1.80E-02
<i>SLC5A9</i>	-0.98	1.72E-03
<i>GYS2</i>	-0.98	4.79E-02
<i>PIPOX</i>	-0.98	4.24E-04
<i>TRNP1</i>	-0.98	9.91E-03
<i>SLC22A10</i>	-0.97	3.26E-02
<i>SLC17A3</i>	-0.97	7.29E-04
<i>CRYM</i>	-0.97	2.21E-04
<i>CEACAMP6</i>	-0.96	3.57E-03
<i>FLJ22763</i>	-0.96	1.33E-02
<i>BAMBI</i>	-0.96	3.66E-03
<i>CYP4X1</i>	-0.95	4.43E-03
<i>NR1I2</i>	-0.95	1.40E-02
<i>SUSD3</i>	-0.95	3.85E-02
<i>AKR1D1</i>	-0.94	1.54E-02
<i>SLC22A1</i>	-0.94	3.92E-03
<i>NAT8B</i>	-0.94	9.30E-03
<i>CCL16</i>	-0.94	6.13E-04
<i>CEBPA</i>	-0.93	2.74E-03
<i>FMO5</i>	-0.92	6.99E-04
<i>PGLYRP2</i>	-0.91	1.26E-02
<i>MOGAT2</i>	-0.91	1.21E-03
<i>PDE5A</i>	-0.91	2.05E-03
<i>PKLR</i>	-0.90	6.51E-03
<i>LOC100509129</i>	-0.90	2.81E-02
<i>BMP2</i>	-0.89	5.48E-03
<i>PDZK1P1</i>	-0.89	1.51E-02
<i>OLFM2</i>	-0.88	1.04E-02
<i>KLHL6-AS1</i>	-0.88	3.75E-02
<i>UGT2B10</i>	-0.88	9.00E-03
<i>MAMLD1</i>	-0.88	9.38E-03
<i>HOGA1</i>	-0.87	3.05E-02
<i>HGD</i>	-0.87	6.95E-05
<i>LOC100506870</i>	-0.87	1.21E-02
<i>AADAT</i>	-0.87	9.47E-03
<i>PDZK1</i>	-0.86	2.88E-02
<i>NAT8</i>	-0.86	2.21E-02
<i>PLLP</i>	-0.86	3.78E-02
<i>EHHADH</i>	-0.85	8.14E-04
<i>BDH1</i>	-0.84	2.27E-02
<i>ACADL</i>	-0.84	4.53E-02
<i>ACSM2A</i>	-0.84	2.22E-02
<i>PRAMEF16</i>	-0.83	8.25E-03

Gene symbol	log <sub>2</sub> FC	P-value <sup>a</sup>
<i>ABCG2</i>	-0.83	4.58E-04
<i>SULT2A1</i>	-0.83	2.22E-02
<i>DMGDH</i>	-0.83	3.02E-03
<i>FGFR2</i>	-0.82	1.48E-03
<i>LAMA3</i>	-0.82	9.66E-03
<i>AGPAT9</i>	-0.82	6.16E-03
<i>ABCC2</i>	-0.81	3.68E-03
<i>ENTPD5</i>	-0.81	1.38E-02
<i>CAVI</i>	-0.81	7.10E-03
<i>UPBI</i>	-0.81	3.17E-02
<i>HAO2</i>	-0.80	2.04E-02
<i>CMBL</i>	-0.80	3.00E-03
<i>FBP1</i>	-0.80	7.03E-03
<i>APOC1P1</i>	-0.79	1.21E-02
<i>LOC389602</i>	-0.79	1.57E-03
<i>ACY3</i>	-0.79	1.54E-02
<i>GLYATL1</i>	-0.78	7.54E-03
<i>MME</i>	-0.78	1.33E-02
<i>SLC6A1</i>	-0.78	5.94E-03
<i>SLC38A3</i>	-0.78	1.50E-02
<i>AKR1C4</i>	-0.78	2.93E-03
<i>MLLT11</i>	-0.77	1.93E-02
<i>SLC22A25</i>	-0.77	3.30E-02
<i>ANKRD29</i>	-0.77	2.17E-02
<i>SLCO1B3</i>	-0.77	2.21E-02
<i>JAG1</i>	-0.77	2.99E-02
<i>UGT2B11</i>	-0.77	4.92E-02
<i>RDH5</i>	-0.77	1.58E-02
<i>TMEM158</i>	-0.77	7.20E-03
<i>PKHD1</i>	-0.77	5.88E-03
<i>SCGN</i>	-0.76	4.10E-02
<i>HAO1</i>	-0.76	1.79E-02
<i>BCO2</i>	-0.76	2.82E-02
<i>FSTL1</i>	-0.75	1.59E-02
<i>C1orf130</i>	-0.74	6.10E-03
<i>HDAC6</i>	-0.74	3.10E-02
<i>DIAPH3</i>	-0.74	5.19E-03
<i>SMAD6</i>	-0.74	3.46E-03
<i>NT5E</i>	-0.74	5.30E-03
<i>TXNRD1</i>	-0.73	1.64E-03
<i>BCHE</i>	-0.73	6.22E-03
<i>IFI44</i>	-0.73	4.03E-02
<i>PPP1R3B</i>	-0.73	1.15E-02
<i>AGMO</i>	-0.72	1.06E-02
<i>GADD45A</i>	-0.72	7.73E-03
<i>DZIP3</i>	-0.72	1.17E-02
<i>ANXA3</i>	-0.72	1.92E-02
<i>SLC30A4</i>	-0.71	1.46E-02
<i>HAAO</i>	-0.71	1.40E-03
<i>GCNT4</i>	-0.71	5.15E-05
<i>MRAS</i>	-0.71	1.10E-02
<i>APBA1</i>	-0.71	6.15E-03
<i>CYP2C19</i>	-0.71	1.69E-03
<i>GSTA1</i>	-0.71	2.47E-02
<i>PIR-FIGF</i>	-0.71	1.76E-02
<i>RGN</i>	-0.71	7.47E-04
<i>LRRC31</i>	-0.70	2.55E-02
<i>EPHA1</i>	-0.70	3.19E-02
<i>EPPK1</i>	-0.70	4.29E-02
<i>RBP5</i>	-0.70	1.28E-03
<i>NQO1</i>	-0.70	9.84E-03
<i>ASPDH</i>	-0.70	2.76E-02
<i>EMP3</i>	-0.69	2.25E-03
<i>FREM2</i>	-0.69	8.01E-03
<i>ASF1A</i>	-0.69	8.23E-03
<i>OGDHL</i>	-0.69	7.42E-03
<i>SLC3A1</i>	-0.69	5.61E-04
<i>GBP7</i>	-0.69	1.85E-02
<i>SCARA3</i>	-0.68	4.52E-02
<i>WEE1</i>	-0.68	3.15E-03
<i>LIPH</i>	-0.68	2.19E-04
<i>VIL1</i>	-0.68	4.91E-03
<i>HRCT1</i>	-0.67	3.30E-02
<i>ZNF470</i>	-0.67	7.90E-03

SUPPLEMENTS

Gene symbol	log <sub>2</sub> FC	P-value <sup>a</sup>
<i>ACOT2</i>	-0.67	2.77E-03
<i>NSAP11</i>	-0.67	4.09E-02
<i>ACOT1</i>	-0.67	4.73E-02
<i>CLRN3</i>	-0.67	9.97E-03
<i>SMAD7</i>	-0.67	3.05E-02
<i>DPYS</i>	-0.67	1.15E-02
<i>CES3</i>	-0.67	3.44E-02
<i>STAP2</i>	-0.66	8.46E-04
<i>FAM162A</i>	-0.66	3.69E-03
<i>KLRC3</i>	-0.66	1.68E-02
<i>SORL1</i>	-0.66	4.66E-02
<i>EDA2R</i>	-0.66	3.63E-03
<i>EXTL2</i>	-0.65	3.17E-02
<i>COX2</i>	-0.65	1.24E-03
<i>PECR</i>	-0.65	1.07E-03
<i>CALML4</i>	-0.65	3.84E-02
<i>COQ3</i>	-0.65	2.99E-02
<i>AMT</i>	-0.65	8.56E-03
<i>TRAF1</i>	-0.65	6.31E-03
<i>NPY6R</i>	-0.65	1.77E-03
<i>ENPP3</i>	-0.65	4.58E-02
<i>TP53I3</i>	-0.65	5.31E-03
<i>MOGAT3</i>	-0.65	1.93E-02
<i>ALDH5A1</i>	-0.65	5.72E-03
<i>CABLES1</i>	-0.64	1.73E-02
<i>SLC39A10</i>	-0.64	1.17E-02
<i>ANKRD2</i>	-0.64	2.84E-03
<i>RUSC2</i>	-0.64	1.87E-02
<i>SLC7A9</i>	-0.64	2.52E-04
<i>CSRP2BP</i>	-0.64	3.15E-02
<i>PLA2G12B</i>	-0.64	2.24E-02
<i>RUNDC3B</i>	-0.64	3.15E-02
<i>LOC283194</i>	-0.64	2.83E-02
<i>RNF128</i>	-0.64	3.24E-02
<i>RNU7-71P</i>	-0.63	3.58E-02
<i>BAG2</i>	-0.63	1.29E-02
<i>PROZ</i>	-0.63	1.90E-03
<i>SLC22A3</i>	-0.63	8.03E-03
<i>MARVELD3</i>	-0.63	3.47E-02
<i>FMNL2</i>	-0.63	1.05E-02
<i>SNORD115-45</i>	-0.63	3.39E-02
<i>NRG1</i>	-0.63	3.25E-02
<i>MTTP</i>	-0.63	4.46E-02
<i>FASTKD1</i>	-0.62	9.76E-03
<i>ADH6</i>	-0.62	1.08E-02
<i>SPATS2L</i>	-0.62	4.15E-04
<i>C1orf98</i>	-0.62	4.12E-02
<i>MPDZ</i>	-0.62	1.21E-02
<i>TRPC5</i>	-0.61	3.24E-03
<i>LIF</i>	-0.61	1.62E-02
<i>DLAT</i>	-0.61	4.10E-03
<i>SNORD98</i>	-0.61	1.42E-02
<i>SNAI2</i>	-0.61	9.86E-03
<i>ACSS3</i>	-0.61	3.68E-02
<i>TTK</i>	-0.61	3.86E-02
<i>AQP11</i>	-0.61	7.99E-03
<i>CAP2</i>	-0.61	3.54E-04
<i>BDH2</i>	-0.60	2.93E-03
<i>TYMS</i>	-0.60	2.58E-03
<i>RDH12</i>	-0.60	1.29E-02
<i>VSNL1</i>	-0.60	3.85E-02
<i>LOC440570</i>	-0.60	1.52E-02
<i>OXER1</i>	-0.60	1.74E-03
<i>ENC1</i>	-0.60	2.30E-02
<i>CCDC112</i>	-0.60	2.52E-02
<i>HPS3</i>	-0.60	5.56E-03
<i>TM6SF2</i>	-0.60	4.62E-02
<i>CYP2A7</i>	-0.60	3.38E-02
<i>RAB7B</i>	-0.60	2.71E-03
<i>FGF2</i>	-0.59	4.64E-02
<i>LOC643401</i>	-0.59	2.23E-03
<i>C3orf25</i>	-0.59	1.11E-02
<i>OR2M7</i>	-0.59	2.37E-02
<i>CTGF</i>	-0.59	1.13E-02

Gene symbol	log <sub>2</sub> FC	P-value <sup>a</sup>
<i>TIMM8A</i>	-0.59	6.33E-03
<i>WDPCP</i>	-0.59	3.16E-02
<i>SKA3</i>	-0.59	1.73E-02
<i>CABYR</i>	-0.59	2.07E-02
<i>EID3</i>	-0.59	2.81E-02
<i>BAAT</i>	-0.59	2.95E-04
<i>ITGA7</i>	-0.59	1.17E-02
<i>PSG8</i>	-0.59	2.80E-02
<i>HADH</i>	-0.59	2.54E-03
<i>POLR3C</i>	-0.59	7.95E-03

Log<sub>2</sub>FC = log 2 fold change, IL-6 compared to control. Values represent mean for N = 4 gene chips per group

<sup>a</sup> Two groups paired t-test

SUPPLEMENTS

**Supplement Table 2** Quantitative PCR analysis to verify differentially expressed genes in IL-6-challenged PHH.

Gene symbol	Microarray (N = 4)			qPCR discovery set (N = 4)			qPCR validation set (N = 11)			
	log2FC	95% CI	P-value <sup>a</sup>	log2FC	95% CI	P-value <sup>a</sup>	log2FC	95% CI	P-value <sup>a</sup>	Adj. P-value <sup>b</sup>
<i>ABCB1</i>	-0.49	-1.21 , 0.23	0.1198	-0.65	-1.15 , -0.16	<b>0.0122</b>	-0.80	-1.20 , -0.40	<b>0.0005</b>	<b>0.0080</b>
<i>ABCC2</i>	-0.81	-1.12 , -0.50	<b>0.0037</b>	-1.30	-1.49 , -1.10	<b>&lt;0.0001</b>	-1.07	-1.32 , -0.81	<b>&lt;0.0001</b>	<b>&lt;0.0032</b>
<i>ABCG2</i>	-0.83	-0.99 , -0.67	<b>0.0005</b>	-1.07	-1.66 , -0.48	<b>0.0036</b>	-0.96	-1.44 , -0.48	<b>0.0006</b>	<b>0.0090</b>
<i>CCL2</i>	1.58	0.59 , 2.57	<b>0.0148</b>	2.39	0.61 , 4.16	0.1202	1.44	0.76 , 2.12	<b>0.0119</b>	0.0952
<i>CRP</i>	3.71	1.33 , 6.10	<b>0.0158</b>	6.74	4.66 , 8.82	0.1639	6.22	5.16 , 7.27	<b>0.0277</b>	0.1410
<i>CYP1A1</i>	-0.42	-1.27 , 0.42	0.2088	-0.78	-1.12 , -0.43	<b>0.0021</b>	-1.00	-1.93 , -0.07	0.5731	0.8160
<i>CYP1A2</i>	-1.25	-1.66 , -0.84	<b>0.0024</b>	-2.03	-2.78 , -1.27	<b>0.0002</b>	-2.31	-2.83 , -1.78	<b>&lt;0.0001</b>	<b>&lt;0.0032</b>
<i>CYP2A6</i>	-2.26	-3.43 , -1.09	<b>0.0087</b>	-3.98	-6.34 , -1.62	<b>0.0010</b>	-2.67	-3.69 , -1.65	<b>&lt;0.0001</b>	<b>&lt;0.0032</b>
<i>CYP2B6</i>	-1.06	-1.43 , -0.69	<b>0.0028</b>	-1.51	-2.46 , -0.56	<b>0.0029</b>	-1.52	-1.93 , -1.11	<b>&lt;0.0001</b>	<b>&lt;0.0032</b>
<i>CYP2C19</i>	-0.71	-0.92 , -0.50	<b>0.0017</b>	-0.83	-1.58 , -0.07	<b>0.0297</b>	-0.79	-1.36 , -0.23	<b>0.0096</b>	0.0880
<i>CYP2C8</i>	-2.34	-3.24 , -1.43	<b>0.0037</b>	-2.18	-3.56 , -0.81	<b>0.0034</b>	-1.47	-2.14 , -0.80	<b>&lt;0.0001</b>	<b>&lt;0.0032</b>
<i>CYP2C9</i>	-1.82	-3.15 , -0.49	<b>0.0222</b>	-1.74	-2.80 , -0.69	<b>0.0012</b>	-1.42	-1.84 , -1.00	<b>&lt;0.0001</b>	<b>&lt;0.0032</b>
<i>CYP2D6</i>	-0.43	-1.05 , 0.19	0.3241	-1.04	-2.33 , 0.26	<b>0.0430</b>	-0.89	-1.34 , -0.45	<b>0.0006</b>	<b>0.0090</b>
<i>CYP2E1</i>	1.05	0.13 , 1.97	<b>0.0361</b>	2.28	-0.68 , 5.23	0.3130	0.44	-0.15 , 1.03	0.1182	0.4730
<i>CYP3A4</i>	-2.26	-3.69 , -0.83	<b>0.0151</b>	-4.00	-6.69 , -1.31	<b>0.0007</b>	-2.77	-3.42 , -2.11	<b>&lt;0.0001</b>	<b>&lt;0.0032</b>
<i>CYP3A5</i>	-1.14	-1.62 , 0.66	<b>0.0049</b>	-2.01	-3.01 , -1.02	<b>0.0006</b>	-1.82	-2.28 , -1.36	<b>&lt;0.0001</b>	<b>&lt;0.0032</b>
<i>CYP3A7</i>	-1.51	-2.16 , -0.86	<b>0.0051</b>	-3.60	-5.46 , -1.75	<b>&lt;0.0001</b>	-2.28	-3.43 , -1.14	<b>0.0017</b>	<b>0.0221</b>
<i>CYP7A1</i>	-1.78	-3.71 , 0.15	0.0606	-3.43	-7.56 , 0.71	<b>0.0061</b>	-3.45	-4.74 , -2.15	<b>&lt;0.0001</b>	<b>&lt;0.0032</b>
<i>GSTA2</i>	-1.11	-1.69 , -0.54	<b>0.0085</b>	-2.01	-2.58 , -1.43	<b>0.0002</b>	-1.99	-2.42 , -1.56	<b>&lt;0.0001</b>	<b>&lt;0.0032</b>
<i>GSTM1</i>	0.15	-0.17 , 0.47	0.2360	-0.68	-2.55 , 1.19	0.1077	-0.84	-1.47 , -0.21	<b>0.0133</b>	0.0952
<i>GSTP1</i>	-0.11	-0.61 , 0.38	0.5209	-0.57	-1.15 , 0.00	<b>0.0423</b>	-0.37	-0.74 , 0.00	0.1642	0.4930
<i>NAT1</i>	-0.24	-0.43 , -0.06	<b>0.0247</b>	-0.52	-1.24 , 0.20	0.0816	-0.51	-0.85 , -0.18	<b>0.0080</b>	0.0880
<i>NAT2</i>	-0.40	-0.70 , -0.11	<b>0.0221</b>	-0.86	-1.65 , -0.07	<b>0.0164</b>	-0.88	-1.20 , -0.56	<b>&lt;0.0001</b>	<b>&lt;0.0032</b>
<i>SLC10A1</i>	-1.82	-2.50 , -1.13	<b>0.0035</b>	-2.63	-3.16 , -2.10	<b>&lt;0.0001</b>	-2.29	-2.74 , -1.85	<b>&lt;0.0001</b>	<b>&lt;0.0032</b>
<i>SLC22A7</i>	-0.47	-0.74 , -0.20	<b>0.0121</b>	-0.54	-1.29 , 0.20	0.1062	-0.90	-1.29 , -0.51	<b>0.0003</b>	<b>0.0051</b>
<i>SLCO1B1</i>	-1.00	-2.16 , 0.16	0.0717	-1.34	-2.64 , -0.04	<b>0.0123</b>	-1.24	-1.69 , -0.80	<b>&lt;0.0001</b>	<b>&lt;0.0032</b>
<i>SOCS3</i>	1.71	1.53 , 1.89	<b>&lt;0.0001</b>	3.94	3.27 , 4.62	<b>0.0054</b>	3.84	2.97 , 4.71	<b>0.0083</b>	0.0880
<i>SOD2</i>	0.18	-0.09 , 0.45	0.1217	0.76	0.25 , 1.27	<b>0.0304</b>	0.74	0.57 , 0.92	<b>&lt;0.0001</b>	<b>&lt;0.0032</b>
<i>SULT1A1</i>	-0.21	-0.48 , 0.06	0.0883	0.00	-1.91 , 1.92	0.6254	-0.13	-1.73 , 1.47	0.4081	0.8160
<i>SULT1B1</i>	1.07	0.37 , 1.76	<b>0.0164</b>	1.30	-0.20 , 2.80	0.1163	0.88	0.28 , 1.47	<b>0.0033</b>	<b>0.0396</b>
<i>TPMT</i>	-0.13	-0.20 , -0.06	<b>0.0116</b>	-0.35	-0.69 , -0.02	<b>0.0318</b>	-0.27	-0.46 , -0.08	<b>0.0235</b>	0.1410
<i>UGT2B7</i>	-0.32	-0.80 , 0.16	0.1269	-1.22	-1.65 , -0.78	<b>0.0007</b>	-1.46	-1.61 , -1.30	<b>&lt;0.0001</b>	<b>&lt;0.0032</b>

Log2FC = log2 fold change IL-6 compared to control, <sup>a</sup>Paired t-test, <sup>b</sup>Bonferroni-Holm multiple testing adjusted (Holm, 1979), Abbreviations: CI, confidence interval

**Supplement Table 3** Significantly enriched GO terms in the category “*biological process*” in IL-6-challenged PHH.

GO ID	Description	Number of genes in term	P-value <sup>a</sup>	Adj p-value <sup>b</sup>
GO:0044281	small molecule metabolic process	134	1.45E-18	7.48E-15
GO:0042221	response to chemical stimulus	165	7.23E-18	3.73E-14
GO:0009410	response to xenobiotic stimulus	28	2.80E-15	1.45E-11
GO:0006805	xenobiotic metabolic process	27	4.39E-15	3.05E-11
GO:0071466	cellular response to xenobiotic stimulus	27	5.21E-15	2.27E-11
GO:0006629	lipid metabolic process	79	5.90E-15	2.69E-11
GO:0006956	complement activation	16	3.61E-14	1.86E-10
GO:0042737	drug catabolic process	10	4.47E-14	2.42E-10
GO:0006082	organic acid metabolic process	69	4.70E-14	2.31E-10
GO:0055114	oxidation-reduction process	71	1.05E-13	5.43E-10
GO:0019752	carboxylic acid metabolic process	64	2.59E-13	1.34E-09
GO:0042493	response to drug	40	2.91E-13	1.50E-09
GO:0042738	exogenous drug catabolic process	9	3.37E-13	1.74E-09
GO:0006952	defense response	69	1.91E-12	9.84E-09
GO:0006958	complement activation, classical pathway	13	2.56E-12	1.32E-08
GO:0008202	steroid metabolic process	31	5.36E-12	2.77E-08
GO:0017144	drug metabolic process	12	1.59E-11	8.19E-08
GO:0006954	inflammatory response	37	1.79E-11	9.24E-08
GO:0050896	response to stimulus	255	2.13E-11	1.10E-07
GO:0010033	response to organic substance	105	3.23E-11	1.67E-07
GO:0006959	humoral immune response	19	4.58E-11	2.36E-07
GO:0002455	humoral immune response mediated by circulating immunoglobulin	13	5.23E-11	2.70E-07
GO:0010038	response to metal ion	31	6.59E-11	3.40E-07
GO:0006953	acute-phase response	13	7.25E-11	3.74E-07
GO:0033993	response to lipid	49	1.53E-10	7.88E-07
GO:0010035	response to inorganic substance	37	2.18E-10	1.13E-06
GO:0070887	cellular response to chemical stimulus	92	2.19E-10	1.13E-06
GO:0006950	response to stress	133	3.17E-10	1.63E-06
GO:0031960	response to corticosteroid stimulus	21	4.70E-10	2.43E-06
GO:0048545	response to steroid hormone stimulus	33	9.22E-10	4.76E-06
GO:0051384	response to glucocorticoid stimulus	20	9.62E-10	4.96E-06
GO:0044255	cellular lipid metabolic process	54	2.07E-09	1.07E-05
GO:0032787	monocarboxylic acid metabolic process	35	2.82E-09	1.45E-05
GO:0014070	response to organic cyclic compound	46	3.31E-09	1.71E-05
GO:0009725	response to hormone stimulus	53	4.09E-09	2.11E-05
GO:0009611	response to wounding	61	5.14E-09	2.65E-05
GO:0002460	adaptive immune response based on somatic recombination of immune receptors built from immunoglobulin superfamily domains	17	2.58E-08	1.33E-04
GO:0033273	response to vitamin	14	2.74E-08	1.41E-04
GO:0046395	carboxylic acid catabolic process	23	3.28E-08	1.69E-04
GO:0002526	acute inflammatory response	13	4.21E-08	2.17E-04
GO:0006957	complement activation, alternative pathway	7	4.97E-08	2.56E-04
GO:0007584	response to nutrient	20	6.95E-08	3.59E-04
GO:0016042	lipid catabolic process	24	7.62E-08	3.93E-04
GO:0016098	monoterpenoid metabolic process	5	7.83E-08	4.04E-04
GO:0002250	adaptive immune response	17	1.32E-07	6.81E-04
GO:0031667	response to nutrient levels	27	1.53E-07	7.89E-04
GO:0051707	response to other organism	40	1.80E-07	9.31E-04
GO:0006955	immune response	55	2.39E-07	1.23E-03
GO:0016064	immunoglobulin mediated immune response	13	2.48E-07	1.28E-03
GO:0009991	response to extracellular stimulus	28	2.54E-07	1.31E-03
GO:0031100	organ regeneration	11	2.67E-07	1.38E-03
GO:0002237	response to molecule of bacterial origin	22	2.88E-07	1.49E-03
GO:0019724	B cell mediated immunity	13	3.81E-07	1.97E-03
GO:0032496	response to lipopolysaccharide	21	4.47E-07	2.31E-03
GO:0009607	response to biotic stimulus	40	6.47E-07	3.36E-03
GO:0006520	cellular amino acid metabolic process	33	6.50E-07	3.34E-03
GO:0009617	response to bacterium	29	7.89E-07	4.07E-03
GO:0009820	alkaloid metabolic process	5	1.54E-06	7.94E-03
GO:0006066	alcohol metabolic process	23	1.82E-06	9.42E-03
GO:0010043	response to zinc ion	9	1.98E-06	1.02E-02
GO:0002684	positive regulation of immune system process	34	2.03E-06	1.05E-02
GO:0048878	chemical homeostasis	39	2.10E-06	1.09E-02
GO:0002376	immune system process	74	2.24E-06	1.15E-02
GO:0070989	oxidative demethylation	5	3.01E-06	1.55E-02
GO:0006720	isoprenoid metabolic process	12	3.30E-06	1.70E-02
GO:0010817	regulation of hormone levels	20	3.37E-06	1.74E-02
GO:0042445	hormone metabolic process	16	3.44E-06	1.78E-02
GO:0002443	leukocyte mediated immunity	15	3.59E-06	1.85E-02
GO:0045087	innate immune response	32	3.76E-06	1.94E-02
GO:0042592	homeostatic process	53	4.14E-06	2.14E-02

## SUPPLEMENTS

---

<b>GO ID</b>	<b>Description</b>	<b>Number of genes in term</b>	<b>P-value<sup>a</sup></b>	<b>Adj p-value<sup>b</sup></b>
GO:0019229	regulation of vasoconstriction	9	4.26E-06	2.20E-02
GO:0010951	negative regulation of endopeptidase activity	15	5.62E-06	2.90E-02
GO:0051186	cofactor metabolic process	22	6.29E-06	3.25E-02
GO:0019627	urea metabolic process	5	9.05E-06	4.67E-02

---

<sup>a</sup> Fisher's Exact Test p-value

<sup>b</sup> Bonferroni adjusted p-value for multiple testing

**Supplement Table 4**  
Differentially regulated genes ( $p \leq 0.05$ ,  $FC \geq 1.5$  and  $\leq -1.5$ ) in livers of patients with elevated CRP ( $> 10\text{mg/l}$ ) compared to normal CRP ( $\leq 1\text{mg/l}$ ).

Gene symbol	Log2 FC	P-value <sup>a</sup>
<i>SPINK1</i>	5.43	6.24E-04
<i>PLA2G2A</i>	4.49	3.77E-04
<i>SAA2</i>	4.46	1.34E-06
<i>SAA1</i>	4.42	2.74E-05
<i>CCL20</i>	3.14	1.01E-02
<i>GPX2</i>	2.89	2.80E-05
<i>LCN2</i>	2.88	2.32E-03
<i>CSAG3A</i>	2.40	2.56E-03
<i>UBD</i>	2.20	3.77E-03
<i>RASD1</i>	2.20	7.86E-03
<i>AKR1B10</i>	2.09	4.67E-02
<i>APOA4</i>	2.07	2.77E-03
<i>FLJ39743</i>	2.01	2.34E-03
<i>COL1A1</i>	1.97	4.55E-02
<i>HKDC1</i>	1.80	2.57E-02
<i>IL32</i>	1.79	4.69E-03
<i>LBP</i>	1.70	2.25E-04
<i>TIMD4</i>	1.59	4.95E-04
<i>TMEM45B</i>	1.53	1.19E-02
<i>SLC5A6</i>	1.49	4.03E-03
<i>SLC35C1</i>	1.43	2.18E-03
<i>G0S2</i>	1.41	4.28E-02
<i>CCBP2</i>	1.40	3.24E-03
<i>HTRA1</i>	1.39	1.41E-03
<i>RARRES1</i>	1.39	2.39E-02
<i>SOCS1</i>	1.35	2.15E-02
<i>ACSL4</i>	1.32	1.03E-02
<i>SLPI</i>	1.32	4.60E-06
<i>PALLD</i>	1.32	1.11E-02
<i>IHPK3</i>	1.32	2.17E-02
<i>ACSS1</i>	1.31	3.03E-02
<i>RAP1GAP</i>	1.30	5.50E-03
<i>LILRA3</i>	1.26	3.56E-03
<i>RNASE1</i>	1.26	1.44E-03
<i>FLOT2</i>	1.25	3.25E-03
<i>MVP</i>	1.24	3.81E-04
<i>VWA1</i>	1.23	5.45E-04
<i>COL4A1</i>	1.22	2.58E-02
<i>C1QB</i>	1.21	5.67E-04
<i>CXCR7</i>	1.20	4.80E-02
<i>GBP2</i>	1.18	7.45E-03
<i>MT1H</i>	1.18	5.05E-03
<i>KCTD17</i>	1.18	3.94E-03
<i>LOC401115</i>	1.18	3.52E-03
<i>CRP</i>	1.16	2.97E-22
<i>VSIG4</i>	1.15	1.35E-04
<i>LGALS4</i>	1.15	2.20E-02
<i>LRG1</i>	1.14	1.20E-04
<i>F2RL1</i>	1.14	1.65E-02
<i>EVL</i>	1.13	3.14E-04
<i>GPX3</i>	1.13	1.57E-04
<i>MID1IP1</i>	1.11	3.53E-02
<i>IFI30</i>	1.11	2.94E-04
<i>PPP2R1B</i>	1.10	1.01E-04
<i>PIK3AP1</i>	1.10	3.56E-03
<i>TIMP1</i>	1.09	1.27E-02
<i>TM4SF5</i>	1.09	2.06E-04
<i>C1QA</i>	1.08	1.65E-05
<i>SUSD4</i>	1.08	4.74E-02
<i>LOC284422</i>	1.08	8.45E-03
<i>SLC38A1</i>	1.06	1.64E-02
<i>SCNN1A</i>	1.06	4.82E-02

Gene symbol	Log2 FC	P-value <sup>a</sup>
<i>TMOD1</i>	1.04	2.03E-02
<i>MGC87042</i>	1.04	1.30E-02
<i>CSTB</i>	1.04	2.11E-03
<i>GPNMB</i>	1.04	4.58E-02
<i>MARCO</i>	1.03	2.55E-04
<i>EPDR1</i>	1.03	4.71E-03
<i>CD163</i>	1.03	1.08E-03
<i>SOD2</i>	1.03	6.65E-04
<i>CIQC</i>	1.02	5.63E-04
<i>CREB3L3</i>	1.01	8.63E-04
<i>ANXA5</i>	1.01	8.22E-03
<i>AQP12A</i>	1.01	3.54E-04
<i>PLTP</i>	1.00	8.12E-03
<i>MFSD2</i>	1.00	1.45E-02
<i>C1orf112</i>	1.00	7.93E-03
<i>ALPL</i>	0.99	5.43E-03
<i>CHRD2</i>	0.98	1.46E-03
<i>IMPA2</i>	0.97	1.55E-03
<i>NQO1</i>	0.97	2.37E-02
<i>RHOQ</i>	0.97	6.54E-03
<i>CXCL6</i>	0.97	2.62E-02
<i>MSN</i>	0.96	1.69E-03
<i>MT1M</i>	0.95	2.57E-02
<i>IFI6</i>	0.94	1.85E-02
<i>MYOM1</i>	0.94	1.06E-02
<i>ADORA3</i>	0.93	1.98E-03
<i>ANKRD33</i>	0.93	1.19E-03
<i>SQSTM1</i>	0.93	6.80E-03
<i>PIGR</i>	0.92	1.82E-03
<i>SI00A11</i>	0.92	3.92E-02
<i>MAPK13</i>	0.92	2.46E-02
<i>GOLM1</i>	0.91	5.03E-03
<i>LOC646310</i>	0.91	1.19E-02
<i>TAX1BP3</i>	0.91	2.52E-02
<i>TMCO3</i>	0.91	2.81E-02
<i>VAMP5</i>	0.90	3.73E-04
<i>IQGAP3</i>	0.90	1.43E-02
<i>CFD</i>	0.89	1.09E-02
<i>SLCIA3</i>	0.89	5.41E-03
<i>KLHL5</i>	0.89	6.57E-03
<i>LOC388610</i>	0.89	1.38E-02
<i>FCAMR</i>	0.89	4.85E-03
<i>TMC5</i>	0.89	2.68E-02
<i>IDH2</i>	0.88	6.60E-03
<i>ACTN1</i>	0.88	4.11E-03
<i>CDC20</i>	0.86	3.47E-02
<i>AKR1B1</i>	0.86	1.37E-02
<i>HAVCR2</i>	0.86	8.94E-04
<i>TRPM4</i>	0.86	4.77E-03
<i>TUBB2A</i>	0.86	1.03E-03
<i>ATF7IP</i>	0.86	1.99E-05
<i>CHSY3</i>	0.85	1.24E-03
<i>NRXN2</i>	0.85	7.37E-04
<i>LOC653888</i>	0.85	6.16E-03
<i>CD68</i>	0.85	8.30E-04
<i>CFHR5</i>	0.85	2.96E-03
<i>NCOA7</i>	0.84	1.55E-02
<i>TUBA4A</i>	0.84	1.66E-02
<i>TKT</i>	0.83	2.14E-03
<i>DDEFL1</i>	0.83	2.07E-04
<i>GMDS</i>	0.83	7.47E-03
<i>LOC284988</i>	0.82	4.44E-02
<i>LYVE1</i>	0.82	3.43E-03
<i>WWC1</i>	0.82	6.91E-03
<i>EML2</i>	0.82	3.71E-03
<i>CLPTMIL</i>	0.82	1.15E-02
<i>ITIH4</i>	0.82	8.46E-04
<i>JPH1</i>	0.81	2.33E-02
<i>SLC7A5</i>	0.81	2.81E-02
<i>TMSB10</i>	0.81	7.98E-03
<i>CAP2</i>	0.81	7.55E-03
<i>HYOU1</i>	0.80	1.76E-02
<i>SCPEP1</i>	0.80	1.79E-03
<i>BAIAP2L2</i>	0.80	9.66E-03

Gene symbol	Log2 FC	P-value <sup>a</sup>
<i>FKBP11</i>	0.79	7.35E-03
<i>FGL1</i>	0.79	3.37E-03
<i>SLCO4A1</i>	0.79	2.15E-02
<i>ARHGEF16</i>	0.79	3.02E-04
<i>M6PRBP1</i>	0.79	1.32E-02
<i>NUSAP1</i>	0.78	1.73E-03
<i>KDELR3</i>	0.78	1.33E-02
<i>ITGB2</i>	0.78	5.60E-03
<i>SULT2A1</i>	0.78	1.18E-04
<i>WBP5</i>	0.78	1.92E-02
<i>CTSD</i>	0.78	8.13E-04
<i>CYP21A2</i>	0.77	1.70E-02
<i>CCDC64</i>	0.77	2.20E-02
<i>CSF1R</i>	0.77	1.73E-03
<i>ZYX</i>	0.77	2.27E-02
<i>HCP5</i>	0.76	1.13E-03
<i>MMD</i>	0.76	2.19E-02
<i>WDR54</i>	0.76	1.47E-02
<i>TMBIM1</i>	0.75	1.73E-03
<i>RGS4</i>	0.75	1.61E-02
<i>OBFC2A</i>	0.75	2.92E-03
<i>LOC643319</i>	0.74	3.01E-02
<i>FOLR2</i>	0.74	1.25E-04
<i>GPR37</i>	0.74	2.66E-03
<i>STOM</i>	0.73	3.70E-03
<i>MFGE8</i>	0.73	3.38E-02
<i>NPL</i>	0.73	2.73E-03
<i>CFL1</i>	0.73	1.61E-02
<i>NAMPT</i>	0.73	2.61E-03
<i>A4GALT</i>	0.73	1.71E-02
<i>LOC650803</i>	0.72	2.83E-02
<i>TEAD2</i>	0.71	6.26E-03
<i>TUBA1C</i>	0.71	3.16E-02
<i>FAM129B</i>	0.70	2.71E-02
<i>NMT2</i>	0.70	1.34E-03
<i>HK3</i>	0.70	1.47E-03
<i>CD93</i>	0.70	6.55E-03
<i>C6orf206</i>	0.70	9.54E-04
<i>HIST1H1C</i>	0.70	4.15E-03
<i>FSCN1</i>	0.70	1.58E-02
<i>STAMBPL1</i>	0.70	1.34E-02
<i>ITIH3</i>	0.70	4.89E-02
<i>FLJ10986</i>	0.70	4.73E-03
<i>NNMT</i>	0.70	7.03E-03
<i>C15orf52</i>	0.69	4.06E-02
<i>AGXT2</i>	0.69	1.19E-02
<i>SLC39A14</i>	0.69	1.10E-02
<i>MTHFD1L</i>	0.69	1.63E-02
<i>IRX3</i>	0.68	8.40E-04
<i>LOC643416</i>	0.68	1.08E-02
<i>SERINC2</i>	0.68	1.32E-02
<i>IFNGR2</i>	0.68	8.17E-03
<i>DHRS13</i>	0.68	5.78E-03
<i>SLC2A10</i>	0.68	4.50E-03
<i>TSC22D4</i>	0.68	2.09E-03
<i>BIRC3</i>	0.67	2.31E-02
<i>TNFRSF21</i>	0.67	1.96E-02
<i>LOC440731</i>	0.67	4.81E-02
<i>ZNF541</i>	0.67	5.46E-04
<i>ALDH4A1</i>	0.67	1.95E-02
<i>DFNA5</i>	0.67	1.55E-02
<i>H2AFY2</i>	0.67	2.62E-02
<i>TRIM8</i>	0.67	9.54E-03
<i>PPT1</i>	0.67	2.54E-03
<i>FCER1G</i>	0.66	6.51E-03
<i>DDIT4</i>	0.66	9.82E-05
<i>AK1</i>	0.66	1.21E-03
<i>TOP2A</i>	0.66	3.68E-02
<i>SEPN1</i>	0.66	6.50E-03
<i>MS4A7</i>	0.66	4.15E-03
<i>TUBB2C</i>	0.66	1.57E-02
<i>SEC14L1</i>	0.66	2.98E-04
<i>CCL23</i>	0.65	1.67E-02
<i>SLC2A6</i>	0.65	4.34E-02

SUPPLEMENTS

Gene symbol	Log2 FC	P-value <sup>a</sup>
<i>INHBE</i>	0.65	1.53E-02
<i>TMED3</i>	0.65	2.96E-02
<i>CLNS1A</i>	0.65	9.21E-04
<i>C9</i>	0.65	2.04E-03
<i>TLN2</i>	0.65	3.67E-02
<i>PRKCE</i>	0.65	1.45E-02
<i>SLC7A7</i>	0.65	4.61E-03
<i>SH3BGRL3</i>	0.65	5.16E-03
<i>LITAF</i>	0.65	7.37E-03
<i>ADCY9</i>	0.65	4.98E-03
<i>DKFZp686O24166</i>	0.64	4.45E-02
<i>IGFBP7</i>	0.64	3.12E-02
<i>TP53I3</i>	0.64	1.27E-04
<i>PIAS4</i>	0.64	3.27E-03
<i>DRAM</i>	0.64	3.57E-03
<i>ST6GALNAC4</i>	0.64	2.47E-02
<i>HLA-B</i>	0.64	5.41E-04
<i>YIPF1</i>	0.64	8.19E-05
<i>EPSTI1</i>	0.64	2.29E-02
<i>RPL39L</i>	0.64	1.20E-02
<i>SLC16A3</i>	0.63	3.29E-02
<i>NPC2</i>	0.63	4.82E-03
<i>TLR5</i>	0.63	4.16E-03
<i>SPIRE1</i>	0.63	3.74E-02
<i>HK2</i>	0.63	2.39E-02
<i>TPP1</i>	0.63	2.04E-04
<i>PDZK1IP1</i>	0.63	3.32E-02
<i>TMEM149</i>	0.63	3.20E-02
<i>PARP1</i>	0.63	7.46E-03
<i>SERPINB1</i>	0.62	3.36E-02
<i>RAB31</i>	0.62	1.64E-02
<i>HNI</i>	0.62	1.45E-02
<i>FLJ20160</i>	0.62	4.70E-02
<i>TNFAIP2</i>	0.62	5.66E-03
<i>SPI1</i>	0.62	6.79E-03
<i>YWHAH</i>	0.62	5.72E-03
<i>PRSS3</i>	0.62	5.48E-04
<i>PAQR4</i>	0.62	7.24E-03
<i>GRAMD1A</i>	0.61	4.38E-03
<i>RFX5</i>	0.61	2.89E-03
<i>TUBB4Q</i>	0.61	3.40E-02
<i>TUBA1B</i>	0.61	1.29E-02
<i>LY96</i>	0.61	1.31E-02
<i>CYP8B1</i>	0.61	4.16E-02
<i>TUBB3</i>	0.61	3.96E-02
<i>PPA1</i>	0.61	5.92E-03
<i>TNFAIP8L3</i>	0.61	2.20E-02
<i>LTBR</i>	0.60	3.17E-03
<i>SUSD1</i>	0.60	6.10E-03
<i>IFNGR1</i>	0.60	1.88E-02
<i>C14orf129</i>	0.60	1.57E-02
<i>STEAP1</i>	0.60	3.43E-02
<i>MORC4</i>	0.60	3.95E-02
<i>Sep09</i>	0.60	2.99E-03
<i>LAPTM5</i>	0.60	6.72E-03
<i>SRPX2</i>	0.60	3.32E-02
<i>RNASE6</i>	0.59	4.14E-04
<i>CARM1</i>	0.59	1.83E-05
<i>CALR</i>	0.59	1.35E-02
<i>RET</i>	0.59	1.78E-02
<i>HPS5</i>	0.59	3.75E-04
<i>GOLPH3</i>	0.59	3.32E-03
<i>LOC144481</i>	-0.59	3.81E-03
<i>MUTYH</i>	-0.59	6.76E-03
<i>C11orf54</i>	-0.59	2.24E-02
<i>GBE1</i>	-0.59	1.58E-02
<i>C6orf60</i>	-0.59	3.67E-03
<i>GHR</i>	-0.59	3.05E-02
<i>LOC732058</i>	-0.60	2.07E-02
<i>SLC16A2</i>	-0.60	3.66E-02
<i>PPP1R10</i>	-0.60	6.89E-03
<i>ACSM2A</i>	-0.60	4.91E-02
<i>AHNAK</i>	-0.60	3.33E-02

Gene symbol	Log2 FC	P-value <sup>a</sup>
<i>HINT2</i>	-0.60	1.28E-02
<i>UBL3</i>	-0.60	2.54E-03
<i>CAT</i>	-0.60	1.47E-02
<i>TMEM195</i>	-0.61	2.27E-02
<i>CYFIP2</i>	-0.61	6.24E-03
<i>PON3</i>	-0.61	1.66E-02
<i>ZSCAN18</i>	-0.61	1.27E-02
<i>LOC641825</i>	-0.61	2.92E-03
<i>TMEM86B</i>	-0.61	1.75E-02
<i>SARDH</i>	-0.61	6.61E-03
<i>TGDS</i>	-0.61	2.60E-02
<i>ST3GAL3</i>	-0.61	4.24E-03
<i>ELOVL2</i>	-0.61	2.05E-02
<i>RAD54L2</i>	-0.62	3.99E-02
<i>TMEM14A</i>	-0.62	1.02E-02
<i>SORL1</i>	-0.62	9.32E-03
<i>C1orf53</i>	-0.62	1.23E-02
<i>PHLPP</i>	-0.62	1.48E-02
<i>LOC729776</i>	-0.62	9.74E-03
<i>VPS37D</i>	-0.62	2.15E-03
<i>MGC70857</i>	-0.62	9.05E-04
<i>PDE3B</i>	-0.62	6.10E-04
<i>XRCC6BP1</i>	-0.62	4.32E-03
<i>PTP4A1</i>	-0.62	5.02E-03
<i>AADAC</i>	-0.62	1.21E-02
<i>SLC2A4RG</i>	-0.62	2.35E-02
<i>C11orf71</i>	-0.62	1.15E-02
<i>LOC648399</i>	-0.62	5.53E-04
<i>LAG3</i>	-0.63	1.34E-02
<i>GLYCTK</i>	-0.63	1.92E-02
<i>ACSM2B</i>	-0.63	2.08E-02
<i>KBTBD11</i>	-0.63	4.05E-03
<i>ZNF622</i>	-0.63	5.85E-03
<i>DEPDC7</i>	-0.63	3.65E-02
<i>LOC730432</i>	-0.64	1.52E-02
<i>TUBE1</i>	-0.64	1.06E-02
<i>SAMD4A</i>	-0.64	1.96E-03
<i>LOC644322</i>	-0.64	5.38E-03
<i>TM7SF3</i>	-0.64	8.07E-07
<i>ZNF511</i>	-0.64	5.42E-03
<i>DPP4</i>	-0.64	2.73E-02
<i>OCEL1</i>	-0.64	1.92E-02
<i>C5orf33</i>	-0.65	1.77E-02
<i>PHYH</i>	-0.65	2.84E-02
<i>CHAD</i>	-0.65	3.70E-02
<i>LEPR</i>	-0.65	3.97E-03
<i>C18orf17</i>	-0.65	2.93E-02
<i>GAMT</i>	-0.65	3.61E-02
<i>MAN1C1</i>	-0.65	4.72E-02
<i>UGT2B15</i>	-0.65	3.83E-02
<i>ALDH7A1</i>	-0.65	2.69E-02
<i>SFXN2</i>	-0.65	2.79E-02
<i>FLJ23754</i>	-0.65	1.58E-06
<i>AMT</i>	-0.66	2.88E-02
<i>GPNPAT1</i>	-0.66	8.49E-04
<i>MYL5</i>	-0.66	4.18E-03
<i>TCPI10L</i>	-0.66	2.35E-02
<i>CCT6B</i>	-0.66	3.37E-03
<i>SLC19A3</i>	-0.66	4.66E-03
<i>MGMT</i>	-0.66	6.84E-03
<i>ENPP1</i>	-0.67	6.98E-03
<i>IRF8</i>	-0.67	4.43E-04
<i>PPARGC1A</i>	-0.67	2.70E-02
<i>EHHADH</i>	-0.67	2.63E-02
<i>NUDT8</i>	-0.67	1.84E-02
<i>NPAL1</i>	-0.67	9.50E-04
<i>KIAA0999</i>	-0.68	1.64E-03
<i>RPL15</i>	-0.68	8.39E-05
<i>PBLD</i>	-0.68	2.12E-02
<i>HAPLN4</i>	-0.68	2.59E-02
<i>PDE7B</i>	-0.68	2.25E-03
<i>NAT8</i>	-0.68	2.03E-02
<i>ALDH5A1</i>	-0.69	3.57E-02
<i>SLC27A5</i>	-0.69	3.54E-02

Gene symbol	Log2 FC	P-value <sup>a</sup>
<i>OXER1</i>	-0.69	1.12E-02
<i>GUCA2B</i>	-0.69	2.87E-03
<i>C8orf40</i>	-0.69	3.27E-02
<i>IVD</i>	-0.69	1.56E-02
<i>WNT11</i>	-0.69	3.40E-05
<i>EPB41LAB</i>	-0.69	6.04E-03
<i>ARMC6</i>	-0.69	5.65E-03
<i>THEM2</i>	-0.69	1.68E-02
<i>DAO</i>	-0.70	5.34E-03
<i>CACNA1H</i>	-0.70	3.15E-02
<i>BDH1</i>	-0.70	9.64E-03
<i>RTN4</i>	-0.70	3.22E-02
<i>GCKR</i>	-0.70	3.81E-03
<i>SH3PXD2A</i>	-0.70	1.97E-02
<i>AMACR</i>	-0.70	1.05E-02
<i>GRAMD1C</i>	-0.70	1.75E-02
<i>MAMDC4</i>	-0.70	9.20E-04
<i>HOMER2</i>	-0.70	2.77E-02
<i>MRPL23</i>	-0.70	3.62E-04
<i>TMEM116</i>	-0.70	7.13E-03
<i>CYP2C18</i>	-0.71	1.05E-02
<i>GADD45A</i>	-0.72	3.46E-02
<i>ANKRD37</i>	-0.72	2.73E-02
<i>MPND</i>	-0.72	4.36E-02
<i>UPB1</i>	-0.72	9.77E-03
<i>GYS2</i>	-0.73	5.58E-03
<i>PON1</i>	-0.73	3.14E-02
<i>AASS</i>	-0.74	1.88E-02
<i>SDC2</i>	-0.74	2.76E-02
<i>HLF</i>	-0.74	2.16E-02
<i>SAT2</i>	-0.74	2.18E-02
<i>HGD</i>	-0.74	1.62E-02
<i>TRPM8</i>	-0.75	2.45E-02
<i>SORD</i>	-0.75	5.31E-03
<i>GCLM</i>	-0.75	2.70E-03
<i>MOGAT1</i>	-0.75	3.67E-02
<i>KLKB1</i>	-0.75	2.89E-02
<i>UNC93A</i>	-0.75	3.38E-03
<i>LOC643031</i>	-0.75	2.42E-02
<i>CLDN14</i>	-0.76	9.62E-03
<i>PCK2</i>	-0.76	2.23E-02
<i>AQP11</i>	-0.76	3.24E-02
<i>C9orf95</i>	-0.76	1.57E-02
<i>MYOM2</i>	-0.76	3.42E-02
<i>PROX1</i>	-0.77	2.27E-03
<i>HDC</i>	-0.78	1.82E-03
<i>UGT2B11</i>	-0.78	1.43E-02
<i>C9orf165</i>	-0.79	1.26E-03
<i>C10orf65</i>	-0.79	2.36E-02
<i>CTH</i>	-0.79	5.83E-03
<i>ABCA8</i>	-0.79	1.18E-02
<i>NP</i>	-0.79	2.03E-03
<i>LIME1</i>	-0.79	1.48E-02
<i>A1CF</i>	-0.79	1.57E-03
<i>POLR2I</i>	-0.80	1.66E-03
<i>C7orf55</i>	-0.80	4.01E-03
<i>VIPRI</i>	-0.80	1.14E-02
<i>DCXR</i>	-0.80	1.63E-02
<i>TIGA1</i>	-0.80	1.44E-03
<i>DCDC5</i>	-0.81	1.79E-02
<i>SLC44A4</i>	-0.81	1.57E-02
<i>SIRT5</i>	-0.81	5.13E-03
<i>HSD17B8</i>	-0.81	3.21E-02
<i>EXPH5</i>	-0.81	1.15E-02
<i>IL27</i>	-0.81	4.79E-03
<i>MACROD1</i>	-0.81	2.18E-02
<i>ba16L21.2.1</i>	-0.82	1.63E-02
<i>NR1I3</i>	-0.82	2.19E-02
<i>PECR</i>	-0.82	2.77E-02
<i>AKR7A3</i>	-0.82	1.01E-02
<i>IRS1</i>	-0.82	3.65E-03
<i>UNQ830</i>	-0.83	8.80E-03
<i>LOC728811</i>	-0.83	1.17E-02
<i>PSMAL</i>	-0.83	7.62E-03

SUPPLEMENTS

Gene symbol	Log2 FC	P-value <sup>a</sup>
SCARNA9	-0.83	2.40E-02
ACAA1	-0.83	2.89E-02
DMGDH	-0.83	3.15E-03
HAO2	-0.84	2.19E-02
ACSM3	-0.84	1.69E-02
GLS2	-0.84	9.95E-03
CYP4A11	-0.85	4.60E-02
NCAM2	-0.85	4.11E-03
F13B	-0.86	1.46E-02
LOC731777	-0.86	6.98E-05
AFM	-0.86	1.97E-02
PEX11G	-0.87	8.13E-03
G6PC	-0.87	1.53E-02
GREM2	-0.88	5.31E-03
ACOX2	-0.88	1.08E-02
SLC22A1	-0.89	3.32E-02
GRHPR	-0.90	3.00E-03
NTHL1	-0.90	2.27E-02
DACT2	-0.90	1.38E-04
RGN	-0.90	2.15E-02
TMPRSS6	-0.90	8.08E-03
RCL1	-0.90	2.27E-02
GPAM	-0.90	8.57E-03
KCNN2	-0.90	1.11E-02
WDR23	-0.91	8.08E-03
XDH	-0.91	3.33E-03
HAAO	-0.91	5.96E-03
UGT2B10	-0.91	3.18E-02
ENO3	-0.91	1.20E-02
CYP39A1	-0.92	4.10E-02
C9orf103	-0.93	3.84E-02
ACADSB	-0.93	1.92E-02
RDH5	-0.93	4.96E-02
PCOLCE	-0.93	1.81E-03
LOC143941	-0.93	3.89E-02
ZNF533	-0.93	2.04E-02
FOLH1	-0.93	6.91E-03
MAP2K1	-0.95	1.54E-03
PRODH	-0.95	1.04E-02
LOC643692	-0.96	1.52E-03
PACSIN3	-0.97	1.85E-03
LOC645378	-0.97	3.08E-03
C5orf13	-0.97	2.18E-02
CYP4A22	-0.97	1.23E-03
VSNL1	-0.98	1.88E-02
TBX15	-0.98	3.79E-02
ABCG2	-0.98	4.63E-03
LOC647169	-0.98	1.48E-02
N4BP2L1	-0.99	3.73E-03
SLC47A1	-1.00	2.13E-02
SLCO1B1	-1.00	1.20E-03
GATM	-1.00	4.63E-02
PRR6	-1.00	1.10E-03
CNDP1	-1.01	4.48E-02
CXCL2	-1.01	4.24E-02
TM7SF2	-1.01	1.16E-02
XPNPEP2	-1.02	6.72E-03
SLC3A1	-1.04	8.98E-03
ALDH1L1	-1.04	1.08E-02
SEC14L2	-1.04	1.06E-02
CFHR4	-1.04	4.65E-02
PXMP2	-1.05	1.19E-03
ABP1	-1.05	4.91E-08
KMO	-1.05	1.02E-02
THRSP	-1.06	1.58E-02
ASPA	-1.07	1.43E-03
THOP1	-1.08	2.40E-02
DPT	-1.09	1.35E-03
OVGP1	-1.09	1.05E-03
CYP2A7	-1.10	4.11E-02
RBP5	-1.10	3.71E-02
ASCL1	-1.10	8.01E-03
CUX2	-1.11	4.45E-02
AGXT2L1	-1.11	7.47E-03

Gene symbol	Log2 FC	P-value <sup>a</sup>
UGT2B17	-1.11	4.89E-03
HGFAC	-1.11	1.12E-02
IYD	-1.13	1.40E-02
SLC1A2	-1.13	4.84E-03
MPDZ	-1.13	1.46E-03
PPP1R3C	-1.14	2.74E-02
ASB9	-1.14	7.65E-03
SOCS2	-1.15	1.99E-02
SLC39A5	-1.16	1.85E-02
ADH6	-1.17	5.29E-03
LIPC	-1.18	1.08E-02
SLC17A3	-1.19	6.61E-04
FXYP1	-1.19	2.19E-02
IGFALS	-1.19	3.94E-02
GBA3	-1.20	1.61E-02
SNORD13	-1.22	1.27E-02
SERPINA5	-1.22	1.40E-02
SLC17A1	-1.23	2.65E-04
INDOL1	-1.23	1.81E-02
LOC554235	-1.26	7.09E-03
CA2	-1.26	7.62E-03
SLC20A2	-1.29	8.42E-04
FNDC5	-1.31	4.99E-02
LOC339766	-1.32	2.87E-04
CYP2A6	-1.40	3.84E-03
PHGDH	-1.41	1.78E-02
ADH4	-1.43	2.82E-02
GLYAT	-1.44	9.61E-03
AKR1D1	-1.45	3.89E-02
CMBL	-1.47	1.14E-02
SCG5	-1.48	1.50E-03
DAK	-1.48	2.80E-04
ZG16	-1.55	1.28E-02
AGPAT9	-1.57	3.17E-05
PCOLCE2	-1.58	1.52E-02
CYP3A43	-1.59	2.19E-02
SLC6A1	-1.60	1.45E-02
GNMT	-1.62	2.40E-02
ITIH2	-1.62	3.89E-03
SLC22A10	-1.66	1.72E-05
BHMT	-1.73	1.95E-02
DNMT3L	-1.76	4.27E-04
OAT	-1.82	1.61E-04
CYP1A2	-1.90	4.06E-02
SRD5A2	-1.92	5.52E-03
GSTA1	-1.97	1.91E-02
CYP2C19	-1.99	1.11E-02
PFKFB1	-2.02	2.07E-03
GSTA2	-2.06	1.41E-02
BCHE	-2.07	9.79E-04
HEPACAM	-2.07	1.07E-02
GSTA5	-2.10	6.64E-03
BBOX1	-2.13	5.96E-03
HSD17B13	-2.26	2.07E-03

Log2FC = log2 fold change, elevated CRP compared to normal. Values represent mean for for N = 7 (CRP hi.) and N = 98 (CRP norm.) arrays per group

<sup>a</sup> Two groups Welch's t

**Supplement Table 5** Significantly enriched GO terms in the category “*biological process*” in patients with elevated CRP (> 10mg/l) compared to normal CRP (≤ 1mg/l).

GO ID	Description	Number of genes in term	P-value <sup>a</sup>	Adj. p-value <sup>b</sup>
GO:0044281	small molecule metabolic process	167	1.58E-27	8.01E-24
GO:0006082	organic acid metabolic process	98	1.29E-26	6.51E-23
GO:0019752	carboxylic acid metabolic process	90	2.59E-24	1.31E-20
GO:0006520	cellular amino acid metabolic process	54	1.13E-16	5.72E-13
GO:0046395	carboxylic acid catabolic process	34	1.89E-14	9.57E-11
GO:0055114	oxidation-reduction process	78	2.54E-14	1.28E-10
GO:0032787	monocarboxylic acid metabolic process	44	9.12E-13	4.62E-09
GO:0006805	xenobiotic metabolic process	24	5.58E-11	2.83E-07
GO:0071466	cellular response to xenobiotic stimulus	24	7.43E-11	3.76E-07
GO:0006629	lipid metabolic process	77	7.62E-11	3.86E-07
GO:0008202	steroid metabolic process	32	1.03E-10	5.23E-07
GO:0009410	response to xenobiotic stimulus	24	2.23E-10	1.13E-06
GO:0009063	cellular amino acid catabolic process	21	1.76E-09	8.92E-06
GO:0006575	cellular modified amino acid metabolic process	22	2.88E-08	1.46E-04
GO:0008652	cellular amino acid biosynthetic process	20	5.55E-08	2.81E-04
GO:0046415	urate metabolic process	7	1.58E-07	7.99E-04
GO:0009069	serine family amino acid metabolic process	11	2.24E-07	1.13E-03
GO:0006081	cellular aldehyde metabolic process	11	4.33E-07	2.19E-03
GO:0051186	cofactor metabolic process	26	5.93E-07	3.00E-03
GO:0044255	cellular lipid metabolic process	52	9.81E-07	4.97E-03
GO:0070887	cellular response to chemical stimulus	90	1.09E-06	5.53E-03
GO:0009056	catabolic process	102	3.49E-06	1.77E-02
GO:0051258	protein polymerization	11	3.97E-06	2.01E-02
GO:0008206	bile acid metabolic process	9	4.21E-06	2.14E-02

<sup>a</sup> Fisher's Exact Test p-value

<sup>b</sup> Bonferroni adjusted p-value for multiple testing

**Supplement Table 6** Common significantly enriched GO terms in the category “*biological process*” in IL-6-challenged PHH and livers of patients with elevated CRP (> 10mg/l) compared to normal CRP (≤ 1mg/l).

GO ID	Description	Number of genes in term	P-value <sup>a</sup>	Adj. p-value <sup>b</sup>
GO:0006805	xenobiotic metabolic process	14	1.00E-12	5.00E-09
GO:0071466	cellular response to xenobiotic stimulus	14	1.10E-12	5.50E-09
GO:0009410	response to xenobiotic stimulus	14	2.31E-12	1.16E-08
GO:0044281	small molecule metabolic process	44	3.85E-12	1.93E-08
GO:0055114	oxidation-reduction process	28	1.07E-11	5.38E-08
GO:0006082	organic acid metabolic process	27	2.85E-11	1.42E-07
GO:0019752	carboxylic acid metabolic process	25	1.54E-10	7.71E-07
GO:0006629	lipid metabolic process	27	1.39E-09	6.94E-06
GO:0046395	carboxylic acid catabolic process	12	1.71E-08	8.56E-05
GO:0042738	exogenous drug catabolic process	4	6.81E-07	3.40E-03
GO:0042737	drug catabolic process	4	1.46E-06	7.30E-03
GO:0006520	cellular amino acid metabolic process	14	1.85E-06	9.23E-03
GO:0017144	drug metabolic process	5	2.09E-06	1.05E-02
GO:0032787	monocarboxylic acid metabolic process	13	2.33E-06	1.16E-02
GO:0044255	cellular lipid metabolic process	18	4.24E-06	2.12E-02

<sup>a</sup> Fisher's Exact Test p-value

<sup>b</sup> Bonferroni adjusted p-value for multiple testing